



UNIVERSITAT DE
BARCELONA

Transcriptome analysis and functional characterization of *Plasmodium vivax* spleen and bone marrow dependent genes and the role of the extracellular vesicles in cryptic niche formation

Alberto Ayllon Hermida

ADVERTIMENT. La consulta d'aquesta tesi queda condicionada a l'acceptació de les següents condicions d'ús: La difusió d'aquesta tesi per mitjà del servei TDX (www.tdx.cat) i a través del Dipòsit Digital de la UB (diposit.ub.edu) ha estat autoritzada pels titulars dels drets de propietat intel·lectual únicament per a usos privats emmarcats en activitats d'investigació i docència. No s'autoritza la seva reproducció amb finalitats de lucre ni la seva difusió i posada a disposició des d'un lloc aliè al servei TDX ni al Dipòsit Digital de la UB. No s'autoritza la presentació del seu contingut en una finestra o marc aliè a TDX o al Dipòsit Digital de la UB (framing). Aquesta reserva de drets afecta tant al resum de presentació de la tesi com als seus continguts. En la utilització o cita de parts de la tesi és obligat indicar el nom de la persona autora.

ADVERTENCIA. La consulta de esta tesis queda condicionada a la aceptación de las siguientes condiciones de uso: La difusión de esta tesis por medio del servicio TDR (www.tdx.cat) y a través del Repositorio Digital de la UB (diposit.ub.edu) ha sido autorizada por los titulares de los derechos de propiedad intelectual únicamente para usos privados enmarcados en actividades de investigación y docencia. No se autoriza su reproducción con finalidades de lucro ni su difusión y puesta a disposición desde un sitio ajeno al servicio TDR o al Repositorio Digital de la UB. No se autoriza la presentación de su contenido en una ventana o marco ajeno a TDR o al Repositorio Digital de la UB (framing). Esta reserva de derechos afecta tanto al resumen de presentación de la tesis como a sus contenidos. En la utilización o cita de partes de la tesis es obligado indicar el nombre de la persona autora.

WARNING. On having consulted this thesis you're accepting the following use conditions: Spreading this thesis by the TDX (www.tdx.cat) service and by the UB Digital Repository (diposit.ub.edu) has been authorized by the titular of the intellectual property rights only for private uses placed in investigation and teaching activities. Reproduction with lucrative aims is not authorized nor its spreading and availability from a site foreign to the TDX service or to the UB Digital Repository. Introducing its content in a window or frame foreign to the TDX service or to the UB Digital Repository is not authorized (framing). Those rights affect to the presentation summary of the thesis as well as to its contents. In the using or citation of parts of the thesis it's obliged to indicate the name of the author.



Transcriptome analysis and functional characterization of *Plasmodium vivax* spleen and bone marrow dependent genes and the role of the extracellular vesicles in cryptic niche formation

Alberto Ayllon Hermida

Doctoral thesis dissertation presented to apply for the degree of doctor at the University of Barcelona

Doctoral Program in Medicine and Translational Research

School of Medicine and Health Sciences

University of Barcelona

September 2024

Directed by:

M^a Carmen Fernández Becerra (ISGlobal, Hospital Clínic – Universitat de Barcelona. IGTP, Badalona)

Hernando A. Del Portillo Obando (ICREA at ISGlobal, Hospital Clínic – Universitat de Barcelona. IGTP, Badalona)

Tutor:

Sara M. Soto González (ISGlobal, Hospital Clínic – Universitat de Barcelona)

A mis padres i a la Gal·la

“Find what you love and let it kill you.”

– **Charles Bukowski** –

ACKNOWLEDGMENTS | AGRAÏMENTS

Y si fuera, mi vida una escalera, me la he pasado entera buscando el siguiente escalón. Supongo que este difícil escalón merece agradecer a mucha gente.

Primero de todo, agradecer a Carmen y Hernando, por haberme dado la oportunidad de entrar en este maravilloso grupo como un iluso estudiante de máster, que no sabía muy bien donde se metía, pero que a través de vuestra ayuda, respaldo y guía ha descubierto en la investigación científica una verdadera pasión. Gracias por haberme hecho crecer tantísimo científicamente y personalmente. De verdad.

A tots els PVREX, actuals i passats; Marc, simplement gràcies per tot: per l'ajut experimental, pel suport moral, pels cotilleos, però sobretot perquè gràcies a tu aquesta tesi ha sortit, ja que sense tu, el lab se hunde. Núria Sima, gràcies pels consells, per l'ajut i per la teva experiència, tant al lab com fora d'ell. Ha estat genial que arribessis al lab, perquè ens has forçat a revitalitzar-nos una mica fora del IGTP. Berta, la niña Berta, gràcies per sempre estar disposada a ajudar, per sempre estar disposada a escoltar i pels coneixements nous que has portat al grup. Sincerament, crec que tens un futur increïble com a científica. Paula, gracias por la organización, por tenerlo todo siempre apuntado, pero también por tu alegría. Nil, gràcies per la passió que mostres i per apropar-nos la complexitat de la física. Iris, gracias por las charlas musicales, por siempre estar dispuesta a ayudar. Nos vemos en los conciertos. Melisa, simplemente decirte que eres una verdadera inspiración y que me siento afortunado de haber podido ver tu pasión por la ciencia como compañero tuyo. Sergio, gracias por las birras y por las charlas de scape rooms. Nuria Cortés, gràcies pels pàdels, per les birres i per les converses. Vam passar els moments més estranys del món junts a un lab del Clínic, però com ho vam fer junts, diria que va ser inclús divertit. Gràcies també als PVREX passats, amb els que vaig coincidir al començament d'aquest camí, la Miriam, l'Aleix i la Haruka.

Però el grup de PVREX no estaria complert sense les moltes visites que hem tingut durant aquests cinc anys que he format part. Mis panitas, Carlos y Jahnnyer: gracias mis senseis por haber traído la alegría a nuestro laboratorio, por ser tan rigurosos y por ser unos grandes científicos, opero, sobre todo, por ser mejores personas. Carlos, en casa de mi madre siempre tendrás un plato en la mesa, y en la discoteca con mis amigos un trago esperándote. Jahnnyer, pese a que seas más merengue que Santiago Bernabéu, siempre estaré encantado de ir contigo al Camp Nou o al Palau Blaugrana. Gracias a los dos, mis panas. Nos vemos en Colombia. Christian, gracias por las risas, por las cenas, por las fiestas... Ah sí, y por los congresos. Fue una suerte que este mundo nos hiciera conocernos. Then, also I'd like to thanks to Pia, first, for being just an amazing person, and second, for allowing me to be your mentor, because I've never would have thought of having a better mentee. Your future is extremely bright, I'm sure. Barbarinha, *rapazinha*, ánimo con el sprint final, pero sobre todo por haber aparecido por el lab, por tu alegría, por los congresos, por nuestras minivacaciones en Palestina, por sacarme las mejores fotos de viaje que nunca he tenido. Obrigado por todo. Por último, gracias Raúl por la vitalidad, por haber encajado en el grupo des del minuto o. Eres una persona encantadora, inteligente y trabajador. Mucha suerte con la tesis que se acerca.

Also, I'd like to thank Prof. Bernd Giebel for having me in your lab in Essen. I've really felt welcome from the very first moment and I've really enjoyed experiencing another lab. I'm sure in the near future we will continue collaborating. Also, I'd like to thank Yanis for being so nice with me during my stay, making it super easy to stay in Essen. Thanks for the drinks, the football matches and diners. I'm sure that in the near future we will see again.

Gràcies als nostres col·laboradors, tant a l'ISGlobal com a fora; Alfred Cortés i tots els epimalarios, Oriol, Elisabet, Alba i Neus, gràcies per l'ajut científic, per les discussions de clonatge, per la resolució de dubtes que tan disposats sempre heu estat, però també per les cerveses, les xerrades i els riures durant el BioMalPar. También quiero agradecer a Mariona Graupera y en especial a Ane

Larrinaga por la ayuda con el single cell, por la predisposición para discutir los resultados pese a que al principio me sonaba todo un poco a chino. Gracias.

Gracias Lili, Xavi y Aleix. Gracias por los cafeses, por los cigarros, por las charlas, por las cenas, por las fiestas, por los brunchs, por las barbacoas, por los Overcooked... La verdad que ha sido una suerte poder compartir con vosotros todos mis sufrimientos, angustias, preocupaciones, pero también las alegrías y las buenas noticias. Me habéis alegrado la resistencia. Os quiero mucho.

Gràcies a tota la gent meravellosa que he conegut gràcies al doctorat: a els tuberculosis (Marta, Ninuka, Kaori, Maria, Pablo), a les EVs Clinic (Julia i Marina), als IVECAT (Marta Clos, Sergio, Marta Sanroque, Miriam, Marcel·la, Ana, Marta Monguió). Ha estat un plaer coincidir en aquest camí.

Gracias madre, gracias por todo. Me has inculcado a fuego que el esfuerzo y el sacrificio es el camino, y creo que así lo he hecho. Gracias por apoyarme en todo momento, por la confianza que has puesto en mí. Emilio, espero que estés orgulloso. Creo que sí que lo estarás. Gracias por todo papa. Sin vosotros, no hubiera llegado hasta aquí. Gracias por los esfuerzos que habéis hecho desde siempre.

Gracias a mi familia, primos, tíos/as, por vuestro apoyo e interés por mí. Especialment al Borja, el meu germà, per haver estat allà en els meus moments mes foscos i per fer-me tiet. Us estimo.

Gràcies als meus amics de la uni, Aina, Anna T, Anna R, Nuria, Maria, Veneno, Murgui, Fanto, Tere, pels anys meravellosos que hem passat d'ençà que ens coneixem i els que ens queden per venir...

Gracias a mis amigos de toda la vida, por llevar 5 años pensando que trabajo en la NASA, pero ser mi vía de escape en formato de cenas, fiestas, risas y, últimamente en formato bodas (y de más estafas piramidales). Os quiero a todos mis Dobles, Cristina, Sara.

I per acabar, però més important, a tu Gal·la. No puc descriure amb paraules com estic d'agraït que hagi aparegut a la meua vida. M'has ajudat i recolzat sempre i de manera incondicional, i mai en aquesta vida t'ho podré tornar. Enhorabona també a tu perquè aquesta tesi és tant teua com meua gairebé. Gràcies per ser la millor parella de món, per la paciència durant aquest (llarg i dur) viatge, per donar-me escalf quan més ho he necessitat i per empènyer-me a perseguir els meus somnis. Podria estar 80 pàgines més escrivint les coses que tinc a agrair-te, però ens les quedem per nosaltres.

Gràcies a tots. Sin vosotros, este camino hubiese sido mucho más complicado y aburrido.

TABLE OF CONTENTS

LIST OF ABBREVIATIONS	17
LIST OF ARTICLES IN THE THESIS	21
SUMMARY	23
<i>Introduction</i>	23
<i>Hypothesis and objectives</i>	24
<i>Methods & key results</i>	24
<i>Conclusions</i>	25
RESUM	27
<i>Introducció</i>	27
<i>Hipòtesi i objectius</i>	28
<i>Mètodes i resultats clau</i>	28
<i>Conclusions</i>	29
1. INTRODUCTION	31
1.1 MALARIA	33
1.1.1 History of malaria	33
1.1.2 The revelation of the malaria pathogen	34
1.1.3 The global burden of malaria disease	36
1.1.4 Pathology in malaria	38
1.1.5 <i>P. falciparum</i> , the deadliest parasite	41
1.1.6 No longer benign: The <i>P. vivax</i> malaria disease	41
1.1.7 Molecular basis of malaria pathology	43
1.1.7.1 <i>P. falciparum</i> : the var multigenic family	43
1.1.7.2 <i>P. vivax</i> multigene families	45
1.1.8 Control measures	47
1.1.8.1 Diagnosis of <i>vivax</i> malaria	47
1.1.8.2 Treatment, control and prevention of <i>P. vivax</i> malaria	49
1.1.9 <i>P. vivax</i> parasite biology	53
1.1.9.1 Life cycle of <i>P. vivax</i>	53
1.1.10 Cryptic niches	56
1.1.10.1 The presence of <i>P. vivax</i> in the bone marrow	57
1.1.10.2 The presence of <i>P. vivax</i> in the spleen	59
1.1.11 Genomic editing of <i>Plasmodium</i> species	63
1.1.11.1 Genomic editing to study <i>P. vivax</i> biology	65
1.2 EXTRACELLULAR VESICLES	67
1.2.1 Origin, biogenesis and composition	68
1.2.2 Extracellular vesicle purification and characterization	72
1.2.2.1 Isolation of extracellular vesicles	72

1.2.2.2	<i>Characterization of isolated EVs</i>	78
1.3	EXTRACELLULAR VESICLES IN MALARIA	82
1.3.1	<i>Biogenesis, uptake and cargo of EVs in malaria</i>	82
1.3.2	<i>Cell-to-cell communication in malaria</i>	84
1.3.3	<i>EVs role in malaria pathology: vascular dysfunction, severe malaria and placental malaria</i>	86
1.3.4	<i>P. vivax-derived EVs and its role in cryptic infections</i>	87
2.	HYPOTHESIS AND OBJECTIVES	89
2.1	HYPOTHESIS	91
2.2	OBJECTIVES	91
3.	MATERIALS, METHODS & RESULTS	93
3.1	ARTICLE 1: <i>PLASMODIUM VIVAX</i> SPLEEN-DEPENDENT GENES ENCODE ANTIGENS ASSOCIATED WITH CYTOADHESION AND CLINICAL PROTECTION	95
3.2	ARTICLE 2: <i>PLASMODIUM VIVAX</i> SPLEEN-DEPENDENT PROTEIN 1 AND ITS ROLE IN EXTRACELLULAR VESICLES-MEDIATED INTRASPLENIC INFECTIONS	117
3.3	ARTICLE 3: MORPHOLOGICAL AND TRANSCRIPTIONAL CHANGES IN HUMAN BONE MARROW DURING NATURAL <i>PLASMODIUM VIVAX</i> MALARIA INFECTIONS	141
3.4	ARTICLE 4 (UNPUBLISHED): TRANSCRIPTIONAL ANALYSIS OF <i>PLASMODIUM VIVAX</i> DURING ACUTE INFECTIONS IN THE HUMAN BONE MARROW	159
4.	DISCUSSION	183
	<i>Vivax malaria, a classically neglected disease</i>	185
	<i>P. vivax cryptic infections</i>	186
	<i>Cryptic niches: The spleen</i>	187
	<i>Cryptic niches: The BM</i>	189
	<i>The role of EVs for P. vivax infection</i>	193
	<i>Limitations & Summary</i>	195
5.	CONCLUSIONS	197
6.	BIBLIOGRAPHY	201
6.1	REFERENCES	203
7.	ANNEX I	233

LIST OF ABBREVIATIONS

ACT	artemisinin-based combination therapy	dUC	Differential ultracentrifugation
AF4	asymmetrical flow filed-flow fractionation	EBIs	erythroblastic islands
AL	artemether-lumefantrine	ELISA	enzyme-linked immunosorbent assay
ALIX	ALG-2 interacting protein X	EM	Electron microscopy
AS-AQ	artesunate-amodiaquine	ESCRT	endosomal sorting complexes required for transport
AS-MQ	artesunate-mefloquine	EVs	extracellular vesicles
AS-PY	artesunate-pyronaridine	G6PD	glucose-6-phosphate dehydrogenase
BBA	Bead-Based Assay	G6PDd	G6PD deficiency
BC	Before Christ	GATA1	Globin Transcription Factor 1
BCA	bicinchoninic acid	GO	Gene ontology
BM	bone marrow	GPI	glycosylphosphatidylinositol
BALB/c	Rag2null IL2rynull	hEVs	healthy donors EVs
Ca2+	calcium	HSC70	heat shock cognate 71kDa protein
CD36	Platelet glycoprotein 4	hSF	human Spleen fibroblasts
CD71/TFRC	transferrin receptor	HSP70	heat shock 70 kDa protein
CM	cerebral malaria		
cryo-EM	cryo-electron microscopy		
CSP	circumsporozoite surface protein		
DBP	Duffy Binding Protein		
DHA-PPQ	dihydro-artemisininpiperazine		
DIC	direct immune-affinity capture		
DNA	desoxyribonucleic acid		

ICAM-1 Intercellular adhesion molecule-1	<i>P. falciparum</i> <i>Plasmodium falciparum</i>
IFAs Immunofluorescence assay	<i>P. malariae</i> <i>Plasmodium malariae</i>
IL interleukin	<i>P. ovale</i> <i>Plasmodium ovale</i>
ILVs intraluminal vesicles	<i>P. vivax</i> <i>Plasmodium vivax</i>
iRBC infected Red Blood Cells	PB Peripheral blood
IRS indoor residual spraying	PCR polymerase chain reaction
ITNs insecticide treated mosquito nets	PHIST Poly-Helical Interspersed Sub-Telomeric
LAMP Lysosomal-associated membrane protein	piRNA PIWI-interacting RNA
LC–MS/MS liquid chromatography coupled to MS	pLDH pan-genus antigen lactate dehydrogenase
lncRNAs long non-coding RNAs	pRBCs parasitized Red Blood
miRNA micro RNAs	PvCSP <i>P. vivax</i> Circumsporozoite surface protein
mRNA messenger RNA	PvDBP <i>P. vivax</i> Duffy Binding protein
MS mass spectrometry	PvEVs <i>P. vivax</i> extracellular vesicles
MSP merozoite surface protein	PvMSP1 <i>P. vivax</i> Merozoite surface protein 1
MVBs multivesicular bodies	PvRBP2a <i>P. vivax</i> reticulocyte-binding protein 2a
MVs Microvesicles	
NHP non-human primates	
NTA Nanoparticle tracking analysis	

Pvs25, Pvs28, Pvs230, Pvs16 *P. vivax* sexual stage 25, 28, 230 and 16

qRT-PCR quantitative reverse transcription PCR

RBC Red Blood Cell

RDT rapid diagnostic test

RNA ribonucleic acid

rRNA ribosomal RNA

RT room temperature

RT-PCR reverse transcription PCR

RTS,S Mosquirix

scRNA small cytoplasmic RNA

SDS-PAGE sulfate polyacrylamide gel electrophoresis

SEC Size-exclusion chromatography

snoRNA small nucleolar RNA

snRNA small nuclear RNA

Spp. species

SRP RNA signal recognition particle RNA

TEM transmission electron microscopy

TGN trans-Golgi network

TNF tumor necrosis factor

tRNA transfer RNA

vault RNA vault ribonucleic acid

WHO World Health Organization

7SK-RNA 7SK small nuclear RNA

LIST OF ARTICLES IN THE THESIS

Thesis in compendium of publications format, composed by three published articles and two manuscripts in preparation.

Objective 1

- Carmen Fernandez-Becerra, Maria Bernabeu, Angélica Castellanos, Bruna R. Correa, Thomas Obadia, Miriam Ramirez, Edmilson Rui, Franziska Hentzschel, Maria López-Montañés, **Alberto Ayllon-Hermida**, Lorena Martin-Jaular, Aleix Elizalde-Torrent, Peter Siba, Ricardo Z. Vêncio, Myriam Arevalo-Herrera, Sócrates Herrera, Pedro L. Alonso, Ivo Mueller, Hernando A. del Portillo. *Plasmodium vivax* spleen-dependent genes encode antigens associated with cytoadhesion and clinical protection. *Proc Natl Acad Sci U S A*. 2020 Jun 9. 117(23):13056-13065.
 - IF: 11.1. Q1 Multidisciplinary Sciences
- Marcelo AM Brito, Bàrbara Baro, Tainá C Raiol, **Alberto Ayllon-Hermida**, Izabella P Safe, Katrien Deroost, Erick F G Figueiredo, Allyson G Costa, Maria del P Armengol, Lauro Sumoy, Anne C G Almeida, Bidossessi W Hounkpe, Erich V De Paula, Càrmen Fernandez-Becerra, Wuelton M Monteiro, Hernando A del Portillo, Marcus V G Lacerda. Morphological and Transcriptional Changes in Human Bone Marrow During Natural *Plasmodium vivax* Malaria Infections. *The Journal of Infectious Diseases*. 2022 Apr 1. Vol. 225 Issue 7 Pages 1274–1283.
 - IF: 8.4. Q1 Infectious Diseases
- **Alberto Ayllon-Hermida**, Marcelo A. M. Brito, Bàrbara Baro, Marcus V. G. Lacerda, Lauro Sumoy, Hernando A. del Portillo, Carmen Fernandez-Becerra. Transcriptional analysis of *Plasmodium vivax* during acute infections in the human bone marrow.
 - Unpublished

Objective 2 & 3:

- **Alberto Ayllon-Hermida**, Marc Nicolau-Fernandez, Ane M. Larrinaga, Iris Aparici-Herraiz, Elisabet Tintó-Font, Oriol Llorà-Battle, Agnes Orban, Maria Fernanda Yasnot, Mariona Graupera, Manel Esteller, Jean Popovici, Alfred Cortes, Hernando A. del Portillo, Carmen Fernandez-Becerra. *Plasmodium vivax* spleen-dependent protein 1 and its role in extracellular vesicles-mediated intrasplenic infections. *Front. Cell. Infect. Microbiol*. 2024 May 17. Vol. 14
 - IF: 5,7 Q1 Infectious Diseases

SUMMARY

Introduction

Plasmodium vivax is the most widespread malaria parasite, with 2.8 billion people at risk across regions from Southeast Asia to the Americas. In 2022 alone, approximately 6.9 million clinical cases were reported worldwide (1). Classically considered less severe than *P. falciparum*, *vivax* malaria can lead to serious complications such as severe anaemia, thrombocytopenia, acute respiratory distress, splenic rupture and even death (2). One of the major challenges with controlling *P. vivax* is its resilience to elimination compared to *P. falciparum*. This difficulty has driven the need for a deeper understanding of the parasite's pathobiology and epidemiology (3,4).

Among the factors contributing to *P. vivax* pathophysiology is the subtelomeric multigenic *vir* family (5). Unlike the clonally expressed *var* genes in *P. falciparum*, *vir* genes from different subfamilies are co-expressed, leading to a broader expression pattern. This broad expression might explain why acquired immunity in *vivax* malaria develops much faster than in *P. falciparum* (6,7).

Research over the past decade has increasingly shown that *P. vivax* uses both the bone marrow (BM) and spleen as key organs in its life cycle. The BM serves for sexual differentiation and parasite growth, as evidenced by the presence of infected reticulocytes in BM aspirates (8–10). Similarly, the spleen harbours significantly higher densities of *P. vivax*-infected red blood cells (RBCs) compared to peripheral blood (11,12). These findings suggest that both the BM and spleen act as cryptic niches for the parasite, contributing to its persistence and the potential for causing anaemia(8,13).

Recently, extracellular vesicles (EVs) have emerged as novel intercellular communicators, not only between parasite populations but also between parasites (14) and their human hosts (15). However, the exact role of EVs in

vivax malaria, in particular in forming these cryptic niches within hematopoietic organs is not fully understood.

Hypothesis and objectives

We hypothesize that during natural *P. vivax* infections, the spleen and BM, reticulocyte-rich tissues, serve as cryptic niches which favour parasite growth and differentiation. Additionally, we postulate that these processes involve specific *P. vivax* proteins whose transcription depend on the BM and spleen and that EVs play a crucial role in facilitating cryptic niche formation.

The main objective is to identify, validate, and functionally characterize *P. vivax* genes that are dependent on the spleen and BM for expression. We aim to clarify the role these genes play during acute vivax malaria and to uncover how EVs contribute to cryptic niche formation.

Methods & key results

This thesis is presented as a compendium of articles, including three published peer-reviewed articles and one manuscript in preparation.

In the first article, we carried out experimental infections in both splenectomized and spleen-intact *Aotus* monkeys. We performed transcriptional analysis on highly purified and synchronized parasite populations to investigate the influence of the spleen on *P. vivax* gene expression. Our results identified 67 coding genes, primarily located in subtelomeric regions, that were spleen-dependent for their expression. These antigens were recognized by naturally acquired immune responses. Additionally, the antigen VIR14 (PVX_108770) was shown to mediate cytoadherence to human spleen fibroblasts (hSFs). We also found that antibodies against PVX_114580 were associated with clinical protection against *P. vivax*.

In the second article, we functional characterize the PVX_114580 protein, named as *P. vivax* Spleen Dependent Protein 1 (PvSDP1). Due to the absence of

in vitro culture for *P. vivax*, we used CRISPR/Cas9 to generate a *P. falciparum* 3D7 transgenic line expressing PvSDP1. Binding assays with this transgenic line to hSFs, previously stimulated with plasma-derived EVs from *P. vivax* patients (PvEVs), revealed a significant increase in the adhesion between 3D7_PvSDP1 parasites and hSFs, which was partially inhibited by antibodies against PvSDP1. Moreover, we confirmed that PvSDP1 is expressed on the surface of infected reticulocytes in *P. vivax* field isolates. Single-cell RNAseq of PvEV-stimulated hSFs revealed upregulation of specific adhesin genes, highlighting the role of EVs in niche formation.

In the third article, we performed global RNAseq analysis of BM aspirates from three patients infected with vivax malaria. We observed downregulation of genes related to RBCs maturation, such as *gata1*, a major transcription factor for erythropoiesis, and enzymes *alas1* and *alas2*, indicating ineffective erythropoiesis during acute vivax malaria.

Finally, in the manuscript in preparation, we used RNAseq data to investigate the *P. vivax* transcriptome within the BM. We found that gametocyte-specific genes were actively transcribed, and comparison with peripheral blood transcriptome (16) revealed a set of 116 genes preferentially expressed in the BM. Among those, we observed an over representation of *vir* genes, accounting for 55 of the preferentially expressed genes. These findings suggest that the BM environment uniquely influences the expression of *vir* genes, potentially contributing to the persistence and cytoadherence of *P. vivax* in this tissue.

Conclusions

This thesis reveals the critical role of the spleen and BM in regulating *P. vivax* gene expression. A total of 67 spleen-dependent genes were identified, many located in subtelomeric regions. The antigen PVX_108770 (VIR14) showed high reactivity with sera from children in Papua New Guinea and was involved in adhesion to spleen fibroblasts. Antibodies against PVX_114580 (PvSDP1) were linked to protection against clinical malaria and PvSDP1 was further characterized using CRISPR/Cas9 and was found to localize to the parasite

membrane in both transgenic lines and natural infections. In the BM, *P. vivax* parasites downregulated erythropoiesis-related genes and preferentially expressed *vir* genes, indicating the BM's role in supporting parasite persistence and cytoadherence. Remarkably, EVs obtained from *P. vivax* patients enhanced the expression of adhesins in hSFs, promoting reticulocyte binding and splenic niche formation. This is the first evidence of the physiological role of EVs in malaria and contributing molecular insights into asymptomatic intrasplenic infections.

RESUM

Introducció

Plasmodium vivax és el paràsit de la malària més estès, amb 2,8 mil milions de persones en risc a regions del sud-est asiàtic fins a les Amèriques. El 2022 es van reportar 6,9 milions de casos clínics globals (1). Encara que tradicionalment es consideri menys greu que *P. falciparum*, la malària per *P. vivax* pot provocar complicacions greus, com anèmia severa, trombocitopènia, dificultat respiratòria aguda, ruptura esplènica i fins i tot la mort (2). Un dels reptes principals per al seu control és la seva major resistència a l'eliminació en comparació amb *P. falciparum*, cosa que subratlla la necessitat de conèixer millor la seva patobiologia i epidemiologia (3,4).

Un factor clau en la fisiopatologia de *P. vivax* és la família multigènica subtelomèrica *vir* (5). A diferència dels gens *var* de *P. falciparum*, els gens *vir* de diverses subfamílies s'expressen simultàniament, donant lloc a una expressió més àmplia. Això podria explicar per què la immunitat adquirida en *P. vivax* es desenvolupa més ràpidament que en *P. falciparum* (6,7).

Estudis recents mostren que *P. vivax* utilitza tant la medul·la òssia (BM) com la melsa com a nínxols clau. La BM serveix per a la diferenciació sexual i creixement del paràsit, com demostra la presència de reticulòcits infectats en aspirats de BM (8–10). La melsa, en canvi, alberga major densitat de glòbuls vermells infectats (11,12) suggerint que ambdós òrgans actuen com nínxols crítics que afavoreixen la persistència del paràsit i l'anèmia (8,13).

Les vesícules extracel·lulars (VEs) han aparegut com a noves comunicadores intercel·lulars, tant entre paràsits com amb l'hoste humà (14,15), però el seu paper en la formació dels nínxols crítics encara no es comprèn del tot.

Hipòtesi i objectius

Hipotetitzem que durant les infeccions naturals per *P. vivax*, la melsa i la BM, teixits rics en reticulòcits, actuen com a nínxols críptics que afavoreixen el creixement i la diferenciació del paràsit. A més, postulem que aquests processos involucren proteïnes específiques de *P. vivax* a la melsa i la BM, i que les VEs tenen un paper crucial en la facilitació de la formació d'aquests nínxols críptics.

L'objectiu principal és identificar, validar i caracteritzar funcionalment els gens de *P. vivax* que depenen de la melsa i la BM per a la seva expressió. Esperem aclarir el paper que tenen aquests gens durant la malària de vivax i descobrir com contribueixen les VEs a la formació dels nínxols críptics.

Mètodes i resultats clau

Aquesta tesi es presenta com un compendi d'articles, que inclou tres articles revisats per parells i un manuscrit en preparació.

En el primer article, vam realitzar infeccions experimentals en micos *Aotus* tant esplenectomitzats com amb melsa intacta. Vam dur a terme una anàlisi de transcriptòmica dels paràsits altament sincronitzats per investigar la influència de la melsa en l'expressió de gens del paràsit. Els resultats van identificar 67 gens codificants, principalment localitzats en regions subtelomèriques, que depenien de la melsa per a la seva transcripció. A més, es va demostrar que l'antigen VIR14 (PVX_108770) mediava l'adhesió cel·lular a fibroblasts esplènics humans (hSFs). També vam trobar que els anticossos contra PVX_114580 estaven associats amb protecció clínica contra *P. vivax*.

En el segon article, vam caracteritzar funcionalment la proteïna PVX_114580, que vam anomenar Proteïna Dependent de la Melsa de *P. vivax* 1 (PvSDP1). Degut a l'absència de cultiu *in vitro* per a *P. vivax*, vam utilitzar CRISPR/Cas9 per generar una línia transgènica de *P. falciparum* 3D7 expressant PvSDP1. Els assaigs d'adhesió d'aquesta línia amb hSFs, prèviament estimulats amb VEs derivades de plasma de pacients amb *P. vivax* (VEsPv), van revelar un augment estadísticament significatiu de l'adhesió entre els paràsits 3D7_PvSDP1 i els

hSFs, que va ser parcialment inhibida pels anticossos contra PvSDP1. A més, vam confirmar que PvSDP1 s'expressa a la superfície dels reticulòcits infectats en aïllats de camp de *P. vivax*. L'anàlisi RNAseq d'una sola cèl·lula dels hSFs estimulats per VEsPv va revelar una sobreexpressió de gens d'adhesines, destacant el paper de les VEs en la formació de nínxols.

En el tercer article, vam dur a terme una anàlisi RNAseq global d'aspirats de BM de tres pacients infectats amb malària de vivax. Vam observar una regulació a la baixa de gens relacionats amb la maduració dels globuls vermells, com *gata1*, un factor de transcripció clau per a l'eritropoesi, i els enzims *alas1* i *alas2*, que indiquen una eritropoesi ineficaç durant la malària de vivax aguda.

Finalment, vam utilitzar les dades de RNAseq per investigar el transcriptoma de *P. vivax* dins de la BM. Vam trobar transcripció activa de gens específics dels gametòcits, i comparant amb el transcriptoma de la sang perifèrica (16) es va revelar un conjunt de 116 gens expressats de manera preferent en la BM. Entre aquests, vam observar una sobrerrepresentació de gens *vir*, amb 55 d'aquests gens expressats preferent a la BM. Aquests descobriments suggereixen que l'entorn de la BM influeix de manera única en l'expressió dels gens, potencialment contribuint a la persistència i l'adhesió cel·lular de *P. vivax* al teixit.

Conclusions

Aquesta tesi revela el paper crític de la melsa i la BM en la regulació de l'expressió dels gens de *P. vivax*. Es van identificar un total de 67 gens dependents de la melsa, molts localitzats a regions subtelomèriques. L'antigen VIR14 va mostrar una alta reactivitat amb sèrum infantils de Papua Nova Guinea i està implicat en l'adhesió a hSFs. Els anticossos contra PvSDP1 es van vincular amb la protecció clínica contra la malària i PvSDP1 es va caracteritzar funcionalment mitjançant CRISPR/Cas9, demostrant la seva localització de membrana. A la BM, els paràsits de *P. vivax* van reduir l'expressió dels gens relacionats amb l'eritropoesi i van mostrar una sobreexpressió de gens *vir*, cosa que indica el paper clau de la BM en la persistència del paràsit. A més, les VEsPv

van augmentar l'expressió de adhesines als hSFs, promovent l'adhesió de reticulocits infectats i la formació del nínxol a la melsa. Aquesta és la primera evidència del rol fisiològic de les VEs en el context de malària, contribuint a aclarir les bases moleculars de les infeccions asimptomàtiques dintre de la melsa.

1.1 Malaria

1.1.1 History of malaria

Human history has probably been deeply influenced by malaria parasites since the dawn of civilization (17). First mentions of a disease with compatible symptomatology to malaria date almost 5000 years ago, in the Nei Ching (the Chinese Canon of Medicine) around 2700 BC. Mesopotamian tablets from 2000 BC (18), Egyptian papyri from around 1500 BC and Hindu texts around the 6th century BC refer to an ancient feverish illness very likely to be human malaria (19). During Ancient Greece, poets, philosophers and physicians like Homer, Empedocles of Agrigento or Hippocrates, as early as 850 BC, were conscious of the characteristic poor health status, malarial fevers and enlarged spleens observed in people living in villages or settings where waterlogged, swampy and marshy areas were located.

Malaria arrived in Europe from the African rain forest, travelling down the Nile to the Mediterranean, then spreading east to the Fertile Crescent, and north to Greece. Greek traders and colonists brought it into the Apennine Peninsula, striking the Roman Empire. Roman soldiers and merchants would ultimately carry the parasite as far north as England and Denmark and all over the Empire (18). Malaria parasites have been detected even in Royal Families from ancient Egypt, and even results using molecular tools suggest that the most probable cause of death for Tutankhamen was an avascular bone necrosis associated with *P. falciparum* malaria (20).

Demographic growth experienced in India and China drove people into semitropical southern zones that favored malaria. Millions of peasants who left the Yellow River for hotter and more humid rice paddies bordering the Yangtze had to face the striking of malaria and other mosquito and water-borne diseases. This phenomenon was happening for centuries causing the lagged development of China's south lands compared to northern regions of the country (18).

Though some scientists speculate that *P. vivax* could have been introduced by the earliest New World immigrants through the Bering Strait, there is no historical evidence of malaria in the Americas until European explorers, conquistadores, and colonizers imported *P. malariae* and *P. vivax* as microscopic cargo (21). Then, *P. falciparum* might have been introduced to the New World by African slaves protected by genetic defences such as the Duffy negativity. By 1750, both *P. vivax* and *P. falciparum* were present from the tropics of South America to the Mississippi valley to New England (18). Significantly, malaria served as the driving force behind the establishment of the United States' foremost public health institution, the Centers for Disease Control and Prevention (22)

1.1.2 The revelation of the malaria pathogen

For millennia, the idea that malarial fevers were caused by miasmas rising from swamps persisted and it is widely believed that the word “malaria” comes from the Italian words “*mala aria*” meaning “bad air”.

Back in 1880, Charles Louis Alphonse Laveran, a French military doctor, started to carefully study malaria disease, which was an enormous problem in the army, investigating the clinical manifestations and anatomic pathology of the ill soldiers. Laveran found that the presence of granules of a black pigment in blood smears was a constant in the malaria cases he investigated, so, when he was looking at the microscope the blood of a soldier, he saw crescent-shaped bodies besides small dots of pigments (18). In the end, he identified four distinct forms of the malaria parasites within human blood, corresponding to different stages of its life cycle: including the female and male gametocyte, schizont, and trophozoite stages (**Figure 1**) (23). This finding earned him the Nobel Prize for the discovery of the single-celled protozoan that caused malaria. Initially, Ettore Marchiafava and Angelo Celli, two eminent Italian malariologists, were not convinced by Laveran's findings. However, Laveran managed to persuade one of the most eminent microbiologists of all time, Louis Pasteur, what in the end, also convinced Marchiafava and Celli.

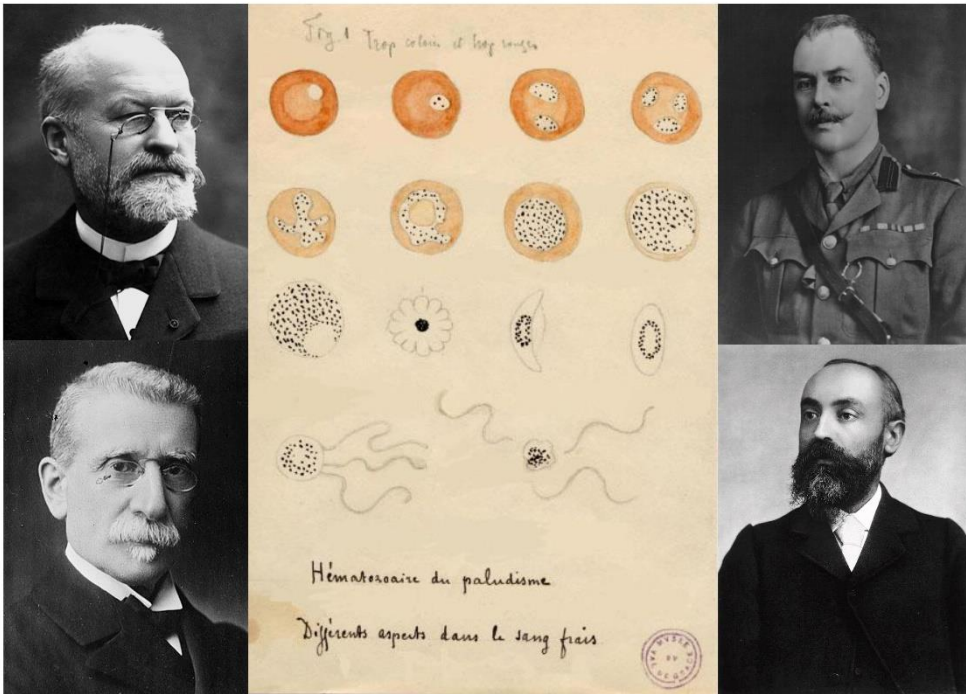


Figure 1. First original drawings from Charles Louis Alphonse Laveran (23) and pictures of the first discoverers of the malaria parasites. Top left: Charles Laveran, top right: Sir Ronald Ross, bottom left: Ettore Marchiafava, bottom right: Angelo Celli.

In the years that followed, Marchiafava and Celli, in collaboration with the renowned Camillo Golgi, described several species of malaria protozoa parasites responsible for benign and malignant tertian fevers (*P. vivax* and *P. falciparum*) and those causing quartan fevers (*P. malariae*) (24,25).

But it was Sir Ronald Ross, an army surgeon of the British-Indian Medical Service, who was the first to complete the *Plasmodium* life cycle, demonstrating that it can be transmitted from an infected patient towards a mosquito bite and then back to an uninfected individual. However, his initial observations were made on avian malaria parasites (26). In 1902, Ross received the Nobel Prize for discovering the mosquito stages of malaria. The credits for confirming the human malaria life cycle in the mosquito belongs to a group of Italian scientists comprising Giovanni Battista Grassi, Amico Bignami and Giovanni Bastianelly. Grassi, an expert entomologist, conducted an experiment involving a healthy volunteer from a malaria-free region who was infected by the bite of an infected

Anopheles claviger mosquito and subsequently developed tertian malaria, thus confirming anopheline mosquitoes as the vector for human malaria (18).

Ultimately, the life cycles of *P. falciparum*, *P. vivax*, and *P. malariae* were described in the human and mosquito host, and proved that only female anopheline mosquitoes could transmit malaria (19).

1.1.3 The global burden of malaria disease

According to the latest World malaria report, over 249 million cases of malaria were estimated in 2022. The World Health Organization (WHO) African Region is the region with the highest burden of the disease, accounting for approximately 94% of all malaria cases (**Figure 2**).

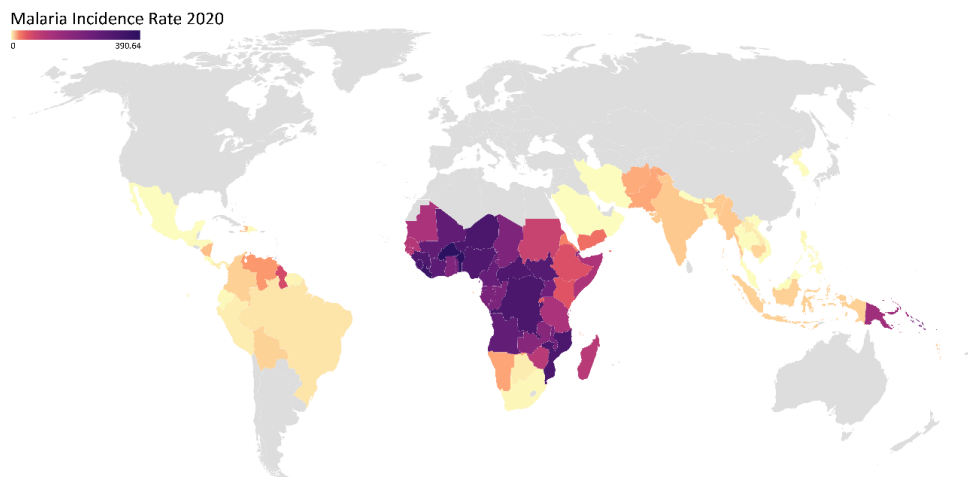


Figure 2. Distribution of malaria incidence in 2020. Figure generated with Datawrapper (27).

The WHO Global Malaria Programme is responsible for coordinating the WHO’s global efforts to control and eliminate malaria. Its work is guided by the “Global technical strategy for malaria 2016-2030” adopted by the WHO Assembly in May 2015 and updated in 2021 (28). The WHO’s main objective is to achieve malaria elimination in 35 countries by 2030 as well as reduce the number of cases and associated mortality by 90% globally (29). Significant progress has been made in combating *P. falciparum*, the deadliest species of malaria, with mortality dropping from 864,000 deaths in 2000 to 586,000 in

2015, further decreasing to 576,000 by 2019. Nevertheless, in 2020, there was a 9.55% rise in malaria fatalities compared to 2019, reaching an estimated 631,000 deaths; with approximately 55,000 additional deaths probably attributed to service disruptions during the COVID-19 pandemic. In 2021 and 2022, the number of deaths reduced again around 3.7% with slightly over 600,000 estimated deaths. Despite this increase, there was a notable decrease in the proportion of malaria deaths occurring in children under 5 years old, declining from 87% in 2000 to 76% in 2022. Altogether, this data indicates that effective control measures are being taken against *P. falciparum* worldwide (1).

In contrast, an increase in the proportion of new *P. vivax* cases have been observed in endemic areas where *P. falciparum* and *P. vivax* coexist (30). Notably, this upsurge extends to countries in sub-Saharan Africa, such as Namibia and Botswana, where the prevalence of the Duffy-negative phenotype was previously thought to have virtually eradicated *P. vivax* infections (3,31). This finding is consistent with observations made by Isaac K. Quaye and the Pan African Vivax and Ovale Network (PAVON), who collected reports of *P. vivax* (and *P. ovale*) infections in over 25 African countries, both in direct surveys at each country but also from travellers/migrant population from those countries (32) (**Figure 3**). To achieve the goal of malaria eradication, a renewed focus on understanding the biology and epidemiology of *P. vivax* is imperative, given its resilience to elimination efforts.

The latest World Malaria Report estimated that 2.8 billion people living in areas at risk of transmission of *P. vivax*, which is responsible for 6.9 million clinical cases in 2022. Despite representing 3% of total worldwide burden of the malaria infection, in countries like India, *P. vivax* accounts for 46% of all cases in the region or in the WHO Region of the Americas where it represents 72% of total malaria cases (1). However, it is important to recognize that the burden of the *P. vivax* parasite is significantly underestimated, as approximately 70 to 90% of infections are completely asymptomatic, with an extremely low number of circulating parasites, rendering current diagnostic methods ineffective for parasite detection (33,34).

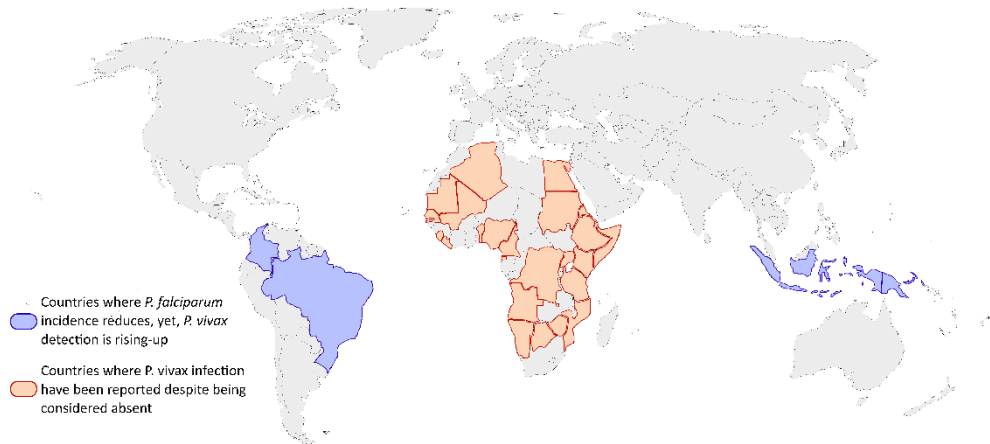


Figure 3. *P. vivax* resilience map. Adapted from (3,32).

Notably, these sub-microscopic and asymptomatic infections can still produce gametocytes, which are potentially infectious to *Anopheles* mosquitoes, thereby facilitating parasite transmission and the spread of infection (35–37).

1.1.4 Pathology in malaria

Plasmodium species, which are protozoan parasites from the Alveolate clade, share a common ancestor to ciliates, dinoflagellates and other apicomplexans (38). To date, *Plasmodium* genus consist of over 200 species, infecting mammals, birds and reptiles, and malaria parasites generally tend to be host-specific, due to a very long adaptation process to the specific host (39). From all species identified, *Plasmodium falciparum*, *Plasmodium vivax*, *Plasmodium malariae*, *Plasmodium ovale* (two subspecies – *P. ovale curtisi* and *P. ovale wallikeri*) and *Plasmodium knowlesi* are the five-known species of the genus that causes malaria in humans (39,40). The first two species, *P. falciparum* and *P. vivax* are the most common species and are responsible for the largest public health burden (41). An overview of the main differences among the five species known to infect human individuals can be found in **Table 1**.

The pathophysiology of uncomplicated malaria is characterised by fever, which is caused by the major rupture of erythrocytes, macrophage ingestion of merozoites, and/or the presence of trophozoites in the bloodstream or spleen loaded with malaria antigens (39). This process triggers the release of tumor

necrosis factor α (TNF- α). The fever associated with malaria is notable for its periodic nature, which varies depending on the species of the parasite. For instance, *P. vivax* and *P. ovale* infections typically cause tertian fever, occurring every 48 hours as their schizonts mature and rupture infected red blood cells (iRBCs). On the other hand, *P. malariae* is linked to quartan fever, with a 72-hour cycle. In the case of *P. falciparum* malaria, fever may occur every 48 hours but often presents with an irregular pattern, lacking a clear periodicity (42).

Table 1. Summary of main differences among *Plasmodium* species causing human infections. Adapted from (39,41,43–46).

Variable	<i>Plasmodium falciparum</i>	<i>Plasmodium vivax</i>	<i>Plasmodium ovale</i>	<i>Plasmodium malariae</i>	<i>Plasmodium knowlesi</i>
Geographical distribution	Worldwide tropical regions	Worldwide tropical regions	Worldwide	Worldwide	Malaysia and neighbouring areas
Infected red cells	All	Young cells	Young cells	Old cells	All
Duration of erythrocytic schizogony (45)	48h but generally irregular	48h (tertian)	48h (tertian)	72h (quartian)	24h (quotidian)
Morphological differences in blood smears (46)	<ul style="list-style-type: none"> • Numerous rings • Smaller rings • Very low or no trophozoites or schizonts • Crescent-shaped gametocytes 	<ul style="list-style-type: none"> • Enlarged erythrocytes • Schüffner's dots • "Ameboid" trophozoites • All stages present in PB 	<ul style="list-style-type: none"> • Similar to <i>P. vivax</i> • Compact trophozoite • Fewer merozoites in schizont • Elongated erythrocyte 	<ul style="list-style-type: none"> • Compact parasite • Trophozoites tend to have a band shape • Merozoites in rosette • All stages present in PB 	<ul style="list-style-type: none"> • Trophozoites, pigment spreads inside cytoplasm • Multiple invasion & high parasitaemia, like <i>P. falciparum</i> • All stages present in PB
Onset of gametocyte production	Gametocytes appear ≈10 th day following the first day of fever (44).	Continuous, from early rounds of asexual cycle, as early as the 6 th day (44).	Continuous from early rounds of asexual cycle, appearing even a little earlier than <i>P. vivax</i> (44).	Probably from early rounds of asexual cycle, after a prepatent period (16-59 days). Gametocytes emerges with asexual parasites (47).	Unknown (gametocytes identified in some of the naturally infected malaria patients) (48).
Recurrence relapse	Unknown (hypnozoites not observed yet)	Well documented, with latency periods from <2 weeks to >1 year and varies systematically by geographic region. Hypnozoites in liver are the main source of recurrence (49–51).	Clinical cases reported (52). Hypnozoites not observed yet and molecular evidence for a causal relationship between dormant liver stages and subsequent relapses unavailable (53,54).	Unknown (hypnozoites not observed yet)	Unknown (hypnozoites not observed yet)
Recrudescence	Known to occur (latent period usually < 2 months, but can be > 2 years (52).	Unknown	Unknown	Known to occur (latent period can be > 40 years (55).	Unknown

1.1.5 *P. falciparum*, the deadliest parasite

One of the key features during severe malaria of *P. falciparum* is the cytoadhesive properties of mature trophozoites and schizonts to different host cells, from endothelial cells (56), uninfected erythrocytes in a phenomenon known as rosetting (57), clumping and bridging to other iRBC through platelets (58,59) or to placental cells (60,61). The accumulation of parasites in organs such as the brain, lungs, or placenta can result in blood flow obstruction, hypoxia, and tissue damage, potentially leading to organ failure and fatal malaria (62). Cytoadhesion is widely recognized as the mechanism by which the parasite evades splenic clearance. This is supported by observations in splenectomised patients infected with *P. falciparum*, who exhibit reduced parasite sequestration in tissues, leading to the presence of mature parasite stages in the peripheral blood circulation (63,64).

For example, the binding of PfEMP1 on infected RBCs to intercellular adhesion molecule-1 (ICAM-1) and cluster of differentiation 36 (CD36) on brain endothelial cells facilitates sequestration, contributing to the development of cerebral malaria (65,66). Additionally, parasite-derived toxins play a critical role in the pathogenesis of severe malaria (67). Glycosylphosphatidylinositol (GPI), a glycolipid that can exist in both protein-bound and free forms, triggers macrophages to overproduce cytokines such as TNF- α and interleukin-1 (IL-1) (68). While cytokines are essential for the immune response against pathogens like the malaria parasite (69), excessive production leads to high-grade fever, increased expression of endothelial receptors, and elevated nitric oxide production. These effects can cause local tissue damage and suppress erythrocyte production in the bone marrow (70).

1.1.6 No longer benign: The *P. vivax* malaria disease

Vivax malaria is a complex illness characterized by chills, vomiting, malaise, headache, fever and myalgia. However, these symptoms may resemble those of other diseases or different types of malaria. In vivax malaria, higher fevers are

often observed more frequently than in falciparum malaria, correlating with the moment of the schizont rupture. For many years, *P. vivax* was considered “benign” compared to the more severe clinical complications caused by *P. falciparum*. However, this perception has changed dramatically in recent years, as reports of severe disease, including death, have been attributed to *P. vivax*. Indeed, vivax malaria can become a chronic condition that may persist for years if left untreated (2,71–73).

Early investigations into vivax malaria in non-endemic regions were based on studies of experimentally induced cases and observations of returned US military personnel. A case series from the 1940s involving 195 non-immune adult prison volunteers deliberately infected with the Chesson strain of *P. vivax* (74), reported that, aside from fever, prevalent symptoms included headache, decreased appetite, nausea, muscle pain, abdominal discomfort, eye pain, chest pain, cough, weakness, and dizziness (74). Additionally, common clinical findings included vomiting, splenomegaly, nosebleeds (epistaxis), urticaria, diarrhoea, swelling (edema without specification), jaundice, and hepatomegaly. Within the first 7 days of illness, there was an average decrease in haemoglobin (Hb) levels of 2.9 g/dL. Over a 15-day period, five participants experienced a mean Hb drop of 6.4 g/dL (74,75).

When examining the more severe consequences of vivax malaria, splenic rupture has been identified as one of the most serious clinical manifestations. Although rare, it has led to fatal outcomes in numerous cases (76). In addition to splenic rupture, severe anaemia (13), respiratory distress, malnutrition (77) and possibly coma (71,78,79) have been also reported to be caused by *P. vivax* (73).

In endemic regions, young children and pregnant women are particularly vulnerable to the adverse clinical impacts of infection with *P. vivax*. Although vivax malaria during pregnancy has been less studied and reported compared to *P. falciparum*, evidence suggests that *P. vivax* does not sequester in the placenta (80,81). However, *P. vivax* can still have detrimental effects on the fetus by

inducing maternal anemia, triggering a robust local inflammatory reaction, and causing a significant reduction in mean birth weight (82,83).

Because *P. vivax* has historically been perceived as a “benign” disease, it has attracted less focus from researchers, policymakers, and funding agencies. As a result, there is a pressing need to refocus efforts on this disease to prevent underreporting, especially since severe symptoms may be mistakenly attributed to co-infection with *P. falciparum* or misdiagnosed entirely. Establishing a clear and accurate differential diagnosis between *P. falciparum* and *P. vivax* using more sensitive and specific techniques than RDTs and microscopy is crucial for the appropriate detection and treatment of vivax malaria infections. This is particularly critical in regions where both types of malaria coexist, as mixed infections are often overlooked by microscopy personnel.

1.1.7 Molecular basis of malaria pathology

Current research into the mechanisms underlying *P. falciparum* pathogenesis has uncovered novel insights that are being used for control strategies for the disease, such as vaccine development (84). However, our understanding of the molecular basis of *P. vivax* pathology remains significantly less developed compared to what is known about *P. falciparum*. The distinct biological differences between these two species highlight the need for increased research efforts to bridge the knowledge gaps surrounding *P. vivax* pathobiology.

1.1.7.1 *P. falciparum*: the var multigenic family

As mentioned above, cytoadherence is a key feature in *P. falciparum* malaria, strongly linked with disease severity and fatality rate. Host molecules such as CD36 (85), ICAM-1 (86), thrombospondin (TSP), P-selectin, chondroitin sulphate A (CSA), and protein C receptor have been identified as receptors that bind iRBCs to the endothelium (87).

The main cytoadhering ligand from *P. falciparum* is the erythrocyte membrane protein 1 (PfEMP1) (66,88). PfEMP1 proteins are part of the subtelomeric multigene family named *var* genes (89–91), composed by 60 different genes in

the genome of the 3D7 strain (92). Interestingly, *P. falciparum* expresses a single *var* gene during schizont stage within an iRBC at a time, maintaining all other members of the family in a transcriptionally silent state, being able to switch the expressed *var* gene under specific situations in a process known as antigenic variation (**Figure 4**) (93,94). This antigenic variation enables the parasite to escape the host immune system that is finally developed slowly and after many exposures, humans might not be refractory to malaria parasites (62). In Figure 4, a graphical representation of PfEMP1 capabilities are represented.

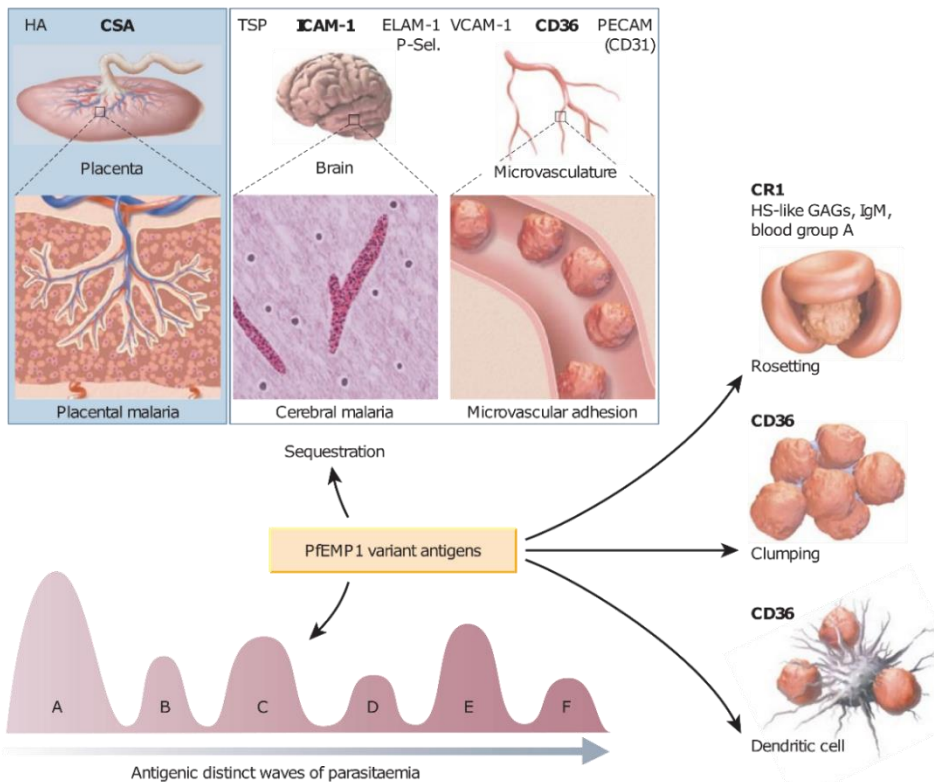


Figure 4. PfEMP1 variant antigens capabilities of binding to different tissues and cells through different receptors. The different properties of PfEMP1 – sequestration for evading spleen-dependent killing and antigenic variation for evading antibody-dependent killing – contribute to the virulence and pathogenesis of *P. falciparum* and are essential for survival of the parasite. HA, hyaluronic acid; TSP, thrombospondin; ELAM-1, endothelial/leukocyte adhesion molecule 1; P-Sel., P-selectin; VCAM-1, vascular cell adhesion molecule 1; PECAM (CD31), platelet endothelial cell adhesion molecule 1; CR1, complement receptor 1; HS-like GAGs, heparin sulphate-like glycosaminoglycans; IgM, immunoglobulin M. Reproduced from (62).

Besides *var* genes, *P. falciparum* subtelomeric domains contain another hypervariable multigenic families, such as the repetitive interspersed family (*rif*) or the subtelomeric variant open reading frame (*stevor*). Recent results have suggested that the RIFIN and STEVOR proteins, together with PfEMP1, are also important for the sequestration of iRBCs and the pathogenesis of severe malaria (95–97).

1.1.7.2 *P. vivax* multigene families

Back in 2001, our group reported the existence of *P. vivax* variant genes, the *vir* family, through the construction and sequencing of a yeast artificial chromosome library containing a clone representing the subtelomeric region of a *P. vivax* chromosome (5,98). The *vir* family was composed of 31 *vir* genes grouped into 6 different subfamilies, termed A to F (**Figure 5**). *Vir* genes share a similar structure among them, consisting in a 3 exons structure; the first one is very short, the second one contains transmembrane domain and a third exon of uniform length. The variant nature and subtelomeric localization of *vir* genes initially suggested their primary role in antigenic variation. This hypothesis was further supported by their subcellular localization at the reticulocyte membrane and their immunogenicity during natural infections (5). However, early studies on expression patterns during natural infections indicated that *vir* genes are not clonally expressed like the *var* genes from *P. falciparum* (6). Single-cell RT-PCR analysis demonstrated that at least two distinct subfamilies of *vir* genes are transcribed simultaneously, and immunofluorescence assays (IFA) confirmed the co-expression of proteins from different subfamilies within the same parasite (6,99).

After these initial observations the landmark paper describing the complete genome sequence of the *P. vivax* Salvador-I strain revealed the presence of 346 *vir* genes divided in 12 subfamilies (A-L) (100). Remarkably, over 1200 *vir* genes including 27 subfamilies were more recently identified from a new reference strain (PvO1), together with draft assemblies of isolates from China (PvCO1) and Thailand (PvTO1) (101).

Interestingly, the trait that *vir* genes do not undergo allelic exclusive expression, results in a vast repertoire of *vir* genes abundantly expressed in isolates at any given time. There was no significant difference in the recognition of VIR proteins by immune sera from first-infected and multiple-infected patients, suggesting that VIR proteins play a major role in natural *P. vivax* infections. However, the data do not fully support a role for antigenic variation and the development of long-term immunity through variant-specific antibodies against VIR proteins, and further studies are needed to clarify the function of *vir* genes, particularly in relation to *P. vivax*'s invasion of reticulocytes and its passage through the spleen (6).

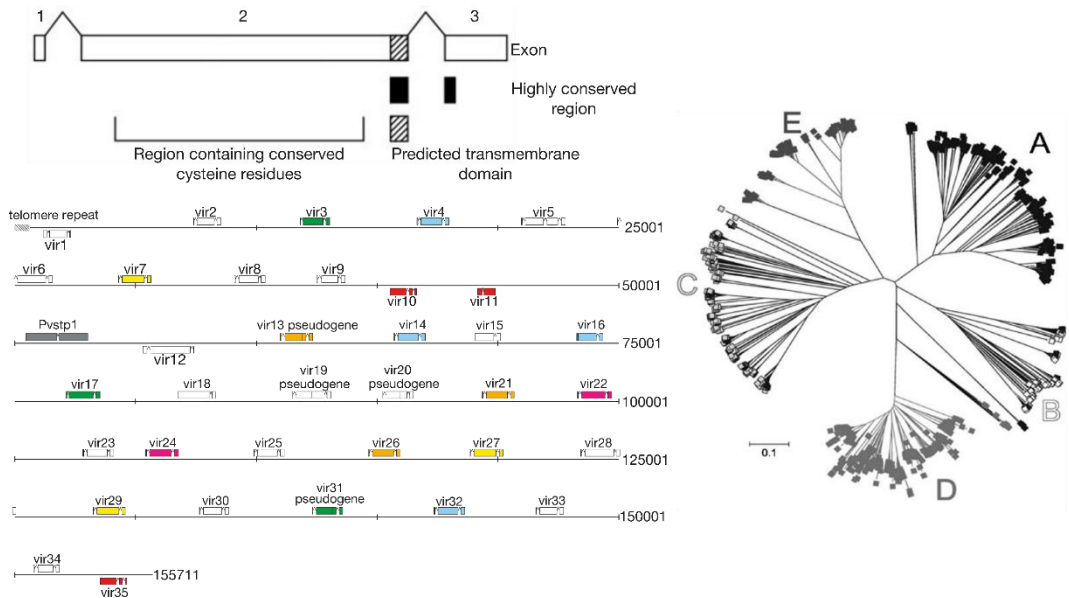


Figure 5. *Vir* multigenic family. Schematic representation of the classical three exon structure of the *vir* genes. Order and orientation of predicted genes and pseudogenes, with coloured subfamilies based on the degree of homology (5). Consensus tree of aminoacidic sequences of VIR proteins subfamilies (A-E) from *P. vivax* (102).

Besides *vir* genes, eight multigene subfamilies were identified in subtelomeric regions in Sal-I reference genome (103). These multigene families were termed from *pv-fam-A* to *pv-fam-E*, and *pv-fam-G* to *pv-fam-I*. Of notable interest are two gene families: first, the PvTRAG (Pv-fam-a) family, composed of 36 genes, one of which gene encodes a protein localized to the caveola-vesicle complex in infected erythrocytes and has been shown to trigger a humoral immune response during natural infections (104).

Altogether, efforts in recent years to elucidate the role of VIR proteins during vivax malaria (6,99,105–107), have identified some functions mediated by this superfamily of genes, such as cytoadherence -particularly to splenic cells – and their involvement in generating an immune response. However, further research is needed to characterize the members of the *vir* superfamily to fully understand the range of functions this multigenic family may play in vivax malaria.

1.1.8 Control measures

1.1.8.1 Diagnosis of vivax malaria

Diagnosing malaria requires examining a Giemsa-stained blood smear under a microscope or using a rapid diagnostic test (RDT), which is an immunochromatographic assay containing a monoclonal antibody against *Plasmodium* antigens. These tools are indispensable because relying solely on clinical signs and symptoms cannot differentiate it from other febrile illnesses, and even less distinguish between *P. falciparum* or other plasmodia versus *P. vivax* infection (1). While microscopy offers greater sensitivity, specificity, detailed parasite count and stage detection than RDT, the availability of microscopy services in healthcare centres within endemic regions may not always be enough (108). Additionally, microscopy examinations require excellent training to effectively distinguish between parasite stages and different plasmodia species. A negative diagnosis is reached after examining at least 200 fields of a thick blood smear without detecting any parasite form. The detection limit for expert microscopists is typically established around 10–20 parasites per microliter of blood (109,110). In areas where the quality of microscopy services cannot be assured, the WHO recommend the use of RDT (111).

RDTs are widely available commercial products, produced by various manufacturers. The sensitivity and specificity of RDTs can vary depending on the commercial provider and the species they are designed to diagnose. In general, *P. falciparum* is detected more reliably than *P. vivax* (112). The

detection of malaria through RDT is based on identifying a pan-genus antigen, lactate dehydrogenase (pLDH), in combination with *P. falciparum* histidine-rich protein 2 (pHRP2). A positive result for both antigens indicates the presence of *P. falciparum* alone or in combination with another species, while positivity for pLDH and negativity for the pHRP2 suggests an infection by a *Plasmodium* species distinct from *P. falciparum*. Specific RDTs designed for the detection of *P. vivax* are based on the aldolase antigen detection, but these tests are generally less sensitive and specific, making them more suitable for diagnosing acute vivax malaria (113). It is important to note that HRP2 can remain detectable in the blood for up to 28 days after the initiation of antimalarial therapy (114). Due to this "persistent antigenemia", these tests are not reliable for assessing parasite clearance post-treatment, and may result in false positives in patients recently treated for malaria. In contrast, pLDH is cleared from the bloodstream rapidly following parasite death, often even faster than the dead parasites themselves (111).

In the context of malaria elimination, particularly with a focus on *P. vivax*, detecting low-level parasitaemia using molecular techniques is of crucial importance. The most widely applied and validated molecular diagnostic test is nested PCR amplification of the ribosomal 18S RNA subunit (115). The detection limit for PCR can be as low as 0.004 parasites per μl (116), making it significantly more sensitive at low levels of parasitaemia and less prone to observer error compared to microscopy. However, the widespread use of PCR is limited by logistical challenges, the need for specially trained technicians, access to well-equipped laboratories, which are often available in low-income countries and other resource-poor endemic regions where *P. vivax* is prevalent.

To conclude, the diagnosis of *P. vivax* primarily relies on RDTs and microscopy, which are considered adequate tools for case management. However, to accelerate malaria eradication efforts, more sensitive and easily deployable field methods are needed to detect and treat sub-microscopic *P. vivax* infections.

1.1.8.2 Treatment, control and prevention of *P. vivax* malaria

Effective treatment for malaria is a key component in the fight against the disease. Malaria treatment varies depending on factors such as the parasite species, the epidemiology of the affected region, and the clinical symptoms. For *P. falciparum* infections, the recommended first-line treatment is artemisinin-based combination therapy (ACT), which includes a combination of an artemisinin derivative and a quinine derivative. Common ACT regimens include artemether-lumefantrine (AL) and artesunate-amodiaquine (AS-AQ), artesunate-pyronaridine (AS-PY), artesunate-mefloquine (AS-MQ) and dihydroartemisinin-piperaquine (DHA-PPQ) (108,117).

P. vivax, due to the dormant hypnozoite stages, needs a different drug regimen to effectively combat the infection. The combination of chloroquine and primaquine was traditionally the preferred treatment for vivax malaria. However, the emergence of chloroquine-resistant parasites has led to a shift in treatment strategy towards using of chloroquine plus DHA-PPQ combined with primaquine. Primaquine and tafenoquine are the two drugs that target the hypnozoite stage in the liver, but unfortunately, they can cause mild to severe acute haemolytic anaemia in patients with glucose-6-phosphate dehydrogenase (G6PD) deficiency (118). Therefore, diagnosing G6PD deficiency in patients with vivax malaria is crucial for effective treatment and *P. vivax* management. Regrettably, the majority of vivax malaria cases are treated outside hospital settings, often at home or in non-clinical environments. Moreover, even among hospitalized patients, the lack of available technology and tools for G6PD deficiency diagnosis frequently results in the unintended administration of primaquine to G6PD-deficient patients, leading to haemolytic anaemia and, in severe cases, death (119).

Global malaria control and elimination heavily rely on insecticidal measures, primarily through vector control strategies such as insecticide-treated mosquito nets (ITNs) and indoor residual spraying (IRS) (120). ITNs combine pyrethroids with the physical barrier of the net, while IRS uses organophosphate and neonicotinoid insecticides to treat surfaces where mosquitoes rest during blood

meal periods. Despite these efforts, resistance has emerged against key insecticide classes, including pyrethroids, organophosphates, carbamates, and organochlorines. From 2010 to 2020, 88 countries reported insecticide resistance, with 78 confirming resistance to at least one insecticide in at least one malaria vector species (**Figure 6**)(1). Thus, there is an urgent need to develop new insecticides and interventions to maintain effective vector control (120).

Apart from drugs, insecticides, and ITNs, vaccines are the most cost-effective tools for controlling malaria. In 2021, WHO recommended the RTS,S vaccine to prevent malaria among children living in regions with moderate to high transmission rates of *P. falciparum* malaria. To date, more than 2 million children have received at least one dose of the vaccine through the WHO-coordinated Malaria Vaccine Implementation Programme in Ghana, Kenya and Malawi (1). In October 2023, WHO also recommended a second safe and effective malaria vaccine, R21 (121,122).

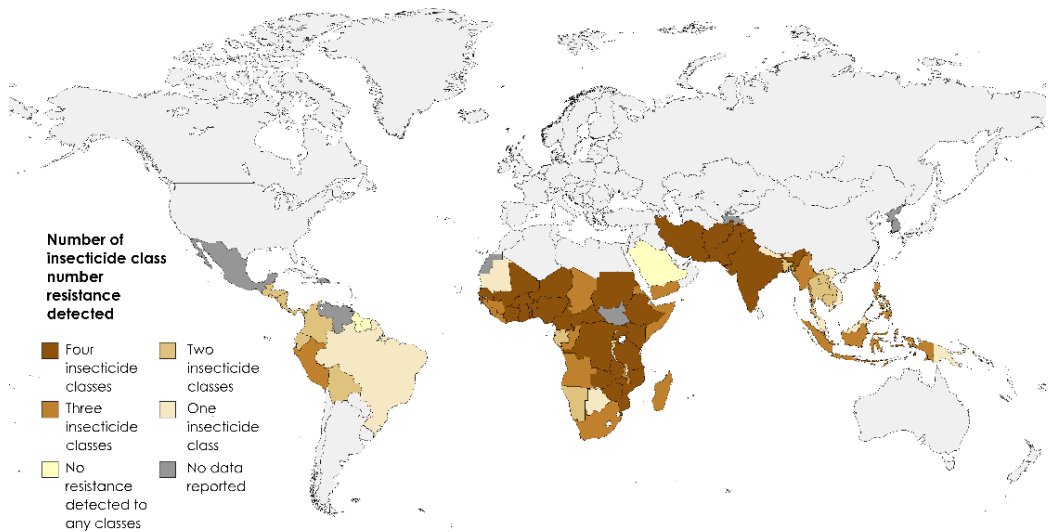


Figure 6. Number of insecticides to which resistance was confirmed in at least one malaria vector in at least one monitoring site, 2010-2020. Adapted from (1).

Unfortunately, the RTS,S and R21 vaccines do not cross-protect against *P. vivax*. Therefore, there is an urgent need to discover new antigens and novel vaccine approaches against this neglected human malaria parasite. The vaccine development scenario for *P. vivax* is meagre. Currently, there are some

candidate vaccines targeting distinct antigens in early clinical phases, which confer only partial protection, and even fewer are in preclinical trials (123,124).

Plasmodium vivax malaria vaccine candidate targets the circumsporozoite protein (PvCSP) are well advanced. Various vaccine formulations, such as VMPO01 (125,126), CSV-S (127), and Rv21 (128), have shown promise in inducing immune responses in preclinical and clinical studies, but challenges remain in achieving sterile protection. Ongoing studies aim to optimize vaccine efficacy, improve immune responses, and assess protection in diverse populations. On the other hand, Pvs25 plays a crucial role in the survival and transformation of *Plasmodium vivax* ookinetes within the mosquito, making it a key target for transmission-blocking vaccines. Various studies have explored its potential as a vaccine candidate, and despite having good results in first stages of development (129–131), those candidates which reached phase I clinical trials in humans showed either moderate reduction of transmissibility in membrane feeding assays of mosquitoes (132) but more worryingly, some have shown a strong reactogenicity, including adverse events including erythema nodosum, forcing to stop further research (133). Additionally, a vaccine using irradiated sporozoites is in phase 1/2a of the clinical trial (**Table 2**) (134,135).

The Duffy Binding protein (PvDBP), a critical protein for reticulocyte invasion, have been also targeted as vaccine candidate. Antibodies targeting PvDBP, especially PvDBP-II, have shown efficacy in blocking invasion and reducing infection (136,137). Vaccines based on PvDBP-II have demonstrated strong immunogenic responses and protection in preclinical studies (137–142). Additionally, viral vector-based vaccines encoding PvDBP-II have shown promising immunogenicity and strain-transcending antibody responses in early clinical trials (142–146).

It is evident that there is a significant gap between *P. falciparum* and *P. vivax* vaccine development and research. Therefore, it is crucial to maintain efforts and funding to advance vaccine development against *P. vivax*.

Table 2. *Plasmodium vivax* vaccines in clinical trials. Reproduced from (153).

Candidate	Phase	Key Findings	Clinical Trial Number	References
Preerythrocytic stage vaccines				
VMP001	1/2a	Recombinant PvCSP with adjuvant AS01B. Reduction of parasitaemia, but low efficacy.	NCT01157897	(147)
Peptides N R&C	1b/2	PvCSP derived from long synthetic peptides (LSP) with Montanide ISA 720 and 51. Long-lasting antibody response, with 36.6% efficacy in naïve volunteers	NCT0108184	(148,149)
PvRAS	1/2a	<i>P. vivax</i> irradiated sporozoite. Poor cellular response and 42% efficacy	NCT01082341	(150)
Blood-stage vaccines				
ChAd63-MVA-PvDBPII	1a/2a	Heterologous <i>prime-boost</i> regimen with recombinant viral vectors ChAd63-MVA-PvDBPII. Induction of antibodies that inhibit interaction with reticulocytes, humoral and cellular response, 50% of strain-transcendent immunity.	NCT01816113	(151)
PvDSPII-GLA-SE	1	Recombinant PvDBPII with GLA-SE adjuvant. High production of specific antibodies can inhibit interaction with reticulocytes and strain-transcendent response.	CTRI/2016/09/007289	(142)
Transmission-blocking vaccines				
Pvs25	1	Recombinant Pvs25 with Montanide ISA 51 adjuvants. Good induction of antibodies and 30% reduction in infected mosquitoes. High reactivity	NCT00295581	(152)

1.1.9 *P. vivax* parasite biology

Malaria continues to exert a significant toll on both human health and economy, remaining one of the most incapacitating and potentially lethal infectious diseases. As previously mentioned, the disease is caused by protozoan parasites of the phylum Apicomplexa from the genus *Plasmodium* (17). Apicomplexa stands out as the only extensive taxonomic group comprised entirely of parasitic organisms, specifically obligate intracellular parasites. These organisms are characterized by the presence of an evolutionarily distinct apical complex, which is crucial for host invasion (154).

The Apicomplexa phylum comprises four distinct groups: the coccidians, the gregarines, the haemosporidians and the piroplasmids. These groups are categorized based on their phenotypic traits, including their host and/or vector preferences and the tissues they invade. While over 120 *Plasmodium* species infect mammals, birds, and reptiles, only five species can infect humans: *Plasmodium falciparum*, *Plasmodium vivax*, *Plasmodium ovale*, *Plasmodium malariae*, and *Plasmodium knowlesi* (17,155).

Compared to *P. falciparum*, *P. vivax* is not only found in tropical areas but is also widespread in temperate regions. These species can survive in climatically unfavoured areas and stay in dormant stages in the liver of its human host for several years. In addition to the hypnozoite stage, there are other unique features of *P. vivax* biology that strongly support the view that *P. vivax* will be the last human malaria parasite to be eliminated.

1.1.9.1 Life cycle of *P. vivax*

The human malaria life cycle involves different phases of the parasite within various cells and tissues across both human and mosquito hosts. It begins when an infected female *Anopheles* mosquito bites a human, initiating the infection process. Of approximately 515 *Anopheles* species, only 30–40 are considered significant malaria vectors. In a given geographical area, multiple species may coexist, each one exhibiting unique biting and resting behaviours, along with

varying preferences for human or animal hosts. Consequently, transmission efficiency and susceptibility to anti-mosquito measures can differ significantly among species (29).

Initially, most of the injected sporozoites migrate through the skin cells, infiltrate skin capillaries, and eventually reaching the liver via the bloodstream. Upon arrival in the liver, the parasites penetrate the sinusoidal endothelium and each settle within a single hepatocyte (4). This invasion is mediated by the circumsporozoite protein (CSP), the most abundant surface protein of the sporozoite stage. Cleavage of the CSP by a parasite protease exposes an adhesive domain at its carboxy-terminus, which facilitates hepatocyte invasion (156). Following hepatocyte infection, the parasitophorous vacuole membrane forms triggering parasite schizogony. In most *Plasmodium* species, parasites rapidly multiply as liver schizonts, eventually giving rise to exo-erythrocytic merozoites. These merozoites are released in clusters, known as merozoites, into the bloodstream, typically within approximately 10 days (157).

An important characteristic of the *P. vivax* life cycle is its ability to form dormant liver stages known as hypnozoites. These hypnozoites can reactivate weeks, months, or even years later, leading to the development of blood stages and the onset of typical symptoms of vivax malaria, which results in relapses (50,158). Relapses can sustain transmission as sexual gametocytes may also be produced. The biological factors that trigger the switch between dormant and active stages remain unknown. Although the role of stress in bird malaria have been observed to be playing a role, the exact mechanism by which hypnozoites initiate relapses remains unclear (159,160).

Once *P. vivax* merozoites enter the bloodstream, they preferentially invade reticulocytes (if not exclusively), which are immature red blood cells, and initiate intra-erythrocytic replication, starting the asexual stage of the life cycle (4,161). Reticulocytes comprise about 1 to 2% of total circulating cells in peripheral blood. The evolutionary reason for *P. vivax*'s preference for this cell type remains unclear, but it has been hypothesized that avoiding high

parasitaemia might be a contributing factor (162). This preference complicates the continuous *in vitro* culture for *P. vivax*.

Invasion by *P. vivax* occurs through the interaction of specific merozoite proteins with host cell receptors, facilitating entry into the cell (163). The Duffy receptor on red blood cells is crucial for *P. vivax* reticulocyte invasion, mediated by the ligand Duffy Binding Protein (PvDBP) (164). Additionally, the transferrin receptor, known as CD71, has been identified as a key molecular receptor for *P. vivax* targeting of reticulocytes (165,166). CD98, a protein expressed on the surface of immature reticulocytes, also interacts with *P. vivax* reticulocyte-binding protein 2a (PvRBP2a) on the merozoite surface. Therefore, CD98, alongside CD71, is proposed as a host membrane protein directly associated with *P. vivax* reticulocyte tropism (167).

Once inside the reticulocyte, the merozoite begins the asexual cycle, which takes approximately 48 hours. After invasion, the first stage observable is the “ring stage”, during which parasite proteins are exported into the host cell. The parasite then develops into the “trophozoite stage”, characterized by rapid biomass growth and hemoglobin digestion, which is converted into hemozoin within the parasite's food vacuole. Finally, the parasite progresses to the “schizont stage”, where it undergoes schizogony, producing multiple daughter merozoites. Upon rupture of the infected reticulocyte, these merozoites are released and invade new RBCs (4).

Throughout blood stage infection, some parasites develop into sexual forms, appearing in peripheral blood circulation earlier than those of *P. falciparum*. This process, known as gametogenesis, occurs within the human host. These sexual stages can be detected before or at the onset of clinical symptoms, which provides an advantage for infection transmission. As a result, sexual parasites may be transmitted to *Anopheles* mosquitoes during a blood meal before infected individuals exhibit clinical symptoms (4,168,169).

Gametocytes are ingested by *Anopheles* mosquitoes during blood meal, initiating the sexual phase of *P. vivax* life cycle. *Anopheline* mosquitos have

adapted to outdoor and daytime biting behaviors, which reduces the efficacy of control measures relying solely on ITNs. In the mosquito midgut, fertilization occurs between male and female gametes, forming an ookinete that traverses the mosquito midgut, and encysts in the epithelial layer, forming an oocyst. Eventually, the oocyst releases newly formed sporozoites that migrate to the mosquito salivary glands, thus restarting the life cycle of the parasite (4). The full life cycle is depicted in **Figure 7**.

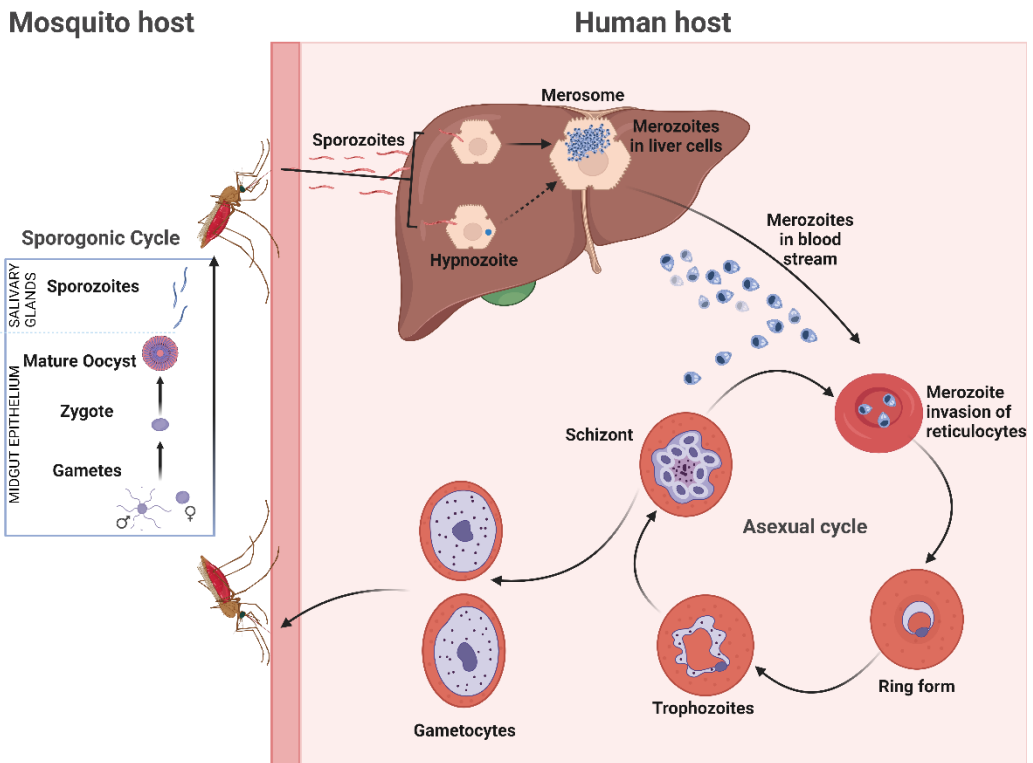


Figure 7. Classical life cycle of *Plasmodium vivax*. Adapted from (4). Figure generated with BioRender.com.

1.1.10 Cryptic niches

For over the decades, hypnozoites have been considered the dormant form of the parasite responsible for relapses as well as for asymptomatic infections (51,158,170). However, beyond hypnozoites, asymptomatic infections of *P. vivax* present a significant challenge towards malaria elimination efforts (9,33). An analysis of sub-microscopic infections identified in 31 cross-sectional surveys across 12 countries found that, on average, 69.5% of all *P. vivax* blood-

stage infections were sub-microscopic. In a subset of these surveys, 89–100% of these sub-microscopic infections were asymptomatic (33). Consequently, in many regions, the prevailing form of *P. vivax* infection is both sub-microscopic and asymptomatic. Due to their asymptomatic nature, these infections are less likely to be treated. Combined with the latent reservoir of hepatic hypnozoites, these infections persist longer within a population, thereby perpetuating parasite transmission (171,172) and representing a major impediment to the elimination of *P. vivax*.

Recent findings have also revealed hidden erythrocytic reservoirs beyond the liver, notably with *P. vivax* establishing cryptic erythrocytic infections in the bone marrow and spleen. These sites serve as significant sources of asymptomatic infections, and parasites residing in these niches appear to evade the human immune system and remain inaccessible to antimalarial drugs (173). Therefore, there is a critical need to intensify research efforts in this area.

1.1.10.1 The presence of *P. vivax* in the bone marrow

The bone marrow (BM) is the principal hematopoietic organ and the major source of newly generated cells in adults. Despite comprising less than 5% of the total body mass, it produces approximately 200 billion red blood cells, 10 billion white blood cells and 400 billion platelets per day (174). Erythropoiesis refers to the expansion and differentiation of hematopoietic stem cells into mature erythrocytes, a process that initially occurs within erythroblastic islands (EBIs). These islands consist of specialized macrophages that interact with developing erythroid cells. Within EBIs, chromatin condenses, most organelles and the nucleus are eliminated, and the cell membrane and cytoskeleton undergo remodelling. Additionally, haemoglobin synthesis occurs during erythroid cell development. Disruptions to these processes can lead to pathophysiological conditions such as anaemia (175,176).

The first descriptions of the parasite in the BM were made using autopsy material by Ettore Marchiafava and Amico Bignami (25). Subsequent studies confirmed the presence of *P. falciparum* in the BM of malaria patients (177,178).

More recent quantitative evidences demonstrated that the human BM is a major place for parasite growth and sexual differentiation. Young gametocytes have been found in reticulocytes associated with EBIs in the BM (11). Molecular studies of BM from children in Mozambique have also observed the accumulation of immature gametocytes in the tissue compared to peripheral blood (179). Specifically, it has been shown that *P. falciparum* can impede the enucleation of primary erythroblasts, allowing the parasite to complete gametocytogenesis within these cells before reaching the circulating blood, where it is transmitted to the *Anopheles* mosquito to complete the life cycle (180).

Initial examinations of sternal BM aspirates from patients with *P. vivax* confirmed the presence of the parasites within the organ. Although this finding was recognized in the late 19th century, relatively few studies have examined BM changes during *P. vivax* infections compared to *P. falciparum*. In 1989, a study reported that among 9 Thai adults infected with *P. vivax*, who were suffering from dyserythropoiesis and ineffective erythropoiesis and none of them had detectable parasites in the BM (181). These findings have raised skepticism about the initial observations of *P. vivax* parasites in the human BM. However, more recent studies have reported the presence of *P. vivax* following both autologous and heterologous bone marrow transplantation (182,183).

In 2017, our group provided the first unequivocal demonstration that *P. vivax*-infected reticulocytes were present in the BM aspirate of an infected individual with unusual high parasitaemia. Microscopic analysis of the BM aspirate revealed all parasite stages in higher proportions than in peripheral blood, with the exception of young trophozoites. Additionally, morphological signs of ineffective erythropoiesis and dyserythropoiesis were observed, which were confirmed by transcriptional changes in miRNAs and small RNA profiles during the acute phase of malaria infection (**Figure 8**) (10).

This finding was later demonstrated using experimental infection of non-human primates (NHP) with *P. vivax*, where the presence of the parasite in the BM parenchyma was observed in 13 *Aotus* and *Saimiri* monkeys (12).

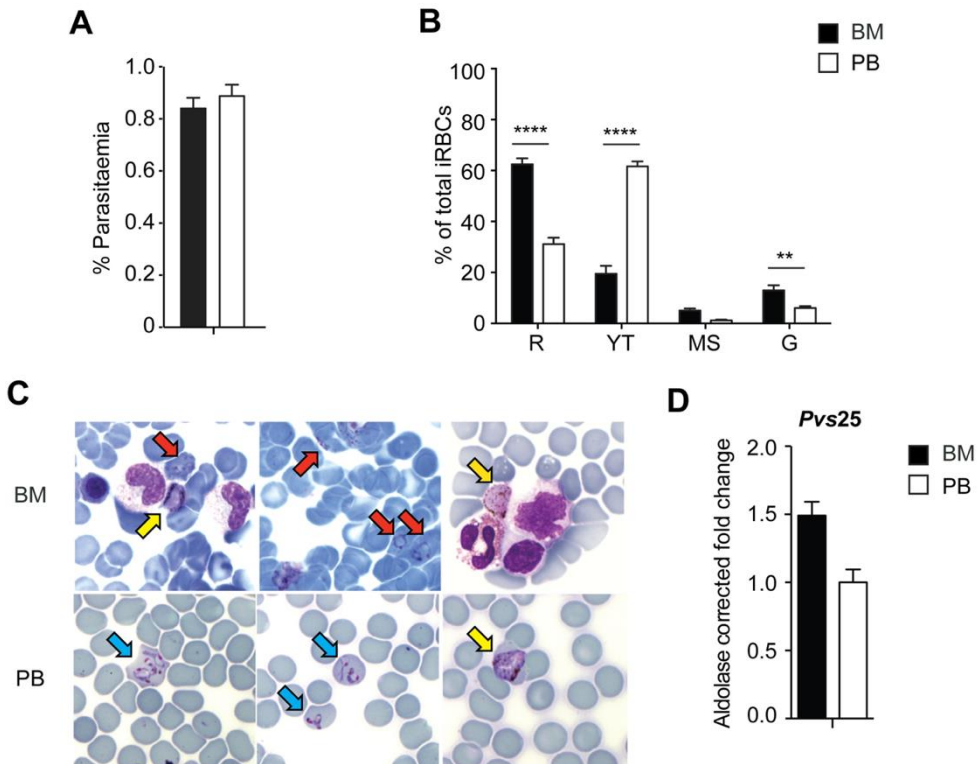


Figure 8. Comparison of *P. vivax* load and life stages in bone marrow aspirate and peripheral blood on admission. (A) Parasitaemia in bone marrow aspirate and peripheral blood at the day of admission. (B) Parasite stage distribution in bone marrow and peripheral blood (C) Representative Giemsa-stained images of *P. vivax* in the bone marrow (BM, upper row) illustrating rings (red arrows) and gametocytes (yellow arrows) and in peripheral blood (PB, lower row) illustrating young trophozoites (blue arrows) and gametocytes (yellow arrow). Arrows indicate infected cells. (D) Relative RT-qPCR quantification of *pvs25* transcripts in bone marrow and peripheral blood samples obtained at admission. Reproduced with permission from (10).

Kho et al concluded that, based on their conservative estimations, the asexual parasite biomass detected in the BM during infection is around 0.1% (8,184). This report suggests that BM infections are primary involved in gametocyte development, whereas the majority of the asexual stages happen in the spleen.

1.1.10.2 The presence of *P. vivax* in the spleen

The spleen has been considered a mysterious organ since ancient times. Despite the ongoing interest from thinkers and researchers over the centuries, our understanding of the spleen's functions and related diseases remains incomplete (185). During embryonic development, the spleen functions as a

hematopoietic organ, supporting various components of the erythroid, myeloid, megakaryocytic, lymphoid, and monocyte-macrophage systems. It plays a significant site for lymphopoiesis, containing approximately 25% of the body's total lymphoid mass. Additionally, under abnormal circumstances, the spleen may serve as a site for extramedullary hematopoiesis (186).

The primary function of the spleen is to destroy damaged, old or *Plasmodium*-parasitized RBCs (187). As previously mentioned, to evade splenic clearance, mature stages of *P. falciparum* adhere to endothelial receptors using variant surface proteins. This mechanism enables the sequestration of parasitized red blood cells (pRBCs) within the microvasculature of internal organs, particularly involving mature stages from the parasites, which are observed in small proportions in circulation (56). In contrast, while infected reticulocytes containing mature stages of *P. vivax* are found in peripheral circulation, it was widely believed for a considerable period that this human malaria parasite did not sequester in the microvasculature.

Contrary to this long-held belief, that *P. vivax* does not sequester, a particular study revealed that infected reticulocytes from a rodent malaria species prone to targeting reticulocytes adhere to spleen barrier cells of fibroblastic origin. This interaction serves to protect parasites from macrophage destruction (188). Subsequent studies have documented the *in vitro* cytoadherence of *P. vivax*-infected reticulocytes to human cells and tissues cryosections (189).

The earliest evidence of intrasplenic infections in natural cases was observed in a 19-year-old non-immune patient who underwent splenectomy following a spleen rupture. IFA imaging of the spleen revealed intact *P. vivax*-infected reticulocytes outside macrophages in the splenic cords. This parasite detection was performed using immunofluorescence confocal microscopy using antibodies against VIR proteins (**Figure 9**). Additionally, immunohistochemical staining showed white pulp expansion and hypercellularity in the splenic red pulp. This case provides the first detailed

immunohistopathological analysis of an untreated human spleen infected with *P. vivax*, suggesting the likelihood of intrasplenic infections (9).

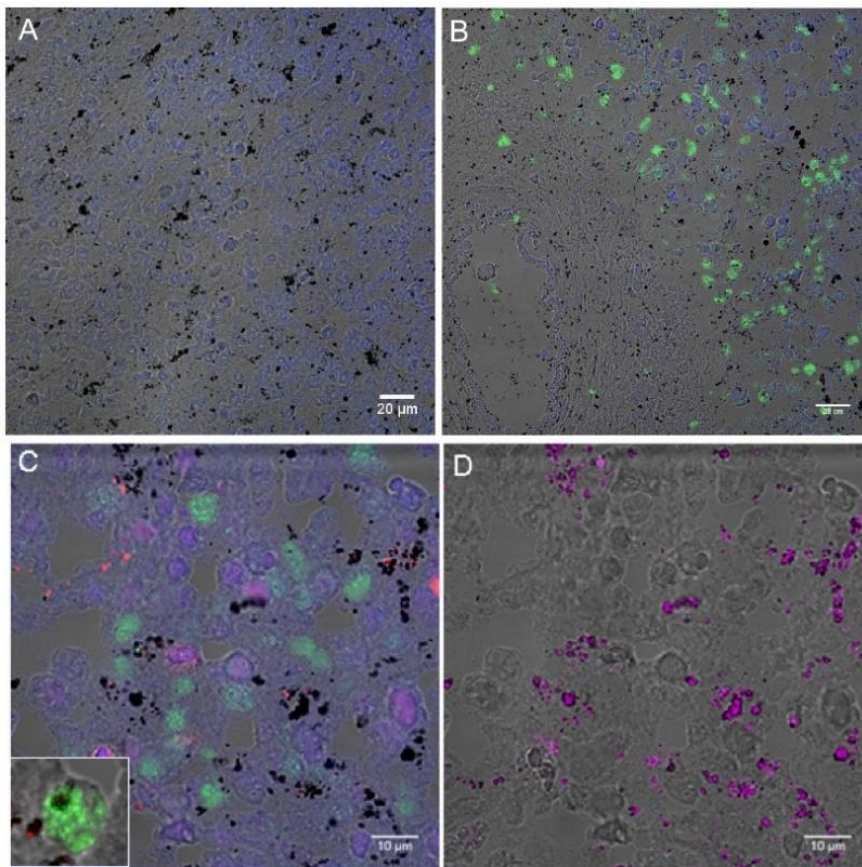


Figure 9. Immunohistofluorescence images of *P. vivax*-infected spleen sections. (A) Spleen section showing *P. vivax* parasites mostly in the cords of the red pulp as detected by polyclonal antibodies against VIR proteins. (B) Negative control using preimmune sera. Nuclei are shown in blue and the bright field image of the tissue in gray. Scale bar: 20 μm . (C) Double staining showing CD68 macrophages in red and parasites stained in green. Scale bar is 10 μm . (D) Reflection contrast (magenta) was used to detect parasite pigment. Reproduced from (9).

This evidence prompted the scientific community to speculate about a more complex role for the spleen in human malaria, specifically the potential accumulation of viable *Plasmodium*-infected red blood cells within this organ. Recently, a substantial number of untreated patients undergoing splenectomy in a highly endemic area for both *P. falciparum* and *P. vivax* in Papua (Indonesia) were found to have non-phagocytosed parasitized red blood cells concentrated in the spleen, as determined by pathological and molecular

examinations of these tissues, compared to peripheral blood. Notably, the authors identified a previously undetected biomass of both *P. falciparum* and *P. vivax*, with a higher concentration for *P. vivax*. This finding led to the conclusion that chronic vivax malaria primarily represents a cryptic erythrocytic infection of the spleen (8,184). The density of *P. vivax*-infected reticulocytes in the spleen was found to be 3,590 times higher than in circulating peripheral blood, which is significantly greater than the estimated spleen-to-circulating blood density ratio in *P. falciparum* infection (median 289) (**Figure 10**) (8,184).

Another study by the same research group demonstrated that, in the spleen, all blood stages of *P. vivax* except for sexual stages were found to accumulate, with higher densities of intact parasites compared to peripheral blood. These parasites account for approximately 95.1% of the total *P. vivax* biomass in the body. These observations suggest that the spleen functions as a site for both the accumulation and potential destruction of *P. vivax* parasites, with the majority of the asexual blood stage life cycle occurring there. The underlying reason for this tropism remains unclear, but it appears to be a major contributing factor to anaemia (13).

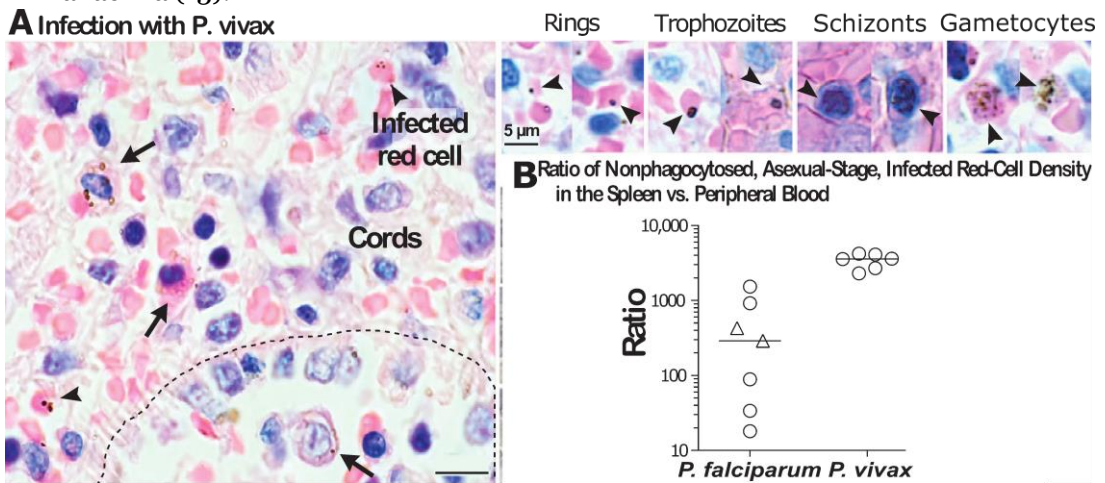


Figure 10. Accumulation of intact, asexual-stage *P. vivax* in the spleens of patients with asymptomatic infection. (A) Tissue sections of the spleen were stained with Giemsa and assessed for the presence of infection with *P. vivax*. (B) Ratio of asexual-stage infected red-cell density in the spleen versus circulating peripheral blood was higher with *P. vivax* than with *P. falciparum*. Circles represent untreated patients and triangles represent recently treated patients. Adapted and reproduced from (8).

Overall, the data presented in this section suggest the need for a new paradigm in *P. vivax* research that includes these cryptic infections in the BM and the spleen as part of its life cycle (**Figure 11**). Although the molecular mechanisms underlying the parasite's tropism towards these hematopoietic organs remain unclear, there is an urgent need to further investigate how these cryptic niches are formed and their implications for vivax malaria pathogenesis and symptomatology.

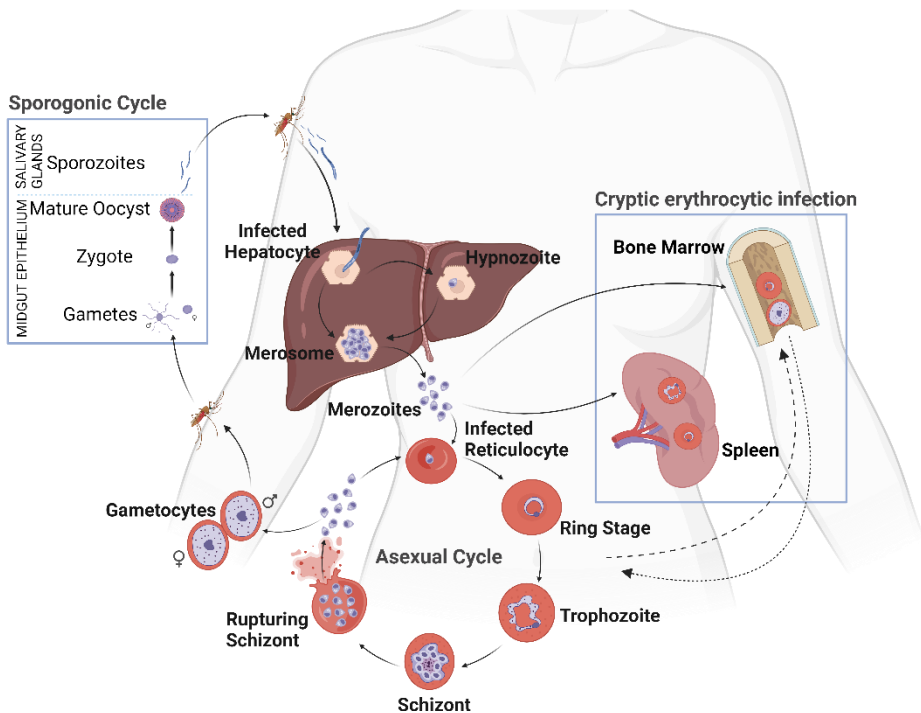


Figure 11. Life cycle of *Plasmodium vivax* incorporating the parasite cryptic niches. Adapted from (190).

1.1.11 Genomic editing of *Plasmodium* species

The ~30 Mb genomes of *Plasmodium* parasites encode approximately 5,000 genes, yet the functions of most remain unknown (191). This is largely due to the limited functional annotations derived from sequence homology and the lower genetic tractability of *Plasmodium* compared to many model organisms. Recent technical advances have enabled genome-wide forward and reverse genetic screens in *Plasmodium*. Notably, the first malaria parasite to be transfected was *Plasmodium gallinaceum* in 1993 (192).

The development of genetic manipulation techniques for *P. falciparum* in the 1980s- 1990s was crucial for advancing the study of malaria biology. Since first transfections of *P. falciparum* parasites (193–196), genetically modified *P. falciparum* parasites have been used to investigate various aspects of the disease, including red blood cell invasion (197), metabolic processes (198,199), drug resistance mechanisms (200,201), gametocyte development (202), and mosquito transmission (203). However, the biological and genetic differences between *P. falciparum* and other human malaria parasites limit its suitability as a model for studying these other species. Additionally, the lack of robust long-term *in vitro* culture systems for *P. vivax* and other human malaria parasites has hindered genetic manipulation efforts for these species.

However, in recent years, the adaptation of CRISPR (Clustered Regularly Interspaced Short Palindromic Repeats) and CRISPR-associated protein 9 (CRISPR/Cas9) technology has significantly improved the efficiency of gene editing at the single gene level (204).

Research into DNA repair has advanced significantly with methods that induce site-specific DNA breaks. In genome editing technologies, double-strand breaks (DSBs) in DNA can be repaired through homologous recombination with donor DNA or nonhomologous end-joining (NHEJ), which can introduce mutations at the target site (205). In *Plasmodium* parasites, the canonical NHEJ (cNHEJ) pathway is deficient, so repair primarily occurs via homology-directed repair (HDR) when a donor template is available (206). This deficiency in the cNHEJ pathway results in fewer unintended mutations or off-target effects. Although *Plasmodium* can use microhomology-mediated end joining (MMEJ), which employs small homologous regions near the DSB to repair the damage and can create potential indels, this process is relatively uncommon (206,207).

CRISPR/Cas9 editing of *P. falciparum* relies on either one- or two-plasmid system to deliver the Cas9 nuclease, guide RNA (gRNA), and DNA repair template (**Figure 12**). Although numerous Cas proteins have been identified through bioinformatics and experimental studies, Cas9 and its variants from *Streptococcus pyogenes* (SpCas9) are the most commonly used in *Plasmodium*

genome editing (204). The high Adenine-Thymine (AT) content of the *P. falciparum* genome complicates the recognition of gRNA binding sites near the SpCas9 PAM sequence (-NGG) and the cloning of repair templates. The dihydrofolate reductase (*dhfr*) gene is the most frequently used drug-selectable marker for selecting modified parasites in CRISPR/Cas9 genetic modifications (203,208–210). To minimize the likelihood of unintended genomic mutations, the DNA repair template should be linear, with two gRNAs creating cut positions at the locus of interest, or by using a Cas9 cut position flanking the DNA repair template on the plasmid (**Figure 12**).

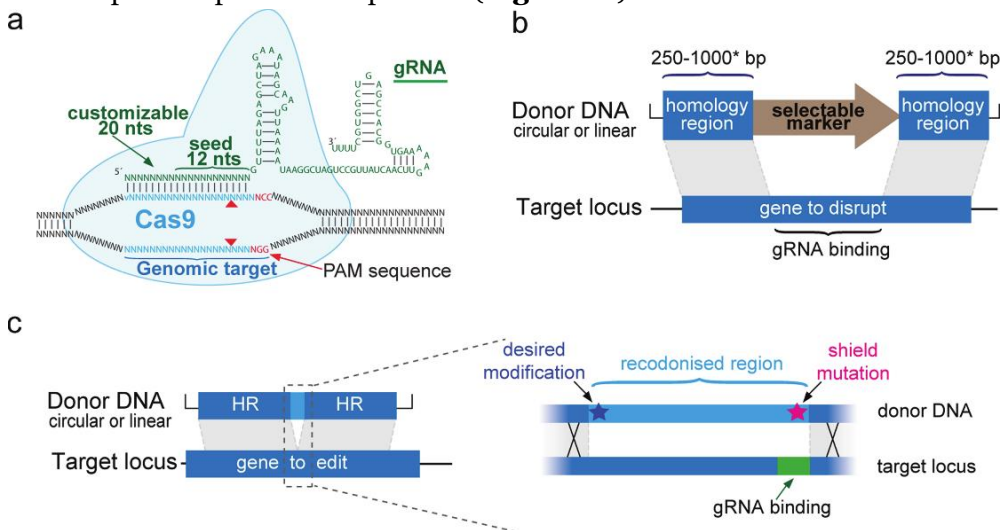


Figure 12. Schematic representation of the molecular mechanisms of CRISPR/Cas9 genome editing tool. (A) Cas9 is directed to a specific genomic target by the first 20 nt of the gRNA, resulting in the generation of a double-strand break (red triangles). Donor design for **(B)** a typical gene-disruption experiment in *P. falciparum* and **(C)** marker-free genome editing of a point mutation. Silent ‘shield mutations’ prevent Cas9-gRNA cleavage of the edited locus. Additional silent mutations spanning the gap between the shield mutations and the desired modification can be introduced to help drive the repair event beyond the mutation-of-interest. Reproduced from (204).

1.1.11.1 Genomic editing to study *P. vivax* biology

The first transfection experiments of *P. vivax* were reported in 2005, where parasites were transiently transfected with episomal plasmids containing the luciferase reporter gene and *P. falciparum* regulatory sequences (211). Significant progress in *P. vivax* transfection was not achieved until 2015, when researchers successfully manipulated the *P. vivax* genome *in vivo* for the first time (212). In this study, Zinc-Finger Nucleases were used to create site-specific

DNA double-strand breaks, introducing point mutations into the *P. vivax dhfr-ts* gene, which rendered the parasites resistant to pyrimethamine. This was the first instance of genome editing in a non-falciparum *Plasmodium* species, demonstrating the potential for site-specific genome editing (212). The experiments were conducted in *Saimiri boliviensis* monkeys and the resistant transfected parasites were selected over three weeks in animals treated with pyrimethamine. This selection method was similar to that used for selecting transgenic *P. knowlesi* (213) and *P. cynomolgi* in rhesus macaques (214–216).

Due to the lack of a robust *in vitro* culture for *P. vivax* and the need to study poorly characterized or uncharacterized genes from the parasite, the heterologous expression of *P. vivax* genes into other *Plasmodium* species has become a valuable approach. This method has been employed since the first report of this rational appeared (217). The feasibility of using heterologous transfection in *P. falciparum* to investigate the subcellular localization and function of *P. vivax* proteins has been widely demonstrated in subsequent studies (105,217–219). Additionally, other non-human malaria parasites have been explored for the heterologous expression of *P. vivax* genes (220–224).

However, reports using the CRISPR/Cas9 system to generate transgenic *Plasmodium* lines expressing *P. vivax* genes have been scarce. Few publications, have investigated this approach as a feasible method for generating transgenic lines of other *Plasmodium* expressing vivax malaria parasite proteins (203,220,222,225). Notably, two of these studies utilized *P. knowlesi* as the parental parasite for transfection, while two others used *P. falciparum*. In this thesis, we employed CRISPR/Cas9 to generate a stable transgenic *P. falciparum* line expressing previously uncharacterized hypothetical *P. vivax* gene (226).

The use of the novel CRISPR/Cas9 system will allow the scientific community to gain a deeper understanding of the biology of *P. vivax* and its pathophysiology. Additionally, the recent advances in the culture adaptation of *P. knowlesi*, combined with the implementation of CRISPR/Cas9 in this parasite (220,222), are expected to further our understanding of *P. vivax* biology in the coming years.

1.2 Extracellular vesicles

Extracellular vesicles (EVs) are a heterogeneous group of small, double lipid bilayers particles secreted by nearly all organisms, from bacteria to humans, and are present in biological fluids such as plasma, urine or even cerebrospinal fluid, among others, providing insights into normal and pathological processes (227–229). EVs are broadly classified into two main categories: microvesicles and exosomes, differentiated by their size, biogenesis and composition. Microvesicles (MVs), also known as microparticles, are larger (ranging from 100 nm to 1 μ m in diameter) and more variable in shape compared to exosomes (229,230). MVs are formed directly through budding from the plasma membrane, whereas exosomes are generated when cytoplasmic multivesicular bodies (MVBs) fuse with the plasma membrane (230). Exosomes, originating from endocytic processes, typically measure between 30 to 100 nm in diameter (228,231). Both EVs carry distinct biological markers from their parent cells and are enriched with molecules essential to their biogenesis pathways, which are selectively enclosed within them (231).

Exosomes were first described by Rose M. Johnstone and Clifford V. Harding in studies on reticulocytes, which are the target cell for *P. vivax*. Initially, exosomes were thought to function primarily as a mechanism for cellular waste disposal, specifically for the removal of the transferrin receptor during the maturation of reticulocytes into erythrocytes (**Figure 13**) (232,233). However, this concept evolved over time, Graça Raposo and colleagues later demonstrated that B-cell-derived exosomes could induce antigen presentation thereby modulating immune responses (234). Since then, numerous studies have elucidated various functions of EVs, and it is now widely recognized that EVs play crucial roles in cell-to-cell communication, pathogenesis, drug delivery, and as biomarkers for many diseases (228).

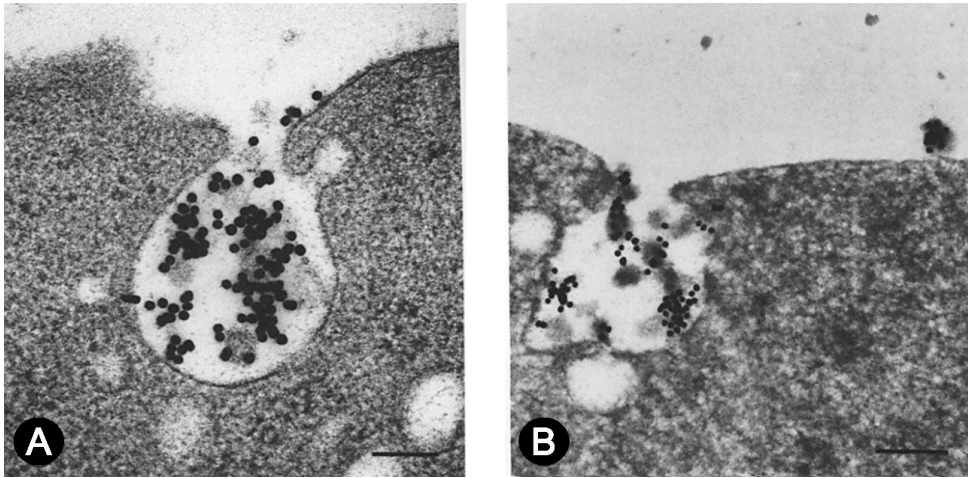


Figure 13. TEM microscopy images of reticulocytes releasing exosomes loaded with Transferrin receptor. (A) View of MVE exocytosis in an unfixed reticulocyte. **(B)** MVE exocytosis with concomitant release of vesicular inclusions. These vesicles often remain attached to the plasma membrane (upper right). Adapted from (233).

1.2.1 Origin, biogenesis and composition

Currently, a wide array of EV subtypes has been characterized due to their secretion by diverse cell types and detection in numerous biological fluids, suggesting potential variations in their biogenesis. In the context of exosomes, the process begins with the invagination of the plasma membrane, leading to the formation of endosomes. These endosomes can fuse with vesicles from the Golgi apparatus, particularly those budding from the trans-Golgi network (TGN) (235,236). Early endosomes subsequently mature to late endosomes, where the endosomal membrane invaginates into the lumen, forming intraluminal vesicles (ILVs). These ILVs accumulate within multivesicular bodies (MVBs), which can then fuse with the plasma membrane, releasing their contents as exosomes into the extracellular environment. Alternatively, MVBs may fuse with lysosomes/autophagosomes for degradation (**Figure 14**) (237). On the contrary, MVs originate from the outward budding and subsequent fission of the plasma membrane. Therefore, the mechanisms underlying the formation of exosomes and MVs differ, leading to distinct cargo compositions: exosomes carry components originating from MVBs, while MVs primarily encapsulate elements from the plasma membrane (**Figure 14**) (230).

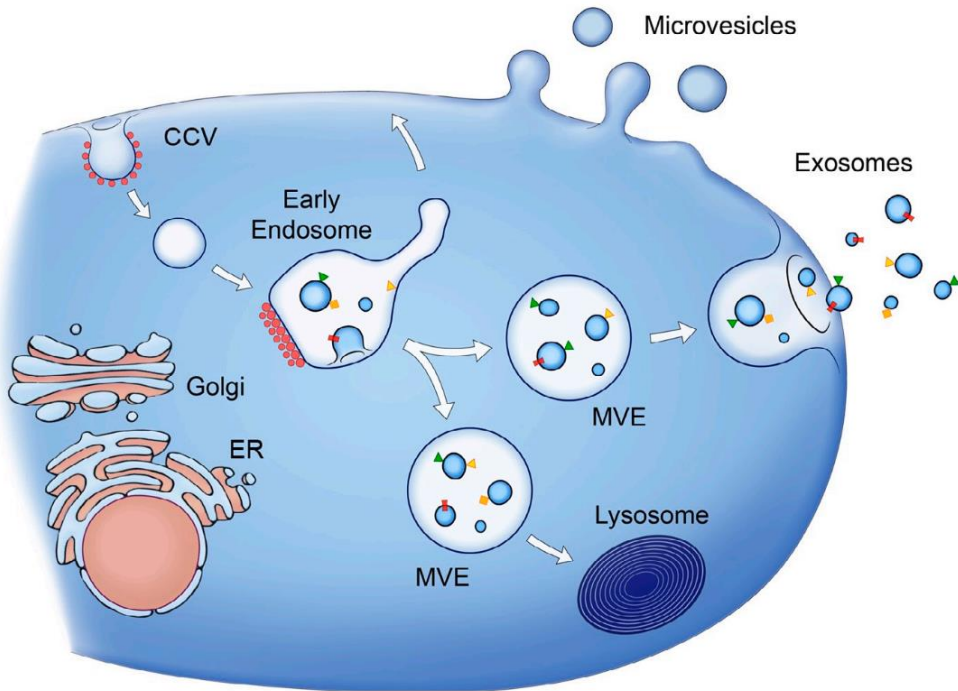


Figure 14. Release of MVs and exosomes. Reproduced from (230).

Despite these differences, both types of EVs share common intracellular mechanisms and classification systems in their biogenesis.

The mechanisms involved in the transportation of EVs are heavily influenced by their biogenesis. Most of our current understanding comes from studies on tumoral or immortalized immune mammalian cell lines. As mentioned earlier, exosomes are small EVs ranging from 30 to 150 nm in size. These particles form from inner budding of the late endosomal membrane, resulting in ILVs within a MVB (238). MVBs can merge with lysosomes for content degradation, a process facilitated by the SNARE system, as well as surface proteins like the HOP complex and GTPase Rab7 associated with MVB membrane (239). However, ILVs coated with EV markers like CD63, LAMP1, or LAMP2 are released as exosomes when the MVB fuses with the cell's plasma membrane (239).

Several mechanisms have been proposed for the release of exosomes from MVBs: i) the involvement of the endosomal sorting complex required for transport (ESCRT) machinery (238,240), ii) the accumulation of CD63 tetraspanin in ILVs (241–243), and iii) the hydrolysis of sphingomyelin into ceramide by neutral sphingomyelinase or phosphatidylcholine into phosphatidic acid by phospholipase D2 (231,244). Consequently, exosome release can proceed through both ESCRT-dependent and -independent pathways (**Figure 15**).

The ESCRT machinery plays a crucial role in organizing MVB proteins within ILVs. Five ESCRT complexes have been identified: 0, I, II, III, and III associated. After ILV formation, MVBs are directed toward the plasma membrane for fusion and budding, facilitated by molecules such as LAMP1 (239), TSG101, ALIX, VSP4, syntenin-1 (245), Rab8b, Rab11, Rab27, the Rab effector otoferlin, and potentially other Rab proteins (245,246). Tetraspanins such as CD63, CD9, and CD81 are notably prevalent in exosomes, with CD63 often considered characteristic of endosome-derived exosomes (247).

Variations in protein mediators during EV formation and release have been observed across different biological origins and cell lines (231). Notably, even within the same cell line, distinct EV subpopulations with unique physicochemical characteristics can be identified under varying conditions, such as different stages of pathogen life cycles, laboratory settings, or external stressors (248–250). However, the ESCRT complex remains highly conserved across kingdoms, likely originating from an early evolutionary event driven by concerted evolution (251,252). Interestingly, ESCRT molecules are also involved in the biogenesis of viruses and retroviruses, facilitating the incorporation of viral cargo into infected cell exosomes for dissemination to neighbouring cells (253,254).

The cargo sorted into EVs can include various proteins, such as chaperones like heat shock 70 kDa protein (HSP70) and heat shock cognate 71 kDa protein (HSC70), which assist in sequestering cytosolic proteins into ILVs (229,255).

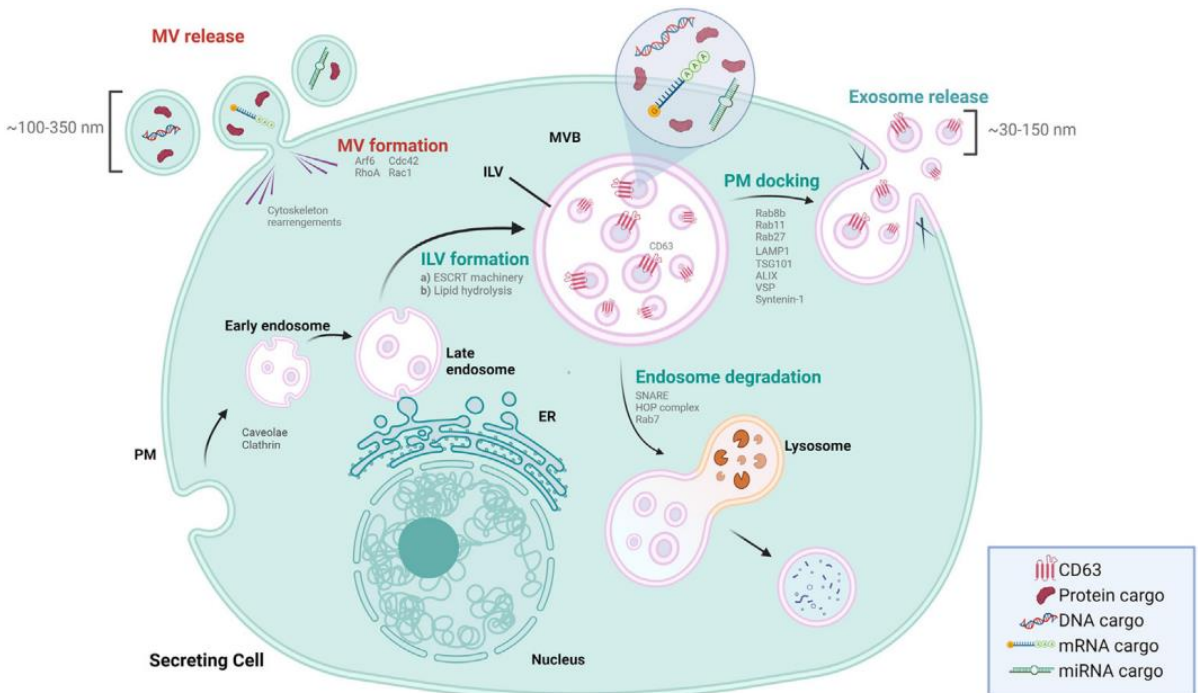


Figure 15. Canonical pathways of EV biogenesis and release. ER: endoplasmic reticulum, ILV: intraluminal vesicles, MVB: multivesicular body, MV: microvesicles, PM: plasma membrane. Reproduced from (252).

Additionally, GPI-anchored proteins are likely incorporated due to their affinity for lipid domains and lipid rafts, potentially contributing directly to ILV formation (256). EV cargo also contains nucleic acids, including mRNAs, non-coding RNAs (such as microRNAs), and DNA sequences (257,258). Recent studies have reassessed exosome composition and emphasized the selective sorting of RNA into exosomes (259).

Notably, *in silico* analysis has identified a specific EXOmotif (GGAG) that governs the loading of miRNAs into exosomes and promotes binding to heterogeneous ribonucleoprotein A2B1 (hnRNPA2B1), which regulates miRNA loading (260–262). However, many questions remain regarding RNA sorting into EVs and the regulatory mechanisms involved, highlighting the need for further research to explore the roles of other RNA-binding proteins and RNA motifs.

The machinery driving MV biogenesis involves alterations in lipid and protein composition, as well as changes in Ca^{2+} levels (263). This process includes the reorganization of membrane phospholipids, such as the translocation of phosphatidylserine from the inner membrane to the outer membrane, which induces membrane curvature and cytoskeletal restructuring, ultimately leading to membrane budding and MV formation (264). Cholesterol is also a critical lipid contributor to MV biogenesis (265). Cytoskeletal components, particularly the RHO family of small GTPases and RHO-associated protein kinase (ROCK), play significant roles in MV formation (266). The cargo of MVs is influenced by its proximity to the lipids of the inner leaflet of the plasma membrane, facilitated by plasma membrane anchors (palmitoylation, prenylation and myristoylation) and the formation of high-order complexes, concentrate them into small membrane domains from which new MVs bud (267). However, the targeting mechanism of nucleic acids inside MVs and their subsequent delivery to the cell surface remains unclear.

While distinct biogenesis, cargo and composition differences exist among EVs, particularly between exosomes and MVs, as discussed in the last part of this thesis, debates continue regarding the various subsets of EVs and their classification. Consequently, precise isolation and characterization methods are crucial in the field to establish clearer classification among EVs. Here, the MISEV guidelines (268) should be followed to assure the reproducibility, rigor and clarity of any EVs preparation used and/or analysed in any kind of research.

1.2.2 Extracellular vesicle purification and characterization

1.2.2.1 Isolation of extracellular vesicles

Before discussing the state-of-art isolation and purification methods, it is important to note that there is currently no gold-standard technology for EVs isolation. However, this section will present the relevant methods to this thesis.

Differential ultracentrifugation (dUC) was one of the first techniques developed for EV isolation (**Figure 16**) (269). Despite its widespread use, dUC can be

impractical due to its complexity and the need for specialized equipment, which may be unavailable in laboratories with limited resources, especially in low- and middle-income countries. The method can be performed varying distinct parameters such as rotor selection, washing steps, centrifugal forces, and duration, all of which must be adjusted based on sample volume and viscosity (270). Typically, initial centrifugations at $400 \times g$ and $2,000 \times g$ are used to remove dead cells and cell debris, followed by centrifugation at $10,000 \times g$ to isolate apoptotic bodies and larger vesicles. A filtration step through a $0.22 \mu\text{m}$ filter may follow to eliminate particles larger than 200 nm (271). The final step involves ultracentrifugation at $100,000 \times g$ to pellet small EVs (exosomes) (269), which are then washed and may undergo a second ultracentrifugation at $100,000 \times g$ (272).

However, dUC has several drawbacks, including protein aggregation, coprecipitation of soluble protein contaminants (such as albumin in plasma), and potential rupture or fusion, which can affect the physical properties of the exosomes and the downstream analysis (273). To address these limitations, alternative isolation techniques suitable for small sample volumes are recommended.

More stringent methods can be employed to eliminate soluble contaminants and protein aggregates, such as floatation in a density barrier or in a density gradient after dUC. These techniques improve EV purity and enable the classification of EV subtypes, with exosomes typically having densities between 1.15 and 1.19 g/ml (**Figure 16**) (269,274). Such approaches have been utilized to study EV heterogeneity and biology. For example, performing a sucrose density gradient after dUC can further enhance exosome purity by removing protein contaminants (275).

Density gradient techniques separate EVs based on physical characteristics like size and shape, allowing them to migrate to their equilibrium buoyant density within a continuous or discontinuous gradient. In a continuous gradient, formed by ultracentrifugation of layers containing 5–60% iodixanol, EVs migrate to their respective densities, while the discontinuous gradient consists

of serial layers of 5 to 60% iodixanol/sucrose maintaining density separation. EVs are often found in the 35-40% sucrose layer. Samples can be loaded either at the top for upward migration or at the bottom for downward migration. The densities of each layer and the solution used (iodixanol or sucrose) are adjusted based on the desired EVs subpopulation to be isolated. After EVs separation, each fraction must be washed to remove excess solution before further analysis. However, this method is time-consuming, requires trained operators, and necessitates a specialized ultracentrifuge.

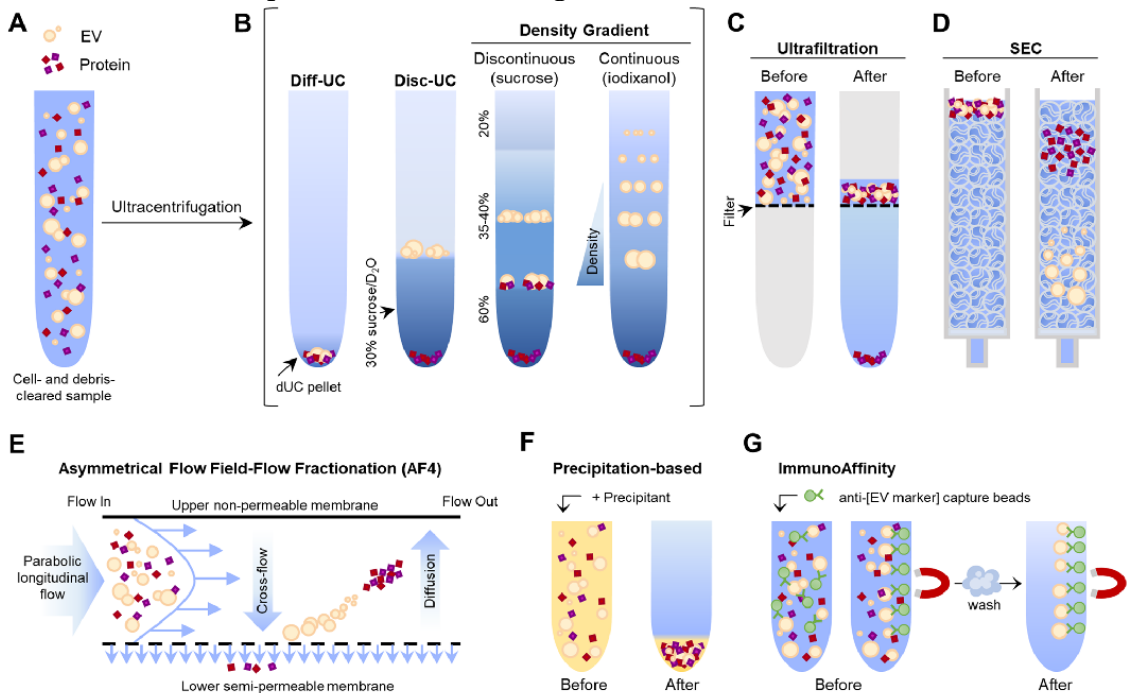


Figure 16. Graphical summary of mainly used EV isolation methods. (A) Initial sample (B) Ultracentrifugation to pellet EVs, in all variants, from differential ultracentrifugation to density gradients (C) Ultrafiltration, (D) size-exclusion chromatography (SEC) and (E) asymmetrical flow field-flow fractionation (AF4). (F) Precipitation-based isolation and (G) Direct immune-affinity capture (DIC). Reproduced from (276).

In 2014, Böing et al. revisited the use of size-exclusion chromatography (SEC) for isolating EVs from biofluids (277). This methodology, originally employed at the early studies of EV, was used to demonstrate the presence of EV-encapsulated proteins distinct from soluble molecules (278). SEC separates EVs based on their size as they pass through chromatography columns (**Figure 16**).

These columns yield different elution profiles for EV fractions of varying sizes. Constructed from a porous polymer, comprising the stationary phase (gel filtration matrix or resin) and the mobile phase. Small particles, such as soluble proteins, enter the polymer pores and elute later than EVs, which move more quickly due to their inability to enter the pores.

Since EVs are larger than the polymer pores, they elute more rapidly than proteins alone, with larger vesicles eluting faster than smaller ones (279). SEC is a scalable time- and cost-effective technique that provides high purity and yield of EVs (280). Additionally, compared to other techniques based on the precipitation of EVs using various precipitating agents, such as polyethylene glycol, SEC minimally alter the characteristics of EVs (281)

SEC have been used to isolate EVs from various sources, culture supernatant (282), urine (283), plasma (284) and, of interest for this thesis, from plasma of malaria infected individuals (15). However, soluble protein might elute altogether with EVs, but also lipoproteins and protein aggregates tend to elute from the chromatography column in (or close to) the EVs enriched fractions. This problem can be solved by combining SEC to other methods prior to the sample application on top of the column such as dUC or density gradient ultracentrifugation. SEC enables the concentration of EVs due to the use of ultrafiltration technology. Implementing SEC is relatively straightforward, as its bench-top usage is less expensive compared to alternative methods. Furthermore, the columns can be reused after washing steps and can also be autoclaved (280). Despite these benefits dUC is still the most commonly used technique. However, SEC is increasingly being adopted worldwide, and its use has grown steadily since 2017 (280).

In addition to methods that rely on the physical traits of EVs for isolation, as previously discussed, there are techniques focused on analyzing and/or separation of specific EVs subpopulation based on their surface protein expression. This approach relies on interactions between proteins (antigens) and their antibodies, as well as specific interactions between receptors and their ligands (285). Immunoaffinity methods offer advantages such as rapid

processing, simplicity, suitability for small sample volumes, and compatibility with standard laboratory equipment (**Figure 16**). This methodology has been adapted to use magnetic beads that can be either covalently coated with antibodies directly or with streptavidin, allowing the coupling of any biotinylated capture antibody with high-affinity, allowing posterior separation from the magnetic bead (286–288). Magnetic beads commercially available, directly linked to anti-CD63, -CD9, and -CD81 antibodies either individually or in combination, offer effective options for EV isolation (247,289). These beads can be immobilized on various carriers such as magnetic beads, ELISA plates, or microfluidic devices (290,291). A critical consideration with this approach is the incorporation of a prior purification step to eliminate potential contaminants, such as antibodies, carriers, or soluble proteins present in the sample. This step is particularly important when subsequent functional assays are planned, as failure to remove these contaminants could lead to inaccurate results. Despite this requirement, immunoaffinity isolation remains an excellent option for exploring specific EV populations with distinct biomarkers and for identifying the molecular cargo within EVs. Of interest, this technique has already been employed in the field of *P. vivax* malaria research. In our lab, we investigated the content of CD71+ EVs, captured using CD71-beads, derived from reticulocytes in plasma from *P. vivax*-infected patients and compared them to those from healthy donors (292). This approach enabled the identification of parasite proteins associated with EVs in natural infections with greater extent than previously reported (15).

As discussed earlier, there are multiple methodologies for EV isolation, each with its own strengths and weaknesses, making the selection of a single method challenging. These methods differ in terms of specificity, yield, purity and the volumes that be processed. Therefore, it is crucial to determine the intended downstream applications or methods used after EVs isolation before selecting the most appropriate isolation technique (**Figure 17**).

5 Concentration and isolation methods

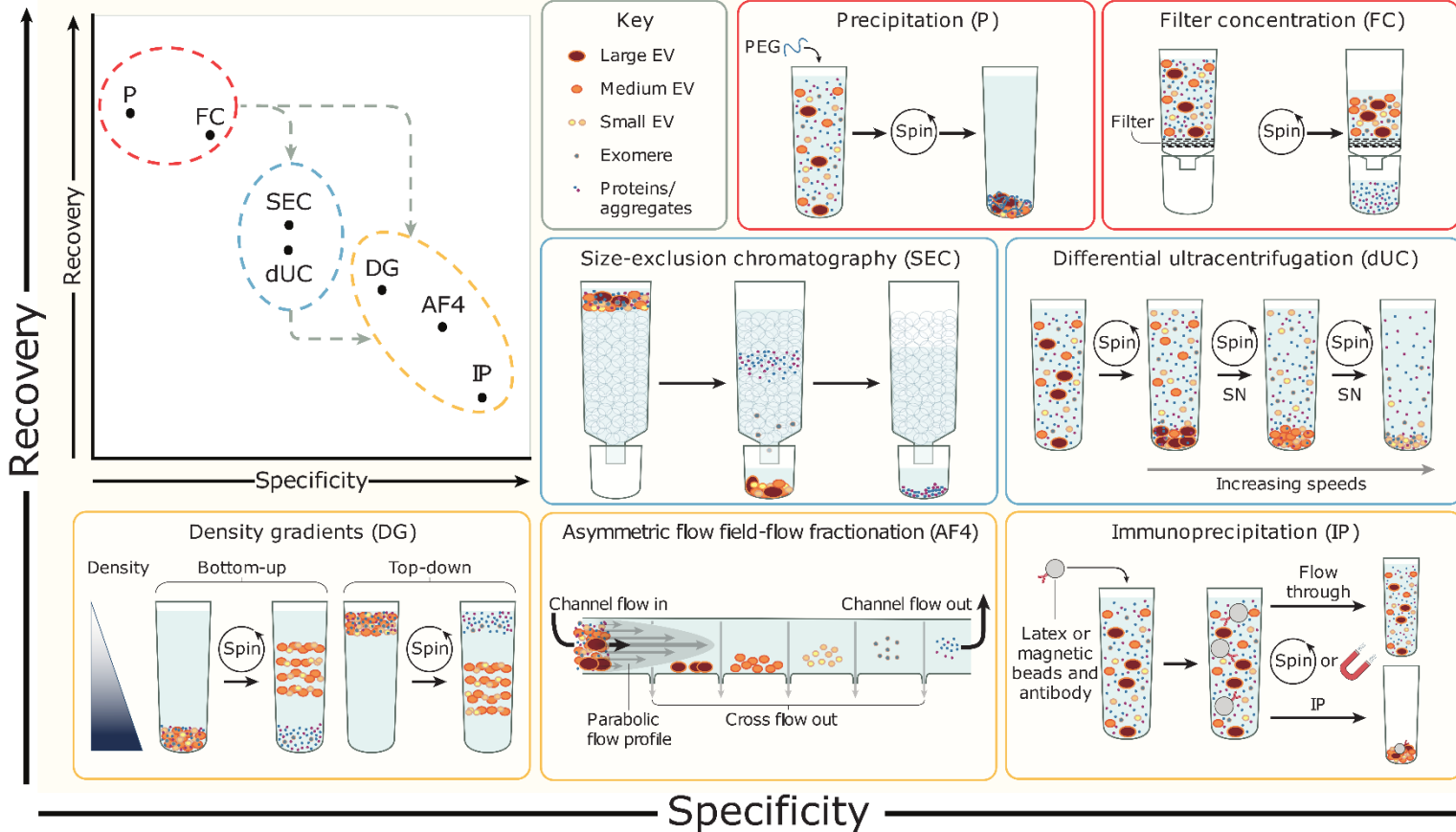


Figure 17. Graphical summary of separation and isolation techniques of EVs. Techniques are organized top-to-bottom and left-to-right based on recovery capacity and specificity of the technique. Adapted from (293).

1.2.2.2 Characterization of isolated EVs

After isolating EVs from any biological source, whether from biological fluids or cell cultures, it is crucial to characterize the EV preparation. This characterization is essential not only to determine the nature, biological function, and origin of the isolated EVs but also to quantify their concentration and composition for subsequent investigations using functional assays or advanced omics techniques. A wide variety of physical and chemical methods are currently employed to characterize EV populations.

One of the main techniques currently used for EV characterization is Nanoparticle Tracking Analysis (NTA). NTA assesses the physical characteristics of EVs and can discern their concentration and size, classically ranging from 10 nm to 2 μm , although newer techniques can measure sizes down to 2.5 nm. By tracking the Brownian motion (294,295) of nanoparticles in a liquid suspension using a laser, NTA captures the trajectory of EV movement (**Figure 18**). Image processing of this movement correlates with the particles' sizes and concentration (296). A key advantage of NTA is its ability to identify various EV populations, including smaller particles as well as offering a straightforward and rapid analysis method, with the added benefit of sample recovery post-measurement (297).

However, proper NTA analysis requires ensuring no particles are detected before sample application by thoroughly washing the measuring cell chamber of the equipment. Additionally, correct and appropriate dilution is crucial to match the concentration range suitable for the equipment, preventing abnormal measurements of EV concentration and size (296). The latest state-of-art NTA machines enable the detection of EV-associated antigens through fluorescent labelling with antibodies and direct particle labeling using lyophilic dyes (298,299).

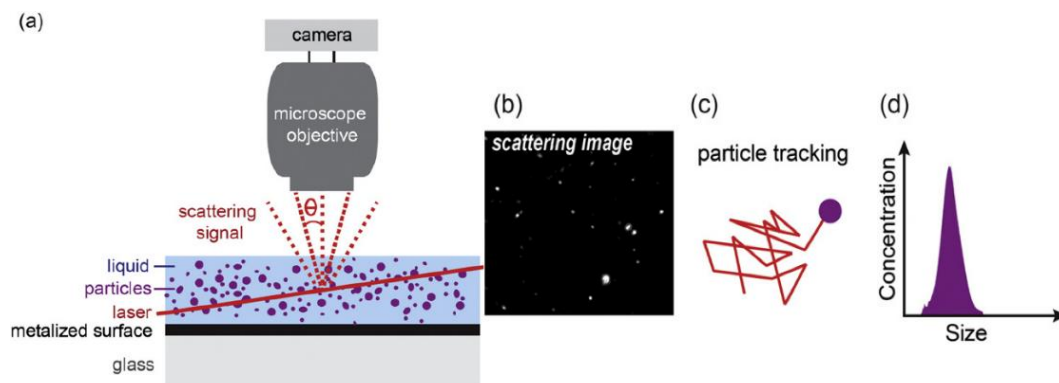


Figure 18. Nanoparticle tracking analysis (NTA). (A) Schematic illustration of the NTA rationale to measure the light scattered from particles measured. (B) scattering of individual particle imaged. (C) Motion tracked of a single particle. (D) NTA extrapolation of size and concentration of measured particles. Reproduced from (300).

Electron microscopy (EM) is commonly used for the characterization of EV structure, morphology, and size. Its use requires specialized equipment and trained personnel (301). EM generates images by directing an electron beam through the sample, resulting in the production of secondary electrons, which are then captured and magnified using various lenses. The two main types of EM used for EV characterization include transmission electron microscopy (TEM) and cryo-electron microscopy (cryo-EM). The primary difference between these techniques lies in the treatment (fixation) and preparation of the sample (297). TEM produces images through electron interference as the electron beam interacts with the sample. Due to the electron beam's wavelength being three orders of magnitude shorter than that of visible light, TEM achieves a resolution of about 1 nm (302). Additionally, TEM's capabilities can be enhanced by immuno-gold labelling, which aids in the collection of biochemical information (303).

Beyond evaluating EVs based on their size and morphology, examining the protein composition within EV preparations is crucial. This is commonly achieved through standard colorimetric detection assays, such as bicinchoninic acid (BCA) or Bradford assays to quantify protein content. Following protein concentration, western blotting is typically performed, employing sodium dodecyl sulfate polyacrylamide gel electrophoresis (SDS-PAGE) followed by protein staining or immunoblotting to identify specific EV cargo (304).

Flow cytometry is a widely employed for analyzing EV surface markers and is one of the most commonly used techniques. Moreover, it allows for the assessment of size and morphology. Flow cytometers analyze samples by capturing scattering and fluorescence signals generated by individual particles illuminated by a laser beam passing through a nozzle. However, conventional flow cytometers typically have a detection limit of around 300 nm, making direct detection of small EVs challenging . To overcome this limitation, newer flow cytometers with enhanced sensitivity in forward scatter detection, fluorescent amplification, and high-resolution imaging have been developed to distinguish stained exosomes from background contaminants (305). Nevertheless, these advanced instruments are costly and not commonly found in most laboratories. Therefore, the bead-based assay (BBA) is a widely adopted alternative, where EVs are coupled to larger beads recognized by fluorescently labeled antibodies targeting specific EV markers, allowing for further analysis by flow cytometry (269,306). This method overcomes the limitations of standard flow cytometers in detecting individual EVs and has been used in several studies, where EVs were coupled to 4µm latex beads, enabling the detection of surface antigens and efficient characterization of EV preparations (15,269,284,306).

Recent advances in "omic" technologies are becoming increasingly crucial for studying the functions and, specially, the molecular composition of EVs (307). Techniques such as proteomic, metabolomic, and microarrays have been employed for detailed molecular characterization of EVs (308). In recent years, 2-D gel electrophoresis and mass spectrometry (MS)-based proteomics have been applied to the EV field, leading to the discovery of novel signalling and secreted proteins with potentially significant physiological roles (309).

Proteomics can detect proteins at attomole levels, allowing efficient analysis of small sample volumes. This process involves the digestion of proteins followed by structural characterization using single-stage and tandem MS. The most commonly used technique in proteomic analysis of EVs is liquid phase chromatography coupled to MS (LC-MS/MS), which combines the physical

separation capabilities of chromatography with the mass analysis provided by MS (310). This technique is advantageous due to its simplicity and effectiveness in analysing hydrophobic and membrane proteins, which are often enriched in EVs. Additionally, these emerging "omic" technologies are expected to provide valuable insights into the structural features of EVs and aid in the development of innovative diagnostic, prognostic, and therapeutic strategies.

Also, characterization of the RNA cargo of EVs is challenging and highly depend on the purification method used. Contaminating RNAs, such as those from the FBS in cell culture media, can obscure human-derived RNAs species due to its similarity to bovine ones (e.g., miR-122) (311). Despite this, the presence of mRNAs, miRNAs and lncRNAs in exosomes and MVs have been consistently confirmed using microarrays and RT-qPCR (312–314). More recently, high-throughput RNA sequencing techniques has identified additional RNA species in EVs, including snRNA, snoRNA, piRNA, vault RNA, Y-RNA, scRNA, SRP-RNA, 7SK-RNA, and various RNA fragments from rRNA and tRNA (315–318).

1.3 Extracellular vesicles in malaria

Research on extracellular vesicle from both host and parasite sources has revealed their crucial roles in disease pathogenesis, susceptibility, intercellular signaling, and immune responses, in both health and disease (319,320). Since the first report on EVs in malaria in 2004 (321) significant progress has been made in understanding the role of EVs during the course of the disease. **Figure 19** represents the key milestones in the historical research on EVs in the malaria field.

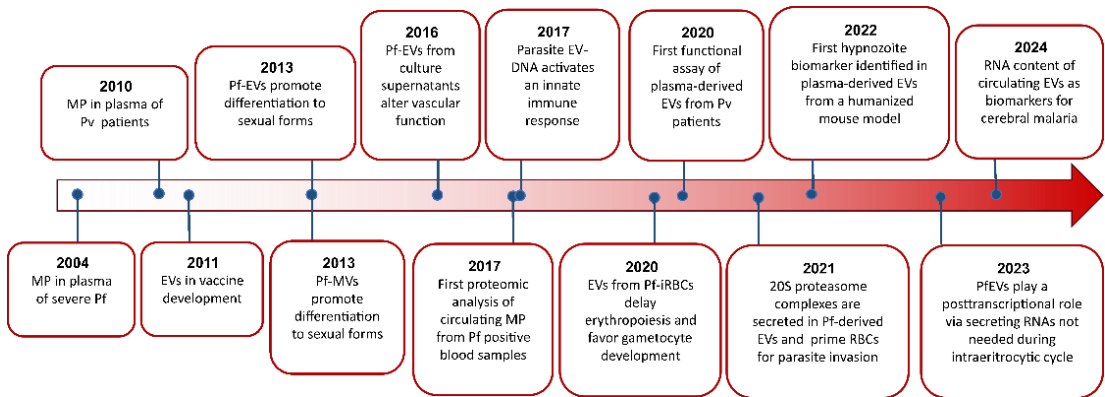


Figure 19. Key milestones in EV research in malaria. Created with InkScape.

1.3.1 Biogenesis, uptake and cargo of EVs in malaria

EVs play a crucial role in the pathophysiology of malaria (322,323). Produced by infected red blood cells (iRBCs) and other host cells, the biogenesis pathways and triggers for EV formation during *Plasmodium* infection remain unclear. Research suggests that circulating EVs increase with disease severity in malaria-infected individuals (321,324,325). Although infected red blood cells lack canonical vesicular trafficking pathways, they release EVs via an alternative endosomal sorting complex required for transport (ESCRT) mechanism (326). In *P. falciparum*, this process is mediated by the ESCRT-III sub-complex, involving PfBro1 and PfVps32/PfVps60 proteins, that are essential for the formation of exosomes and MVs in iRBCs (327). Further research is needed to fully understand these processes and their impact on malaria progression.

EVs from *P. falciparum*-infected red blood cells (Pf-iRBCs) and other host cells interact with host cell membranes to deliver cargo or transmit signalling (15,328–330). Ofir-Birin et al. developed an imaging flow cytometry method to track this internalization, revealing insights into EV-mediated signaling (328). *P. falciparum* exploits host sialylated N-glycans for EV uptake by immune cells, but further research is needed to determine if this applies to other host cells (331).

EVs derived from iRBCs with different stages of the malaria parasite display varying levels of EV markers compared to uninfected RBCs (332). Those originating from Pf-iRBCs are primarily released during later asexual cycle stages, originating from specific subdomains within the iRBC (329,333). These Pf-iRBC-derived EVs consistently contain a mixture of human and parasite-derived biomolecules across various parasite strains, including proteins associated with RBC membranes (e.g., Maurer's clefts, surface membrane proteins, parasitophorous vacuole membrane proteins) and proteins crucial for parasite invasion (e.g., erythrocyte-binding antigens, rhoptry proteins) (329,333,334). The selective loading mechanisms of certain protein families, such as PHIST and Rifin, in late-stage Pf-iRBC EVs suggest a targeted cargo delivery process. Conversely, EVs released during early parasite stages carry PfEMP1, triggering mild cytokine responses and transcriptional alterations in human monocytes, potentially shaping the host-parasite immune interactions during infection (322). Neta Regev-Rudzki's team identified different subtypes of EVs released by Pf-iRBCs, varying in size and protein content. Smaller EVs (10-70nm) carry proteins related to the complement, while larger EVs ones (30-300nm) contain functional 20S proteasome complexes (250,330). They also exhibit distinct abilities to fuse with early endosomes, suggesting different cellular targets (250). Pf-iRBC-derived EVs induce phosphorylation of glycophorin A and RBC membrane channels, impacting parasite invasion (331,335), though further research is needed to fully understand their significance.

Research on EVs from both natural *P. vivax* infections and humanized mouse models infected with *P. vivax* has uncovered several malaria antigens such as MSP7, MSP9, Serine-repeat antigen 1, and HSP70. These antigens show promise for vaccine development and may serve as biomarkers for hypnozoite infection (15,292,336,337). Moreover, MSP1, MSP3, and pHISTc, known for their immunogenic properties, have been identified in multiple proteomic analyses using varied purification methods and sample sources (15,292,336). Additionally, EVs from healthy donors' plasma contain a higher abundance of human proteins compared to those from *P. vivax*-infected patients, suggesting a selective sorting mechanism for human protein cargo during vivax malaria (15).

Besides proteins, EVs from Pf-iRBC-derived EVs contain host and parasite RNA (338,339) and genomic DNA (340). Among the different RNAs that have been reported to be found in Pf-iRBC-derived EVs, two-thirds are from human-origin and one-thirds have parasitic-origin, from miRNAs, tRNAs but also snoRNAs, snRNAs, rRNAs and piRNAs to even mRNA encoding to exported proteins and proteins linked to drug resistance (338,339). Of interest, *Plasmodium* parasites are unable to produce miRNAs (341,342) indicating that miRNAs found in EVs during malaria are originated exclusively from the host. However, parasite antigens appear to influence the production of the host miRNAs (10,343) which subsequently regulate the expression of *P. falciparum* genes through intricate mechanisms (344,345).

1.3.2 Cell-to-cell communication in malaria

EVs are crucial mediators of intercellular communication, delivering their cargo to recipient cells or interacting with receptors on target cell membranes to trigger signaling pathways, even without being internalized (14,15,335,338,345,346). Recent studies have highlighted the essential role of EVs in various cellular processes during malaria infection. EVs released by Pf-iRBCs facilitate communication between parasite and host cells. These EVs, including MVs and exosome-like vesicles, are internalized by iRBCs, promoting

the generation of parasite transmission stages by transferring parasite or host factors (**Figure 20**) (14,328). EVs from Pf-iRBCs can inhibit erythropoiesis *in vitro*, potentially aiding the development of gametocyte stages in immature red blood cells (180). Additionally, circulating EVs from *P. vivax*-infected patients signal human spleen fibroblasts, enhancing cytoadherence and contributing to the formation of splenic niches in vivax malaria (15). These vesicles also carry DNA, which can be transferred to other iRBCs or host cells, impacting parasite virulence and host immune responses. For instance, EVs can transfer drug resistance genes between parasites, modulate host gene expression through the STING-dependent DNA sensing pathway, and present plasmodial antigens, influencing immune responses during infection (14,340).

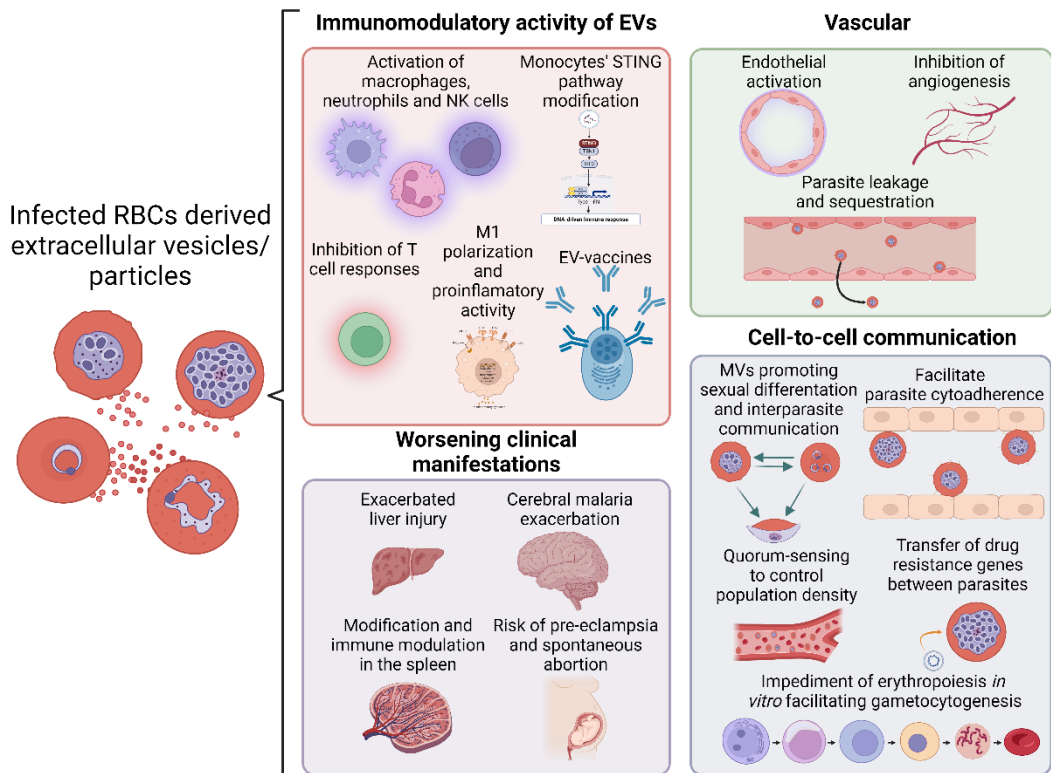


Figure 20. Overview of effects caused by extracellular vesicles derived from infected RBCs. Adapted from Annex I. Created with BioRender.

Proteomic analysis of late-stage parasite EVs has revealed the presence of invasion-related proteins, suggesting roles in antigen presentation and immune modulation (328). Furthermore, EVs from severe malaria strains induce

stronger monocyte responses than those from non-severe strains, though miRNAs seem not to play a major role in this process (347). In vivax malaria, patient-derived plasma EVs interact more with spleen cells than those from healthy donors, indicating a role in immune modulation (348). Lastly, a quorum-sensing role for Pf-iRBC EVs has been proposed, where EVs from high parasite density cultures regulate the parasite population (322). Collectively, these findings underscore the multifaceted roles of EVs in malaria pathogenesis and host-parasite interactions (**Figure 20**).

1.3.3 EVs role in malaria pathology: vascular dysfunction, severe malaria and placental malaria

EVs play critical roles in malaria-related vascular dysfunction. Elevated levels of red-cell MVs in *P. falciparum* malaria patients correlate with disease severity and vascular issues (325). Spleen clearance significantly contributes to the removal of these MVs, as splenectomised patients exhibit increased MV levels. MVs from infected red blood cells iRBCs modulate endothelial cell responses, leading to altered barrier properties, increased pro-inflammatory cytokines, endothelial activation, leakage, and parasite sequestration (345,349).

Severe malaria, primarily caused by *P. falciparum* but also by *P. vivax* and *P. knowlesi*, features vital organ dysfunction, from impaired consciousness, acidosis, hypoglycaemia, severe anaemia, renal impairment, jaundice, pulmonary edema and bleeding from various sites, all characterized by hyperparasitaemia (350). MVs are pivotal in the pathogenesis of cerebral malaria, with studies showing reduced MV numbers and procoagulant activity in mice lacking the *abca1* gene (351). Polymorphisms in the *abca1* gene are associated with plasma MV levels in malaria patients, influencing disease severity (352). EVs loaded with miR-451a and let-7i-5p have shown anti-inflammatory potential during heme-induced inflammation, correlating with reduced *P. falciparum* counts (353). In cerebral malaria (CM), EVs contribute to endothelial activation, adhesion of Pf-iRBCs, and release of endothelial MVs (65,321,325,354). Recently, EVs in circulation have been proved to be useful

markers for cerebral malaria severity as they do contain transcripts derived from cerebral cells, correlating with disease severity (355). These features prove their involvement in cell-to-cell interactions, signalling, inflammation, coagulation, and vascular function as well as their utility as disease markers. Elevated endothelial MVs and TNF- α levels are distinctive in CM and revert to baseline post-infection (356). These MVs carry procoagulant and pro-inflammatory properties, exacerbating endothelial damage. EVs from infected RBCs influence microglial gene expression, increasing TNF α and reducing IL-10, thereby altering immune responses (352,357,358). Finally, during placental malaria, active infection is not associated with changes in MV concentrations but affects miRNA expression in placental MVs. Specifically, miR-517c, part of the C19MC cluster, is overexpressed in mothers with placental malaria and linked to increased placental weight, pre-eclampsia, and recurrent spontaneous abortion, indicating its potential as a biomarker for placental malaria (359).

Overall, EVs play multifaceted roles in malaria pathogenesis, influencing vascular dysfunction, immune responses, and disease severity across various forms of malaria, including cerebral and placental malaria.

1.3.4 *P. vivax*-derived EVs and its role in cryptic infections

In the context of *P. vivax* and their cryptic niches, a recent study from our group utilized circulating EVs from patients infected with *P. vivax* (PvEVs) to investigate their interactions with human spleen cells *in vitro*. In this study, it was possible to identify *P. vivax* proteins associated with plasma-derived EVs from vivax malaria patients using size-exclusion chromatography and mass spectrometry (15). This research, also provided insights into the pathophysiological processes involving the spleen in vivax malaria (15). This study showed that PvEVs were taken up by human spleen fibroblasts (hSFs), inducing the expression of ICAM-1 via NF- κ B nuclear translocation. Following hSF activation by PvEVs, *P. vivax*-reticulocytes exhibited increased adhesion to the stimulated cells with PvEVs (**Figure 21**) (15). These findings offered new

insights into the mechanisms of *P. vivax* pathology, highlighting the roles of cytoadherence and sequestration in the spleen.

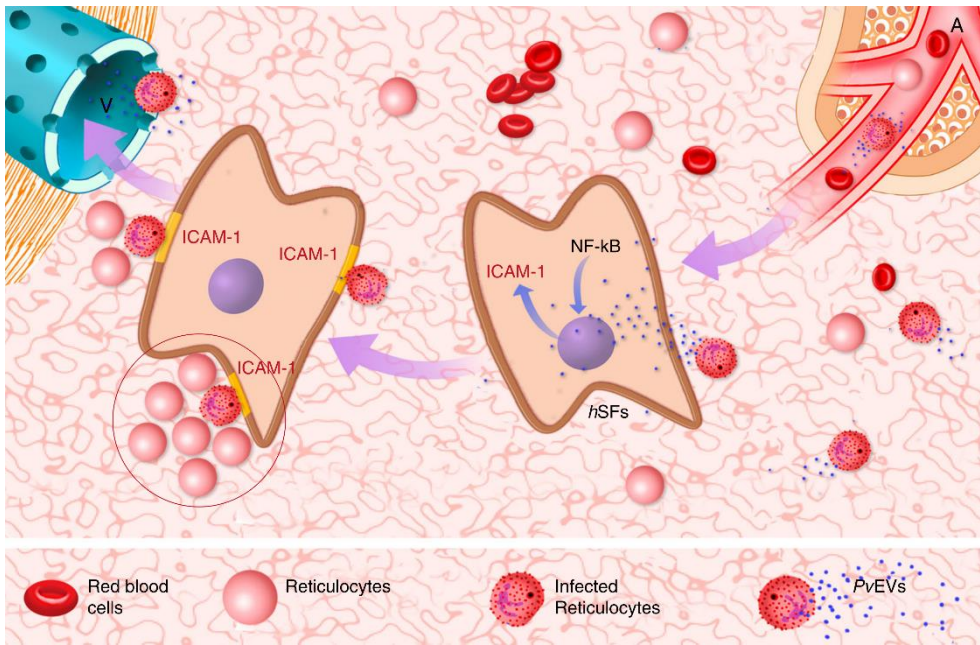
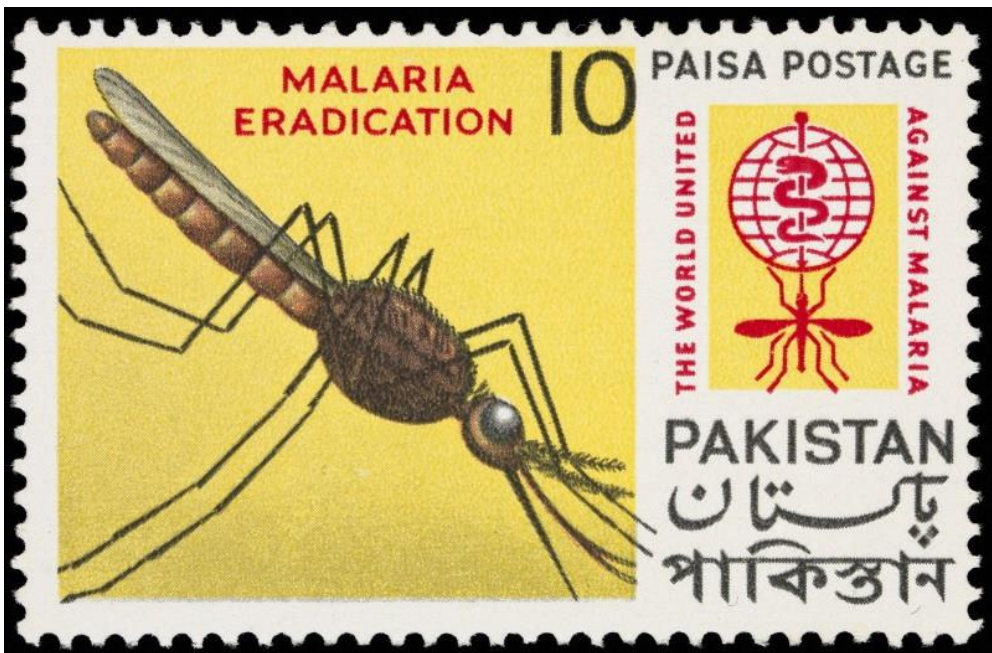


Figure 21. Spleen model of the physiological role of EVs in *P. vivax*. Circulating plasma-derived extracellular vesicles from infected cells (PvEVs) enter the microvasculature of the spleen and are uptake by human spleen fibroblasts (hSFs). This event signals NF- κ B for translocation to the nucleus and transcription of ICAM-1. After translation of ICAM-1 and expression at the surface of hSFs, infected reticulocytes bind to these cells in a niche rich in reticulocytes (circled) where parasites can invade and multiply. A, arteriole; V, venule. Reproduced from (15).

Regarding the proteomic profiling of the circulating EVs from patients, using direct immunoaffinity to capture the specific subcellular population of reticulocyte-derived EVs, which express CD71, it was possible to detect a huge variety of parasite proteins in those EVs (292).

Additionally, research using liver-humanized mouse models, which can sustain *P. vivax* infections, has facilitated the study of PvEVs from this source (337). In these models, parasite proteins were also identified in EVs from the plasma, presenting new avenues for researching biomarkers for vivax liver infection, including hypnozoites (337).

2. HYPOTHESIS AND OBJECTIVES



Malaria eradication : the world united against malaria. 10 paise postage stamp showing a mosquito in profile on a yellow background and the International year of malaria symbol.
Picture: L0074987 Wellcome Library, London. Wellcome Images

2.1 Hypothesis

We hypothesize that during natural *P. vivax* infections, the **spleen** and the **bone marrow** constitute **cryptic niches** favouring the growth and differentiation of parasites in these reticulocyte-enriched tissues. In addition, we also postulate that this process involves spleen/bone marrow **specific parasite proteins** and that **extracellular vesicles facilitate** the formation of these **cryptic erythrocytic niches**.

2.2 Objectives

The main objective of this project is the identification, validation and functional characterization of *P. vivax* genes whose expression is spleen and bone marrow dependent to determine their role during acute vivax malaria infection and to unveil the role of extracellular vesicles in these haematopoietic tissues.

Objective 1: Identification and validation of genes differentially expressed in the spleen & bone marrow through global transcriptional and computational analysis.

Objective 2: Generation of *P. falciparum* transgenic lines, using CRISPR/Cas9 technology, expressing some of those genes.

Objective 3: Functional characterization of *P. vivax* genes preferentially expressed in the human spleen and bone marrow and the role of extracellular vesicles in these haematopoietic tissues

3. MATERIALS, METHODS & RESULTS



Members of the Malaria Commission of the League of Nations collecting larvae on the Danube delta, 1929. Photo number: L0011626. Wellcome Images

3.1 Article 1: *Plasmodium vivax* spleen-dependent genes encode antigens associated with cytoadhesion and clinical protection

Objective 1: Identification and validation of genes differentially expressed in the spleen & bone marrow through global transcriptional and computational analysis.

Title: *Plasmodium vivax* spleen-dependent genes encode antigens associated with cytoadhesion and clinical protection.

Authors: Carmen Fernandez-Becerra, Maria Bernabeu, Angélica Castellanos, Bruna R. Correa, Thomas Obadia, Miriam Ramirez, Edmilson Rui, Franziska Hentschel, Maria López-Montañés, **Alberto Ayllon-Hermida**, Lorena Martin-Jaular, Aleix Elizalde-Torrent, Peter Siba, Ricardo Z. Vêncio, Myriam Arevalo-Herrera, Sócrates Herrera, Pedro L. Alonso, Ivo Mueller, Hernando A. del Portillo.

Journal: Proceedings of the National Academy of Sciences of the United States of America.

Year: 2020

Volume: 117

Issue: 23

Pages: 13056 – 13065

Impact Factor: 11.1

Quartile and Research area: Q1 Multidisciplinary Sciences.

DOI: <https://doi.org/10.1073/pnas.1920596117>



Plasmodium vivax spleen-dependent genes encode antigens associated with cytoadhesion and clinical protection

Carmen Fernandez-Becerra^{a,b,1} , Maria Bernabeu^{a,2}, Angélica Castellanos^c , Bruna R. Correia^{d,3}, Thomas Obadia^e, Miriam Ramirez^a, Edmilson Rui^a, Franziska Hentzschel^{a,4}, Maria López-Montañés^e, Alberto Ayllon-Hermida^a, Lorena Martin-Jaular^{a,5} , Aleix Elizalde-Torrent^{a,6}, Peter Siba^f, Ricardo Z. Vêncio^d, Myriam Arevalo-Herrera^c , Sócrates Herrera^c, Pedro L. Alonso^{a,7}, Ivo Mueller^{e,g}, and Hernando A. del Portillo^{a,b,h,1}

^aISGlobal, Hospital Clinic, Universitat de Barcelona, Barcelona 08036, Spain; ^bInstitut d'Investigació Germans Trias i Pujol, Badalona 08916, Spain; ^cCentro de Investigación Científica Caucesco, Cali, Valle, Colombia ^dDepartment of Computing and Mathematics FFCLRP, Ribeirão Preto, Universidade de São Paulo, São Paulo 14040-900, Brazil; ^eDepartment of Parasites and Insect Vectors, Institut Pasteur, Paris 75015, France; ^fPapua New Guinea Institute of Medical Research, Madang, Papua New Guinea; ^gPopulation Health and Immunity Division, The Walter and Eliza Hall Institute of Medical Research, Parkville, VIC 3052, Australia; and ^hInstitució Catalana de Recerca i Estudis Avançats, Barcelona 08010, Spain

Edited by Louis H. Miller, National Institute of Allergy and Infectious Diseases, NIH, Rockville, MD, and approved April 16, 2020 (received for review November 23, 2019)

Plasmodium vivax, the most widely distributed human malaria parasite, causes severe clinical syndromes despite low peripheral blood parasitemia. This conundrum is further complicated as cytoadherence in the microvasculature is still a matter of investigations. Previous reports in *Plasmodium knowlesi*, another parasite species shown to infect humans, demonstrated that variant genes involved in cytoadherence were dependent on the spleen for their expression. Hence, using a global transcriptional analysis of parasites obtained from spleen-intact and splenectomized monkeys, we identified 67 *P. vivax* genes whose expression was spleen dependent. To determine their role in cytoadherence, two *Plasmodium falciparum* transgenic lines expressing two variant proteins pertaining to VIR and Pv-FAM-D multigene families were used. Cytoadherence assays demonstrated specific binding to human spleen but not lung fibroblasts of the transgenic line expressing the VIR14 protein. To gain more insights, we expressed five *P. vivax* spleen-dependent genes as recombinant proteins, including members of three different multigene families (VIR, Pv-FAM-A, Pv-FAM-D), one membrane transporter (SECY), and one hypothetical protein (HYP1), and determined their immunogenicity and association with clinical protection in a prospective study of 383 children in Papua New Guinea. Results demonstrated that spleen-dependent antigens are immunogenic in natural infections and that antibodies to HYP1 are associated with clinical protection. These results suggest that the spleen plays a major role in expression of parasite proteins involved in cytoadherence and can reveal antigens associated with clinical protection, thus prompting a paradigm shift in *P. vivax* biology toward deeper studies of the spleen during infections.

Plasmodium vivax | spleen-dependent genes | cytoadherence | global transcription

Human malaria caused by *Plasmodium vivax* infection (vivax malaria) is a major global health issue. It is the most geographically widespread form of the disease, accounting for 7.5 million annual clinical cases, the majority of cases in America and Asia, and estimation of over 2.5 billion people living under risk of infection (1). The general perception toward vivax malaria has shifted recently, following a series of reports, from being viewed as a benign infection to the recognition of its potential for more severe manifestations, including fatal cases (2–4). However, the underlying pathogenic mechanisms of vivax malaria remain largely unresolved.

Central to the pathology in *Plasmodium falciparum*, the most virulent malaria-causing human species, is the phenomenon of cytoadherence to endothelial receptors mediated by variant surface

proteins that facilitate sequestration of parasitized red blood cells (RBCs) deep in microvasculature (5). The absence of mature parasites in peripheral blood of patients is unequivocal evidence of cytoadherence and parasite sequestration in this species. In contrast,

Significance

In spite of low peripheral blood parasitemia, vivax malaria causes severe disease. This conundrum finds an explanation from reports suggesting that the spleen is a place for parasite sequestration. We performed a global transcriptional analysis of parasites that grew in the presence or absence of the spleen in a nonhuman primate model. We identified 67 spleen-dependent genes, including multigene variant families, and functionally demonstrated specific adherence to human spleen fibroblasts by a member of such families. Moreover, we further demonstrated that spleen-dependent *Plasmodium vivax* genes code for immunogenic proteins during natural infections. Our results indicate that this organ plays an important function in *P. vivax* malaria and call for deeper studies of the role of spleen in *P. vivax* infections.

Author contributions: C.F.-B., M.B., B.R.C., L.M.-J., R.Z.V., M.A.-H., S.H., P.L.A., I.M., and H.A.d.P. designed research; C.F.-B., M.B., A.C., M.R., E.R., F.H., M.L.-M., L.M.-J., A.E.-T., and H.A.d.P. performed research; P.S. contributed new reagents/analytic tools; C.F.-B., M.B., B.R.C., T.O., A.A.-H., R.Z.V., M.A.-H., S.H., I.M., and H.A.d.P. analyzed data; and C.F.-B. and H.A.d.P. wrote the paper.

The authors declare no competing interest.

This article is a PNAS Direct Submission.

This open access article is distributed under [Creative Commons Attribution-NonCommercial-NoDerivatives License 4.0 \(CC BY-NC-ND\)](https://creativecommons.org/licenses/by-nc-nd/4.0/).

Data deposition: All data are freely available through the Gene Expression Omnibus database, <https://www.ncbi.nlm.nih.gov/geo> (accession no. GPL6667).

¹To whom correspondence may be addressed. Email: carmen.fernandez@isglobal.org or hernandoa.delportillo@isglobal.org.

²Present address: European Molecular Biology Laboratory, Barcelona 08003, Spain.

³Present address: Centre for Genomic Regulation, The Barcelona Institute of Science and Technology, Barcelona, Catalonia 08003, Spain.

⁴Present address: Wellcome Centre for Integrative Parasitology, Institute of Infection, Immunity and Inflammation, University of Glasgow, Glasgow 120, United Kingdom.

⁵Present address: INSERM U932, Institut Curie Centre de Recherche, PSL Research University, Paris 75005, France.

⁶Present address: IrsiCaixa AIDS Research Institute, Hospital Germans Trias i Pujol, Badalona, Catalonia 08916, Spain.

⁷Present address: World Health Organization, Geneva 1211, Switzerland.

This article contains supporting information online at <https://www.pnas.org/lookup/suppl/doi/10.1073/pnas.1920596117/-DCSupplemental>.

First published May 21, 2020.

as infected reticulocytes with mature stages of *P. vivax* are detected in peripheral circulation, for a long time it was amply accepted that this human malaria parasite does not sequester in the microvasculature. Against this dogma, in the last decade, different reports have described in vitro cytoadherence of *P. vivax*-infected reticulocytes to

human cells and tissue cryosections (6–8). Moreover, infected reticulocytes were able to cytoadhere under static and flow conditions to cells expressing ICAM-1, a well-known *P. falciparum* receptor, and this binding was partly mediated by VIR proteins (6), a superfamily of variant surface proteins likely

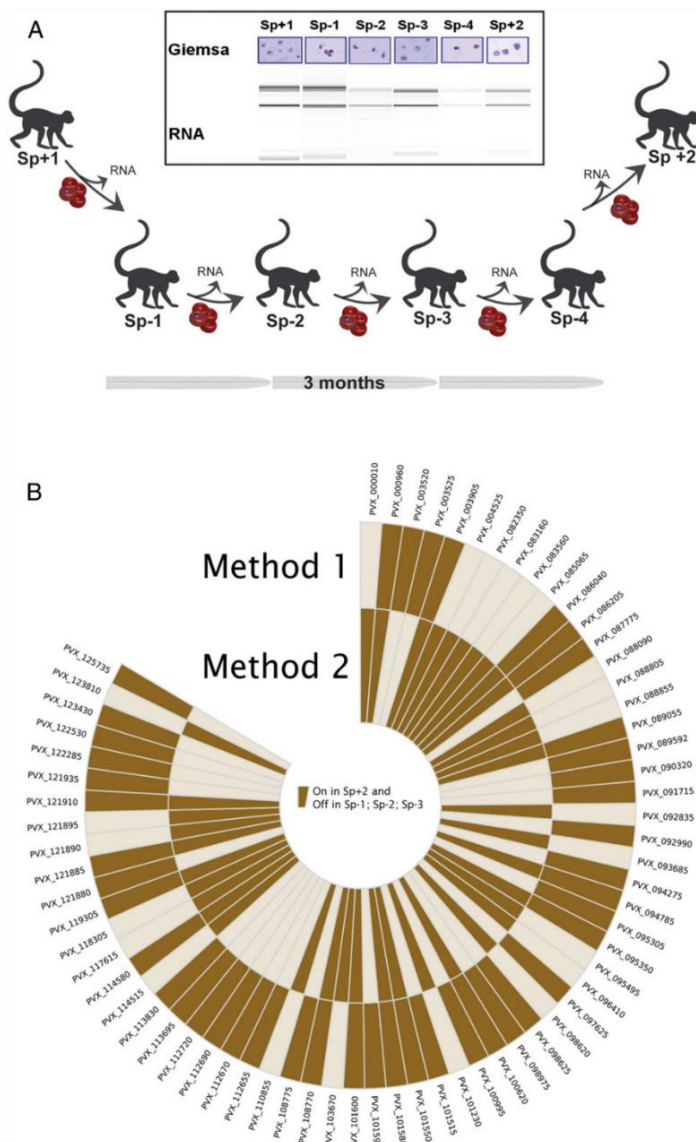


Fig. 1. Identification of *P. vivax* spleen-dependent genes. (A) Scheme of experimental infections and biological samples used for expression analysis. (B) Diagram showing genes only expressed in Sp+2 and negative in the splenectomized monkeys for any of the two algorithms used.

involved in cytoadherence (9, 10). Therefore, even though the exact molecular mechanisms of cytoadherence are not fully elucidated, these observations prompt a paradigm shift in *P. vivax* biology.

Malaria parasites infections induce a dramatic splenic response mostly characterized by variable levels of splenomegaly. This is probably due to the fact that the spleen plays an important dual role in malaria: destruction of infected red blood cells (iRBCs) and expression of parasite antigens, including variant surface proteins involved in pathology (11, 12). Thus, pioneering experiments with *Plasmodium knowlesi* parasites obtained from splenectomized monkeys showed that parasites no longer expressed variant antigens (SICA) on the surface of iRBCs and that immune sera from these animals failed to agglutinate iRBCs with mature stages (13). Upon passage of these parasites into monkeys with intact spleens, however, parasites recovered the expression of SICA antigens, and immune monkey sera showed the agglutinating phenotype. In a more recent study, it has been demonstrated that the spleen plays an important role in controlling the transcriptional and posttranscriptional expression of SICAvary antigens (14). Similar observations on expression of variant proteins were also made in monkey models of *P. falciparum*

(15) and *Plasmodium fragile* (16) as well as in a rodent *Plasmodium chabaudi* model (17). In *P. falciparum* splenectomized patients, iRBCs present low expression of surface variant proteins and appearance of mature stages in peripheral blood, likely due to an impairment of parasite tissue sequestration (18, 19). In addition, in immune (19) and nonimmune individuals (20, 21), the absence of the spleen results in increased disease severity.

Altogether, these data support a major role of the spleen in modulating the expression of variant virulent determinants in malaria involved in cytoadherence. We thus hypothesized that *P. vivax* coding genes whose expression is dependent on an intact spleen will allow the identification of antigens involved in spleen cytoadherence and pathogenesis; to test this hypothesis, we used a global transcriptional approach in experimental *P. vivax* infections of spleen-intact and splenectomized *Aotus* monkeys to identify genes whose expression is spleen dependent.

Results

Identification of *P. vivax* Coding Genes with Intact Spleen-Dependent Expression. To identify *P. vivax* genes whose expression is spleen dependent, a series of experimental infections with the *P. vivax*

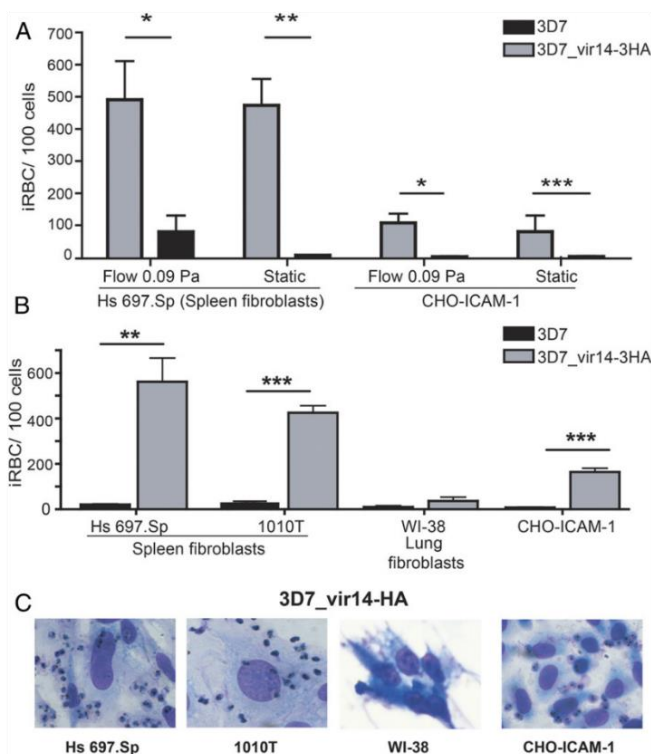


Fig. 2. VIR14 protein mediates adhesion to spleen fibroblasts. A *P. falciparum* transgenic line (3D7_vir14-3HA) previously reported to express VIR14 at the surface of iRBCs (23) showed cytoadhesion to spleen fibroblasts. Cytoadherence was expressed as iRBC per 100 cells. Significant higher binding than the *P. falciparum* 3D7 parental strain is represented by asterisks (unpaired *t* test). Results are shown as the mean of the binding \pm SEM of three to five experiments. (A) Cytoadherence of 3D7 and the *P. falciparum* transgenic line 3D7_vir14-3HA to CHO-ICAM-1 cells and human spleen fibroblasts Hs 697.Sp under static and flow conditions at a wall shear stress of 0.09 Pa. (B) Cytoadherence of 3D7 and 3D7_vir14-3HA to CHO-ICAM-1 cells, lung fibroblasts WI-38, and spleen fibroblasts Hs 697.Sp and 1010T under static conditions. **P* < 0.05; ****P* < 0.001; *****P* < 0.0005. (C) Representative images of cytoadhesion of transgenic line 3D7_vir14-3HA to human spleen fibroblasts Hs 697.Sp (column 1) and 1010T (column 2), lung fibroblasts WI-38 (column 3), and CHO-ICAM-1 (column 4).

Salvador-1 (Sal-1) strain was performed in splenectomized (Sp-) and spleen-intact (Sp+) *Aotus* monkeys (Fig. 1A). After each infection, Giemsa smears were performed daily to determine the time to patency and peak of parasitemias (SI Appendix, Table S1). At peak parasitemias, mature parasites (multinuclei schizonts) were affinity purified (Fig. 1A). Although this purification step drastically reduced the total numbers of iRBCs, it was essential to achieve the highest level of comparability within the dataset. Dual hybridizations comparing the global expression of parasites obtained from the different experimental infections (labeled with Cy5) with a reference pool PvSp-1 obtained from splenectomized monkeys from the Centers for Disease Control and Prevention (CDC) donated by John Barnwell, Malaria Branch, Division of Parasitic Diseases and Malaria, CDC, Atlanta, GA (labeled with Cy3) were performed using an Agilent custom-made array containing 5,038 *P. vivax* coding genes (one 60-base oligonucleotide at every 2 kb) as annotated (10). Use of this reference pool from the CDC was needed due to the limited amounts obtained from our groups of monkeys Sp-1. Of note, sample Sp-4 was not included in these analyses due to insufficient amount of total RNA obtained. All data are freely available through the Gene Expression Omnibus (GEO) database (GEO accession no. GPL6667).

Two different statistical algorithms were used for expression analysis (SI Appendix, Fig. S1). In the first model, probe intensities were compared with negative controls. Average intensity of each probe was compared with the probability density function of the negative controls. If expression probability of negative controls was less than 0.001 compared with the probe, this probe was classified as “on.” If it was greater than 0.05, probe was considered “off.” In the second model, a 0.98 quantile of negative controls intensity was used as a cutoff. Probes presenting average intensity at least 10 times greater than this cutoff were considered on, and the ones with average intensity below the quantile were classified as off. For each model, selected genes were those presenting the following expression pattern: off in Sp-1, Sp-2, and Sp-3 and on in Sp+2. Using these criteria, a total of 67 spleen-dependent genes were identified, with close to 50% of them located in subtelomeric regions and around 26% in chromosome 14 (SI Appendix, Table S2). Genes could be grouped into those pertaining to multigene families, such as variant surface proteins (VIR) and *Pv-fam* genes. In addition, a high number of exported and hypothetical proteins and to a lesser extent, some enzymes and binding proteins were also identified (SI Appendix, Table S2).

VIR14 Protein Mediates Specific Adhesion to Human Spleen Fibroblasts. We have previously hypothesized that variant VIR proteins of *P. vivax* mediate cytoadherence to spleen barrier cells of fibroblastic origin (22). To test this hypothesis, we selected the PVX_108770 gene, encoding for VIR14, as its expression was predicted to be spleen dependent by two different algorithms (SI Appendix, Table S2). In the absence of long-term *P. vivax* in vitro culture, it had been previously used to generate a *P. falciparum* transgenic line (3D7_vir14-human influenza hemagglutinin [HA]) (23). In this transgenic line, VIR14 was localized at the surface of iRBC and showed cytoadhesion to CHO cells expressing the ICAM-1 receptor. To assess the cytoadhesion properties of this VIR protein to spleen fibroblasts, we first tested a commercial spleen fibroblast cell line, Hs 697.Sp (ATCC). This cell line was obtained from a patient who previously had a granulomatous lymph node and Hodgkin's disease without spleen involvement. Compared with the parental strain 3D7, cytoadherence of the transgenic line 3D7_vir14-3HA was significantly higher under flow and static conditions (Fig. 2A and C). Moreover, adhesion to Hs 697.Sp was five times higher than the previously reported adhesion to CHO-ICAM-1 cells. To avoid confounding due to the pathogenic origin of cell line Hs

697.Sp, we generated a spleen fibroblast cell line (1010T) derived from a transplantation donor with a healthy spleen by culturing homogenized spleen cells for 3 wk. The transgenic strain 3D7_vir14-3HA also presented significantly higher adhesion to 1010T fibroblasts compared with the 3D7 parental strain (Fig. 2B and C). To further determine the specificity of adhesion to spleen fibroblasts, static adhesion experiments were done using commercial lung fibroblasts (WI-38). No significant adhesion of the transgenic line 3D7_vir14-3HA was found to the WI-38 lung fibroblasts when compared with the 3D7 parental strain (Fig. 2B and C).

A Member of the Pv-FAM-D Multigene Family Has No Direct Role in Cytoadhesion. To determine if members of other multigene families whose expression was also dependent on an intact spleen cytoadhere to spleen fibroblasts, we generated a *P. falciparum* transgenic line (3D7_PvFamD-3HA) expressing a member of the Pv-FAM-D multigene family identified by both algorithms (PVX_101580). Moreover, to avoid confounding, this transgenic line was generated using the same expression vector that the one used to generate the 3D7_vir14-3HA transgenic line (Fig. 3A) (23). Expression was validated by RT-PCR (Fig. 3A) and indirect immunofluorescence (Fig. 3B and C). Colocalization assays with antibodies raised against conserved intracellular acidic terminal segment of PfEMP1 (anti-ATS) revealed that Pv-FAM-D is located at the iRBCs membrane, partially colocalizing with the cytoplasmic domain of PfEMP1 (Fig. 3B). Lack of a more punctuated pattern as seen in 3D7 with anti-ATS antibodies (24) is likely due to a different fixation procedure, which gives images similar to those of 3D7 smears fixed with methanol (25). Surface expression was further validated in live immunofluorescence assays (Fig. 3C).

Cytoadherence assays showed no significant binding of this transgenic line to human endothelial receptors expressed in CHO cells nor to human Hs 697.Sp or 1010T spleen fibroblasts (Fig. 3D and E). A similar or even lower adhesion than the 3D7 parental strain was found. Additionally, a role in adhesion to lung fibroblasts was excluded as no adhesion of the 3D7_PvFamD-3HA transgenic line was observed to WI-38 lung fibroblasts (Fig. 3E).

Naturally Acquired Immune Responses of *P. vivax* Spleen-Dependent Antigens. To determine if *P. vivax* spleen-dependent antigens are targets of naturally acquired immune responses, a list of genes for complementary DNA (cDNA) amplification and cloning into the pVEXGST1.4d vector was selected for expression as glutathione S-transferase (GST)-tagged proteins using the wheat germ in vitro expression system (SI Appendix, Table S3) (26). Selection criteria were all members pertaining to subtelomeric multigene families (*vir* and *Pv-fam* genes) by any of the two algorithms used. In addition, we also selected the rest of the genes predicted by the two algorithms, excepting those annotated as enzymes or RNA binding proteins. Unfortunately, despite several different attempts, most of the genes, including PVX_101580, were either unclonable or expressed as insoluble products. Therefore, only five genes representing three different multigene families VIR14 (PVX_108770), Pv-FAM-A (PVX_112670), and Pv-FAM-D (PVX_121910); one membrane transporter SECY (PVX_000960); and one hypothetical protein HYP1 (PVX_114580) were expressed as soluble products in the wheat germ system (SI Appendix, Fig. S2) (26). We also expressed a GST-tagged MSPI-19 protein as a control of exposure as this is a highly immunogenic protein in natural vivax infections (27). Immune sera from a retrospective study (28), including 383 children from 1.2 to 5.6 y of age from Papua New Guinea (PNG), were used in multiplex assays as described (26). Recurrence of *P. vivax* in this cohort was high with 91.3 and 76.5% of children

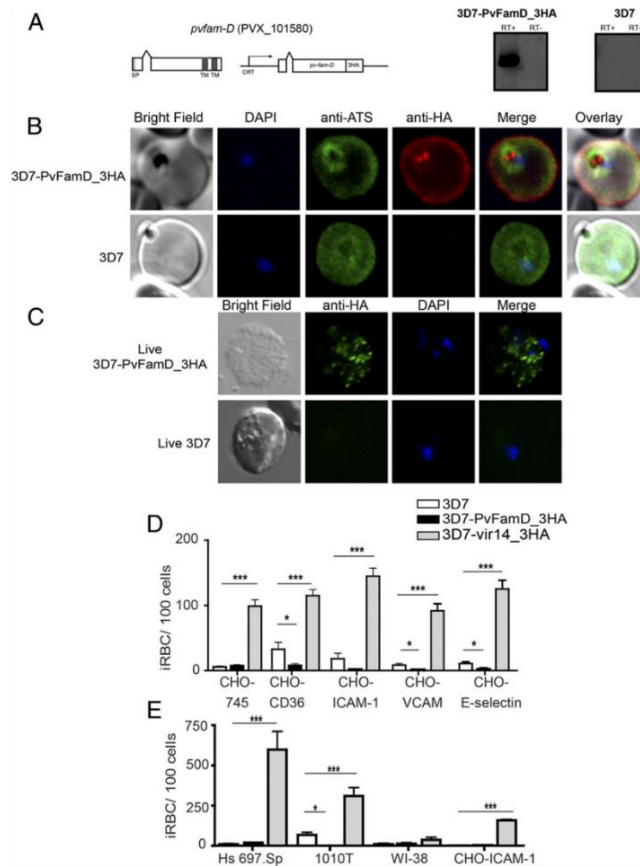


Fig. 3. The multigenic family Pv-FAM-D is expressed in the surface of the *P. falciparum* transgenic line, and it is not implicated into adhesion to endothelial receptors and human spleen and lung fibroblasts. (A) Schematic representation of the Pv-FAM-D expression cassette. SP indicates signal peptide, TM indicates transmembrane domain, CRT indicates promoter region of the chloroquine resistance transporter gene, and 3HA indicates triple human influenza hemagglutinating tags (Left). RT-PCR expression of the *pv-fam-d* gene (Right). RT+ indicates cDNA treated with reverse transcriptase, and RT- indicates not treated. (B) Coimmunofluorescence images of transgenic strain 3D7_PvFamD-3HA (Upper) and 3D7 (Lower) labeled with anti-HA (red), anti-ATS (green), and DAPI for nuclear staining. The first column represents differential interference contrast microscopy (DIC), the fifth column represents the merge of the fluorescent staining, and the sixth column represents the overlay of all five images. (C) Live immunofluorescence assay. The anti-HA (green) antibody recognized the 3D7_PvFamD-3HA transgenic line and did not recognize the 3D7 parental strain (Lower). The first column represents DIC, the third column represents DAPI for nuclear staining, and the fourth column represents the overlay of all images. (D) Cytoadherence to CHO cells expressing endothelial receptors. Cytoadherence was expressed as iRBCs per 100 CHO cells. (E) Cytoadherence to human fibroblasts (Hs 697.Sp, 1010T, and WI-38) and CHO-ICAM-1 cells. Significant differences in cytoadhesion are marked with asterisks (unpaired t test). Results are shown as the mean of the binding \pm SEM of three to five experiments. * $P < 0.05$; *** $P < 0.005$.

experiencing a PCR- or light microscopy-detectable *P. vivax* by week 6, respectively (28).

At baseline, 26.4% (HYP1) and 75.6% (VIR14) of children had antibodies to the spleen-dependent antigens, whereas 67.1% of children had antibodies to the nonspleen-dependent MSP1-19 antigen (Fig. 4A). Antibodies to PvFAM-D2, SECY, and VIR14 were significantly less commonly observed at week 6 than week 0 ($P < 0.01$) but recovered to pretreatment level at week 40 for PvFAM-D2 and Secy. The prevalence of antibodies to MSP1-19, PvFAM-A2, and HYP1 did not change from week 0 to 6 but

decreased significantly by week 40 ($P \leq 0.03$) (Fig. 4A). The prevalence of antibodies to VIR14 and HYP1 increased significantly with age ($P \leq 0.002$), indicating continued natural acquisition of immunity (Fig. 4B), whereas antibodies to PvFAM-D2 and MSP1-19 were significantly more common in children with concurrent *P. vivax* infections (as detected by light microscopy and/or PCR) (Fig. 4C). After adjusting for difference in exposure, children with antibodies against HYP1 (hazard ratio [AHR] = 0.65, confidence interval [CI]95 [0.46, 0.92], $P = 0.01$) showed significant association with protection against clinical

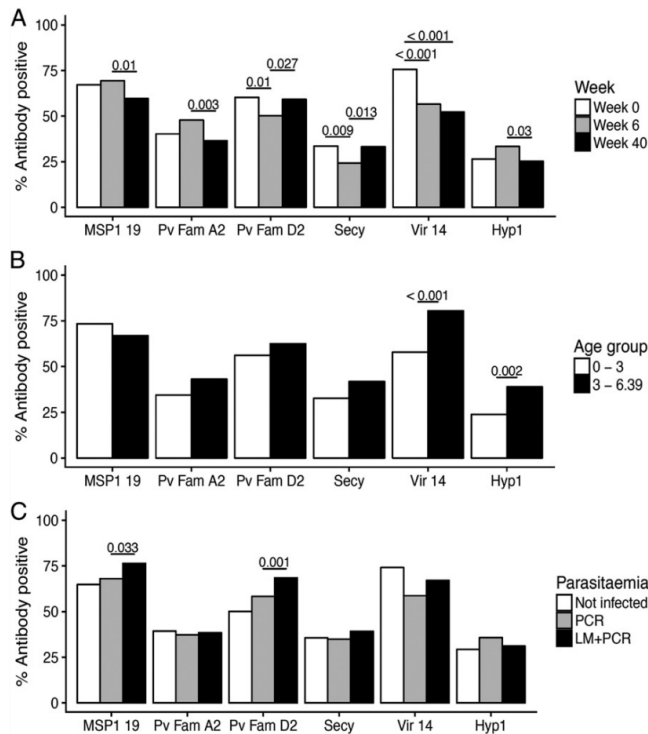


Fig. 4. Prevalence of positive antibody titers according to (A) week of follow-up, (B) age group cut at median, and (C) detectable parasitemia. A positive antibody titer was defined for MFI above mean +2 SD of negative controls. *P* values were adjusted for multiple pairwise comparisons using Tukey's method.

P. vivax episodes during follow-up (SI Appendix, Table S4). Children with antibodies to the spleen-dependent PvFAM-D2, however, tended to be at increased risk of acquiring new *P. vivax* during follow-up (light microscopy [LM] positive: AHR = 1.23, CI95 [0.99, 1.52], *P* = 0.056), although not reaching statistical significance. No associations with risk of *P. vivax* infection or disease were observed for antibodies to any of the other antigens.

Discussion

Analysis of infections in splenectomized hosts has demonstrated that the spleen plays a major role in modulating expression of malaria variant multigene families involved in cytoadherence. To understand the role of the spleen in the expression of *P. vivax* genes, we used experimental *P. vivax* infections in splenectomized and spleen-intact *Aotus* monkeys and performed global transcriptional analyses of highly pure and synchronous parasite populations. We demonstrated that 67 coding genes largely located at subtelomeric regions are dependent on the spleen for expression and that such antigens are targets of naturally acquired immune responses.

Several reports based on global transcriptional analysis using customized microarray platforms (29–31), and more recently, on RNA sequencing (RNA-seq), have been applied to sequence *P. vivax* isolates (32–34). These expression data analyses have identified stage-specific and differentially expressed genes coding for proteins with functions related to parasitic development,

virulence capacity, and/or host–parasite interaction, among others. We customized an Agilent microarray representing all coding genes of the Salvador 1 reference strain (10) and identified genes whose expression was dependent on the presence of the spleen in experimental *P. vivax* infections of spleen-intact and splenectomized *Aotus* monkeys. From the 67 spleen-dependent genes identified, close to 50% were located at subtelomeric regions and pertained to variant multigene families (VIR proteins, Pv-FAM-D proteins, and *Plasmodium* exported proteins) (SI Appendix, Table S2). Genes belonging to these multigene families are among the most expressed genes in isolates obtained from different patients, underscoring the importance of variant antigens in natural infections (29–33). Noticeably, gene PVX_108770 (VIR14) pertaining to the *vir* multigene family and shown here to mediate specific cytoadhesion to human spleen fibroblasts was present in the list of 25 *vir* genes highly expressed in clinical isolates (30). Our previous results showed that *P. vivax* VIR proteins present different subcellular localizations revealing that they might play different functions. Additionally, we demonstrated that VIR members of subfamilies A and D do not mediate cytoadherence, whereas VIR14, pertaining to subfamily C, does (23). It is therefore tempting to speculate that spleen-dependent VIR proteins play a role in antigenic variation and cytoadherence in its strict sense, whereas the function of nonspleen-dependent VIR proteins

remains to be elucidated. In the absence of other supporting data, this remains to be determined.

To assess if *P. vivax* spleen-dependent proteins are targets of naturally acquired immune responses, we expressed five genes representing three different multigene families, one membrane transporter, and one hypothetical protein as soluble proteins in the wheat germ cell-free system. This system has proved robust and reproducible to express soluble, mostly intact, and correctly folded malarial proteins (35). Immunogenicity was evaluated measuring total immunoglobulin G (IgG) antibody levels of sera from a prospective longitudinal study of children from PNG (28). All proteins were immunogenic, albeit at different levels (Fig. 4) (*SI Appendix*). PvFAM-A2 and PvFAM-D2 proteins were recognized by a high percentage of sera. These results are in agreement with members of these families being highly expressed in transcriptional analysis of parasite isolates (32). Furthermore, a recent study showed that these two members of PvFAM proteins, when analyzed as recombinant proteins using sera from the Republic of Korea (36), were also immunogenic. The fact that antibodies to PvFAM-D2 and MSP1-19 were significantly more common in children with concurrent *P. vivax* infections clearly indicates that these two proteins could be associated with an active infection. Recent analysis of naturally acquired antibody responses to *P. vivax* MSP1-19 in an area of unstable malaria transmission in Southeast Asia has shown that antibodies to PvMSP1₁₉ may serve as a serological marker for malaria transmission in that particular study area (37). PvFAM-D2 pertains to a family sharing a conserved N terminus to C terminus protein structure, starting with a signal peptide, followed by Protein Export Elements (PEXEL) motif, antigenic regions containing B cell epitopes, and two transmembrane domains. This topology is only disrupted in two members (PVX_000015 and PVX_118695) where predicted antigenic regions are also observed between the signal peptide and the PEXEL motif (*SI Appendix*, Fig. S3). Further epidemiological studies should determine the value of the PvFAM-D family as markers of exposure. On the other hand, low antibody levels were observed against SECY and HYP1. Noticeably, despite pertaining to the variant *vir* gene family with more than a thousand genes described to date, PVX_108770 (VIR14) presented the highest positivity of all antigens tested, including the highly immunogenic MSP1-19 protein. VIR proteins contain predicted immunogenic conserved globular domains of unknown function (9, 23, 38). Whether such domains elicit cross-reacting antibodies responsible for this high percentage of positivity remains to be demonstrated.

The number of genetically distinct blood-stage infections acquired over time, also known as the molecular force of blood-stage infection (molFOB), is a direct way to measure individual differences in exposure to *P. vivax* infections (39). This parameter has also been shown to be a major predictor of clinical disease in *P. falciparum* (40) and vivax malaria (39). Remarkably, when adjusting for difference in exposure, children with antibodies against HYP1 showed significant association with protection against clinical *P. vivax* episodes during follow-up (*SI Appendix*, Table S4). HYP1 is 100% conserved among *P. vivax* isolates from Mauritania, North Korea, India, and Brazil and 90% among other species, including *Plasmodium inui*, *Plasmodium cynomolgi*, *Plasmodium coatneyi*, and *P. knowlesi* (*SI Appendix*, Fig. S4). These results highlight its value as a target for vaccination against asexual blood stages of *P. vivax* and reinforce the importance of using molFOB in the search for association of clinical protection of vaccine candidates in *P. vivax* in prospective longitudinal studies.

P. vivax remains the most widely distributed human malaria parasite. Due to specific biological features, including dormancy in the liver and a tropism for reticulocytes, its elimination requires an improved understanding of its biology and

pathogenesis (41). One particular open question regards the conundrum of low peripheral blood parasitemia coincident with severe disease. Recent evidence indicates that this seeming discrepancy could be due to the adherent capacity and sequestration of iRBC parasite populations, outside the peripheral blood, and particularly in the spleen (6, 42–46), the bone marrow (47, 48), and with a less degree of certainty, to other organs (3, 6). Our data thus support a model (Fig. 5) in which infected reticulocytes expressing spleen-dependent VIR proteins, represented here by the VIR14 protein, can adhere to the microvasculature of the spleen, in particular to fibrocytic cells expressing ICAM-1. In contrast, as many VIR proteins are not spleen dependent, it is legitimate to speculate that infected reticulocytes expressing such VIR proteins will not cytoadhere. Therefore, they will circulate in peripheral blood, eliciting the acquisition of cross-reacting VIR antibodies due to the presence of conserved immunogenic globular domains (10, 23, 38) as well as of antibodies against other variant proteins such as PvFAM-D coexpressed in these infected reticulocytes. Further studies of spleen-dependent *P. vivax* genes could thus help in unveiling mechanistic insights of spleen cytoadherence in *P. vivax* as well as discovering new antigens for vaccination and markers of exposure. Most relevant, together with hypnozoite and other tissue reservoirs such as the bone marrow, these populations may represent an added challenge for malaria elimination, particularly since cytoadherence to the microvasculature of the spleen will represent a privileged niche where parasites can escape (46), thus prompting a paradigm shift in *P. vivax* biology toward deeper studies of the spleen during infections.

Materials and Methods

Ethics Statement. The serological analyses of plasma samples from cohort participants received ethical clearance by the PNG Institute of Medical Research Institutional Review Board (IRB; IRB 07.20) and the PNG Medical Advisory Committee (07.34). Individual written consent was obtained from the parents or guardians of all children. The consent included a specific approval to investigate their children's immune responses to different malarial antigens and their association with protection.

The Animal Ethical Committee of Universidad del Valle approved the protocol involving *Aotus lemurinus griseimebra* monkeys from the Fundación Centro de Primates in Cali, Colombia. Animals were handled and housed following the National Research Council's *Guide for the Care and Use of Laboratory Animals* (50).

Infections of Aotus Monkeys. Five groups of *A. lemurinus griseimebra* monkeys ($n = 2$ per group), four splenectomized (Sp–1, Sp–2, Sp–3, and Sp–4) and one with spleen (Sp+2), were used. All groups were handled according with animal welfare guidelines and maintained with standard requirements of water and food supplies. Animals were splenectomized by a veterinarian according to standard operational procedures under general anesthesia 4 wk prior to infections.

Spleen-intact (Sp+) and splenectomized (Sp–) animals were infected by intravenous (iv) inoculation of 10^5 iRBCs (500- μ L volume) obtained from a donor monkey previously infected with the *P. vivax* Sal-1 reference strain (10). First recipient group was splenectomized monkeys (Sp–1 group); thereafter, parasites were passaged by iv inoculations through groups Sp–2, Sp–3, Sp–4, and Sp+2. Parasite passages were performed at peak parasitemia (~3 to 4 wk postinoculation); simultaneously, 3 to 4 mL of peripheral blood was collected via femoral vein in heparinized sterile tubes from each animal, and 1-mL aliquots were processed for RNA extractions.

Sample Processing for RNA Isolation and Gene Expression Array. For RNA isolation, blood was first centrifuged at $600 \times g$ for 5 min, and packed RBCs were resuspended at 25% hematocrit in incomplete Roswell Park Memorial Institute medium (iRPMI). Mature *P. vivax* parasites were purified using magnetic MACS LS columns (Miltenyi) as described (51) and preserved into 1 mL of TRIzol for later processing. RNA extraction was performed following the manufacturer's instructions, and 50 ng of each sample was reversely transcribed into cDNA, being subsequently amplified and labeled with Cy5 and Cy3 dye following Agilent's Two-Color Microarray-Based Gene

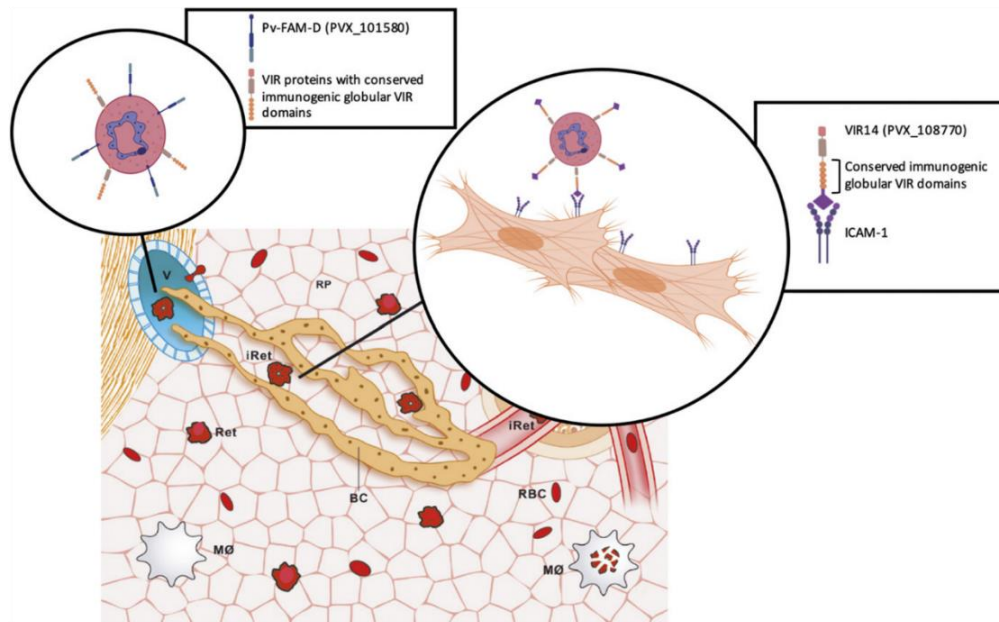


Fig. 5. Spleen cytoadherence mediated by spleen-dependent VIR proteins. Infections by reticulocyte (Ret)-prone malaria parasites induce spleen remodeling and formation of barrier cells (BCs) of fibroblastic origin where infected reticulocytes (iRet) avoid macrophage (M ϕ) clearance (background scheme) (49). *P. vivax* iRet expressing spleen-dependent VIR proteins, here represented by VIR14 (PVX_108770), adhere to human spleen fibroblasts expressing ICAM-1 (*Right Inset*). iRet expressing VIR proteins whose expression is not spleen-dependent will not cytoadhere; thus, reaching peripheral circulation facilitating antigen presentation of conserved immunogenic VIR globular domains (10, 23, 38) as well as other variant antigens such as PvFAM-D (PVX_101580; *Left Inset*). Partially created by BioRender. RP, red pulp; V, venule.

Expression Analysis protocol version 6.5 (Agilent Technologies). Spike-in RNA (Agilent Technologies) was used as internal control. Slides were scanned with Agilent's G2565CA Microarray Scanner System. Dye normalized, background subtracted, and log ratios of sample to reference expression were calculated using Agilent's Feature Extraction Software version 9.5.

Dual hybridizations comparing the global expression of parasites obtained from the different experimental infections (labeled with Cy5) with a reference pool PvSp-1 obtained from splenectomized monkeys from the CDC (donated by John Barnwell; labeled with Cy3) were performed using Agilent's custom-made array containing 5,038 *P. vivax* coding genes (one 60-base oligonucleotide at every 2 kb) as annotated (10). Of note, sample Sp-4 was not included in these analyses due to insufficient amount of total RNA obtained. All data are freely available through the GEO NIH database repository (GEO accession no. GPL6667).

Selection of Spleen-Dependent Genes Based on Microarray Analyses. Two distinct probabilistic models were proposed to identify *P. vivax* genes expressed only in monkeys with intact spleen (*SI Appendix, Fig. S1*), one considering each time point independently (Method 1) and the other considering the entire time series (Method 2). In the first model, probe intensities were compared with negative controls. Each negative control was considered as a realization of a random variable ($I_{(ctrl)}$), and a probability density function was modeled using straightforward Kernel Density Estimation (52) in R programming language's package stats (53). Average intensity of each gene probe (a number, $I_{(probe)}$) was compared with the probability density function of the negative controls. If the negative control would rarely generate intensity signals greater than what was observed for a given probe, we say that this probe is expressed (on). Formally, if $\Pr(I_{(ctrl)} > I_{(probe)}) < 0.001$, then probe is on. Conversely, if negative control could easily generate similar intensity levels that gene probes also can, we say that this probe is not confidently expressed (off). Formally, if $\Pr(I_{(ctrl)} > I_{(probe)}) > 0.05$,

then probe is off. In the second model, a 0.98 quantile of negative control intensity was used as a cutoff. Probes presenting average intensity at least 10 times greater than this cutoff were considered on, and the ones with average intensity below the quantile were classified as off. For each model, selected genes were those presenting the following expression pattern: off in Sp-1, Sp-2, and Sp-3 and on in Sp+2. Intrinsic variability of the log ratio and mean average plot in the different arrays limited the possibility of performing a robust differential *vir* gene expression analysis.

Fibroblasts and CHO Cells Culture. The spleen fibroblast cell line (1010T) was established in our laboratory from a human spleen donated by the Hospital Clinic of Barcelona in accordance with the protocol approved by the Ethics Committee for Clinical Research of the Universitat de Barcelona (no. 041499). Briefly, a portion of the spleen was fragmented into several parts and divided into two tubes to be homogenized by the GentleMACS dissociator. After applying the "Spleen 1" program twice, the sample was centrifuged at $700 \times g$ for 10 min. The obtained pellet was resuspended in complete RPMI supplemented with 10% fetal bovine serum (FBS) (cRPMI) at a final density of 10^8 cells in 30 mL of medium and cultured at 37 °C/5% CO₂. After 2 d, the cell suspension was removed, and only adherent cells were kept in culture for 3 to 4 wk until 100% of confluence was reached before trypsinization.

CHO cells were grown in cRPMI medium, while the commercial fibroblasts Hs 697.Sp (ATCC CRL-7433) and WI-38 (ATCC CCL-75) were cultured in complete Dulbecco's Modified Eagle Medium (supplemented with 10% FBS serum). All cell cultures were maintained at 37 °C/5% CO₂.

***P. falciparum* Static and Flow Cytoadhesion Assays.** Static binding assays were performed as previously described (23). Briefly, 5×10^5 CHO cells (CHO-746, CHO-CD36, CHO-ICAM-1, CHO-VCAM, and CHO-E-Selectine (donated by Artur Scherf, Biology of Host-Parasites Interactions, Institut Pasteur, Paris, France) were seeded in 24-well plates in coverslips (Nunc) and left to attach

for 2 d. Half of the content of a 75-cm² flask of Hs697 Sp, 1010T, and WI-38 cell lines was used to seed 12 wells. In the case of the Hs697 cell line, the cells were seeded 5 d before performing the experiment. Mature asexual blood stages of cultured *P. falciparum* 3D7 strain and the transgenic lines were enriched using a 70% Percoll solution, and parasites were quantified using both a Neubauer chamber and a Giemsa-stained smear. For adhesion experiments, cells were washed with binding medium (RPMI, pH 6.8 supplemented with 10% AB⁺ human plasma), and 500 μ L containing 1×10^6 *P. falciparum* transgenic parasites were added to each well. Each experiment was run in triplicate. Cells and iRBCs were incubated for 1 h at 37 °C in binding medium in a 5% CO₂ incubator, and unbound cells were washed by dipping coverslips twice in binding medium followed by 30 min of gravity wash at a 45° angle. Adhesion experiments with the WI-38 cell line were done in binding medium at a pH of 7.2 to avoid cell clumping. The same medium was used for experiments run in parallel with WI-38, CHO-iCAM-1, and Hs697 Sp cells. For flow cytoadhesion assays, coverslips seeded with either CHO or Hs 697Sp cell lines were mounted in a Cell Adhesion Flow Chamber. The system was connected to a precise infusion/withdrawal pump (model KDS120; KD Scientific) to control the flow of the iRBC suspension through the perfusion chamber; then, 1×10^7 iRBCs were flowed over for a total of 30 min, and binding buffer was flowed over for 10 min to remove unbound cells. The flow rate yielded a wall shear stress of 0.09 Pa, which mimics wall shear stresses in the microvasculature. Static and flow coverslips were fixed in methanol after the washing process and stained with 10% Giemsa for 15 min. Adhesions were quantified in an optical light microscope. Binding experiments were done in triplicate in 3 to 5 independent days. Statistical analysis was done on GraphPad Prism (version 4), and significance was determined by an unpaired t test.

***P. falciparum* Culture, Plasmid Constructs, and Parasite Transfection.** *P. falciparum* parasites were cultured with B+ human erythrocytes (3% hematocrit) in RPMI media (Sigma) supplemented with 10% AB+ human plasma using standard methods (23). *Pv-fam-d* gene (PVX_101580) was amplified from *P. vivax* Sal1 genomic DNA (gDNA) using primers F-PvFamD: GGTACCATGAAAATGAAAAAATAAG; R-PvFamD: ctgcagATTCCTGGTCTTTTTTTTG and was cloned in the KpnI-PstI cloning sites of modified transfection vector pARL1a-3HA (23). The plasmid pARL1a-PvFamD-3HA was transfected into 3D7 parasites by electroporating ring-stage parasites (>5% parasitemia) with 100 μ g of purified plasmid DNA (Qiagen) as previously described (23) using 0.310-kV and 950-F electroporation conditions. Six hours after transfection, 2.5 nM WR99210 was added to the culture media. Parasites were detectable in culture 20 to 30 d after drug selection pressure started.

***P. falciparum* Indirect Immunofluorescence Assays.** Cultured *P. falciparum* 3D7-Pv-fam-D_3HA transgenic line that presents mixed stages was washed in phosphate-buffered saline (PBS) and then fixed with 4% electron microscopy (EM)-grade paraformaldehyde and 0.075% EM-grade glutaraldehyde in PBS (23). Fixed cells were permeabilized with 0.1% Triton X-100 in PBS and blocked for 1 h at room temperature in 3% PBS-bovine serum albumin (BSA). Samples were incubated overnight with primary antibody (rabbit anti-HA [1:50; Molecular Probes] or rat anti-HA [1:50; Roche] and mouse anti-ATS [1:50]) diluted in 3% PBS-BSA followed by 1 h of incubation with secondary antibody (anti-mouse or anti-rat IgG conjugated with Alexa Fluor 488 and anti-rabbit IgG conjugated with Alexa Fluor 594 [1:100; Molecular Probes]) diluted in 3% PBS-BSA. Nuclei were stained in the secondary antibody incubation with 4,6-diamidino-2-phenylindole (DAPI; 2 mg/mL diluted in 3% PBS-BSA). Confocal microscopy was performed using a laser-scanning confocal microscope (TCS-SP5; Leica Microsystems) at microscopy scientific and technical services of Universitat de Barcelona. Images were processed using ImageJ image browser software.

***P. falciparum* Live Immunofluorescence Assays.** Cultured *P. falciparum* transgenic lines were washed in iRPMI and blocked for 1 h at room temperature in 3% RPMI-BSA (PBS-BSA). Samples were incubated for 1 h with rabbit anti-HA [1:50; Molecular Probes] diluted in 3% RPMI-BSA followed by 1 h of incubation with secondary antibody anti-rabbit IgG conjugated with Alexa Fluor 488 [1:100; Molecular Probes] diluted in RPMI. Nuclei were stained in the secondary antibody incubation with DAPI (2 mg/mL). Samples were mounted in Vectashield (Vector Labs), and confocal microscopy was performed using a laser-scanning confocal microscope (TCS-SP5; Leica Microsystems). Images were processed using ImageJ image browser software.

Cloning and Small-Scale Wheat Germ Cell-Free Protein Synthesis. *P. vivax* spleen-dependent genes were amplified from cDNA (Sal-1 strain) by PCR using Platinum Taq DNA Polymerase High Fidelity (Thermo Fisher Scientific)

and the primers listed in *SI Appendix, Table S5*. PCR products were initially cloned into pGEM-T easy vector (Promega) and subcloned into pIVEX1.4d vector (Roche), previously modified by our group, by inserting GST after the 6xHis tag sequence (26). Authenticity of all clones encoding GST-fusion proteins was confirmed by sequencing before expression in the wheat germ cell-free system (Roche). In vitro protein synthesis was done on a 50- μ L scale as described (26) and purified on GST SpinTrap purification columns (GE Healthcare). GST was also expressed separately for immune-reactivity control.

Antibody Measurement by Luminex Technology. For antibody measurement, 1 μ g of each recombinant protein was covalently coated to different MagPlex magnetic carboxylated microspheres (Luminex Corporation) following the manufacturer's instructions. Measurement of total IgG antibodies was performed by multiplex suspension array using the Luminex technology as previously described (54). Briefly, a batch of microspheres, containing 2,000 beads per analyte, was incubated with human plasma samples (1:100 dilution) in duplicates and subsequently, with anti-human IgG biotinylated (Sigma-Aldrich) at 1:4,000 dilution followed by streptavidin-conjugated R-phycoerythrin (R-PE) (1 μ g/mL). Beads were acquired on the BioPlex100 system (Bio-Rad), and results are expressed as median fluorescence intensity. A panel of eight negative controls was included on every plate.

Antibodies to all proteins were measured in a cohort of PNG children aged 1 to 5 y enrolled in a longitudinal cohort study who were randomized to pretreatment with artesunate (7 d), artemisinin (7 d) plus primaquine (14 d), or no treatment and followed up actively for recurrent *Plasmodium* infections and disease for 40 wk. A detailed description of the cohort is given elsewhere (28). Antibodies were measured in samples collected at baseline ($n = 435$), 6 wk after treatment ($n = 408$), and at the end of follow-up ($n = 419$). Antibody mean fluorescent intensities (MFIs) were log transformed, and background values due to antibody reactivity to the GST tag were subtracted as described (54). Cutoffs for antibody positivity were determined for each plate separately by calculating mean +2 SD of the negative control values.

Statistical Analysis. Clinical malaria was defined as fever (axillary temperature ≥ 37.5 °C) or recent history of febrile illness and presence of a concomitant *Plasmodium* sp. infection. Time at risk was counted from the first day after the last treatment dose was administered and up until withdrawal, loss to follow-up, or study completion. Associations between the time to first *Plasmodium* sp. infection (or clinical episode) and treatment options were already investigated in a previous study (28) and relied on Cox proportional hazard regressions using Schoenfeld residuals test to confirm the proportional hazard assumption. In this study, we also included recoded antibody titers as explanatory independent covariates in these regressions.

Recoding of Antibody Titers. To account for plate-to-plate variations and to reflect on antibody level, MFIs were adjusted, platewise, under the assumption that $\log(\text{Ab_tag}) \sim \log(\text{Ab}) + \log(\text{tag})$. A linear model was fitted to each plate and antigen to derive the adjusted MFI value: the minimal tag value that could be detected was hence considered as background noise from the experiment.

Adjusted MFI values from negative controls were used to define a standard reference curve, reflecting the expected values of cross-reactivity that could be expected in individuals who were never exposed to *Plasmodium* parasites. Assuming log-normal distributions of MFI values in this control population, extreme outliers were flagged using Grubb's test recursively (55).

Positivity thresholds were defined plate- and antigenwise as 2 SDs above the mean MFI in negative controls. Patients' adjusted MFIs values were compared against these thresholds and recoded to binomial outcomes (positive/negative). As a sensitivity analysis, a more conservative set of thresholds was computed using 3 SDs.

Logistic regression was used to quantify the associations between baseline positivity and age categories (two groups cut at a median of 3 y old), *Plasmodium* sp. parasitemia, and clinical episodes, while adjusting for the averaged individual molecular force of infection as a proxy for individual exposure to mosquitoes. Temporal trends in prevalence of antibody positivity were estimated using generalized estimating equations with exchangeable correlation structure to account for repeated measurements.

ACKNOWLEDGMENTS. We thank John Barnwell (Malaria Branch, Division of Parasitic Diseases and Malaria, CDC) for the gift of the reference RNA pool PvSp-1 obtained from splenectomized monkeys from the CDC, Artur Scherf (Biology of Host-Parasite Interactions, Institut Pasteur) for the gift of CHO-cells expressing different receptors and Marc Nicolau for technical assistance.

We also thank the anonymous reviewers of this manuscript whose criticisms and suggestions significantly improved its content and quality. This work was supported with funding from the Cellex Foundation. The funder had no role in study design, data collection and analysis, decision to publish, or preparation of the manuscript. The Barcelona Institute for Global Health (ISGlobal) receives support from the Spanish Ministry of Science, Innovation

and Universities through the "Centro de Excelencia Severo Ochoa 2019-2023" Program (CEX2018-000806-S). This research is part of ISGlobal's Program on the Molecular Mechanisms of Malaria, which is partially supported by the Fundación Ramón Areces. ISGlobal and Germans Trias i Pujol Research Institute are members of the Centres de Reserca de Catalunya Program, Generalitat de Catalunya.

1. R. E. Howes *et al.*, Global epidemiology of *Plasmodium vivax*. *Am. J. Trop. Med. Hyg.* **95** (suppl. 6), 15–34 (2016).
2. J. K. Baird, Neglect of *Plasmodium vivax* malaria. *Trends Parasitol.* **23**, 533–539 (2007).
3. M. V. Lacerda *et al.*, Postmortem characterization of patients with clinical diagnosis of *Plasmodium vivax* malaria: To what extent does this parasite kill? *Clin. Infect. Dis.* **55**, e67–e74 (2012).
4. C. Naing, M. A. Whittaker, V. Nyunt Wai, J. W. Mak, Is *Plasmodium vivax* malaria a severe malaria?: A systematic review and meta-analysis. *PLoS Negl. Trop. Dis.* **8**, e3071 (2014).
5. L. H. Miller, D. I. Baruch, K. Marsh, O. K. Doumbo, The pathogenic basis of malaria. *Nature* **415**, 673–679 (2002).
6. B. O. Carvalho *et al.*, On the cytoadhesion of *Plasmodium vivax*-infected erythrocytes. *J. Infect. Dis.* **202**, 638–647 (2010).
7. K. Chotivanich *et al.*, *Plasmodium vivax* adherence to placental glycosaminoglycans. *PLoS One* **7**, e34509 (2012).
8. B. De las Salas *et al.*, Adherence to human lung microvascular endothelial cells (HMVEC-L) of *Plasmodium vivax* isolates from Colombia. *Malar. J.* **12**, 347 (2013).
9. H. A. del Portillo *et al.*, A superfamily of variant genes encoded in the subtelomeric region of *Plasmodium vivax*. *Nature* **410**, 839–842 (2001).
10. J. M. Carlton *et al.*, Comparative genomics of the neglected human malaria parasite *Plasmodium vivax*. *Nature* **455**, 757–763 (2008).
11. H. A. Del Portillo *et al.*, The role of the spleen in malaria. *Cell. Microbiol.* **14**, 343–355 (2012).
12. C. R. Engwerda, L. Beattie, F. H. Amante, The importance of the spleen in malaria. *Trends Parasitol.* **21**, 75–80 (2005).
13. J. W. Barnwell, R. J. Howard, L. H. Miller, Altered expression of *Plasmodium knowlesi* variant antigen on the erythrocyte membrane in splenectomized rhesus monkeys. *J. Immunol.* **128**, 224–226 (1982).
14. S. A. Lapp *et al.*, Spleen-dependent regulation of antigenic variation in malaria parasites: *Plasmodium knowlesi* SICAvax expression profiles in splenic and asplenic hosts. *PLoS One* **8**, e78014 (2013).
15. M. Hommel, P. H. David, L. D. Olligino, Surface alterations of erythrocytes in *Plasmodium falciparum* malaria. Antigenic variation, antigenic diversity, and the role of the spleen. *J. Exp. Med.* **157**, 1137–1148 (1983).
16. S. M. Handunnetti, K. N. Mendis, P. H. David, Antigenic variation of cloned *Plasmodium fragile* in its natural host *Macaca sinica*. Sequential appearance of successive variant antigenic types. *J. Exp. Med.* **165**, 1269–1283 (1987).
17. C. F. Gilks, D. Walker, C. I. Newbold, Relationships between sequestration, antigenic variation and chronic parasitism in *Plasmodium chabaudi* chabaudi—a rodent malaria model. *Parasite Immunol.* **12**, 45–64 (1990).
18. M. Demar, E. Legrand, D. Hommel, P. Esterre, B. Carne, *Plasmodium falciparum* malaria in splenectomized patients: Two case reports in French Guiana and a literature review. *Am. J. Trop. Med. Hyg.* **71**, 290–293 (2004).
19. A. Bachmann *et al.*, Absence of erythrocyte sequestration and lack of multicopy gene family expression in *Plasmodium falciparum* from a splenectomized malaria patient. *PLoS One* **4**, e7459 (2009).
20. S. Loareesuwan, P. Suntharasamal, H. K. Webster, M. Ho, Malaria in splenectomized patients: Report of four cases and review. *Clin. Infect. Dis.* **16**, 361–366 (1993).
21. K. Chotivanich *et al.*, Parasite multiplication potential and the severity of *falciparum* malaria. *J. Infect. Dis.* **181**, 1206–1209 (2000).
22. C. Fernandez-Becerra *et al.*, *Plasmodium vivax* and the importance of the subtelomeric multigene vir superfamily. *Trends Parasitol.* **25**, 44–51 (2009).
23. M. Bernabeu *et al.*, Functional analysis of *Plasmodium vivax* VIR proteins reveals different subcellular localizations and cytoadherence to the ICAM-1 endothelial receptor. *Cell. Microbiol.* **14**, 386–400 (2012).
24. A. G. Maier *et al.*, Skeleton-binding protein 1 functions at the parasitophorous vacuole membrane to traffic PfEMP1 to the *Plasmodium falciparum*-infected erythrocyte surface. *Blood* **109**, 1289–1297 (2007).
25. V. Kumar *et al.*, PHISTC protein family members localize to different subcellular organelles and bind *Plasmodium falciparum* major virulence factor PfEMP-1. *FEBS J.* **285**, 294–312 (2018).
26. E. Rui *et al.*, *Plasmodium vivax*: Comparison of immunogenicity among proteins expressed in the cell-free systems of *Escherichia coli* and wheat germ by suspension array assays. *Malar. J.* **10**, 192 (2011).
27. P. A. Nogueira *et al.*, A reduced risk of infection with *Plasmodium vivax* and clinical protection against malaria are associated with antibodies against the N terminus but not the C terminus of merozoite surface protein 1. *Infect. Immun.* **74**, 2726–2733 (2006).
28. I. Betuela *et al.*, Relapses contribute significantly to the risk of *Plasmodium vivax* infection and disease in Papua New Guinean children 1–5 years of age. *J. Infect. Dis.* **206**, 1771–1780 (2012).
29. S. J. Westenberger *et al.*, A systems-based analysis of *Plasmodium vivax* lifecycle transcription from human to mosquito. *PLoS Negl. Trop. Dis.* **4**, e653 (2010).
30. Z. Bozdech *et al.*, The transcriptome of *Plasmodium vivax* reveals divergence and diversity of transcriptional regulation in malaria parasites. *Proc. Natl. Acad. Sci. U.S.A.* **105**, 16290–16295 (2008).
31. P. A. Boopathi *et al.*, Revealing natural antisense transcripts from *Plasmodium vivax* isolates: Evidence of genome regulation in complicated malaria. *Infect. Genet. Evol.* **20**, 428–443 (2013).
32. A. Kim *et al.*, Characterization of *P. vivax* blood stage transcriptomes from field isolates reveals similarities among infections and complex gene isoforms. *Sci. Rep.* **7**, 7761 (2017).
33. L. Zhu *et al.*, New insights into the *Plasmodium vivax* transcriptome using RNA-Seq. *Sci. Rep.* **6**, 20498 (2016).
34. A. Kim, J. Popovici, D. Menard, D. Serre, *Plasmodium vivax* transcriptomes reveal stage-specific chloroquine response and differential regulation of male and female gametocytes. *Nat. Commun.* **10**, 371 (2019).
35. T. Tsuboi, S. Takeo, T. U. Arumugam, H. Otsuki, M. Torii, The wheat germ cell-free protein synthesis system: A key tool for novel malaria vaccine candidate discovery. *Acta Trop.* **114**, 171–176 (2010).
36. F. Lu *et al.*, Profiling the humoral immune responses to *Plasmodium vivax* infection and identification of candidate immunogenic rophry-associated membrane antigen (RAMA). *J. Proteomics* **102**, 66–82 (2014).
37. Q. Wang *et al.*, Naturally acquired antibody responses to *Plasmodium vivax* and *Plasmodium falciparum* Merozoite Surface Protein 1 (MSP1) C-terminal 19 kDa domains in an area of unstable malaria transmission in Southeast Asia. *PLoS One* **11**, e0151900 (2016).
38. P. Requena *et al.*, *Plasmodium vivax* VIR proteins are targets of naturally-acquired antibody and T cell immune responses to malaria in pregnant women. *PLoS Negl. Trop. Dis.* **10**, e0005009 (2016).
39. C. Koepfli *et al.*, A high force of *Plasmodium vivax* blood-stage infection drives the rapid acquisition of immunity in Papua New Guinean children. *PLoS Negl. Trop. Dis.* **7**, e2403 (2013).
40. I. Mueller *et al.*, Force of infection is key to understanding the epidemiology of *Plasmodium falciparum* malaria in Papua New Guinean children. *Proc. Natl. Acad. Sci. U.S.A.* **109**, 10030–10035 (2012).
41. I. Mueller *et al.*, Key gaps in the knowledge of *Plasmodium vivax*, a neglected human malaria parasite. *Lancet Infect. Dis.* **9**, 555–566 (2009).
42. J. K. Baird, Evidence and implications of mortality associated with acute *Plasmodium vivax* malaria. *Clin. Microbiol. Rev.* **26**, 36–57 (2013).
43. A. Machado Siqueira *et al.*, Spleen rupture in a case of untreated *Plasmodium vivax* infection. *PLoS Negl. Trop. Dis.* **6**, e1934 (2012).
44. M. S. Peterson *et al.*, MaHPIC Consortium, *Plasmodium vivax* parasite load is associated with histopathology in *Saimiri boliviensis* with findings comparable to *P. vivax* pathogenesis in humans. *Open Forum Infect. Dis.* **6**, ofz021 (2019).
45. A. Elizalde-Torrent *et al.*, Sudden spleen rupture in a *Plasmodium vivax*-infected patient undergoing malaria treatment. *Malar. J.* **17**, 79 (2018).
46. R. S. Lee, A. P. Waters, J. M. Brewer, A cryptic cycle in haematopoietic niches promotes initiation of malaria transmission and evasion of chemotherapy. *Nat. Commun.* **9**, 1689 (2018).
47. B. Baro *et al.*, *Plasmodium vivax* gametocytes in the bone marrow of an acute malaria patient and changes in the erythroid miRNA profile. *PLoS Negl. Trop. Dis.* **11**, e0005365 (2017).
48. N. Obaldia 3rd *et al.*, Bone marrow is a major parasite reservoir in *Plasmodium vivax* infection. *mBio* **9**, e00625-18 (2018).
49. L. Martin-Jular *et al.*, Strain-specific spleen remodeling in *Plasmodium yoelii* infections in Balb/c mice facilitates adherence and spleen macrophage-clearance escape. *Cell. Microbiol.* **13**, 109–122 (2011).
50. National Research Council, *Guide for the Care and Use of Laboratory Animals*, (National Academies Press, Washington, DC, ed. 8, 2011).
51. D. T. Trang, N. T. Huy, T. Kariu, K. Tajima, K. Kamei, One-step concentration of malarial parasite-infected red blood cells and removal of contaminating white blood cells. *Malar. J.* **3**, 7 (2004).
52. B. W. Silverman, *Density Estimation*, (Chapman and Hall, London, UK, 1986).
53. R Core Team, *R: A Language and Environment for Statistical Computing*, (R Foundation for Statistical Computing, Vienna, Austria, 2015).
54. C. Fernandez-Becerra *et al.*, Naturally-acquired humoral immune responses against the N- and C-termini of the *Plasmodium vivax* MSP1 protein in endemic regions of Brazil and Papua New Guinea using a multiplex assay. *Malar. J.* **9**, 29 (2010).
55. F. E. Grubbs, Sample criteria for testing outlying observations. *Ann. Math. Stat.* **21**, 27–58 (1950).

SI Appendix

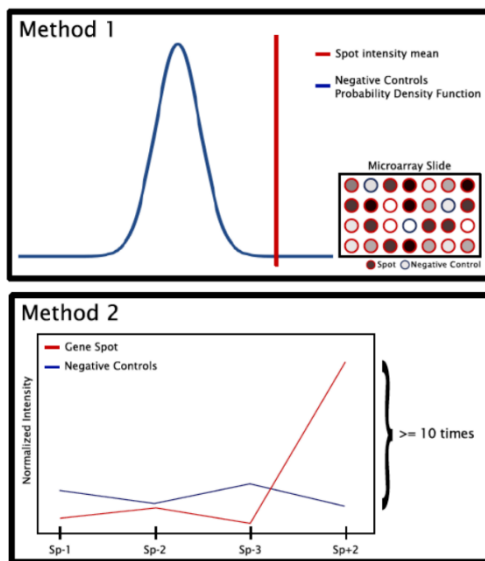


Figure S1. Probabilistic models for identification of *P. vivax* genes expressed only in monkeys with intact spleen. Model 1. In the first model, probe intensities were compared with negative controls. Average intensity of each probe was compared to the probability density function of the negative controls. If expression probability of negative controls was less than 0.001 compared to the probe, this probe was classified as "On", if it was greater than 0.05, probe was considered "Off". **Model 2.** In the second model, a 0.98 quantile of negative controls intensity was used as a cut-off. Probes presenting average intensity at least ten times greater than this cut-off were considered "On", and the ones with average intensity below the quantile were classified as "Off". For each model, selected genes were those presenting the following expression pattern: "Off" in Sp-1, Sp-2, Sp-3 and "On" in Sp+2.

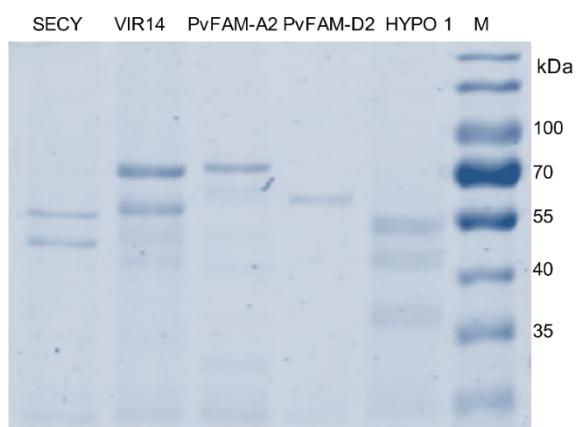


Figure S2. Protein expression using the wheat germ cell-free system. Soluble proteins were analyzed on a 10% SDS-PAGE. Expected size of the proteins are: PV-FAM-D (40 kDa), PV-FAM-A (64 kDa), Hyp1 (54 kDa), SECY (53 kDa), VIR14 (74 kDa). Molecular weight markers (MW) in kDaltons. Expected sizes correspond to GST-fusion proteins, considering GST as 26 kDa.



Figure S3. Conserved Sequence/Motifs of the Pv-FAM-D family. The multiple EM (expectation maximization) for motif elicitation suite (<http://meme-suite.org>), with the following parameters (motif site distribution ZOOPS: zero or one site per sequence; Objective function: E-values of products of p-values; Starting Point Function: E-values of products of p-values; Site strand handling: this alphabet only has one strand; Maxim Number of Motifs: 10; Motif E-value threshold: no limit; Minimum motif with: 6; Maximum motif with: 50; Minimum Sites per Motif: 2; maximum Sites per Motif: 13), was used to discover conserved sequences and motifs. **A.** Motifs and colour representations. **B.** Conserved N-terminus to C-terminus proteins structure, starting with a signal peptide, followed by PEXEL motif, antigenic regions containing b-cell epitopes and two transmembrane domains. This topology is only disrupted in two members (PVX_000015 and PVX_118695) where predicted antigenic regions are also observed between the signal peptide and the PEXEL motif. Highlighted in yellow, members whose expression was dependent on the spleen. Motif consensus sequences are also shown.

TABLE S1. Daily parasitemia and hematocrit of the different experimental groups

		PARASITEMIA																						
Group	Monkey code/ day	8	7	10	11	12	14	17	19	21	24	26	28	30	32	34	36	40	42	44	46	48	51	
G1	354-339	0	0	0,1	0,2	0,5	0,7	0,8	0,8	0,5	0	0	0	0	0	0	0	0	0	0	0	0	0	
Sp-1	051-375	0	0	0,6	1,4	1,6	1,6	0,8	0,7	0,6	1,8	1,5	0,9	0,2	0	0	0	0	0	0	0	0	0	
G2	030-833	0	7	9	11	14	16	18	21	24	25	28	30	32	34	36	40	42	44	46	48	51		
Sp-2	316-879	0	0,1	0,1	0,2	0,4	0,4	1	0,4	0,6	0,8	0,7	0,3	0,1	0,1	0,1	0	0	0,1	0,2	0,2	-0,1		
G3	814-168	0	7	11	13	15	17	18	19	21	24	26												
Sp-3	310-334	0	0,1	0,1	0,1	0,1	0	0,1	0,1	0,2	0,5	0,7												
G4	370-274	0	6	9	11																			
Sp-4	030-302	0	0	0,1																				
G5	856-342	0	10	13	16	18	19	21	22	23	30	33	35	37	40	41	43							
Sp-2	0342	0	0,2	0	0	0,5	0,3	0	0	0	0	0	0	0	0	0	0							
		RNA extraction	Treatment	Deaths																				
		HEMATOCRIT																						
Group	Monkey code/ day	7	10	11	12	14	17	19	21	24	26	28	31	33	35	39								
G1	354-339	48	52	43	37	35																		
Sp-1	051-375	46	42	45	24	22	28																	
G2	030-833	7	9	11	14	16	18	21	24	25	28	30	32	34	36	40	42	44	46	48	51			
Sp-2	316-879	53	53	41	40	34	43	39																
G3	814-168	7	11	13	15	17	18	19	21	24	26													
Sp-3	310-334	38	36	47	36	47	35	33																
G4	370-274	6	9	11																				
Sp-4	030-302	25																						
G5	856-342	10	13	15	16	19	21	22	23	30	33	35	37	40										
Sp-2	0342	48	45	40	40	41	41	43	42															
		RNA extraction	Treatment	Deaths																				

Table S2. *Plasmodium vivax* spleen-dependent genes and chromosomal location

[Gene ID]	[Product Description] PlasmoDB version 45	Description (PlasmoDB version 8.0)	[Chromosome]	Method1	Method2
PVX_087775	E3 ubiquitin-protein ligase, putative	E3 ubiquitin-protein ligase, putative	1	✓	
PVX_088090	hypothetical protein, conserved	hypothetical protein, conserved	1		✓
PVX_093685	Plasmodium exported protein, unknown function	Plasmodium exported protein, unknown function	1		✓
PVX_000010	Plasmodium exported protein, unknown function	Plasmodium exported protein, unknown function	3		✓
PVX_000960	secy-independent transporter protein, putative	secy-independent transporter protein, putative	3		✓
PVX_096410	cysteine repeat modular protein 2, putative	cysteine repeat modular protein 2, putative	3		✓
PVX_003520	knob-associated histidine-rich protein, putative	knob-associated histidine-rich protein, putative	4	✓	
PVX_003525	Plasmodium exported protein, unknown function	Plasmodium exported protein, unknown function	4	✓	
PVX_003905	6-cysteine protein	6-cysteine protein	4	✓	✓
PVX_088805	variable surface protein Vir22/24-like	variable surface protein Vir22/24-like	5		✓
PVX_088855	hypothetical protein, conserved	hypothetical protein, conserved	5		✓
PVX_089055	E3 ubiquitin-protein ligase, putative	E3 ubiquitin-protein ligase, putative	5		✓
PVX_089592	hypothetical protein, conserved	hypothetical protein, conserved	5	✓	
PVX_090320	Vir protein, pseudogene	Vir protein, pseudogene	5	✓	
PVX_004525	variable surface protein Vir16/32-related	variable surface protein Vir16/32-related	6		✓
PVX_110855	hypothetical protein, conserved	hypothetical protein, conserved	6		✓
PVX_098620	hypothetical protein, conserved	hypothetical protein, conserved	7		✓
PVX_098625	hypothetical protein, conserved	hypothetical protein, conserved	7	✓	
PVX_098975	actin-like protein, putative	actin-like protein, putative	7	✓	
PVX_094275	hypothetical protein	hypothetical protein	8	✓	
PVX_094785	hypothetical protein, conserved	hypothetical protein, conserved	8		✓
PVX_095305	hypothetical protein, conserved	hypothetical protein, conserved	8	✓	
PVX_095350	40S ribosomal protein S11, putative	40S ribosomal protein S11, putative	8	✓	✓
PVX_095495	hypothetical protein, conserved	hypothetical protein, conserved	8	✓	✓
PVX_119305	thioredoxin-like redox-active protein, putative	thioredoxin-like redox-active protein, putative	8	✓	✓
PVX_091715	3-phosphoinositide dependent protein kinase-1, putative	3-phosphoinositide dependent protein kinase-1, putative	9	✓	
PVX_092835	hypothetical protein, conserved	hypothetical protein, conserved	9		✓
PVX_092990	tryptophan-rich antigen (Pv-fam-a)	tryptophan-rich antigen (Pv-fam-a)	9	✓	
PVX_097625	merozoite surface protein 8, putative	merozoite surface protein 8, putative	10	✓	
PVX_113695	transcription factor with AP2 domain(s), putative	transcription factor with AP2 domain(s), putative	11	✓	
PVX_113830	myosin-like protein, putative	myosin-like protein, putative	11	✓	
PVX_114515	ethanolaminephosphotransferase, putative	ethanolaminephosphotransferase, putative	11		✓
PVX_114580	hypothetical protein, conserved	hypothetical protein, conserved	11	✓	✓
PVX_082350	hypothetical protein, conserved	hypothetical protein, conserved	12		✓
PVX_083160	rhomboid protease ROM6, putative	rhomboid protease ROM6, putative	12		✓
PVX_083560	Plasmodium exported protein, unknown function	Plasmodium exported protein, unknown function	12		✓
PVX_117615	signal peptide peptidase, putative	signal peptide peptidase, putative	12		✓
PVX_118305	diphospho-CoA kinase, putative	diphospho-CoA kinase, putative	12		✓
PVX_085065	diphthamide synthesis protein, putative	diphthamide synthesis protein, putative	13		✓
PVX_086040	plasmepsin IV, putative	plasmepsin IV, putative	13		✓
PVX_086205	adenyl cyclase alpha, putative	adenyl cyclase alpha, putative	13		✓
PVX_100620	hypothetical protein	hypothetical protein	14	✓	✓
PVX_100995	TPR domain containing protein	TPR domain containing protein	14	✓	
PVX_101230	hypothetical protein, conserved	hypothetical protein, conserved	14		✓
PVX_101515	tryptophan-rich antigen (Pv-fam-a)	tryptophan-rich antigen (Pv-fam-a)	14	✓	
PVX_101550	Plasmodium exported protein, unknown function	Plasmodium exported protein, unknown function	14	✓	✓
PVX_101580*	Pv-fam-d protein	Pv-fam-d protein	14	✓	✓
PVX_101595	Plasmodium exported protein, unknown function	Plasmodium exported protein, unknown function	14	✓	
PVX_101600	variable surface protein Vir16/32-related	variable surface protein Vir16/32-related	14	✓	✓
PVX_121880	Plasmodium exported protein, unknown function	Plasmodium exported protein, unknown function	14	✓	
PVX_121885	cytoadherence linked asexual protein, CLAG, putative	cytoadherence linked asexual protein, CLAG, putative	14	✓	✓
PVX_121890	hypothetical protein, conserved	hypothetical protein, conserved	14		✓
PVX_121895	Plasmodium exported protein, unknown function	Plasmodium exported protein, unknown function	14		✓
PVX_121910	Pv-fam-d protein	Pv-fam-d protein	14	✓	✓
PVX_121935	Plasmodium exported protein, unknown function	Plasmodium exported protein, unknown function	14	✓	
PVX_122285	60S ribosomal protein L24, putative	60S ribosomal protein L24, putative	14	✓	
PVX_122530	telomerase reverse transcriptase, putative	telomerase reverse transcriptase, putative	14	✓	
PVX_123430	hypothetical protein, conserved	hypothetical protein, conserved	14	✓	
PVX_123810	hypothetical protein, conserved	hypothetical protein, conserved	14		✓
PVX_103670	unspecified product	variable surface protein Vir6-like	Not Assigned		✓
PVX_108770*	unspecified product	variable surface protein Vir 14, putative	Not Assigned	✓	✓
PVX_108775	unspecified product	variable surface protein Vir26, truncated, putative	Not Assigned	✓	
PVX_112655	unspecified product	tryptophan-rich antigen (Pv-fam-a)	Not Assigned	✓	
PVX_112670	unspecified product	tryptophan-rich antigen (Pv-fam-a)	Not Assigned	✓	
PVX_112690	unspecified product	tryptophan-rich antigen (Pv-fam-a)	Not Assigned	✓	
PVX_112720	unspecified product	variable surface protein Vir12-related	Not Assigned	✓	
PVX_125735	unspecified product	hypothetical protein	Not Assigned	✓	

Bold: expressed as recombinant proteins in the WGE system

* Expressed as transgenes in *P. falciparum*

Table S3. List of genes selected for amplification and protein expression in the WGE system.

Gene Id	Annotation in PlasmoDB*	Positive Algotirms	CDS Length (bp)	Protein Size (Da)	Expressed in WGE/ Short Name
PVX_000960	secy-independent transporter protein, putative	2	948	37370	yes / SECY
PVX_004525	variable surface protein Vir16/32-related	1	1062	40985	
PVX_088805	variable surface protein Vir22/24-like	1	1077	42643	
PVX_092990	tryptophan-rich antigen (Pv-fam-a)	1	4245	157512	
PVX_094785	hypothetical protein, conserved	2	1797	71934	
PVX_100615	hypothetical protein	2	2439	89230	
PVX_101550	hypothetical protein, conserved	2	711	27952	
PVX_101580	Pv-fam-d protein**	2	1047	41545	
PVX_101600	variable surface protein Vir16/32-related	2	1119	44769	
PVX_103670	variable surface protein Vir6-like	1	1380	52877	
PVX_108770	variable surface protein Vir 14, putative**	2	1230	48425	yes/VIR14
PVX_112655	tryptophan-rich antigen (Pv-fam-a)	1	2079	80685	
PVX_112670	tryptophan-rich antigen (Pv-fam-a)	1	1008	38528	yes/PvFAM-A2
PVX_112690	tryptophan-rich antigen (Pv-fam-a)	1	942	36607	
PVX_112720	variable surface protein Vir12-related	2	1518	59628	
PVX_114580	hypothetical protein, conserved	2	732	28542	yes/HYPO1
PVX_121885	cytoadherence linked asexual protein, CLAG, putative	2	4236	165733	
PVX_121910	Pv-fam-d protein	2	876	33556	yes/PvFAM-D2

* Annotation based on Gene ID: version 8.0 PlasmodDB

** Expressed as transgenes in *P. falciparum*

Table S4. Association with clinical protection

Antigen	<i>P. vivax</i> episode	Adjusted HR	P-value
MSP1_19	LM	1.12 [0.9-1.39]	0.3299
	PCR	1.2 [0.97-1.48]	0.09751
	Clinical	1.36 [1-1.86]	0.05091
PvFAM-A2	LM	1.06 [0.85-1.31]	0.6118
	PCR	0.92 [0.75-1.13]	0.4244
	Clinical	1.08 [0.81-1.45]	0.592
PvFAM-D2	LM	1.23 [0.99-1.52]	0.0557
	PCR	1.09 [0.89-1.34]	0.3888
	Clinical	1.03 [0.77-1.38]	0.8269
VIR14	LM	1.05 [0.82-1.34]	0.713
	PCR	1.22 [0.97-1.54]	0.09394
	Clinical	0.8 [0.58-1.1]	0.1632
SECY	LM	0.85 [0.68-1.06]	0.16
	PCR	0.85 [0.69-1.05]	0.1291
	Clinical	0.74 [0.54-1.01]	0.0612
HYP1	LM	0.88 [0.7-1.11]	0.2831
	PCR	0.88 [0.7-1.09]	0.2418
	Clinical	0.65 [0.46-0.92]	0.01481

Table S5. List of primers selected for amplification of parasite genes for expression in the WGE system

Gene ID	Gene Name	Primer sequence
F_PVX_000960 R_PVX_000960	SECY	cacc gcggccgc ATGAAAACGTTAACCGAGGC ctgcag CTACCTGCGTCTGTAGC
F_PVX_108770 R_PVX_108770	VIR 14	cacc gcggccgc ATGTTTCGATCTGGAAGGAG ctgcag TTAATAATCCAATGTGG
F_PVX_112670 R_PVX_112670	PvFAM-A2	cacccc gcggccgc ATGAGATTGTTACCTGCC ctgcag TTATTTTTCTAATTCITTACACC
F_PVX_114580 R_PVX_114580	HYP1	cacc gcggccgc ATGAAGAGCATTTTGGGCC ctgcag TAAAACTCTTTTGCTTAT
F_PVX_121910 R_PVX_121910	PvFAM-D2	cacc gcggccgc ATGAATAAGTTCAGCCTC ctgcag TTAAGACATTTTATATTC

3.2 Article 2: *Plasmodium vivax* spleen-dependent protein 1 and its role in extracellular vesicles-mediated intrasplenic infections

Objective 2: Generation of *P. falciparum* transgenic lines, using CRISPR/Cas9 technology, expressing some of those genes.

Objective 3: Functional characterization of *P. vivax* genes preferentially expressed in the human spleen and bone marrow and the role of EVs in these haematopoietic tissues.

Title: *Plasmodium vivax* spleen-dependent protein 1 and its role in extracellular vesicles-mediated intrasplenic infections.

Authors: **Alberto Ayllon-Hermida**, Marc Nicolau-Fernandez, Ane M. Larrinaga, Iris Aparici-Herraiz, Elisabet Tintó-Font, Oriol Llorà-Batlle, Agnes Orban, Maria Fernanda Yasnot, Mariona Graupera, Manel Esteller, Jean Popovici, Alfred Cortes, Hernando A. del Portillo, Carmen Fernandez-Becerra.

Journal: Frontiers in Cellular and Infection Microbiology.

Year: 2024

Volume: 14

Issue:

Impact Factor: 5.7

Quartile and Research area: Q1 Infectious Diseases.

DOI: <https://doi.org/10.3389/fcimb.2024.1408451>



OPEN ACCESS

EDITED BY
Benoit Malleret,
National University of Singapore, SingaporeREVIEWED BY
Eun-Taek Han,
Kangwon National University,
Republic of Korea
Jessica Molina-Franky,
City of Hope, United States*CORRESPONDENCE
Hernando A. del Portillo
✉ hernandoa.delportillo@isglobal.org
Carmen Fernandez-Becerra
✉ carmen.fernandez@isglobal.org†PRESENT ADDRESSES
Iris Aparici Herraiz,
BioSystems S.A., Barcelona, Spain
Oriol Llorà-Battle,
Single Cell Discoveries B.V., Utrecht,
NetherlandsRECEIVED 28 March 2024
ACCEPTED 06 May 2024
PUBLISHED 17 May 2024CITATION
Ayllon-Hermida A, Nicolau-Fernandez M,
Larrinaga AM, Aparici-Herraiz I, Tintó-Font E,
Llorà-Battle O, Orban A, Yasnot MF,
Graupera M, Esteller M, Popovici J, Cortés A,
del Portillo HA and Fernandez-Becerra C
(2024) *Plasmodium vivax* spleen-dependent
protein 1 and its role in extracellular vesicles-
mediated intrasplenic infections.
Front. Cell. Infect. Microbiol. 14:1408451.
doi: 10.3389/fcimb.2024.1408451COPYRIGHT
© 2024 Ayllon-Hermida, Nicolau-Fernandez,
Larrinaga, Aparici-Herraiz, Tintó-Font,
Llorà-Battle, Orban, Yasnot, Graupera, Esteller,
Popovici, Cortés, del Portillo and
Fernandez-Becerra. This is an open-access
article distributed under the terms of the
Creative Commons Attribution License (CC BY).
The use, distribution or reproduction in other
forums is permitted, provided the original
author(s) and the copyright owner(s) are
credited and that the original publication in
this journal is cited, in accordance with
accepted academic practice. No use,
distribution or reproduction is permitted
which does not comply with these terms.

Plasmodium vivax spleen- dependent protein 1 and its role in extracellular vesicles-mediated intrasplenic infections

Alberto Ayllon-Hermida^{1,2,3}, Marc Nicolau-Fernandez^{1,2},
Ane M. Larrinaga⁴, Iris Aparici-Herraiz^{1,2†}, Elisabet Tintó-Font¹,
Oriol Llorà-Battle^{1†}, Agnes Orban⁵, María Fernanda Yasnot⁶,
Mariona Graupera^{4,7,8}, Manel Esteller^{7,8,9,10}, Jean Popovici^{5,11},
Alfred Cortés^{1,7}, Hernando A. del Portillo^{1,2,7*}
and Carmen Fernandez-Becerra^{1,2,12*}¹ISGlobal, Barcelona Institute for Global Health, Hospital Clínic-Universitat de Barcelona, Barcelona, Spain, ²GTP Institut d'Investigació Germans Trias i Pujol, Ctra. de Can Ruti, Barcelona, Spain, ³School of Medicine and Health Sciences, University of Barcelona, Barcelona, Spain, ⁴Endothelial Pathobiology and Microenvironment Group, Josep Carreras Leukaemia Research Institute (IJC), Barcelona, Catalonia, Spain, ⁵Malaria Research Unit, Institut Pasteur du Cambodge, Phnom Penh, Cambodia, ⁶Grupo de Investigaciones Microbiológicas y Biomédicas de Córdoba-GIMBIC, Universidad de Córdoba, Montería, Colombia, ⁷ICREA, Institució Catalana de Recerca i Estudis Avançats, Barcelona, Spain, ⁸CIBERONC, Centro de Investigación Biomédica en Red Cancer, Instituto de Salud Carlos III, Madrid, Spain, ⁹Cancer Epigenetics Group, Josep Carreras Leukaemia Research Institute (IJC), Barcelona, Catalonia, Spain, ¹⁰Physiological Sciences Department, School of Medicine and Health Sciences, University of Barcelona (UB), Barcelona, Catalonia, Spain, ¹¹G5 Épidémiologie et Analyse des Maladies Infectieuses, Département de Santé Globale, Institut Pasteur, Paris, France, ¹²CIBERINFEC, ISCIII-CIBER de Enfermedades Infecciosas, Instituto de Salud Carlos III, Madrid, Spain

Recent studies indicate that human spleen contains over 95% of the total parasite biomass during chronic asymptomatic infections caused by *Plasmodium vivax*. Previous studies have demonstrated that extracellular vesicles (EVs) secreted from infected reticulocytes facilitate binding to human spleen fibroblasts (hSFs) and identified parasite genes whose expression was dependent on an intact spleen. Here, we characterize the *P. vivax* spleen-dependent hypothetical gene (PVX_114580). Using CRISPR/Cas9, PVX_114580 was integrated into *P. falciparum* 3D7 genome and expressed during asexual stages. Immunofluorescence analysis demonstrated that the protein, which we named *P. vivax Spleen-Dependent Protein 1* (PvSDP1), was located at the surface of infected red blood cells in the transgenic line and this localization was later confirmed in natural infections. Plasma-derived EVs from *P. vivax*-infected individuals (PvEVs) significantly increased cytoadherence of 3D7_PvSDP1 transgenic line to hSFs and this binding was inhibited by anti-PvSDP1 antibodies. Single-cell RNAseq of PvEVs-treated hSFs revealed increased expression of adhesion-related genes. These findings demonstrate the importance of parasite spleen-dependent genes and EVs from natural infections in the formation of intrasplenic niches in *P. vivax*, a major challenge for malaria elimination.

KEYWORDS

Plasmodium vivax, intrasplenic infections, extracellular vesicles (EVs), CRISPR/Ca9, single-cell RNASeq (scRNASeq), spleen fibroblasts

Introduction

Malaria caused by *Plasmodium vivax* infection (vivax malaria) is a global health issue. *P. vivax* is the most widely distributed human malaria parasite, ranging from South-East Asia to the Americas region, in an area where 2.5 billion people live at risk of transmission (Howes et al., 2016). Almost 7.7 million clinical cases were estimated in 2022 (World Health Organization, 2023). However, current available diagnostic methods only detect a small percentage of infection, as epidemiological field studies estimate that up to 90% of chronic infections are asymptomatic (White et al., 2018) and 50–80% are below the sensitivity of current diagnostics methods (Okell et al., 2012). Moreover, the degree of these infections varies across different endemic regions (Angrisano and Robinson, 2022). A better understanding of these asymptomatic infections is needed if elimination of malaria is to be achieved.

For many years, it was amply accepted that the dormant form of the liver, called hypnozoites (Krotoski et al., 1982; Krotoski, 1985), was the solely responsible for these asymptomatic infections (White, 2011). However, the reticulocyte-rich spleen has recently emerged as a major cryptic niche (Siqueira et al., 2012) where more than 95% of the total parasite biomass has been observed in natural infections (Kho et al., 2021b, 2021a). The reason for this tropism remains unclear, yet it seems a major cause of anemia (Kho et al., 2024). Of interest, parasite genes whose expression is dependent on an intact spleen, have been identified in experimental infections using a nonhuman primate model susceptible to *P. vivax* (Fernandez-Becerra et al., 2020). Moreover, this study suggested that infected reticulocytes expressing spleen-dependent proteins may adhere to the spleen's microvasculature, specifically to fibroblasts expressing ICAM-1.

Extracellular vesicles (EVs) are double membrane particles secreted from cells and have recently emerged as relevant mediators of intercellular communication (Yáñez-Mó et al., 2015). EVs have been classified into two main categories, exosomes and microvesicles, based on their size, biogenesis, and composition (Raposo and Stoorvogel, 2013). Exosomes are 30–100 nm vesicles of endocytic origin that are released after the fusion of multivesicular bodies (MVBs) with the plasma membrane. Microvesicles are larger in size (0.2–2 µm) and originate by budding and shedding from the plasma membrane. Exosomes were firstly described in reticulocytes (Harding et al., 1983; Pan and Johnstone, 1983), the host cell for *P. vivax* invasion in its life cycle. Of note, during their maturation to erythrocytes, reticulocytes selectively remove proteins through the formation of reticulocyte-derived exosomes. Noticeably, it was previously shown that EVs isolated from *P. vivax* individuals can increase the binding capacity to human spleen fibroblasts (hSF) of *P. vivax*-infected reticulocytes *in vitro* via NF-κB nuclear translocation (Toda et al., 2020).

CRISPR/Cas9 editing has accelerated dramatically our ability to test essential metabolic pathways, to conditionally express genes and to generate transgenic parasites which altogether have enabled us to gain better understanding of malaria parasites (Ghorbal et al., 2014; Adjalley and Lee, 2022). Due to the lack of *in vitro* culture, we

used the CRISPR/Cas9 technology to generate a *P. falciparum* 3D7 transgenic line expressing a hypothetical *P. vivax* spleen-dependent gene (PVX_114580) (Fernandez-Becerra et al., 2020), from here on named as *P. vivax* spleen dependent protein 1 (PvSDP1). To functionally characterize it, we have performed binding assays of the transgenic line (3D7_PvSDP1) to hSFs previously stimulated with plasma-derived EVs from *P. vivax* patients (PvEVs). Moreover, we have demonstrated that this binding is partially inhibited when 3D7_PvSDP1 parasites are pre-treated with a polyclonal antibody against PvSDP1 generated in house. Of note, this antibody was also used to show that PvSDP1 is expressed at the surface of infected reticulocytes in *P. vivax* natural infections. Last, we performed single-cell RNAseq of hSFs stimulated with PvEVs from natural infections to get further insights into the formation of parasite intrasplenic niches.

Material and methods

Human plasma samples

Plasma from *P. vivax* patients used in this study was collected at the E.S.E. Hospital San José de Tierralta, Colombia. Signed informed consent was obtained from all patients by the Universidad de Córdoba, Montería (Colombia). Samples from healthy donors were collected at the Hospital Germans Tries I Pujol, Badalona (Spain), with expressed consent from the donors. Information regarding patients' parasitaemia, gender, age and other relevant information can be found in Table EV1. Ten milliliters of peripheral blood were collected in sodium citrate tubes, followed by centrifugation at 400 x g for 10 min at room temperature (RT). The collected plasmas underwent further centrifugation at 2000 x g for 10 min. The resulting plasma supernatant was recovered, aliquoted into 1 ml fractions, and subsequently frozen at -80°C.

Plasmid constructs, parasite culture and transfection

Plasmid pHH1_DiCre_Lisp1, previously described (Llorà-Batlle et al., 2020), underwent modification to incorporate the Chloroquine Resistance Transporter Promoter (CRT Promoter) and a triple hemagglutinin tag (3HA). Initially, the CRT Promoter was excised from the pARL_Vir14 plasmid (Bernabeu et al., 2012) utilizing BglII-PstI restriction enzymes and subsequently ligated into the pBlueScript II KS (+) vector at the BamHI/PstI sites. This construct was then subcloned into the SpeI/PstI sites of the pHH1_DiCre_LISP1 plasmid. The 3HA tag was synthesized through the design and annealing of two complementary primers, F-HA: GGTACCATGCATACTA GTCCGGGTACCCATACGACGTCCAGACTACGCTTAC CCATACGACGTCCCAGACTACGCT and R-HA: CCATACGACGTCCCAGACTACGCTTACCCATACGACGTCCCAGACTACGCTTACGCTTACCCATACGACGTCCCAGACTACGCTTATACTGCAG and cloned into the modified pHH1_DiCre_Lisp1 at

KpnI/PstI sites. A KpnI cloning site was deliberately preserved between the promoter sequence and the 3HA.

The *P. vivax* PVX_114580 gene was amplified from a cDNA template obtained from total RNA of the Sal-I strain (kind gift of Dr. John Barnwell) using primers F-PvSDP1: ACTCGACCCGG GATGGTACCATGAAGAGCAATTTGGGCC and R-PvSDP1: TGGGACGTCGTATGGGTACCAAACCTCTTTGCTTAT TTTTCTTT and Platinum™ Taq (Invitrogen 11304011). PVX_114580 was cloned at the KpnI restriction site using In-Fusion® HD Cloning Plus CE (Takara 638916), following manufacturer's instructions. The generated plasmid, pHH1-CRT-PvSDP1-3HA_LISP1, was cloned into SURE2 Competent Cells (Agilent 200152) and purified using EndoFree Plasmid Maxi Kit (Qiagen 12362).

The *P. falciparum* 3D7 strain was obtained from MR4 BEI Resources (MRA-102) and cultured with B+ human erythrocytes (3% hematocrit) in RPMI media (Sigma 51800-035) supplemented with 0.5% Albumax, 0.23% NaHCO₃, 0.59% HEPES, 0.05% gentamicin and 0.05 mg/ml of hypoxanthine using standard methods (Trager and Jensen, 1976).

P. falciparum 3D7 WT parasites were transfected as described previously (Llorà-Batlle et al., 2020). Briefly, 60 µg of pDC2_Cas9_hDHFryFCU1_LISP1 and 12 µg of pHH1-CRT-PvSDP1-3HA_LISP1 linearized using BsaI site (located in the ampicillin resistance cassette at the backbone of the plasmid) were used for transfection. Seven ml of 8% ring stage-synchronized culture were electroporated (310 V, 950 µF and 2 mm cuvette) with the above-mentioned plasmids. 24 h after electroporation, 10 nM WR99210 was added to the culture and maintained for 4 days. After assessing genomic integration, subcloning by limiting dilution was performed to obtain clonal population of transgenic parasites expressing PvSDP1.

Genomic integration and transcript detection

Genomic DNA from the *P. falciparum* 3D7_PvSDP1 transgenic line was obtained from 10 ml cultures with 10% mature stages parasitaemia by using QIAamp® DNA Blood Mini Kit (Qiagen 51104). Integration was confirmed by PCR using KAPA2G Robust HotStart ReadyMix (Sigma KK5701) with primers used for amplification of PVX_114580, as well as primers targeting the *lisp1* gene.

Total RNA was obtained from 16% mature-stages *P. falciparum* 3D7_PvSDP1 pellet after saponin lysis. Parasites were resuspended in TRIzol™ (Invitrogen 15596026) and incubated for 5 min at RT. Purification of RNA was performed using phenol:chloroform with precipitation in isopropanol. To minimize the risk of DNA contamination, RNA was DNase treated (Invitrogen 8170G). First-strand cDNA synthesis was performed using 1 µg of total RNA quantified via 2200 TapeStation system (Agilent), and the SuperScript™ IV (Invitrogen 18091050) with random hexamers following manufacturer's instructions. For RT-PCR, specific forward primer for PVX_114580 and reverse 3HA Tag primer were used using KAPA2G Robust HotStart ReadyMix.

Western blotting

Trophozoite/schizont parasites were harvested at 15% parasitaemia using LS-MACS separation columns (Miltenyi 130-042-401). Briefly, 12 ml of *P. falciparum* 3D7_PvSDP1 culture was pelleted by centrifugation at 300 x g for 5 min. Cell pellet was resuspended in 4 ml of RPMI and loaded on top of a LS-MACS column previously equilibrated with RPMI. Then, the parasite preparation was allowed to enter the column while being placed in LS-MACS magnet separator. Afterwards, two washes of 8 ml each were applied to the column to remove ring-stage parasites. Finally, 4 ml of RPMI were added to the column and parasites were eluted by removing the column from the magnet and by using the plunger. Parasites were lysed using parasite lysis buffer (PBS, 4% SDS, 0.1% Triton X-100 and 0.05% Protease Inhibitor Cocktail) with 30 min incubation on ice. Samples were boiled and separated in 10% SDS-PAGE, transferred on to Protran® Premium nitrocellulose membrane (Amersham 10600008) and blocked in blocking buffer (PBS, 0.1% Triton, 5% milk powder) overnight at 4°C. Blots were washed and incubated for 1 h with primary antibody [rat anti-HA tag (1:230, Roche 11867423001) and mouse anti-Hsp70 (1:1000) in dilution buffer (PBS, 0.1% Triton, 1% milk powder)]. After incubations, membranes were washed and incubated for 1 h with secondary antibody [IRDye® 680LT Goat anti-Rat IgG Secondary Antibody (1:10000, Li-Cor 926-68029) and IRDye® 800CW Goat-anti-Mouse Antibody (1:10000, Li-Cor 925-32210)]. Bands were visualized using the Li-Cor Odyssey Infrared Scanner.

Immunogenicity prediction and peptide selection

Immunogenicity of PvSDP1 was predicted using online available tools (<http://tools.iedb.org/bcell/>) based in previously published algorithms (Kolaskar and Tongaonkar, 1990; Jespersen et al., 2017) (Figures EV2A-B). Matching regions were detected and those with higher score were used to choose a peptide for synthesis: SFTVIEKKHLSKNFKKC. Synthesized peptide was characterized by an A-HPLC with a Column Luna C18 (4.6Å~ 50mm, 3µm; Phenomenex), a Gradient: Linear B (0.036% TFA in MeCN) into A (0.045% TFA in H₂O) over 15 min with a flow rate of 1 ml/min and detection at 220 nm. Peptide was 97% pure and was resuspended in ultrapure H₂O (MiliQ water), aliquoted and stored in -20°C until use. The peptide was coupled Keyhole limpet hemocyanin (KLH) at the Department of Experimental and Health Sciences – Peptide synthesis Facility of Universitat Pompeu Fabra at Centre for Genomic Regulation (Barcelona-Spain) according to their own standard operational procedures.

Generation of polyclonal antibodies against PvSDP1 and antibody testing through ELISA

Six mice (3 female and 3 male) were immunized following protocols approved by the Catalan Government (CEEA-IGTP 19-

031-HPO). Briefly, 50 µg of the synthetic peptide linked with KLH were used for individual subcutaneous injections. 0.5 ml of whole blood was extracted before immunization. Two distinct boosting injections were performed at day 21 and 42. Finally, at day 49 mice were exsanguinated and 1 ml of blood was collected from each mouse (Figure EV2D). Sera from individual mice was recovered after let it sit blood overnight at 4°C.

Sera collected from the terminal bleed (Day 49) from individual mice were tested for recognition of synthetic peptides of PvSDP1 by ELISA. Flat-bottom 96 well, microtitre ELISA plates were coated with PvSDP1 peptide (100 ng/well) in carbonate-bicarbonate buffer at 4°C overnight. Plates were washed three times using PBS with 0.2% Tween 20 and blocked with 5% skimmed milk in PBS for 2 h at RT. Antigen coated wells were incubated with sera samples (1:100, 1:200 or 1:1000) for 1 h at room temperature, washed and incubated with secondary antibody Goat anti-mouse IgG (Fc): HRP (Sigma A8786) at 1/500 dilution. Optical density was measured at 450 nm using Varioskan Flash equipment (Thermo Scientific) (Figure EV2E).

Indirect immunofluorescence assay

Transgenic parasite slides were prepared as previously described (Bernabeu et al., 2012). Briefly, a 10-ml culture of 10% parasitaemia of mixed stages of the *P. falciparum* 3D7_PvSDP1 transgenic line was washed in PBS and fixed with 4% EM grade paraformaldehyde and 0.075% EM grade glutaraldehyde in PBS. Fixed cells were permeabilized with 0.1% Triton X-100 in PBS and blocked for 1 h at room temperature in 3% PBS-Bovine Serum Albumin (PBS-BSA). A clinical isolate collected from a *P. vivax* malaria patient in Cambodia during field surveys by Institut Pasteur du Cambodge was used for IFA. *P. vivax* parasites were collected from peripheral blood from infected individuals as described (Martinez et al., 2024). Briefly, parasites were enriched by Percoll gradient (57% Percoll in KCl buffer) as described previously (Rangel et al., 2018) and then IFA slides were prepared by depositing cells on them, air dried and fixed with acetone:methanol (90:10) for 10 min and air dried.

Slides were incubated overnight with primary antibody [rabbit anti-HA (1:50, Invitrogen 71-5500) or mouse anti-RESA (1:200, gently donated by Professor Klavs Berzins, Stockholm University, Sweden) or mouse anti-SDP1 sera (1:20) or guinea pig anti-PvMSP1-19 (1:200, homemade) or guinea pig anti-LPI (Bernabeu et al., 2012) (1:200)] diluted in 3% PBS-BSA. After washing, 1 h incubation with secondary antibody [anti-rabbit conjugated with Alexa Fluor 488 (1:200, Invitrogen A11008) or anti-mouse conjugated with Alexa Fluor 546 (1:200, Invitrogen A-10036) or anti-guinea pig conjugated with Alexa Fluor 647 (1:200, Invitrogen A21450)] diluted in 3% PBS-BSA was performed. Nuclei were stained for 10 min with 4,6-diamidino-2-phenylindole (DAPI, 1:1000 in PBS). Then slides were mounted using ProLong™ Gold Antifade mounting media.

Confocal microscopy images were obtained using Abberior Infinity microscope (Abberior Instruments GmbH) using 405 nm, 485 nm, 561 nm excitation laser lines. The fluorescence excitation

and collection was performed using 60x/1.42 oil immersion objective. All acquisition operations were controlled by Lightbox software (Abberior Instruments GmbH). Acquired images were processed using Fiji/ImageJ software (version 1.54, NIH, USA).

Extracellular vesicles isolation, bead based assay characterization & EVs pooling.

EVs from plasma samples of *P. vivax* infected individuals (PvEVs) and healthy donors (hEVs) (Table EV1) were isolated by size-exclusion chromatography (SEC) as previously published (Toda et al., 2020) with some minor modifications. Briefly, 1 ml of plasma was thawed on ice and centrifuged at 2000 x g for 10 min at 4°C. Supernatants were loaded on top of 10 ml handmade Sepharose CL-2B columns (Sigma 17014001), pre-equilibrated with sterile PBS. Fifteen fractions of 500 µl each were collected in 1.5 ml low-protein retention tubes (Eppendorf, 525-0133) with PBS as elution buffer and kept at -80°C until use. Each individual SEC fraction from individual patients was identified by bead-based flow cytometry assessing the presence of CD9, CD63, CD81, CD71 and/or CD5L classical EV markers. Finally, EVs isolated from patient's plasma and healthy donor controls were pooled. To do so, 25 µl of peak quantified fractions of 10 PvEVs and 10 hEVs samples were mixed independently. PvEVs and hEVs pools were generated the day of the stimulation of the hSFs to avoid freezing/thawing.

EVs isolation via direct immunoaffinity capture of CD71+

120 µl of plasma from the same 10 different patients infected with *P. vivax* were pooled to obtain 1.2 ml of pooled sample. Similar procedure and pooling was done with plasma from the same healthy donors (Table EV1). Pooled plasmas were diluted 1:4 in cold PBS and ultracentrifuged at 120,000 x g for four hours in a TH-641 Swinging bucket rotor (Sorvall WX, ThermoFisher Ultracentrifuge 15342177) to pellet total EVs. DIC was performed as previously described (Aparici-Herraiz et al., 2022). Anti-CD71 antibody (Abcam ab214039) was coupled to Magnetic beads from Dynabeads Antibody Coupling Kit (ThermoFisher 14311D). Immediately after the last wash, captured EVs (DIC EVs) were resuspended in 35 µl SB buffer (ThermoFisher 14311D). 5 µl of DIC EVs were used for characterization of EVs by Western Blotting and 30 µl were used for functional assays.

Human spleen fibroblast culture and stimulation with Evs

hSFs were isolated from cadaveric patients from the Transplant Programme at the Hospital Germans Tries I Pujol (Toda et al., 2020). Donation of these organs for use in biomedical research received written consent from family members and was in accordance with the protocol approved by the Ethics Committee for Clinical Research of the Hospital Germans Trias I Pujol. hSFs

were cultured in Dulbecco's modified Eagle's Medium (DMEM) supplemented with 10% fetal bovine serum (FBS) (Gibco, 16000-044) and 1% penicillin/streptomycin solution (Gibco, 15070-063) (cDMEM) at 37°C and 5% CO₂. To assess biocompatibility of the Magnetic Dynabeads with the hSFs, 2.5 x 10⁵ hSFs were cultured for 48 h with the Magnetic Dynabeads coupled to the CD71 antibody (ThermoFisher 14311D). Also, same number of cells were cultured without the beads for comparison. After 48 h, and after trypsinization, cells were counted and viability was assessed using Neubauer Chamber and TrypanBlue counting.

For the functional binding assay, hSFs at 70-80% confluency were trypsinized and 1.5 x 10⁵ hSFs were seeded on 130mm coverslips (Nunc 174950) in 24-well plates in cDMEM. 24h after seeding, only adhered cells were kept and 500 µl of EVs-depleted cDMEM with 50ul of previously pooled PvEVs, hEVs or PBS independently with the SEC-purified EVs or 10 µl of the CD71⁺ captured EVs with the magnetic Dynabeads was added to each well. Each stimulation was performed in technical triplicate and with biological triplicate. EVs stimuli was kept for 48 h at 37°C before performing the functional binding assay with the *P. falciparum* 3D7_PvSDP1 transgenic line.

P. falciparum 3D7_PvSDP1 functional binding assay

Stimulated hSFs were put into contact with *P. falciparum* 3D7_PvSDP1 or *P. falciparum* 3D7 wild type. Cells were washed from growing medium and 500 µl of binding medium (RPMI supplemented with 10% AB serum (Sigma H4522-100ML) at 6.8 pH), added. Afterwards, 7.5 x 10⁵ mature stage parasites purified by LS-MACS (Miltenyi 130-042-401) were added to each well independently. Parasites were incubated at 37°C, 5% CO₂ for 1 h and unbound cells were washed thoroughly 3 times with prewarmed binding medium. Samples were fixed with methanol for 1 min and stained with 10% Giemsa. The number of parasites bound to cells were count twice independently by three different researchers (AAH, MNF, CFB) in 1000 cells of each preparation using bright-field optical microscope (Nikon, Eclipse CYL) with x100/1.25 oil objective. Statistics were calculated using Two-way ANOVA with Sidak's multiple comparisons test.

Binding inhibition assay using anti-PvSDP1 antibody

P. falciparum 3D7_PvSDP1 transgenic line was incubated with sera from immunized mouse with the PvSDP1 immunogenic peptides for 1 h at 37°C at two different concentrations of the antibody (1:5 and 1:20) diluted in binding medium. After incubation, PvEVs-stimulated hSFs were put into contact with *P. falciparum* PvSDP1 and parental *P. falciparum* 3D7. As described before, parasites were incubated at 37°C, 5% CO₂ for 1 h and unbound cells were washed thoroughly 3 times with prewarmed binding medium. Number of parasites bound to cells were counted as described previously by three different researchers (AAH, MNF, CFB).

Single-cell RNA

To further investigate the impact of EVs on hSFs, we conducted 10x single-cell RNA sequencing. A total of 1.5 x 10⁵ hSFs were seeded in a 6-well flat-bottom plate. Once 70-80% confluency was reached, EVs-depleted DMEM was introduced to each well. Subsequently, 100 µl of PvEVs was added to two wells, while 100 µl of PBS was added to two other wells. After 30 h of stimulation, cells were trypsinized and counted using a Neubauer chamber with Trypan Blue for viability assessment. The transcriptome of both stimulated and non-stimulated hSFs were sequenced using the Next GEM Single Cell 3' Reagents kits v3.1 (10x Genomics), following the manufacturer's instructions. A total of 1.6 x 10⁵ hSFs, from both the stimulated and non-stimulated groups, were independently loaded onto the Chromium Controller instrument (10X Genomics) to generate single-cell gel bead-in-emulsions (GEMs).

Single-cell RNA-Seq data processing

Sequencing results from EVs-stimulated and non-stimulated samples, generated with 10X RNAseq, were aligned and quantified against the human reference genome GRCh38 using Cell Ranger software (Version 6.1.2) with default settings. The obtained results from Cell Ranger and the count matrix were read using the Read10X function from the Seurat library (Version 4.9.9). Subsequently, standard procedures in Seurat were employed to analyze the samples, which were initially treated independently and later merged. The analysis began with quality control, removing cells with fewer than 300 genes and those with a mitochondrial RNA content exceeding 10%. Doublets were identified using the DoubletFinder library (Version 2.0.3), integrated into the Seurat pipeline, to discern doublets within each sample. Following filtering, a total of 10,338 cells in the EV-stimulated sample and 8,894 cells in the non-stimulated sample were retained.

Normalization of the samples was performed using the LogNormalize function from Seurat, ensuring global normalization to equalize the total expression of each gene across cells. Subsequently, 2,000 Highly Variable Genes (HVGs) were selected using the FindVariablesFunction. Data were scaled using ScaleData, and dimensionality reduction was conducted based on the previously calculated HVGs. This reduction was achieved using RunPCA from Seurat, considering the first 20 dimensions. To facilitate clustering, the FindNeighbors and FindClusters functions were employed, utilizing the Louvain algorithm. Visualization of clusters was accomplished using UMAP.

Identification of differentially expressed genes

To identify genes that were differentially expressed after stimulation with plasma-derived PvEVs, the FindAllMarkers function from Seurat was employed with default settings. A non-parametric Wilcoxon test with Bonferoni correction was applied for statistical analysis. Subsequently, the DotPlot function from Seurat

was used to visually represent the differentially expressed genes of interest. To further study the clusterization of the samples, Gene ontology enrichment of human proteins for all categories was done with the Database for Annotation, Visualization, and Integrated Discovery (David 6.8) (Huang, Sherman and Lempicki, 2008). Only clusters with more than 50% of treated cells were analyzed.

Single-Cell RNAseq validation through RT and qPCR of EVs-Stimulated hSFs

1.5×10^5 cells were seeded in a flat-bottom 24-well plate in exosome-depleted complete Dulbecco's Modified Eagle Medium (cDMEM), as previously described. Independently, 50 μ l of PvEVs, hEVs, or PBS was added to each well. After 48 hours of stimulation, the supernatant was removed, and 1 ml TRIzolTM (Invitrogen 15596026) was added to each well. Cells were scraped and embedded in the chaotropic agent, followed by incubation for 5 min at room temperature and freezing at -80°C until RNA extraction was performed. Biological triplicates were conducted using three different sets of PvEVs and hEVs.

RNA extraction, as described earlier in this paper, was performed, resuspended in 50 μ l of DNase/RNase-free water, and integrity was assessed using the BioAnalyzer. First-strand cDNA synthesis utilized 1 μ g of total RNA and SuperScriptTM IV (Invitrogen 18091050) with Oligo (dT) primers to match the poly-A tail of mRNA. Quantitative real-time PCR reactions were carried out in technical triplicate for each biological replicate using the Light Cycler 480 Roche system (Life Science). The qPCR reactions were prepared with 5 μ l of TaqMan[®] Fast Advanced Master (Thermo Fisher Scientific), 0.5 μ l of each amplification primer, 2.5 μ l of nuclease-free water, and 2 μ l of cDNA templates.

The PCR program included UNG incubation at 50°C for 2 min, polymerase activation at 95°C for 20 s, followed by 45 cycles of denaturation at 95°C for 1 s, annealing at 60°C for 20 s, and a negative control using 2 μ l of nuclease-free water instead of cDNA. Primers used (ThermoScientific) are listed below. To normalize expression levels (ΔCp), Glyceraldehyde-3-Phosphate Dehydrogenase (*gapdh*) was employed as an endogenous control. The studied genes included CD44 Molecule (Indian Blood Group) (*cd44*), Integrin Subunit Alpha 1 (*itga1*), Intercellular Adhesion Molecule 1 (*icam1*), Thrombospondin 1 (*thbs1*), Fibronectin 1 (*fn1*), Adhesion Molecule with Ig Like Domain 2 (*amigo2*), CD36 molecule (*cd36*), Fibroblast Growth Factor 8 (*fgf8*), Toll Like Receptor 4 (*tlr4*), and C-X-C Motif Chemokine Ligand 12 (*cxcl12*). Expression levels were normalized to the internal reference *gapdh* and calculated using the $2^{-(\Delta\Delta\text{Ct})}$ formula.

Results

Generation of a transgenic *P. falciparum* clonal line expressing PvSDP1

PvSDP1 (PVX_114580) was previously described as a spleen-dependent hypothetical protein associated with clinical protection

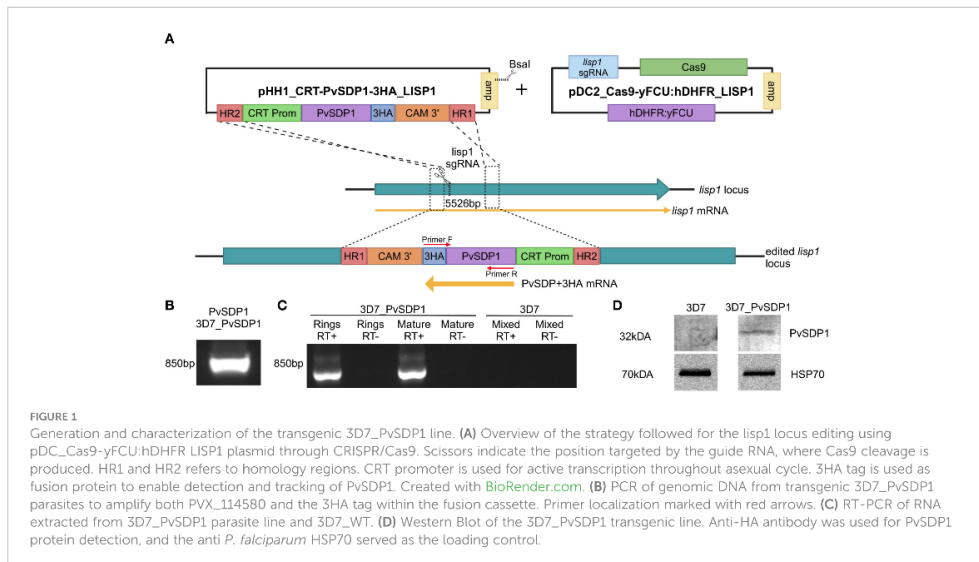
(Fernandez-Becerra et al., 2020). To further understand the function of PvSDP1, we generated transgenic *P. falciparum* 3D7 line expressing it. To do so, we modified the pHH1_DiCre_lisp1 vector (Llorà-Batlle et al., 2020) introducing the Chloroquine Resistance Transporter (CRT) promoter to ensure stable transcription of PvSDP1 through all stages of the intraerythrocytic replicative cycle (Crabb et al., 2004; Bernabeu et al., 2012) (Supplementary Figure 1A). The PvSDP1 construct targets the *lisp1* gene locus and is inserted at position 5523 of this *P. falciparum* gene (Figure 1A). *pvsdp1* was amplified from cDNA of the *P. vivax* Sal-1 strain and cloned into intermediate pHH1_CRT under the control of the *pfprt* promoter region. A triple haemagglutinin (3HA) tag was added at the 3' end of *pvsdp1* to facilitate its detection (Supplementary Figure 1A). DNA sequencing confirmed the correct sequence of the final vector.

Characterization of *P. falciparum* 3D7_PvSDP1

CRISPR/Cas9 enabled to generate efficiently a transgenic line with similar growth pattern when compared to the parental *P. falciparum* 3D7 line (Supplementary Figure 1B), leaving the transgenic *P. falciparum* 3D7_PvSDP1 line marker-free and therefore sensitive to the drug WR99210 (Supplementary Figure 1C). Genotyping of the clonal transgenic line revealed correct integration of the *pvsdp1* gene at the *lisp1* locus detecting both the gene and the HA tag fused to it (Figure 1B). Efficient transcription of *pvsdp1* was detected by RT-PCR of both ring and mature parasites (Figure 1C). In addition, Western Blot analysis using an anti-HA antibody confirmed that the transgenic 3D7_PvSDP1 line correctly expressed the PvSDP1 protein fused to the 3HA-tag (Figure 1D).

Immunofluorescence analysis reveals membrane localization of PvSDP1

To determine the subcellular localization of the PvSDP1 protein in the *P. falciparum* transgenic line, immunofluorescence assays (IFAs) were done using antibodies against HA and the ring-infected erythrocyte surface antigen (RESA), previously used as a membrane surface marker of *P. falciparum* infected red blood cells (iRBCs) (Elizalde-Torrent et al., 2021). Although a faint signal against PvSDP1 is detected in the cytosol of transgenic 3D7_PvSDP1, likely due to the forced overexpression of the PvSDP1 gene, confocal images clearly illustrate localization of the PvSDP1 at the membrane of iRBCs. This is evidenced by the co-localization of signals from the anti-HA antibody with the anti-RESA antibody (Figure 2A). Finally, using anti-HA antibody in combination with a polyclonal antibody raised against PvSDP1 (Supplementary Figure 2), we were able to observe correct targeting of the PvSDP1 to the iRBCs membrane exclusively in the transgenic line 3D7_PvSDP1 (Figure 2B).



PvSDP1 is expressed in the membrane of reticulocytes in natural infections

To confirm the subcellular localization of PvSDP1 in *P. vivax* field isolates, we used the mouse polyclonal antibody produced against PvSDP1 (Supplementary Figure 2) in IFA assays of *P. vivax*-infected reticulocytes obtained from a Cambodian patient. Confocal microscopy demonstrated that PvSDP1 is located at the surface of infected reticulocytes (Figure 3). To further confirm these results, we used the anti-PvSDP1 antibody in combination with an antibody against a long synthetic peptide (LP2) representing conserved VIR motifs, previously shown to be located at the surface of infected reticulocytes (Bernabeu et al., 2012). Colocalization of both anti-LP2 and anti-PvSDP1 antibodies is over 80% confirming membrane localization of the PvSDP1 in *P. vivax* field isolates. The anti-PvSDP1 antibody was also used in combination with an anti-PvMSP1-19 antibody displaying the typical “grape-like” shape surrounding the merozoites surface (Figure 3). Altogether, these results confirmed that PvSDP1 is located at the membrane of infected reticulocytes.

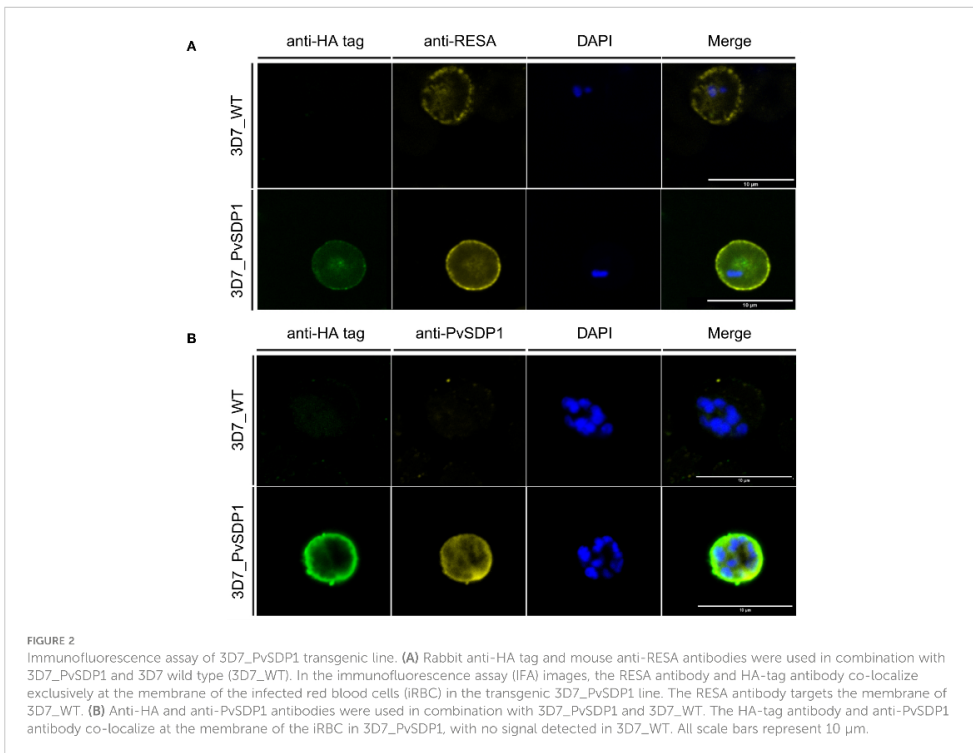
Cytoadherence of *P. falciparum* 3D7_PvSDP1 to human spleen fibroblasts

It was previously shown that EVs isolated from *P. vivax* individuals increased the binding capacity to hSFs (Toda et al., 2020). For functional assays and due to the low peripheral blood volume withdrawn from patients during acute attacks, we purified

plasma-derived EVs using Size Exclusion Chromatography (SEC) and pooled fractions 7, 8 and 9 from ten patients (PvEVs). As controls, we also made a single pool of the same SEC fractions from circulating EVs obtained from ten healthy donors (hEVs). SEC EVs were then characterized by Bead Based Assay (BBA), Nanoparticle Tracking Analysis (NTA) and Stimulated emission depletion (STED) microscopy (Supplementary Figures 3A–D). hSFs were stimulated with PvEVs and hEVs independently for 48h. Subsequently, EV-stimulated hSFs were incubated for 1 hour with the 3D7_PvSDP1 transgenic line as well as the parental 3D7_WT line, followed by thorough washing to remove unbound parasites to the cells. Binding was assessed via light microscopy (Supplementary Figure 4A). Ratios between hSFs and parasites were calculated, and statistics was performed using the Two-Way ANOVA. Binding of *P. falciparum* 3D7_PvSDP1 was significantly increased when hSFs were stimulated with PvEVs, when compared with wild type parasites (Sidak’s multiple comparisons test $p=0061$). Interestingly, this effect was only seen when the hSFs have been stimulated with PvEVs but not with hEVs or control PBS (Figure 4A).

Immunocaptured EVs increase binding to hSFs

We had previously shown that CD71⁺-EVs increased the signal of parasite proteins detection associated with circulating EVs from patients (Aparici-Herraiz et al., 2022). CD71⁺-EVs from patients’ plasma and healthy donors were purified by Direct Immunocapture



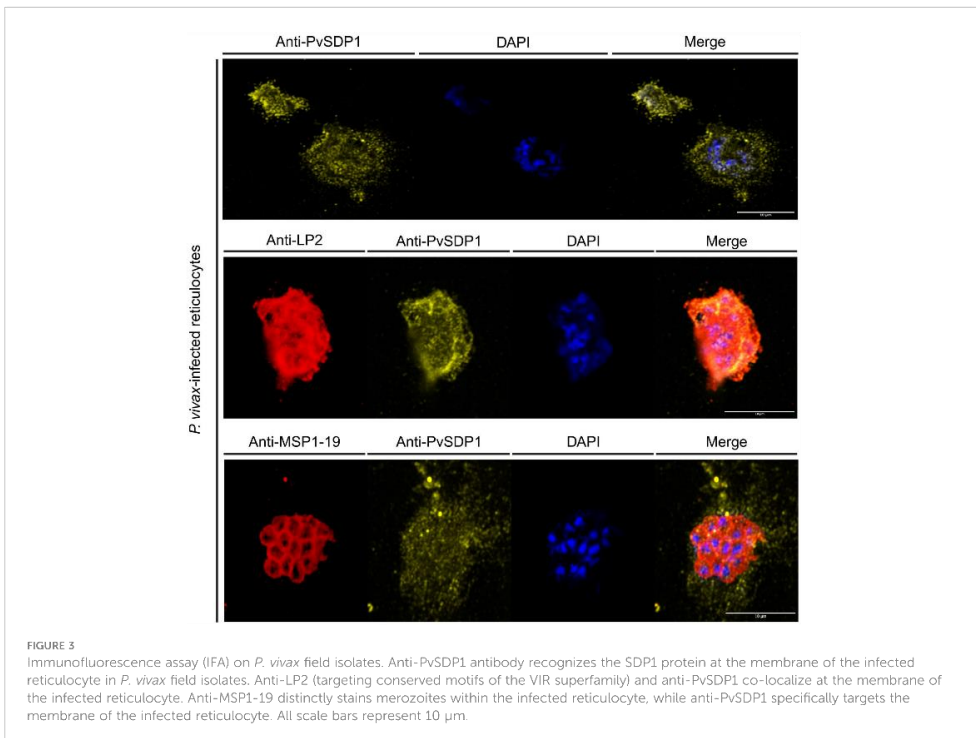
(DIC) using magnetic Dynabeads (ThermoFisher) and characterized by western blot (Supplementary Figure 5A). Beads coupled to CD71 antibodies were directly added to hSFs and cell viability assessed after 48h. There were no changes in growth rates or cell viability in hSFs that have been in contact with the Dynabeads when compared with control non-stimulated cells (Supplementary Figures 5B, C). Next, stimulation of hSFs with CD71⁺-EVs was done and functional binding assays was performed. To compare binding of the transgenic *P. falciparum* 3D7_PvSDP1, stimulation of hSFs was also performed with CD71⁺-hEVs and Dynabeads with the CD71 antibody alone. 3D7_PvSDP1 transgenic parasites showed a significant increased binding capacity to hSFs when stimulated with CD71⁺-PvEVs compared to the parental 3D7_WT (Sidak's multiple comparison test $p < 0.0001$).

Interestingly, there was a significant increase in the binding capacity of the 3D7_PvSDP1 to hSFs previously stimulated with EVs from infection when comparing to healthy EVs or control Dynabeads (Sidak's multiple comparison test, $p < 0.0001$) (Figure 4B). Altogether, DIC immunocaptured CD71⁺-EVs increased the statistical significance of the binding capacity of the transgenic line to hSFs, in comparison to SEC-purified EVs (Figure 4A). Of note, despite thoroughly washing, Dynabeads

were still observed at the surface of hSFs, yet no parasites were observed adhering directly to the magnetic beads (Figure 4B, upper panel).

Anti-PvSDP1 polyclonal antibodies block binding of the transgenic *P. falciparum* 3D7_PvSDP1 line to hSF

To confirm that the increase binding capacity of the transgenic line to hSF was mediated by the PvSDP1 protein, polyclonal antibodies generated against the protein were used in functional binding-inhibition assay. After incubation of the parasites with the antibody, parasites were put into contact with PvEVs-stimulated hSF for 1h as described previously. After thorough washes, binding of the parasites was quantified as previously described (Supplementary Figure 4B). Interestingly, after the incubation with anti-PvSDP1 sera, the transgenic 3D7_PvSDP1 parasites exhibit a reduction in the binding capacity to hSFs when compared to non-blocked 3D7_PvSDP1 parasites (One-way ANOVA $p = 0.0028$ in 1:5 dilution and $p = 0.0082$ in 1:20 dilution) (Figure 4C).



Single-cell RNAseq showed increased adhesion expression in PvEVs-treated hSFs

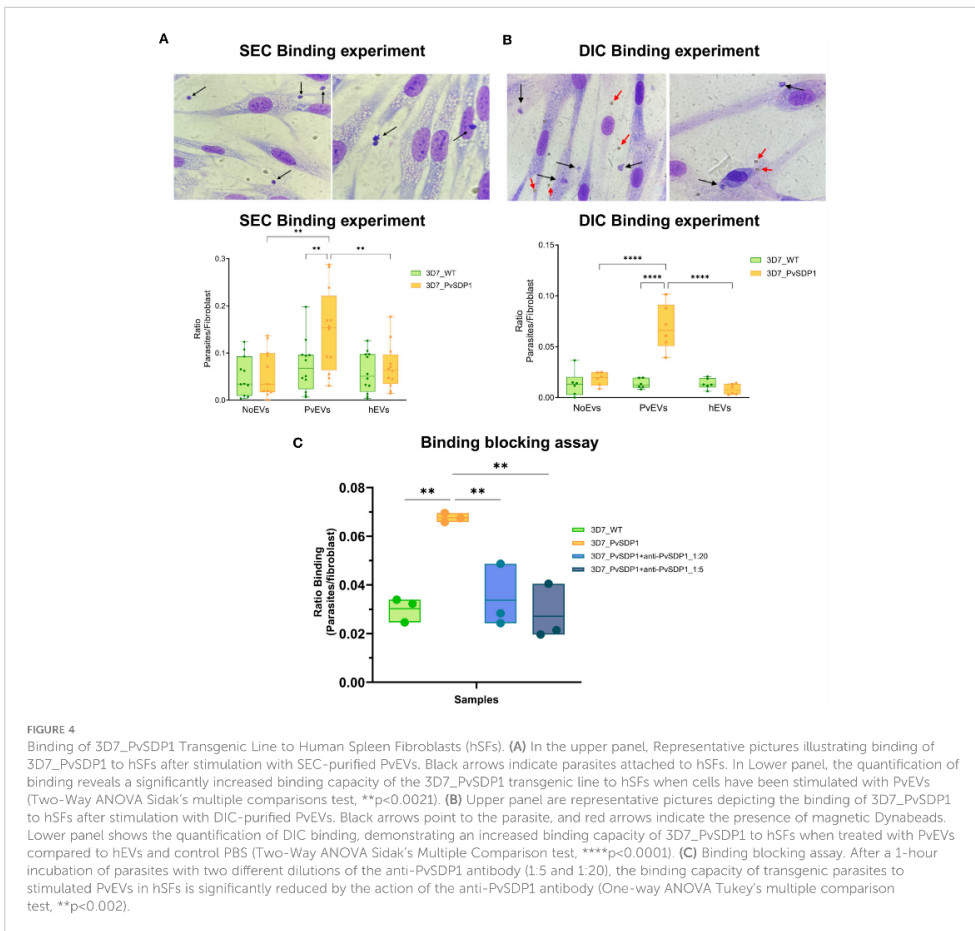
To further investigate the effect of PvEVs over hSFs whole transcriptomic analysis was done by 10X Single-Cell RNAseq. Cells were stimulated for 48h with plasma-derived EVs followed by 10X Gel Beads-in-emulsion (GEM) preparation and amplification. In parallel, untreated hSFs were also incubated for 48h and also used for 10X GEM preparation. Following clusterization of stimulated and non-stimulated cells (Figure 5A), we were able to study the distribution of treated and not-treated cells in each fibroblast cluster (Figure 5B). To gain insight into the genes that define this cluster, a GO enrichment analysis of individual cluster with more than 50% of treated cells was performed. Of note, cell adhesion, cellular compartments related to cellular junction, exosomes and other membrane-related terms and biological processes relevant to binding, were largely enriched in Cluster 1 (Figure 5C). To confirm the increase expression of cell adhesion genes, we used RT-qPCR to check transcription levels of selected adhesins genes, all included in the cell adhesion GO term. CD44 (Dalimot et al., 2022), CD36 (Cabrera et al., 2014) and ICAM1 (Toda et al., 2020) have been previously reported to play an important role in malaria pathophysiology. Here, we were able to observe how after stimulation with EVs coming from infected individuals, hSFs

exhibit a significant increased expression of adhesins like *fn1*, *amigo2*, *icam1*, *thbs1* and *thr4* (Two-way ANOVA test). Also, we observed increased expression of *cd44* and *cd36* although not being statistically significant. hEVs also produced an increase in the expression levels of the assessed genes when compared to control PBS stimulation, however, this effect is significantly smaller than PvEVs (Figure 5D).

Discussion

The presence of asymptomatic infections of *Plasmodium vivax* is a major challenge towards malaria elimination. In recent years, the spleen has emerged as a key player of such infections (Siqueira et al., 2012) where more than 95% of the total parasite biomass is found in this reticulocyte-rich organ (Kho et al., 2021b, 2021a). Here, we have characterized a hypothetical *P. vivax* spleen-dependent gene (PVX_114580) (Fernandez-Becerra et al., 2020), proposed to be named *P. vivax* spleen dependent protein 1 (PvSDP1), and shown that EVs from natural infections facilitate its binding to hSFs; thus, revealing new insights into intrasplenic infections in this species.

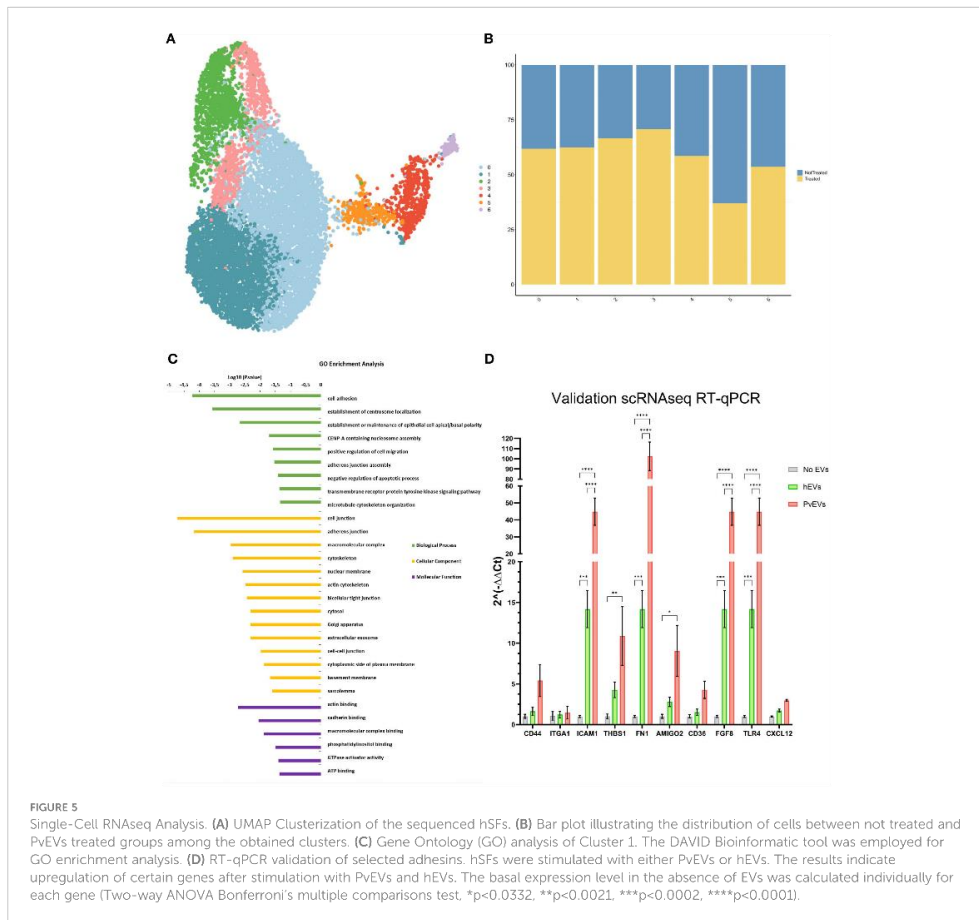
Implementation of CRISPR/Cas9 in malaria research has enabled highly targeted and precise modifications of the malaria



parasite's genome (Ghorbal et al., 2014; Adjalley and Lee, 2022). Advances in studying *P. vivax* genes using this technology enabled to study the role of the CSP protein in *P. vivax* sporozoite formation and infectiveness (Marin-Mogollon et al., 2018). We used CRISPR/Cas9 editing to knock-in PVX_114580 into a non-essential gene for asexual stages of *P. falciparum*, the *lisp1* (Llorà-Battle et al., 2020), under the control of the CRT promoter for constitutive expression during asexual blood stages (Bernabeu et al., 2012). We opted against substituting the *P. falciparum* ortholog (PF3D7_0629600) due to the limited homology with only a 51% identity conservation between them. Also, transcription of the *P. falciparum* 3D7 ortholog through intraerythrocytic cycle is relatively low when compared to more abundant transcripts like *msp1* (PF3D7_0930300) or house-keeping genes like *gapdh* (PF3D7_1462800) (Otto et al., 2010; Chappell et al., 2020). Results corroborated that PVX_114580 is

expressed in asexual blood stages and that PvSDP1 is located at the surface of infected red blood cells (Figures 1, 2).

Surface expression of PvSDP1 allowed testing this protein as a ligand in interactions with hSFs as previously reported for another *P. vivax* variant surface protein (Fernandez-Becerra et al., 2020). Moreover, as such interactions had been shown to be facilitated by EVs from natural infections (Toda et al., 2020), we used EVs isolated by SEC in binding experiments and observed an increase binding capacity of the transgenic parasite line expressing the PvSDP1 protein (Figure 4A). Of importance, for what we believe is the first time, we also used in these assays circulating EVs directly immunocaptured by CD71-antibodies as functional stimuli and showed an increase in the significance of the binding capacity of the transgenic 3D7_PvSDP1 to hSFs when compared to EVs isolated by SEC (Figure 4B). These results are likely due to the increased signal



of parasite proteins associated with circulating EVS detected by proteomic analysis (Aparici-Herraiz et al., 2022). Moreover, these data suggest the use of directly immunocaptured EVs from human plasma in functional assays, thus facilitating studies of their physiological role.

PvSDP1 was initially reported as a hypothetical *P. vivax* gene (PVX_114580) with true orthologues in other malaria species (Carlton et al., 2008) and later shown to be dependent on an intact spleen for expression (Fernandez-Becerra et al., 2020). It exhibits the PEXEL exportation motif (Supplementary Figure 1D) (Pick et al., 2011) which is in accordance with its membrane localization when is heterologously expressed in the *P. falciparum* 3D7 strain, as confirmed by confocal imaging. This localization is further supported by its co-localization with a RESA antigen from *P. falciparum*, previously identified as a membrane-associated protein (Elizalde-Torrent et al., 2021). Noticeably, polyclonal antibodies raised against a synthetic peptide from the

immunogenic region of the protein blocked the binding of PvSDP1 to hSFs after EV uptake, confirming unequivocally its cellular localization on the membrane surface of iRBCs. Moreover, we were able to confirm the surface localization of PvSDP1 in infected reticulocytes from natural infections through co-localization experiments using anti-LP2 antibody. It is worth noting, that the punctate localization pattern observed in infected reticulocytes may be attributed to the different fixation method employed, based on methanol: acetone. Due to the importance of intrasplenic infections in chronic asymptomatic infections in malaria, further studies of PvSDP1 in vaccine development are warranted.

Single-cell RNA analysis area has enabled the identification of signaling mechanisms in *P. vivax* (Sà et al., 2020; Ruberto et al., 2022). To get further insights into the EVs-induced interactions with spleen fibroblasts during *P. vivax* infections, we performed single-cell RNA analysis of hSFs after uptake of EVs from *P. vivax*

patients. GO enrichment analysis revealed an over-representation of terms such as cell adhesion, cellular components related to the cell junction and adherence junctions, among others, in Cluster 1. Indeed, expression levels of certain adhesins (Figure 5D) like *cd36* (Cabrerá et al., 2014; Nguyen et al., 2023), *icam1* (Toda et al., 2020; Gill et al., 2023), *thbs1*, *cd44* (Egan, 2018) or *thbs1* (Kanchan et al., 2015) and genes like *fgf8* (Martin-Jaular et al., 2011) were validated by RT-qPCR and is in accordance with what was previously published (Bernabeu et al., 2012; Toda et al., 2020). Together, these data strongly suggest that EVs from natural infections interact with hSFs increasing the expression of cell adhesins, thus facilitating binding of *P. vivax*-infected reticulocytes and formation of intrasplenic niches.

We are conscious of some limitations of this work: (i) functional studies of PvSDP1 using heterologous expression in *P. falciparum*, might not reveal its sole function in natural infections; (ii) the heterogeneity of human plasma EVs is always a confounding factor; yet, the use of immunocaptured CD71⁺-EVs increases the specificity of reticulocyte-derived EVs; (iii) Single-cell RNA experiments were limited to hSFs requiring future experiments with other spleen cells.

In summary, our research offers insights into how *P. vivax* utilizes circulating EVs to communicate with the human spleen, thereby facilitating the formation of cryptic intrasplenic infections. Additionally, our findings suggest that parasite genes whose expression relies on an intact spleen may serve as ligands for cell adhesins expressed in hSFs. A critical question that remains unanswered is the mechanism underlying the selectivity of EVs to interact with specific cells within this complex organ. Further transcriptional studies of the human spleen using *in vivo* and *in vitro* models as well as from spleen ruptures during asymptomatic infections are necessary for a comprehensive understanding of extracellular vesicle-mediated intercellular communication and intrasplenic infections.

Data availability statement

The datasets presented in this study can be found in online repositories. The names of the repository/repository and accession number(s) can be found below: <https://www.ncbi.nlm.nih.gov/geo/>, GSE255891.

Ethics statement

The studies involving humans were approved by Comité de Ética de la Universidad de Córdoba, Montería, Colombia and Ethics Committee Hospital Germans Trias i Pujol, Badalona (Spain). The studies were conducted in accordance with the local legislation and institutional requirements. The participants provided their written informed consent to participate in this study. The animal study was approved by Comitè Ètic d'Experimentació Animal de l'Institut de Recerca Germans Trias i Pujol. The study was conducted in accordance with the local legislation and institutional requirements.

Author contributions

AA-H: Writing – review & editing, Writing – original draft, Visualization, Validation, Resources, Methodology, Investigation, Formal analysis. MN-F: Writing – review & editing, Validation, Resources, Methodology, Investigation. AL: Writing – original draft, Visualization, Validation, Software, Methodology, Formal analysis, Data curation. IA-H: Writing – review & editing, Resources, Methodology, Investigation. ET-F: Writing – review & editing, Resources, Methodology. OL-B: Resources, Methodology, Writing – review & editing. AO: Resources, Writing – review & editing. MY: Resources, Writing – review & editing. MG: Methodology, Writing – review & editing. ME: Resources, Writing – review & editing. JP: Resources, Writing – review & editing. AC: Resources, Methodology, Writing – review & editing. HP: Writing – review & editing, Writing – original draft, Supervision, Resources, Project administration, Methodology, Funding acquisition, Formal analysis, Conceptualization. CF-B: Writing – review & editing, Writing – original draft, Validation, Supervision, Resources, Project administration, Methodology, Investigation, Funding acquisition, Formal analysis, Conceptualization.

Funding

The author(s) declare financial support was received for the research, authorship, and/or publication of this article. This work was supported by grants from the Spanish Ministry of Science and Innovation (MICINN) (PID2019-111795RB-I00 and PID2022-142908OB-I00), and co-funded by AGAUR-SGR (2021 SGR 01554) and “la Caixa” Foundation (LCF/PR/HR21/52410021). CF-B. is also part of the CIBER-Consorcio Centro de Investigación Biomédica en Red (CB 2021), Instituto de Salud Carlos III, Ministerio de Ciencia e Innovación, and Unión Europea–NextGenerationEU. This research is part of the ISGlobal's Program on the Molecular Mechanisms of Malaria which is partially supported by the Fundación Ramón Areces. We acknowledge support from the Spanish Ministry of Science and Innovation through the Centro de Excelencia Severo Ochoa “2019–2023” Program (CEX2018-000806-S) and support from the Generalitat de Catalonia through the CERCA Program.

Acknowledgments

We kindly acknowledge all participants that have given permission to be included in this project. We also thank Dr. Nuria Sima Teruel for scientific discussions, Berta Barnadas-Carceller and Pia Lucia Dernick for experimental support, Dr. Jakub Chojnacki for access to Abberior Infinity microscope and assistance with confocal imaging and to Dr. Pilar Armengol for her assistance in qRT-PCR experiments. The single cell experiments were performed at the Single Cell Unit of the Josep Carreras Leukaemia Research Institute (IJC). We also thank Toni Lluç and Ana Borges (Bonsai Lab) for all their support and discussion on single-cell RNA technology. Indicated figures were created with BioRender.com.

Conflict of interest

The authors declare that the research was conducted in the absence of any commercial or financial relationships that could be construed as a potential conflict of interest.

Publisher's note

All claims expressed in this article are solely those of the authors and do not necessarily represent those of their affiliated

organizations, or those of the publisher, the editors and the reviewers. Any product that may be evaluated in this article, or claim that may be made by its manufacturer, is not guaranteed or endorsed by the publisher.

Supplementary material

The Supplementary Material for this article can be found online at: <https://www.frontiersin.org/articles/10.3389/fcimb.2024.1408451/full#supplementary-material>.

References

- Adjalley, S., and Lee, M. C. S. (2022). CRISPR/cas9 editing of the plasmodium falciparum genome. *Methods Mol. Biol.* 2470, 221–239. doi: 10.1007/978-1-0716-2189-9_17/COVER
- Angrisano, F., and Robinson, L. J. (2022). Plasmodium vivax – How hidden reservoirs hinder global malaria elimination. *Parasitol. Int.* 87, 102526. doi: 10.1016/j.parint.2021.102526
- Aparici-Herraiz, I., Gualdrón-López, M., Castro-Cavada, C. J., Carmona-Fonseca, J., Yasnot, M. F., Fernández-Becerra, C., et al. (2022). Antigen discovery in circulating extracellular vesicles from plasmodium vivax patients. *Front. Cell Infect. Microbiol.* 11. doi: 10.3389/fcimb.2021.811390
- Bernabeu, M., Lopez, F. J., Ferrer, M., Martín-Jaular, L., Razaname, A., Corradin, G., et al. (2012). Functional analysis of Plasmodium vivax VIR proteins reveals different subcellular localizations and cytoadherence to the ICAM-1 endothelial receptor. *Cell Microbiol.* 14, 386–400. doi: 10.1111/j.1462-5822.2011.01726.x
- Cabrera, A., Neculai, D., and Kain, K. C. (2014). CD36 and malaria: friends or foes? A decade of data provides some answers. *Trends Parasitol.* 30, 436–444. doi: 10.1016/j.pt.2014.07.006
- Carlton, J. M., Adams, J. H., Silva, J. C., Bidwell, S. L., Lorenzi, H., Caler, E., et al. (2008). Comparative genomics of the neglected human malaria parasite Plasmodium vivax. *Nature* 455, 757–763. doi: 10.1038/nature07327
- Chappell, L., Ross, P., Ross, P., Orchard, L., Russell, T. J., Otto, T. D., et al. (2020). Refining the transcriptome of the human malaria parasite Plasmodium falciparum using amplification-free RNA-seq. *BMC Genomics* 21. doi: 10.1186/s12864-020-06787-5
- Crabb, B. S., Rug, M., Gilberger, T. W., Thompson, J. K., Triglia, T., Maier, A. G., et al. (2004). Transfection of the human malaria parasite Plasmodium falciparum. *Methods Mol. Biol.* 270, 263–276. doi: 10.1385/1-59259-793-9-263/COVER
- Dalimot, J. J., Klei, T. R. L., Beuger, B. M., Dikmen, Z., Bouwman, S. A. M., Mombongo-Goma, G., et al. (2022). Malaria-associated adhesion molecule activation facilitates the destruction of uninfected red blood cells. *Blood Adv.* 6, 5798–5810. doi: 10.1182/bloodadvances.2021006171
- Egan, E. S. (2018). Beyond hemoglobin: screening for malaria host factors. *Trends Genet.* 34, 133. doi: 10.1016/j.tig.2017.11.004
- Elizalde-Torrent, A., Trejo-Soto, C., Méndez-Mora, L., Nicolau, M., Ezama, O., Gualdrón-López, M., et al. (2021). Pitting of malaria parasites in microfluidic devices mimicking spleen interendothelial slits. *Sci. Rep.* 11, 22099. doi: 10.1038/s41598-021-01568-w
- Fernández-Becerra, C., Bernabeu, M., Castellanos, A., Correa, B. R., Obadia, T., Ramirez, M., et al. (2020). Plasmodium vivax spleen-dependent genes encode antigens associated with cytoadhesion and clinical protection. *Proc. Natl. Acad. Sci. U.S.A.* 117, 13056–13065. doi: 10.1073/pnas.1920596117
- Ghorbal, M., Gorman, M., MacPherson, C. R., Martins, R. M., Scherf, A., and Lopez-Rubio, J. J. (2014). Genome editing in the human malaria parasite Plasmodium falciparum using the CRISPR-Cas9 system. *Nat. Biotechnol.* 32, 819–821. doi: 10.1038/nbt.2925
- Gill, J., Singh, H., and Sharma, A. (2023). Profiles of global mutations in the human intercellular adhesion molecule-1 (ICAM-1) shed light on population-specific malaria susceptibility. *BMC Genomics* 24 (1), 773. doi: 10.1186/s12864-023-09846-9
- Harding, C., Heuser, J., and Stahl, P. (1983). Receptor-mediated endocytosis of transferrin and recycling of the transferrin receptor in rat reticulocytes. *J. Cell Biol.* 97, 329–339. doi: 10.1083/jcb.97.2.329
- Hoves, R. E., Battle, K. E., Mendis, K. N., Smith, D. L., Cibulskis, R. E., Baird, J. K., et al. (2016). Global epidemiology of Plasmodium vivax. *Am. J. Trop. Med. Hygiene* 95, 15–34. doi: 10.4269/ajtmh.16-0141
- Iluang, D. W., Sherman, B. T., and Lempicki, R. A. (2008). Systematic and integrative analysis of large gene lists using DAVID bioinformatics resources. *Nature Protocols* 4 (1), 44–57. doi: 10.1038/nprot.2008.211
- Jespersen, M. C., Peters, B., Nielsen, M., and Marcotilli, P. (2017). BepiPred-2.0: improving sequence-based B-cell epitope prediction using conformational epitopes. *Nucl. Acids Res.* 45 (W1), W24–W29. doi: 10.1093/nar/gkx346
- Kanchan, K., Pati, S. S., Mohanty, S., Mishra, S. K., Sharma, S. K., Awasthi, S., et al. (2015). Polymorphisms in host genes encoding NOSII, C-reactive protein, and adhesion molecules thrombospondin and E-selectin are risk factors for Plasmodium falciparum malaria in India. *Eur. J. Clin. Microbiol. Infect. Dis.* 34, 2029–2039. doi: 10.1007/s10096-015-2448-0
- Kho, S., Qotrunnada, L., Leonardo, L., Andries, B., Wardani, P. A. I., Fricot, A., et al. (2021a). Evaluation of splenic accumulation and colocalization of immature reticulocytes and Plasmodium vivax in asymptomatic malaria: A prospective human splenectomy study. *PLoS Med.* 18, e1003632. doi: 10.1371/journal.pmed.1003632
- Kho, S., Qotrunnada, L., Leonardo, L., Andries, B., Wardani, P. A. I., Fricot, A., et al. (2021b). Hidden biomass of intact malaria parasites in the human spleen. *New Engl. J. Med.* 384, 2067–2069. doi: 10.1056/NEJMc2023884
- Kho, S., Siregar, N. C., Qotrunnada, L., Fricot, A., Sissoko, A., Shanti, P. A. I., et al. (2024). Retention of uninfected red blood cells causing congestive splenomegaly is the major mechanism of anemia in malaria. *Am. J. Hematol.* 99, 223–235. doi: 10.1002/ajh.27152
- Kolaskar, A. S., and Tongaonkar, P. C. (1990). A semi-empirical method for prediction of antigenic determinants on protein antigens. *FEBS Lett.* 276 (1–2), 172–174. doi: 10.1016/0014-5793(90)80535-Q
- Krotoski, W. A. (1985). Discovery of the hypnozoite and a new theory of malarial relapse. *Trans. R. Soc. Trop. Med. Hyg.* 79, 1. doi: 10.1016/0035-9203(85)90221-4
- Krotoski, W. A., Collins, W. E., Bray, R. S., Garnham, P. C., Cogswell, F. B., Gwadz, R. W., et al. (1982). Demonstration of hypnozoites in sporozoite-transmitted plasmodium vivax infection. *Am. J. Trop. Med. Hyg.* 31, 1291–1293. doi: 10.4269/ajtmh.1982.31.1291
- Llorá-Battle, O., Michel-Todó, L., Wimer, K., Toda, H., Fernández-Becerra, C., Baum, J., et al. (2020). Conditional expression of PfAP2-G for controlled massive sexual conversion in Plasmodium falciparum. *Sci. Adv.* 6. doi: 10.1126/sciadv.aaz5057
- Marin-Mogollon, C., Van Pul, F. J. A., Miyazaki, S., Imai, T., Ramesar, J., Selman, A. M., et al. (2018). Chimeric Plasmodium falciparum parasites expressing Plasmodium vivax circumsporozoite protein fail to produce salivary gland sporozoites. *Malar. J.* 17 (1), 288. doi: 10.1186/s12936-018-2431-1
- Martínez, F. J., White, M., Guillotte-Blisnick, M., Huon, C., Boucharlat, A., Agou, F., et al. (2024). PvDBPI elicits multiple antibody-mediated mechanisms that reduce growth in a Plasmodium vivax challenge trial. *NPJ Vaccines* 9 (1). doi: 10.1038/S41541-023-00796-7
- Martin-Jaular, L., Ferrer, M., Calvo, M., Rosanas-Urgell, A., Kalko, S., Graewe, S., et al. (2011). Strain-specific spleen remodeling in Plasmodium yoelii infections in Balb/c mice facilitates adherence and spleen macrophage-clearance escape. *Cell Microbiol.* 13, 109–122. doi: 10.1111/cmi.2011.13.issue-1
- Nguyen, T. S., Park, J. H., Nguyen, T. K., Nguyen, T. V., Lee, S. K., Na, S. H., et al. (2023). Plasmodium vivax merozoite-specific thrombospondin-related anonymous protein (PvMTRAP) interacts with human CD36, suggesting a novel ligand-receptor interaction for reticulocyte invasion. *Parasit Vectors* 16, 1–11. doi: 10.1186/s13071-023-06631-5
- Okell, L. C., Boucema, T., Griffin, J. T., Ouedraogo, A. L., Ghani, A. C., and Drakeley, C. J. (2012). Factors determining the occurrence of submicroscopic malaria infections and their relevance for control. *Nat. Commun.* 3, 1237. doi: 10.1038/ncomms2241
- Otto, T. D., Wilinski, D., Aseffa, S., Keane, T. M., Sarry, L. R., Böhm, U., et al. (2010). New insights into the blood-stage transcriptome of Plasmodium falciparum using RNA-Seq. *Mol. Microbiol.* 12–24. doi: 10.1111/j.1365-2958.2009.07026.x
- Pan, B.-T., and Johnstone, R. M. (1983). Fate of the transferrin receptor during maturation of sheep reticulocytes in vitro: selective externalization of the receptor. *Cell* 33, 967–978. doi: 10.1016/0092-8674(83)90040-5
- Pick, C., Ebersberger, I., Spielmann, T., Bruchhaus, L., and Burmester, T. (2011). Phylogenomic analyses of malaria parasites and evolution of their exported proteins. *BMC Evol. Biol.* 11, 167. doi: 10.1186/1471-2148-11-167

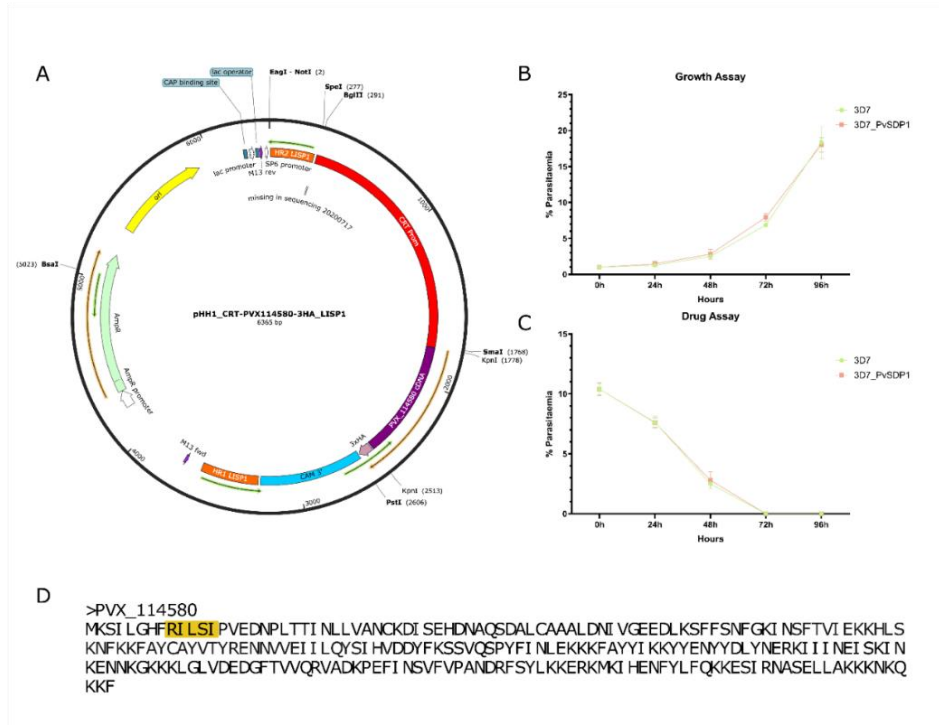
- Rangel, G. W., Clark, M. A., Kanjee, U., Lim, C., Shaw-Saliba, K., Menezes, M. J., et al. (2018). Enhanced ex vivo plasmodium vivax intraerythrocytic enrichment and maturation for rapid and sensitive parasite growth assays. *Antimicrob. Agents Chemother.* 62 (4), e02519-17. doi: 10.1128/AAC.02519-17
- Raposo, G., and Stoorvogel, W. (2013). Extracellular vesicles: Exosomes, microvesicles, and friends. *J. Cell Biol.* 200, 373–383. doi: 10.1083/jcb.201211138
- Ruberto, A. A., Bourke, C., Vantaux, A., Maher, S. P., Jex, A., Witkowski, B., et al. (2022). Single-cell RNA sequencing of Plasmodium vivax sporozoites reveals stage- and species-specific transcriptomic signatures. *PLoS Negl. Trop. Dis.* 16, e0010633. doi: 10.1371/journal.pntd.0010633
- Sá, J. M., Cannon, M. V., Caleon, R. L., Wellem, T. E., and Serre, D. (2020). Single-cell transcription analysis of Plasmodium vivax blood-stage parasites identifies stage- and species-specific profiles of expression. *PLoS Biol.* 18, e3000711. doi: 10.1371/journal.pbio.3000711
- Siqueira, M., Maria, B., Magalha, L., Melo, G. C., Ferrer, M., Castillo, P., et al. (2012). Spleen rupture in a case of untreated plasmodium vivax infection. *PLoS Negl. Trop. Dis.* 6, 1–5. doi: 10.1371/journal.pntd.0001934
- Toda, H., Diaz-Varela, M., Segui-Barber, J., Roobsoong, W., Baro, B., Garcia-Silva, S., et al. (2020). Plasma-derived extracellular vesicles from Plasmodium vivax patients signal spleen fibroblasts via NF-κB facilitating parasite cytoadherence. *Nat. Commun.* 11, 2761. doi: 10.1038/s41467-020-16337-y
- Trager, W., and Jensen, J. B. (1976). Human malaria parasites in continuous culture. *Sci.* (1979) 193, 673–675. doi: 10.1126/science.781840
- White, N. J. (2011). Determinants of relapse periodicity in Plasmodium vivax malaria. *Malar. J.* 10, 1–36. doi: 10.1186/1475-2875-10-297/TABLES/3
- White, M. T., Walker, P., Karl, S., Hetzel, M. W., Freeman, T., Waltmann, A., et al. (2018). Mathematical modelling of the impact of expanding levels of malaria control interventions on Plasmodium vivax. *Nat. Commun.* 9, 3300. doi: 10.1038/s41467-018-05860-8
- World Health Organization (2023) *World malaria report 2022*. Available online at: <https://www.wipo.int/amc/en/mediation/>.
- Yáñez-Mó, M., Siljander, P. R. M., Andreu, Z., Zavec, A. B., Borrás, F. E., Bazas, E. I., et al. (2015). Biological properties of extracellular vesicles and their physiological functions. *J. Extracell. Vesicles* 4, 1–60. doi: 10.3402/jev.v4.27066

SUPPLEMENTARY DATA FILE

Table of Contents

Supplementary Figures	2
Supplementary Figure 1. Characterization of 3D7_PvSDP1 Transgenic Line and Plasmid Map.	2
Supplementary Figure 2. Generation of polyclonal antibodies against PvSDP1.	3
Supplementary Figure 3. Characterization of SEC EVs used for functional assays.	4
Supplementary Figure 4. Schematic representation of functional assays.	5
Supplementary Figure 5. Characterization of DIC-captured EVs and investigation of the effect of Dynabeads over hSFs.	6
Supplementary Table	7
Supplementary Table 1. Information of <i>P. vivax</i> infected individuals and healthy donor controls samples used for functional assay	7

1 Supplementary Figures



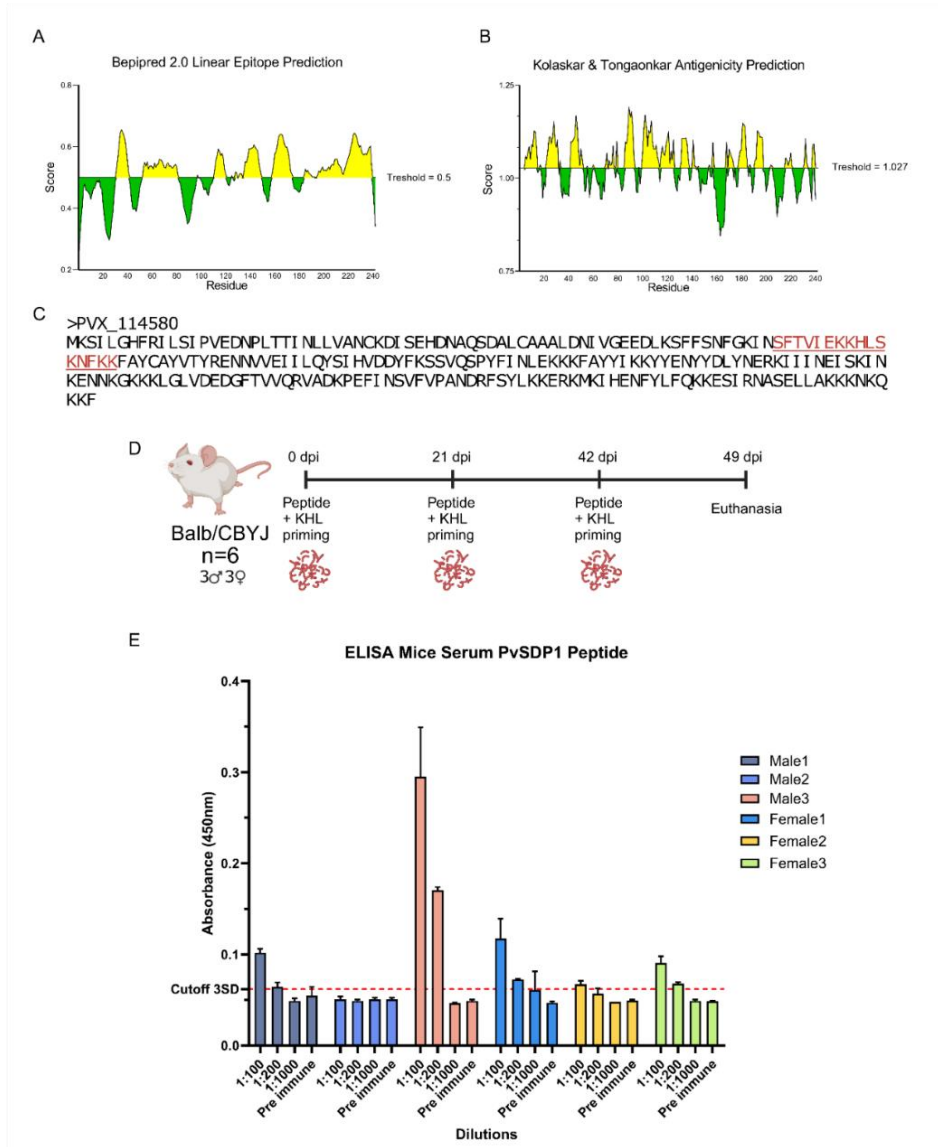
1.1 Supplementary Figure 1. Characterization of 3D7_PvSDP1 Transgenic Line and Plasmid Map.

(A) Plasmid Map containing PVX_114580.

(B) Growth assay comparing parental and transgenic 3D7_PvSDP1 line.

(C) Drug (WR9210) sensitivity assay comparing parental and transgenic 3D7_PvSDP1 line.

(D) Aminoacidic sequence of the SDP1 protein. In yellow, the exportation PEXEL-motif highlighting conserved sequences of this motif (Pick *et al*, 2011).



1.2 Supplementary Figure 2. Generation of polyclonal antibodies against PvSDP1.

(A) Bepipred linear epitope prediction results of the protein sequence of PvSDP1. Immunogenicity of PvSDP1 was predicted using online available tools (<http://tools.icdb.org/bcell/>) (Kolaskar and

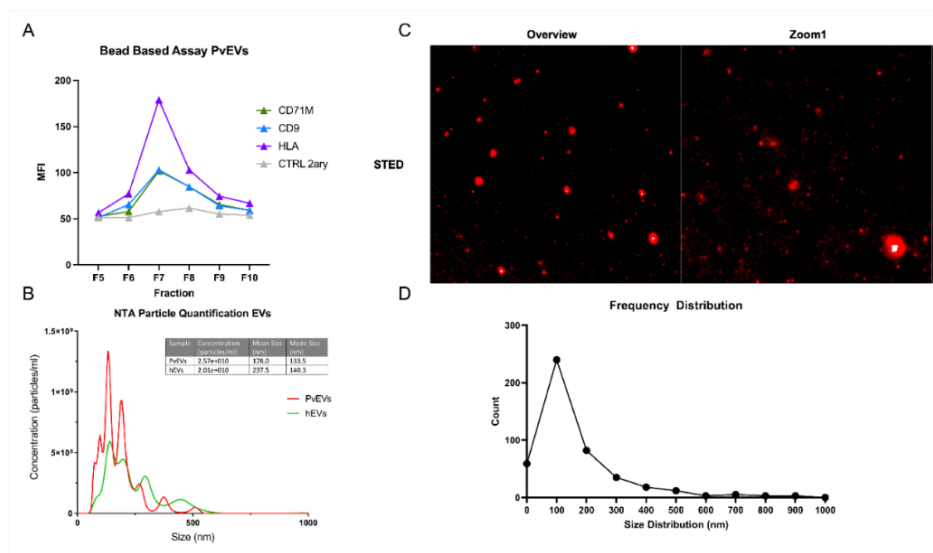
Tongaonkar, 1990; Jespersen et al., 2017), Matching regions were detected and those with higher score were used to choose a peptide for synthesis: SFTVIEKKHLSKNFKKC

(B) Antigenicity Kolaskar-Tongaonkar prediction algorithm of the protein sequence of PvSDP1.

(C) Protein sequence of PvSDP1. Note in red underline is the peptide selected for the immunization of mice.

(D) Immunization strategy of Balb/CBYJ mice using immunogenic synthetic peptide from PvSDP1

(E) ELISA results from mice sera obtained after immunization with PvSDP1 peptides.



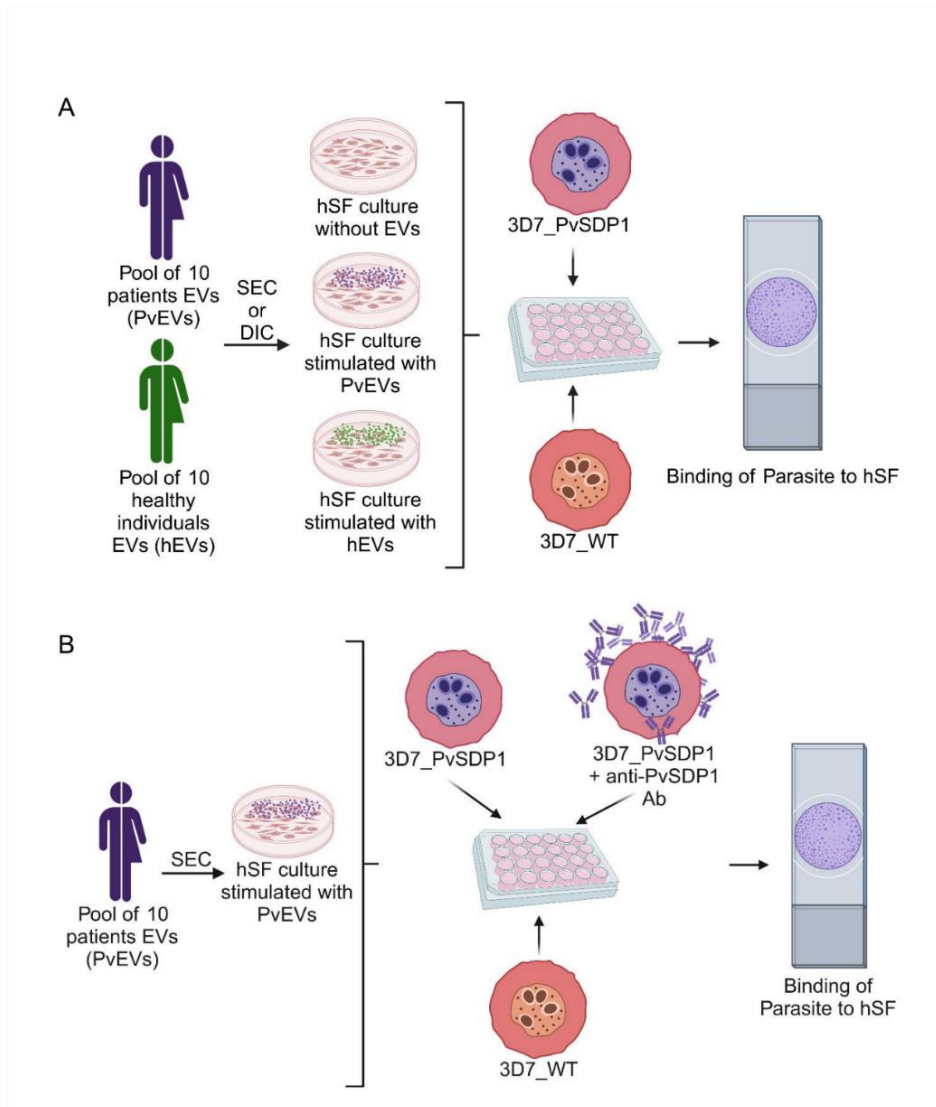
1.3 Supplementary Figure 3. Characterization of SEC EVs used for functional assays.

(A) Representative Bead-based Assay of PvEVs where CD9, HLA, and CD71 served as EV markers in all PvEVs or hEVs SEC.

(B) NTA Particle Quantification of EVs.

(C) Images corresponding to Super Resolution STED Microscopy where DPPE membrane staining is utilized to stain PvEVs.

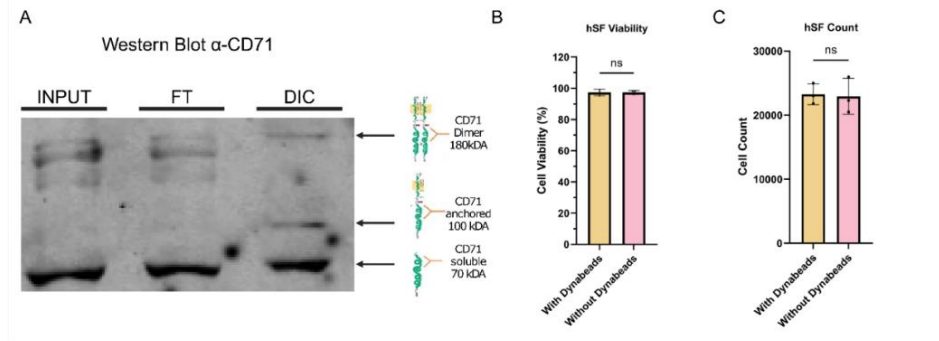
(D) Automated quantification of the Size Distribution of PvEVs Stained with DPPE and Imaged in STED Mode.



1.4 Supplementary Figure 4. Schematic representation of functional assays.

(A) Binding Experiment schematic representation.

(B) Binding inhibition assay using anti-PvSDP1 antibody.



1.5 Supplementary Figure 5. Characterization of DIC-captured EVs and investigation of the effect of Dynabeads over hSFs.

(A) WB of Direct-Immunocaptured CD71+ EVs. In the Direct Immunocapture (DIC) fraction, there is an enrichment in the anchored CD71 form and CD71 dimer, both associated with EVs.

(B) hSFs viability test after incubation for 48 h with magnetic Dynabeads coupled with anti-CD71 antibody.

(C) hSFs count by microscopy using Neubauer Chamber after incubation for 48 h with magnetic Dynabeads coupled with anti-CD71 antibody.

2 Supplementary Table

Patient code	Collection Date	Residence time in malaria endemic area	City	State	Country	Age (years)	Parasitaemia (parasites/ μ l)	Number of previous malaria infections	Gender	Pregnant
B8-04	22/11/2018	130 months	Tierralta	Cordoba	Colombia	31	5200	3	M	
B8-09	28/11/2018	9 months	Tierralta	Cordoba	Colombia	0,75	2100	0	M	
B8-10	28/11/2018	60 months	Tierralta	Cordoba	Colombia	10	2000	0	M	
B8-11	28/11/2018	48 months	Tierralta	Cordoba	Colombia	40	2000	1	M	
B8-12	28/11/2018	48 months	Tierralta	Cordoba	Colombia	4	19310	0	M	
B8-13	29/11/2018	276 months	Tierralta	Cordoba	Colombia	23	18600	2	F	NO
B8-14	30/11/2018	156 months	Tierralta	Cordoba	Colombia	13	2901	3	M	
B8-16	30/11/2018	600 months	Tierralta	Cordoba	Colombia	64	2325	1	F	NO
B8-27	24/05/2019	N/A	Tierralta	Cordoba	Colombia	39	4219	N/A	F	NO
B8-33	06/06/2019	N/A	Tierralta	Cordoba	Colombia	20	2610	N/A	M	
HD-04	11/01/2019	0	Badalona	Barcelona	Spain	34	-	0	M	
HD-05	24/01/2019	0	Badalona	Barcelona	Spain	23	-	0	M	
HD-07	24/01/2019	0	Badalona	Barcelona	Spain	24	-	0	F	NO
HD-09	08/03/2019	0	Badalona	Barcelona	Spain	37	-	0	F	
HD-11	08/03/2019	0	Badalona	Barcelona	Spain	33	-	0	M	
HD-14	18/06/2019	0	Badalona	Barcelona	Spain	25	-	0	F	NO
HD-15	18/06/2019	0	Badalona	Barcelona	Spain	25	-	0	M	
HD-20	18/04/2023	0	Badalona	Barcelona	Spain	24	-	0	F	NO
HD-22	18/04/2023	0	Badalona	Barcelona	Spain	29	-	0	F	NO
HD-23	18/04/2023	0	Badalona	Barcelona	Spain	48	-	0	M	

N/A: Information not available

2.1 Supplementary Table 1. Information of *P. vivax* infected individuals and healthy donor controls samples used for functional assay

3.3 Article 3: Morphological and Transcriptional Changes in Human Bone Marrow During Natural *Plasmodium vivax* Malaria Infections

Objective 1: Identification and validation of genes differentially expressed in the spleen & bone marrow through global transcriptional and computational analysis.

Title: Morphological and Transcriptional Changes in Human Bone Marrow During Natural *Plasmodium vivax* Malaria Infections.

Authors: Marcelo AM Brito, Bàrbara Baro, Tainá C Raiol, **Alberto Ayllon-Hermida**, Izabella P Safe, Katrien Deroost, Erick F G Figueiredo, Allyson G Costa, Maria del P Armengol, Lauro Sumoy, Anne C G Almeida, Bidossessi W Hounkpe, Erich V De Paula, Cármen Fernandez-Becerra, Wuelton M Monteiro, Hernando A del Portillo, Marcus V G Lacerda.

Journal: The Journal of Infectious Diseases.

Year: 2022

Volume: 225

Issue: 7

Pages: 1274-1283

Impact Factor: 8.4

Quartile and Research area: Q1 Infectious Diseases.

DOI: <https://doi.org/10.1093/infdis/jiaa177>

Morphological and Transcriptional Changes in Human Bone Marrow During Natural *Plasmodium vivax* Malaria Infections

Marcelo A. M. Brito,^{1,2,a} Bárbara Baro,^{1,3,a} Tainá C. Raiol,⁴ Alberto Ayllon-Hermida,³ Izabella P. Safe,¹ Katrien Deroost,^{1,b} Erick F. G. Figueiredo,^{1,2} Allyson G. Costa,^{1,2} Maria del P. Armengol,⁵ Lauro Sumoy,⁶ Anne C. G. Almeida,^{1,2} Bidossessi W. Hounkpe,⁶ Erich V. De Paula,^{5,7} Carmen Fernandez-Becerra,^{3,5} Wuelton M. Monteiro,^{1,2} Hernando A. del Portillo,^{3,5,8} and Marcus V. G. Lacerda^{1,2,9}

¹Fundaç o de Medicina Tropical Dr Heitor Vieira Dourado, Manaus, Amazonas, Brazil, ²Universidade do Estado do Amazonas, Manaus, Amazonas, Brazil, ³ISGlobal, Hospital Cl nic–Universitat de Barcelona, Barcelona, Spain, ⁴Fiocruz Bras lia, Oswaldo Cruz Foundation, Bras lia, Brazil, ⁵Institut d’Investigaci n Ci ncies de la Salut Germans Trias i Pujol, Badalona, Spain, ⁶University of Campinas, Campinas, S o Paulo, Brazil, ⁷Hematology and Hemotherapy Foundation from Amazonas State, Manaus, Amazonas, Brazil, ⁸Instituci  Catalana de Recerca i Estudis Avançats, Barcelona, Spain, and ⁹Instituto Le nidas & Maria Deane, Fiocruz, Manaus, Amazonas, Brazil

Background: The presence of *Plasmodium vivax* malaria parasites in the human bone marrow (BM) is still controversial. However, recent data from a clinical case and experimental infections in splenectomized nonhuman primates unequivocally demonstrated the presence of parasites in this tissue.

Methods: In the current study, we analyzed BM aspirates of 7 patients during the acute attack and 42 days after drug treatment. RNA extracted from CD71⁺ cell suspensions was used for sequencing and transcriptomic analysis.

Results: We demonstrated the presence of parasites in all patients during acute infections. To provide further insights, we purified CD71⁺ BM cells and demonstrated dyserythropoiesis and inefficient erythropoiesis in all patients. In addition, RNA sequencing from 3 patients showed that genes related to erythroid maturation were down-regulated during acute infections, whereas immune response genes were up-regulated.

Conclusions: This study thus shows that during *P. vivax* infections, parasites are always present in the BM and that such infections induced dyserythropoiesis and ineffective erythropoiesis. Moreover, infections induce transcriptional changes associated with such altered erythropoietic response, thus highlighting the importance of this hidden niche during natural infections.

Keywords. *Plasmodium vivax*; bone marrow aspirates; natural infections; ineffective erythropoiesis; RNA sequencing.

SIGNIFICANCE STATEMENT

Analysis of bone marrow aspirates from 7 patients with *Plasmodium vivax* malaria revealed parasites and erythropoietic defects in all of them. Global transcription identified genes related to such defects, highlighting the importance of this hidden niche during infections.

Plasmodium vivax is the most widely distributed human malaria parasite and is responsible for 7 million yearly clinical cases, including many causing severe disease or death [1]. Studies of the

human bone marrow (BM) during *P. vivax* malaria infections are scarce, even though the presence of parasites in this tissue was first acknowledged in 1894 [2]. Moreover, sternal puncture evaluation as an alternative method for malaria diagnosis revealed parasite enrichment in the BM compared with peripheral blood [3]. Nuclear abnormalities in erythroblasts, a common feature of dyserythropoiesis, were first observed in vivax malaria [4]. In contrast, an electron microscopic study of the human BM during *P. vivax* attacks in anemic children revealed BM dyserythropoiesis and ineffective erythropoiesis in the absence of parasites [5]. Unequivocal evidence for the presence of parasites in the BM using molecular markers, as well as observations on BM dyserythropoiesis and ineffective erythropoiesis, however, were recently reported in a clinical case [6]. In addition, experimental *P. vivax* infections in splenectomized monkeys also revealed that the BM is a niche for parasites during active infections [7].

The mechanisms leading to dyserythropoiesis and ineffective erythropoiesis during malaria are not fully understood, especially for *P. vivax*. However, findings from studies in human patients, animal models, and in vitro studies all seem to support the idea that an inadequate erythropoietic response is due to the presence of parasites or their products during infections as

Received 9 January 2020; editorial decision 31 March 2020; accepted 8 June 2020; published online June 18, 2020.

^aM. A. M. B. and B. B. contributed equally to this work.

^bPresent affiliation: Francis Crick Institute, London, United Kingdom.

Correspondence: Hernando A. del Portillo, Barcelona Institute for Global Health and Institut d’Investigaci n, Germans Trias i Pujol, Carretera de Can Ruti, Cami de les Escoles, Badalona (Barcelona) 08916, Spain (hernandoa.delportillo@isglobal.org).

The Journal of Infectious Diseases[®] 2022;225:1274–83

  The Author(s) 2020. Published by Oxford University Press for the Infectious Diseases Society of America. This is an Open Access article distributed under the terms of the Creative Commons Attribution-NonCommercial-NoDerivs licence (<http://creativecommons.org/licenses/by-nc-nd/4.0/>), which permits non-commercial reproduction and distribution of the work, in any medium, provided the original work is not altered or transformed in any way, and that the work is properly cited. For commercial re-use, please contact journals.permissions@oup.com. DOI: 10.1093/infdis/jiaa177

well as host immune responses [8]. Synchronous *in vitro* differentiation of reticulocytes and erythrocytes from hematopoietic stem cells [9] offered the possibility of studying vivax infections *in vitro* during erythropoiesis. Using such methods, intact and lysed *P. vivax*-infected cells were shown to suppress erythroid development by promoting cell cycle arrest [10, 11]. Moreover, *in vivo* studies using *Plasmodium yoelii*, a murine malaria species that shares some biological features with *P. vivax*, showed that infected cells as well as parasite-conditioned media have been shown to induce secretion of tumor necrosis factor (TNF) in mouse macrophages [12], which in turn have been shown to suppress erythropoiesis *in vitro* through TNF release [13]. Clinical data indicate that erythropoietic defects are associated with the presence of the parasites in the BM, independent of anemic status or levels of circulating erythropoietin [5, 14].

The proinflammatory cytokines TNF and interferon (IFN) γ have also been shown to inhibit erythropoiesis [15, 16] by interfering in the expression of transcriptional factors controlling erythropoiesis and by with the production of erythropoietin [8]. In contrast, interleukin 10, an anti-inflammatory cytokine, has been suggested to protect surrounding cells from erythropoietic defects by regulating the expression of surface and soluble TNF receptor [17]. Of interest, hemozoin (a by-product of hemoglobin digestion produced by malaria parasites) can suppress erythropoiesis *in vitro* in the absence of TNF, although addition of TNF synergized with hemozoin to inhibit erythropoiesis [18]. This was confirmed *in vivo* for *Plasmodium falciparum* infections in children [19]. *In vitro* cultures of erythroblasts exposed to hemozoin have shown changes in cell cycle regulation, as well as down-regulation of Globin Transcription Factor 1 (GATA-1), a master transcription factor of erythropoiesis [20]. Finally, serum proteome profiles of nonanemic and anemic patients infected with *P. vivax* showed changes in several physiological pathways, including oxidative stress, cytoskeletal regulation, lipid metabolism, and complement cascades [21].

The data reviewed above clearly indicate that, during malaria acute attacks, parasites and products in the BM could affect normal erythropoiesis. Noticeably, most of the data have been studied in *P. falciparum* and have not yet been directly investigated in *P. vivax*. In the current study, to provide insights into alterations of the human BM during natural infections, we evaluated morphological as well as transcriptional changes in BM aspirates obtained from patients with *P. vivax* malaria during acute attacks and 42 days after drug treatment.

METHODS

Ethical Statements

The protocol was reviewed and approved by the Ethics Review Board of the Fundação de Medicina Tropical Heitor Vieira Dourado (PB_1.065.022/2015), where adult patients presenting with positive diagnoses of vivax malaria (microscopy) were enrolled after providing signed informed consent. All participants were treated

according to recommendations for the treatment of uncomplicated *P. vivax* malaria from the Brazilian Ministry of Health, which included chloroquine for 3 days (600 mg/d on day 1, and 450 mg on days 2 and 3), followed by primaquine for 7 days (30 mg/d). BM punctures were performed, with use of appropriate needles, aseptic conditions, and local anesthesia, by an expert physician.

Sample Collection and Hematological Characterization

At days 0 (diagnosis visit) and 42 (convalescence visit), 4 mL of BM aspirates from iliac crest was obtained. Hematological parameters were measured using a Sysmex KX-28N hematology analyzer. The percentage of BM blood in the aspirate (BM purity) was calculated as follows: $[1 - (\text{total nonnucleated cells BM} / \text{total nonnucleated cells PB}) \times (\text{total nucleated cells PB} / \text{total nucleated cells BM})]$, where PB represents peripheral blood [22].

CD71 Purification of Aspirates

CD71⁺ cells were enriched as described elsewhere [6]. After plasma removal, blood cells were washed twice with ice-cold incomplete Roswell Park Memorial Institute (RPMI) 1640 medium, resuspended at 30% hematocrit and filtered through a 50- μ m cell strainer. Cell suspensions were brought to 50% hematocrit and incubated with CD71 microbeads for 15 minutes at 4°C (Miltenyi Biotech). Magnetic isolation was done with LS (Miltenyi Biotech, USA) columns. Cell suspensions were loaded into a prewet column and allowed to flow. Of the recovered CD71⁺ pellet, 2 μ L was used for a smear, 2 μ L was used for staining with anti-CD71 and anti-glycophorin A (Miltenyi Biotech), to confirm purification, and the rest was resuspended in Trizol reagent and kept at -80°C until RNA extraction. Thin smears containing CD71⁺ cells were stained with rapid panoptic stain to quantify erythroid cells and leukocyte contaminants with light microscopy.

Quantitative and Qualitative Analysis With Light Microscopy

Panoptic-stained thin smears containing CD71⁺ cells were used for dyserythropoiesis counts. The erythroid precursors were classified as basophilic, polychromatic, or orthochromatic erythroblasts. A total of 1000 red cell precursors were counted by 3 different viewers. Reticulocytes were counted in brilliant cresyl blue-stained thin smears.

Parasite Count

Malaria parasitemia was estimated using Giemsa-stained thin blood smears. A total of 10 000 enucleated red blood cells were counted, and the parasitemia was calculated as the percentage of infected red blood cell. Whole BM and whole peripheral blood were used for these counts. *P. vivax* monoinfection on admission and absence of parasites at convalescence were confirmed by means of quantitative polymerase chain reaction (qPCR) [23].

Total RNA Isolation

CD71⁺ cells were resuspended in 200 μ L of Trizol reagent and kept at -80°C until RNA extraction. After thawing, the cell

suspensions were vigorously homogenized by mixing with 200 μL of chloroform and incubated at room temperature for 15 minutes. The resultant mix was cold centrifuged (at 4°C and 12 000g for 15 minutes). The supernatant was mixed with isopropanol and incubated overnight. Ethanol 75% was used for RNA precipitation, and the resultant pellet was suspended in diethyl pyrocarbonate-treated water and kept at -80°C until RNA sequencing. Aliquots were used for integrity analysis and concentration measurement with the High Sensitivity RNA ScreenTape system (Agilent Technologies). RNA quality control was performed by the translational genomics core facility at El Instituto de Investigación Germans Trias y Pujol (IGTP).

Messenger RNA Sequencing Library Construction, Sequencing, and Bioinformatic Analysis

CD71⁺ fractions were used for transcriptomic studies. Material from 3 patients (patients 1, 3, and 15) had enough RNA quality (RNA integrity number >7) in both days 0 and 42, to generate RNA sequencing libraries using the TruSeq stranded messenger RNA kit (Illumina). Next-generation sequencing library preparation and Illumina sequencing were performed by the Genomics Unit of the Center for Genomic Regulation. Samples showed excellent sequence quality scores (score >30; approximately 250 million reads sequenced in a single lane). The quality of raw data was checked using FastQC software, version 0.11.9 (<https://www.bioinformatics.babraham.ac.uk/projects/fastqc/>). The reads were mapped to the human genome (Ensembl GRCh38.p10) using Bowtie 2 [24] software, version 2.3.5.1, and Samtools [25] and HTSeq-count [26] software, version 0.11.0 were used to count aligned reads. Clustering and differential expression analysis were performed using the DESeq2 software package, version 1.29. Statistical cutoffs for significant differences in gene expression were set for adjusted *P* values (<.05) and absolute fold change (>1.2). To identify human genes affected by *P. vivax*, we compared the resulting data from samples obtained from 3 patients during acute malaria infection to samples obtained during convalescence from the same 3 patients.

Functional Enrichment Analysis

Gene set enrichment analysis (GSEA) in preranked mode was performed using the GSEA tool [27] and the fast GSEA implementation of the preranked GSEA algorithm implemented in the fgsea package in R software [28]. Analyses were performed using preranked paired sample individual and average log₂ fold change or the signed minus log-adjusted *P* value as the metric. To visualize GSEA results, we used Enrichment Map [29]. Gene ontology terms found to be enriched using the significant differentially expressed genes were visualized with the ClueGO Cytoscape plug-in [30].

Reverse-Transcription qPCR Assays to Validate Gene Expression

A set of genes related to erythropoiesis and with different patterns of expression during infection was selected to confirm

expression by means of reverse-transcription qPCR. Five aliquots of messenger RNA from different patients were used to measure transcripts for genes *GATA1*, *ALAS1*, *ALAS2*, *ARID3A*, *NFE*, and *TALI*, using as calibrator the *GAPDH* gene (*Homo sapiens* constitutively expressed gene). The qPCR assays were performed using triplicates for each sample and repeated twice for quality control. Day 42 samples were used to determine a threshold for transcript expression.

Cytometry Bead Array

Chemokines, anaphylatoxins, and cytokines in the peripheral blood and BM were measured by means of Cytometric Bead Array (BD Biosciences). Human chemokine, anaphylatoxin and T-helper (Th) 1/Th2/Th17 cytokine kits (BD Biosciences) were used, following the manufacturer's guidelines and protocols. A FACSCanto II flow cytometer (BD Biosciences) was used for sample acquisition, and FCAP-Array software (version 3; Soft Flow) was used to calculate the levels of each molecule's levels (in picograms per milliliter pg/mL and as the mean fluorescence intensity).

RESULTS

Presence of *P. vivax* Parasites in the Human BM During Acute Vivax Malaria

We confirmed *P. vivax* mono-infection for all patients by means of qPCR (Supplementary Table 1). Examination of peripheral blood thin smears during acute infections revealed a wide range of *P. vivax* parasitemia (parasite count, 299–12 792/ μL) among the 7 patients included in this study. Noticeably, we observed *P. vivax* parasites in BM aspirates from all patients, and quantification of BM parasitemia in Giemsa-stained smears revealed overall similar parasitemia in BM and peripheral blood (Figure 1A). At microscopy, no nucleated cell was seen to be infected by *P. vivax*. We next attempted to characterize *P. vivax* stage distribution in BM aspirates compared with peripheral blood and did not observe any statistically significant difference in parasite stage distribution (Figure 1B).

Dyserythropoiesis and Ineffective Erythropoiesis as Common Features in *P. vivax*-Infected Patients

Supplementary Table 2 summarizes essential hematological and clinical data on admission (day 0) and during convalescence (day 42) for all patients studied. Absence of parasites at day 42 was confirmed by means light microscopy (not shown) and qPCR (Supplementary Table 1). Five patients presented normal levels of hemoglobin at admission, and 2 were mildly anemic (patients 9 and 13), with a significant change in hemoglobin levels (decrease >20%) during infection, which levels returning to normal by day 42. We used CD71-coated microbeads to purify erythroid cells from each BM aspirate. CD71 enrichment was very efficient, presenting a median yield of 88.7% (interquartile range, 73.4%–95.7%). White blood cell contamination was estimated using light microscopy (median, 2.6%; interquartile

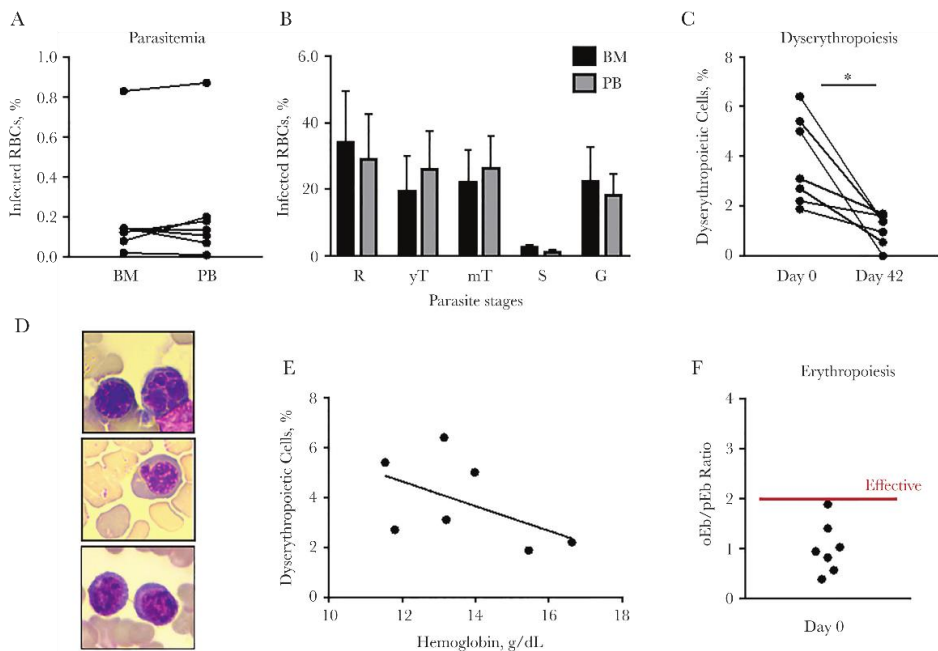


Figure 1. *Plasmodium vivax* parasites in bone marrow (BM), dyserythropoiesis, and inefficient erythropoiesis during active *P. vivax* infections. *A*, Parasitemia in BM aspirates and peripheral blood (PB) on admission (day 0). Percentage of infected red blood cells (RBCs; $n = 10\,000$ enucleated RBCs); values represent means ($n = 3$). *B*, Parasite stage distribution in BM and PB on admission ($n = 200$ infected RBCs). Abbreviations: G, gametocytes; mT, mature trophozoites; R, rings; S, schizonts; yT, young trophozoites. *C*, Dyserythropoiesis in BM aspirates on admission (day 0) compared with convalescence (day 42), shown as percentage of dyserythropoietic cells ($n = 1000$ erythroid cells); values represent means ($n = 3$). * $P < .05$ (paired Student *t* test). *D*, Representative images of dyserythropoietic cells. Rapid panoptic–stained BM CD71⁺ fraction smears showing erythroblast presenting a dysplastic nucleus (top), erythroblast presenting a budding nucleus (middle), and cytoplasmic bridge between erythroblasts (bottom). *E*, Comparison of dyserythropoiesis (percentage of dyserythropoietic erythroblasts) and hemoglobin levels on admission. *F*, Ineffective erythropoiesis in BM aspirates on admission (day 0). Polychromatic and orthochromatic erythroblasts were quantified ($n = 200$ erythroblasts). The ratio of orthochromatic to polychromatic erythroblasts (oEb/pEb ratio) was used as a proxy of inefficient erythropoiesis. Red line indicates effective erythropoiesis (oEb/pEb ratio approximately 2); ratios < 2 indicate a defective maturation of polychromatic into orthochromatic erythroblasts (ineffective erythropoiesis).

range, 1.2%–7.7%). All erythroblast stages were found after purification, and they closely mimicked the original composition of the BM aspirate (not shown). Because proportions of polychromatic and orthochromatic erythroblasts were faithfully maintained on purification, we used the CD71⁺ fraction to quantify dyserythropoiesis and ineffective erythropoiesis.

Interestingly, we observed dyserythropoiesis in all patients recruited, which significantly decreased after recovery from the infection (Figure 1C). Dyserythropoietic cells included erythroblasts presenting dysplastic or irregularly shaped nuclei, budding or multiple nuclei and cytoplasmic bridge between erythroblasts (Figure 1D). Nuclear abnormalities were the most common observation and were predominantly seen in polychromatic erythroblasts, as described elsewhere [5].

Dyserythropoiesis in patients with *P. vivax* malaria has been reported to be most marked with higher levels of anemia, although no statistical correlation was found. Similarly, we also

observed a trend toward a higher dyserythropoiesis with lower hemoglobin levels, although it was not statistically significant ($P = .23$) (Figure 1E). Hemoglobin levels and dyserythropoiesis were not related to levels of parasitemia. This is in accordance with the finding that *P. vivax* can cause anemia even at low levels of parasitemia [31].

To assess ineffective erythropoiesis during *P. vivax* acute infection, we quantified the different erythroblast maturation stages in the BM. During healthy (effective) erythropoiesis, the proportions of proerythroblasts and basophilic, polychromatic, and orthochromatic erythroblasts are 1:2:4:8, because there is a cell duplication for each step of maturation [32]. Because orthochromatic and polychromatic erythroblasts are the most abundant cells in the BM, we used the ratio of orthochromatic to polychromatic erythroblasts to quantify ineffective erythropoiesis (Figure 1F). In normal conditions, this ratio is about 2 (effective). The ratio was < 2 in all *P. vivax*-infected patients,

suggesting that ineffective erythropoiesis is common during active *P. vivax* infection.

Surprisingly, we did not observe any relationship between levels of dyserythropoiesis and ineffective erythropoiesis. On the other hand, ineffective erythropoiesis was not related to parasitemia, as we observed for dyserythropoiesis. According to the stage of development of erythropoietic lineage, 66% of polychromatic and 34% of orthochromatic erythroblasts were dyserythropoietic. Proerythroblasts and basophilic erythroblasts with dyserythropoiesis signals were not found. In conclusion, although dyserythropoiesis and ineffective erythropoiesis were reported in the BM of anemic children [5] and of an anemic adult from a clinical case report [6], we found these phenomena to be a hallmark of all *P. vivax* infections in the BM, as they are also present in nonanemic patients.

Use of CD71 Purification of BM Aspirates in Specific Transcriptomic Studies of Erythropoiesis in Patients

CD71⁺ fractions were used for transcriptomic studies. Material from 3 patients [1, 5, 13] had enough RNA quality on both days 0 and day 42 to generate RNA libraries. A pipeline for bioinformatics analysis of the data is shown in [Supplementary Figure](#)

1. To identify genes related to clinical conditions, the resulting data from these 3 patients during acute malaria were compared with data from the same patients during convalescence. The overall alignment rate into the reference human genome ranged from 86.71% to 99.15%, with a mean of 26 064 genes mapped, of which 52.5% corresponded to protein coding genes. Differential expression analysis comparing samples from days 0 and 42 revealed a total of 274 genes with significantly different expression (adjusted $P < .05$) during acute vivax malaria compared with convalescence, most of them up-regulated. All data are freely available through the Gene Expression Omnibus NIH database repository (GSE136046).

Principal component analysis showed differential clustering of samples from days 0 and 42, indicating a distinct composition and/or expression profile for *P. vivax* active infection compared with convalescence ([Figure 2A](#)). Indeed, heat maps showed differential expression profiles for each patient during active infections and after drug treatment ([Figure 2B](#)). Noticeably, GSEA showed heme synthesis and chromatin silencing terms significantly enriched at day 42 and immune response terms enriched at day 0 ([Figure 2C](#), [Supplementary Figure 2](#), and [Supplementary Table 3](#)).

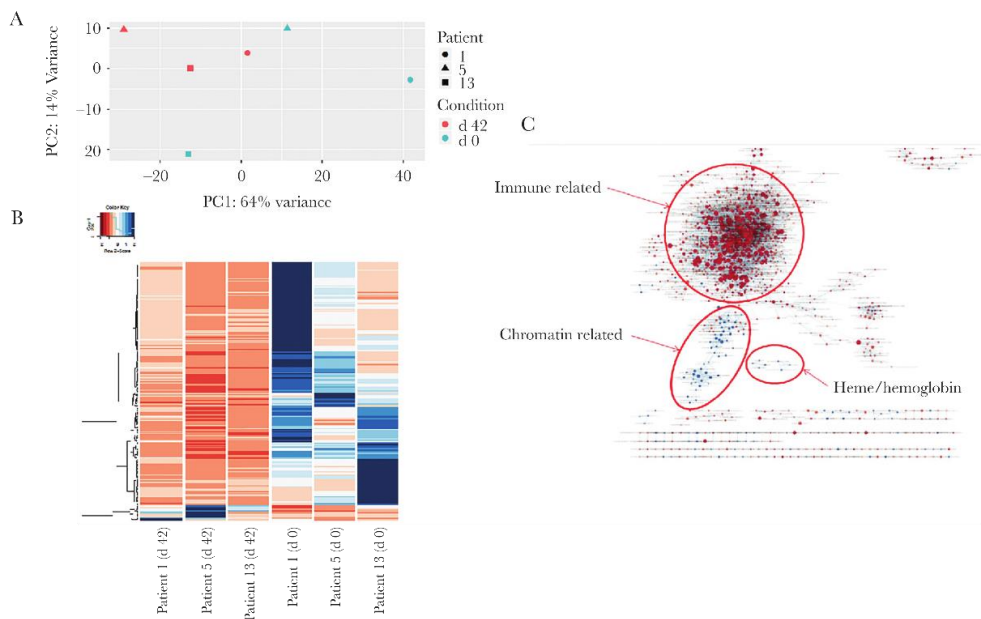


Figure 2. Principal component analysis, heat map, and gene set enrichment analysis (GSEA). *A*, Principal component analysis based on global normalized RNA sequencing gene counts by sample and condition. The day 42 sample group is in red, and the day 0 sample group in blue; patients 1, 5, and 13 are represented with a circle, a triangle, and a square, respectively. Abbreviations: PC1, principal component 1; PC2, principal component 2. *B*, Heat map of gene expression based on normalized mapped read counts of statistically significant (adjusted $P < .05$) differentially expressed genes, considering all samples (columns). *C*, Gene ontology enrichment map showing a network of gene ontology terms (C5 MaSigDB collection) corresponding to gene sets found significant at a false discovery rate of <math><0.25</math> on performing preranked GSEA using the signed minus log-adjusted P value as metric (signed meaning that the direction of change is kept). Red: up-regulated at 0 days, down at 42; blue: down-regulated at 0 day, up at 42.

Gene Expression Validation

We used reverse-transcription qPCR to validate the expression of the aforementioned genes on days 0 and 42 for the 3 individual patients. Figure 3A shows the down-regulation of genes related to erythropoiesis (*ALAS1*, *ALAS2*, *NFE*, *TAL1*, *ARID3A*, and *GATA1*). Figure 3B shows a trend in negative correlation between parasitemia and the expression of such genes.

Use Cytokine Measurement to Reveal Inflammatory BM Environment

We quantified cytokines in BM aspirates and peripheral blood plasma during acute *P. vivax* infection and convalescence in the 7 patients studied (Figure 4C). Although we found a small increase in TNF and IFN- γ during infection, values were almost negligible. Larger values were obtained for interleukin 17A for some samples, but no significant difference was observed between infection and convalescence, for either BM or peripheral blood. In contrast, strong signals were detected for interleukin 6 and 10, which were increased during active *P. vivax* infection in both BM and peripheral blood plasma, in accordance with previous reports [33, 34]. In addition to cytokines, genes involved in the complement cascade, such as the 3 C1q chains (A, B, and C) and receptors for C3a and C5, were found to be up-regulated in CD71⁺ cells during active *P. vivax* infection.

DISCUSSION

In our study, 3 of the 7 patients showed 2–3-fold parasite enrichment in the BM. Thus, although parasitemia in the BM and peripheral blood are often similar, parasite enrichment in the BM can occur, as reported elsewhere [6]. To complicate matters, there is also the possibility that during aspiration, adhered cells were not analyzed. BM biopsies would solve the technical issue, but that is a more invasive and painful procedure. In fact, cases of vivax malaria where parasites have been exclusively found

in this tissue have been described [35]. However, similarly to what has been described in a clinical case [6], we observed a trend toward enrichment of rings, schizonts, and gametocytes. However, owing to common low parasitemias hampering reliable differential counting, generating antibodies or identifying molecular markers specific for each parasite stage is required for confident quantification of *P. vivax* stages. No nucleated cell in BM was seen to be infected by *P. vivax*. That has been reported elsewhere in 1 patient with severe anemia [36].

One interesting group of genes that was found significantly to be down-regulated in the BM during active infection, the erythroid maturation genes, including *GATA1*, the major transcription factor driving erythropoiesis [37], as well as *NFE*, *TAL1*, and *ARID3A*, nuclear factors involved in erythroid maturation [38]. In addition, 2 enzymes involved in heme biosynthesis that are induced during erythropoiesis, *ALAS-1* and *ALAS-2*, were also found among this group of down-regulated genes. All genes were indeed down-regulated during infections, with the exception of *NFE* in patient 13. Interestingly, fold changes >4 were observed for *GATA-1*, *NFE*, *TAL-1*, and *ALAS-2* in patient 5, who was nonanemic and the patient presenting the most marked dyserythropoiesis and ineffective erythropoiesis.

Decreased expression of the enzymes *ALAS-1* and *ALAS-2* could be a result of the ineffective erythropoiesis observed during active infections or could be due to enrichment of polychromatic respect to orthochromatic erythroblasts in these samples. In contrast, *GATA-1* has been found to be constantly and similarly expressed during erythroblast differentiation [37, 38]. Thus, different erythroblast composition due to ineffective erythropoiesis is less likely to explain substantial changes in the expression of *GATA-1*, suggesting that *GATA-1* down-regulation is directly caused by *P. vivax*, in our sample. However, *GATA-1* modulation has also been described for other anemic

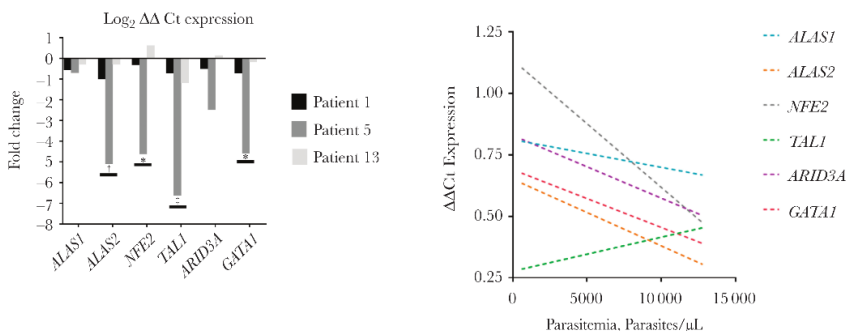


Figure 3. Transcriptional validation and correlation of hemozoin with inefficient erythropoiesis. A, Relative expression of erythropoietic genes in patients (patients 1, 5, and 13). Threshold level 0 was determined based on transcriptional levels at day 42. Logarithmic fold change scale is shown on the y-axis. Statistical significance was calculated using 2-way analysis of variance, with differences considered significant at $P \leq .05$. * $P < .05$; † $P < .03$; ‡ $P < .001$. B, Correlation between parasitemia and expression levels assessed with quantitative polymerase chain reaction (Delta-Delta Cycle Threshold [$\Delta\Delta Ct$]). For all genes, except *TAL1*, low expression was correlated with high parasitemia.

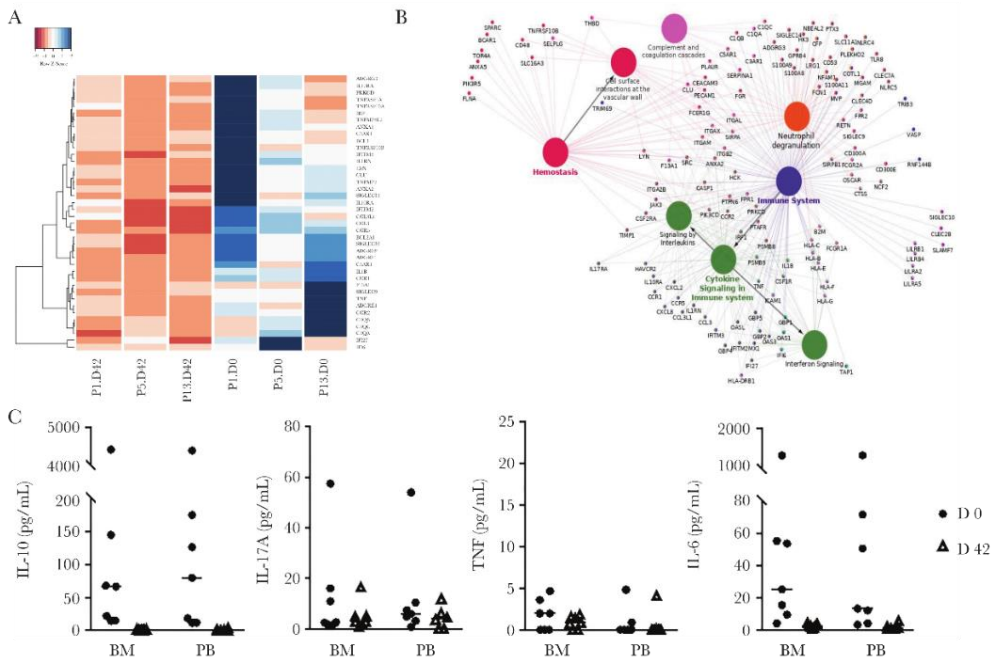


Figure 4. Immune-related genes and cytokine profile. *A*, Heat map of gene expression for innate immunity related genes based on normalized mapped read counts of statistically significant differentially expressed genes. Clustering was performed with genes in the enriched innate immunity gene ontology category (rows) for each sample (columns). Gradient colors range from red to blue, representing lower to higher expression. *B*, Clustering of up-regulated inflammatory genes based on gene ontology clustering (ClueGO tool). Only high-expression transcripts with significant differences (adjusted $P < .05$) were used. *C*, Comparison of cytokine levels between bone marrow (BM) aspirate and peripheral blood (PB), in both visits, measured by means of Cytometric Bead Array (n = 7). Absolute values were used for plotting and to calculate mean values for each group. Abbreviations: IL-6, interleukin 6; IL-10, interleukin 10; IL-17A, interleukin 17A; TNF, tumor necrosis factor.

conditions, such as that caused by 3'-Azido-3'-deoxythymidine and sickle cell anemia [39, 40].

In erythroblast cultures, it has been found that hemozoin induces down-regulation of GATA-1, resulting in erythropoiesis defects [20]. Thus, we explored the relationship between parasitemia in the BM aspirates of these patients and expression levels. GATA-1, NFE, ALAS-1, and ALAS-2 seemed to be more down-regulated in those samples with higher parasitemia, although this correlation was weak (Figure 3B).

Overall, taking into account the results of published in vitro studies and our transcriptomic study, it is legitimate to speculate that *P. vivax* and, likely, hemozoin produced by parasites, induces GATA-1 down-regulation in the erythroid lineage, resulting in ineffective erythropoiesis in the BM. Finally, GATA-1 is also a master regulator of megakaryopoiesis and platelet production, and thrombocytopenia is also present in most active *P. vivax* infections [41].

Another cluster of significantly differentially expressed genes was related to the immune response. These genes were up-regulated during active *P. vivax* infection compared with

convalescence (Figure 4A). Functional enrichment and network analyses confirmed such results (Figure 4B). The erythroblastic island, where erythropoiesis occurs, presents a specific immune microenvironment regulating erythroblast differentiation around a central macrophage; CD71⁺ cells are immunomodulatory and are capable of producing cytokines and chemokines [42]. TNF, as well as its receptors TNF receptor superfamily 1A, 10A, and 10B, were found up-regulated during active *P. vivax* infection. TNF inhibits erythropoiesis through several proposed mechanisms, including blockage of GATA-1 transcriptional activity. Several genes induced by TNF, as well as IFN- γ , were also found to be up-regulated during active *P. vivax* infection and are pathways related to erythropoiesis inhibition and apoptosis.

Complement activation could thus lead to phagocytosis of these cells, contributing to ineffective erythropoiesis. Moreover, annexin A2 and A5, which serve as ligands for C1q on apoptotic cells [43], were also found to be up-regulated during infection. Overall, these results suggest that the inflammatory microenvironment regulating erythroblast development could be profoundly disturbed by

the inflammatory response to active *P. vivax* infection, leading to apoptosis and phagocytosis of erythroblasts.

In summary, during active vivax malaria infections, parasites are always found in the BM and induce dyserythropoiesis and ineffective erythropoiesis, independent of patients' anemic status. Such defects are related to transcriptional changes affecting immune-related genes as well as erythropoietic-related genes, which were seemingly orchestrated by GATA-1 down-regulation. The question thus remains why *P. vivax* has chosen CD71⁺ reticulocytes, mostly found in the BM, as a host cell while actively inducing erythropoietic defects during infection.

Our group has postulated that *P. vivax* infections also induce spleen remodeling facilitating adherence of infected reticulocytes to the spleen [44], and this postulation has received support from 2 clinical cases of spleen rupture [45, 46]. Thus, in addition to the BM, the spleen seems another niche rich in reticulocytes where the parasites can multiply. In fact, formation of hematopoietic niches and extramedullary erythropoiesis in the spleen is prevalent in benign clinical hematological disorders [47], and in other infections innate immune activation initiates extramedullary hematopoiesis [48]. Further investigations on the BM as a new parasite niche, and its link to anemia and splenomegaly are warranted. Studies in asymptomatic population infected with this parasite are also relevant and must be pursued, to elucidate the consequences of chronic infection and what happens in niches such as BM.

Data presented herein should be considered as pioneering but preliminary analysis of erythropoiesis in a few patients with *P. vivax* malaria, in whom BM aspirates were made possible. The major question that still persists is the specificity of such findings to *P. vivax* infection or to a more general inflammatory systemic disease.

Supplementary Data

Supplementary materials are available at *The Journal of Infectious Diseases* online. Consisting of data provided by the authors to benefit the reader, the posted materials are not copyedited and are the sole responsibility of the authors, so questions or comments should be addressed to the corresponding author.

Notes

Acknowledgments. We thank all patients and healthy donors that participated in these studies. We thank the El Instituto de Investigación Germans Trias y Pujol (IGTP) Cytometry Unit for fluorescence-activated cell sorting services, IGTP Translational Genomics Unit for RNA quality control services, and IGTP High Content Genomics and Bioinformatics (and Susanna Aussó) for their contribution to RNA sequencing data quality control, differential gene expression, and functional genomic analyses. We thank the Center for Genomic Regulation's Genomics Unit for

next-generation sequencing services. ISGlobal and IGTP are members of the CERCA Programme, Generalitat de Catalunya.

Author contributions. Conception and coordination of study: H. A. d. P. and M. V. G. L.

Performance of experiments: M. A. M. B., B. B., A. A. H., K. D., E. F. G. F., A. G. C., A. C. G. A., B. W. H., E. V. D. P., and C. F. B. Data analysis: M. A. M. B., B. B., A. A. H., K. D., M. d. P. A., E. V. D. P., C. F. B., WM, H. A. d. P., and M. V. G. L. Bioinformatic analysis: T. C. R. and L. S. Obtaining of bone marrow aspirates: I. P. S. and M. V. G. L. Drafting of manuscript: M. A. M. B., B. B., K. D., T. C. R., and H. A. d. P. All authors read and approved the content of the manuscript.

Financial support. This work was supported by Coordenação de Aperfeiçoamento de Pessoal de Nível Superior (grant 71/2013 and Science Without Borders fellowships to M. A. M. B. and K. D.); Fundação de Amparo à Pesquisa do Estado do Amazonas (grant PRONEM 009/2011, ProAM-Estado fellowship to B. B., and funding for M. V. G. L.'s laboratory); the Sao Paulo Research Foundation (B. W. H. and E. V. D. P.); CNPq (fellowships to W. M. M., E. V. D. P., and M. V. G. L. and funding for M. V. G. L.'s laboratory); the Brazilian Ministry of Health (funding for M. V. G. L.'s laboratory); and the Ministerio Español de Economía y Competitividad (grant SAF2016-80655-R to the laboratory of C. F. B. and H. A. d. P.).

Potential conflicts of interest. All authors: No reported conflicts. All authors have submitted the ICMJE Form for Disclosure of Potential Conflicts of Interest. Conflicts that the editors consider relevant to the content of the manuscript have been disclosed.

References

1. World Health Organization. World malaria report 2018. Geneva, Switzerland: World Health Organization, 2018.
2. Marchiafava E, Bignami A. On Summer-Autumn Malarial Fevers [Translated by J. Harry Thomson], Chap. 7, Vol. CL. London: The New Sydenham Society, 1894; 92–119.
3. Aitken GJ. Sternal puncture in the diagnosis of malaria. *Lancet* 1943; 242:466–8.
4. Knüttgen HJ. Knochenmark befunde bei malaria tertiana. *Z Tropenmed Parasitol*. 1949; 1:178–94.
5. Wickramasinghe SN, Looareesuwan S, Nagachinta B, White NJ. Dyserythropoiesis and ineffective erythropoiesis in *Plasmodium vivax* malaria. *Br J Haematol* 1989; 72:91–9.
6. Baro B, Deroost K, Raiol T, et al. *Plasmodium vivax* gametocytes in the bone marrow of an acute malaria patient and changes in the erythroid miRNA profile. *PLoS Negl Trop Dis* 2017; 11:e0005365.
7. Obaldia N, Meibalan E, Sa JM, et al. Bone marrow is a major parasite reservoir in *Plasmodium vivax* infection. *MBio* 2018; 9:e00625-18.

8. Pathak VA, Ghosh K. Erythropoiesis in malaria infections and factors modifying the erythropoietic response. *Anemia* **2016**; 2016:9310905.
9. Giarratana MC, Kobari L, Lapillonne H, et al. Ex vivo generation of fully mature human red blood cells from hematopoietic stem cells. *Nat Biotechnol* **2005**; 23:69–74.
10. Panichakul T, Payuhakrit W, Panburana P, Wongborisuth C, Hongeng S, Udomsangpetch R. Suppression of erythroid development in vitro by *Plasmodium vivax*. *Malar J* **2012**; 11:173.
11. Panichakul T, Ponnikorn S, Roytrakul S, et al. *Plasmodium vivax* inhibits erythroid cell growth through altered phosphorylation of the cytoskeletal protein ezrin. *Malar J* **2015**; 14:138.
12. Bate CA, Taverne J, Playfair JH. Malarial parasites induce TNF production by macrophages. *Immunology* **1988**; 64:227–31.
13. Weiss L, Johnson J, Weidanz W. Mechanisms of splenic control of murine malaria: tissue culture studies of the erythropoietic interplay of spleen, bone marrow, and blood in lethal (strain 17XL) *Plasmodium yoelii* malaria in BALB/c mice. *Am J Trop Med Hyg* **1989**; 41:135–43.
14. Verhoef H, West CE, Kraaijenhagen R, et al. Malarial anemia leads to adequately increased erythropoiesis in asymptomatic Kenyan children. *Blood* **2002**; 100:3489–94.
15. Dufour C, Corcione A, Svahn J, et al. TNF-alpha and IFN-gamma are overexpressed in the bone marrow of Fanconi anemia patients and TNF-alpha suppresses erythropoiesis in vitro. *Blood* **2003**; 102:2053–9.
16. Miller KL, Schooley JC, Smith KL, Kullgren B, Mahlmann LJ, Silverman PH. Inhibition of erythropoiesis by a soluble factor in murine malaria. *Exp Hematol* **1989**; 17:379–85.
17. Kurtzhals JA, Adabayeri V, Goka BQ, et al. Low plasma concentrations of interleukin 10 in severe malarial anaemia compared with cerebral and uncomplicated malaria. *Lancet* **1998**; 351:1768–72.
18. Casals-Pascual C, Kai O, Cheung JO, et al. Suppression of erythropoiesis in malarial anemia is associated with hemozoin in vitro and in vivo. *Blood* **2006**; 108:2569–77.
19. Aguilar R, Moraleda C, Achtman AH, et al. Severity of anaemia is associated with bone marrow haemozoin in children exposed to *Plasmodium falciparum*. *Br J Haematol* **2014**; 164:877–87.
20. Skorokhod OA, Caione L, Marrocco T, et al. Inhibition of erythropoiesis in malaria anemia: role of hemozoin and hemozoin-generated 4-hydroxynonenal. *Blood* **2010**; 116:4328–37.
21. Ray S, Patel SK, Venkatesh A, et al. Clinicopathological analysis and multipronged quantitative proteomics reveal oxidative stress and cytoskeletal proteins as possible markers for severe vivax malaria. *Sci Rep* **2016**; 6:24557.
22. Holdrinet RS, von Egmond J, Wessels JM, Haanen C. A method for quantification of peripheral blood admixture in bone marrow aspirates. *Exp Hematol* **1980**; 8:103–7.
23. Melo GC, Monteiro WM, Siqueira AM, et al. Expression levels of *pvcrt-o* and *pvm-dr-1* are associated with chloroquine resistance and severe *Plasmodium vivax* malaria in patients of the Brazilian Amazon. *PLoS One* **2014**; 9:e105922.
24. Langmead CJ, McClung CR, Donald BR. A maximum entropy algorithm for rhythmic analysis of genome-wide expression patterns. *Proc IEEE Comput Soc Bioinform Conf* **2002**; 1:237–45.
25. Li H, Handsaker B, Wysoker A, et al; 1000 Genome Project Data Processing Subgroup. The Sequence Alignment/Map Format and SAMtools. *Bioinformatics* **2009**; 25:2078–9.
26. Anders S, Pyl PT, Huber W. HTSeq—a Python framework to work with high-throughput sequencing data. *Bioinformatics* **2015**; 31:166–9.
27. Subramanian A, Tamayo P, Mootha VK, et al. Gene set enrichment analysis: a knowledge-based approach for interpreting genome-wide expression profiles. *Proc Natl Acad Sci U S A* **2005**; 102:15545–50.
28. Sergushichev AA, Loboda AA, Jha AK, et al. GAM: a web-service for integrated transcriptional and metabolic network analysis. *Nucleic Acids Res* **2016**; 44:W194–200.
29. Merico D, Isserlin R, Stueker O, Emili A, Bader GD. Enrichment map: a network-based method for gene-set enrichment visualization and interpretation. *PLoS One* **2010**; 5:e13984.
30. Bindea G, Mlecnik B, Hackl H, et al. ClueGO: a Cytoscape plug-in to decipher functionally grouped gene ontology and pathway annotation networks. *Bioinformatics* **2009**; 25:1091–3.
31. Castro-Gomes T, Mourão LC, Melo GC, Monteiro WM, Lacerda MV, Braga ÉM. Potential immune mechanisms associated with anemia in *Plasmodium vivax* malaria: a puzzling question. *Infect Immun* **2014**; 82:3990–4000.
32. Hu J, Liu J, Xue F, et al. Isolation and functional characterization of human erythroblasts at distinct stages: implications for understanding of normal and disordered erythropoiesis in vivo. *Blood* **2013**; 121:3246–53.
33. Fernandes AA, Carvalho LJ, Zanini GM, et al. Similar cytokine responses and degrees of anemia in patients with *Plasmodium falciparum* and *Plasmodium vivax* infections in the Brazilian Amazon region. *Clin Vaccine Immunol* **2008**; 15:650–8.
34. Hojo-Souza NS, Pereira DB, de Souza FS, et al. On the cytokine/chemokine network during *Plasmodium vivax* malaria: new insights to understand the disease. *Malar J* **2017**; 16:42.
35. Lacerda MVG de, Hipólito JR, Passos LN da M. Chronic *Plasmodium vivax* infection in a patient with splenomegaly and severe thrombocytopenia. *Rev Soc Bras Med Trop* **2008**; 41:522–3.

36. Ru YX, Mao BY, Zhang FK, et al. Invasion of erythroblasts by *Plasmodium vivax*: A new mechanism contributing to malarial anemia. *Ultrastruct Pathol* **2009**; 33:236–42.
37. Welch JJ, Watts JA, Vakoc CR, et al. Global regulation of erythroid gene expression by transcription factor GATA-1. *Blood* **2004**; 104:3136–47.
38. Kerenyi MA, Orkin SH. Networking erythropoiesis. *J Exp Med* **2010**; 207:2537–41.
39. Spiga MG, Weidner DA, Trentesaux C, LeBoeuf RD, Sommadossi JP. Inhibition of β -globin gene expression by 3'-azido-3'-deoxythymidine in human erythroid progenitor cells. *Antiviral Res* **1999**; 44:167–77.
40. Bacon ER, Dalyot N, Filon D, Schreiber L, Rachmilewitz EA, Oppenheim A. Hemoglobin switching in humans is accompanied by changes in the ratio of the transcription factors, GATA-1 and SP1. *Mol Med* **1995**; 1:297–305.
41. Lacerda MVG, Mourão MPG, Coelho HC, Santos JB. Thrombocytopenia in malaria: who cares? *Mem. Inst. Oswaldo Cruz* **2011**; 106:52–63.
42. Chasis JA, Mohandas N. Erythroblastic islands: niches for erythropoiesis. *Blood* **2008**; 112:470–8.
43. Martin M, Leffler J, Blom AM. Annexin A2 and A5 serve as new ligands for C1q on apoptotic cells. *J Biol Chem* **2012**; 287:33733–44.
44. Fernandez-Becerra C, Yamamoto MM, Vêncio RZ, Lacerda M, Rosanas-Urgell A, del Portillo HA. *Plasmodium vivax* and the importance of the subtelomeric multigene vir superfamily. *Trends Parasitol* **2009**; 25:44–51.
45. Elizalde-Torrent A, Val F, Azevedo ICC, et al. Sudden spleen rupture in a *Plasmodium vivax*-infected patient undergoing malaria treatment. *Malar J* **2018**; 17:79.
46. Machado Siqueira A, Lopes Magalhães BM, Cardoso Melo G, et al. Spleen rupture in a case of untreated *Plasmodium vivax* infection. *PLoS Negl Trop Dis* **2012**; 6:e1934.
47. Miwa Y, Hayashi T, Suzuki S, et al. Up-regulated expression of CXCL12 in human spleens with extramedullary haematoopoiesis. *Pathology* **2013**; 45:408–16.
48. Jackson A, Nanton MR, O'Donnell H, Akue AD, McSorley SJ. Innate immune activation during *Salmonella* infection initiates extramedullary erythropoiesis and splenomegaly. *J Immunol* **2010**; 185:6198–204.

SUPPLEMENTARY INFORMATION

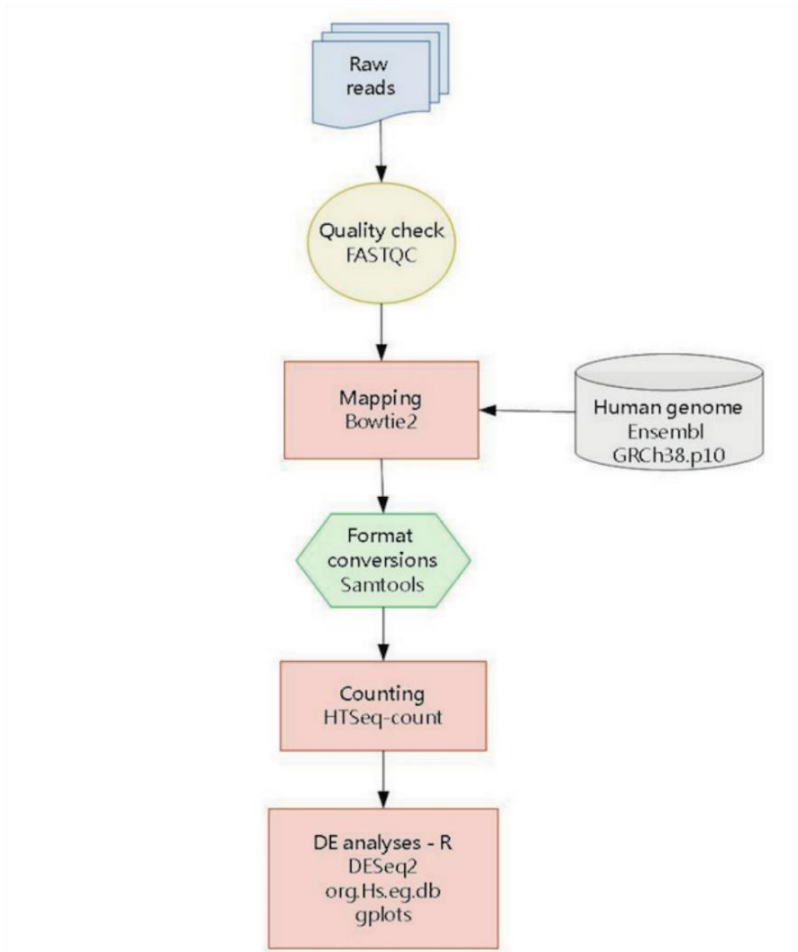


Figure S1. RNA-seq pipeline for differential gene expression analysis, including quality check of RNA-seq libraries and mapping into *Homo sapiens* genome Ensembl GRCh38.p10.

Supplementary Table 1. qPCR analysis of *P. vivax* and *P. falciparum* in bone marrow aspirates at D0 and D42.**Table S1.1.** Amplification conditions.

Assay	Stage	Step	Temperature	Time
Qmal (<i>18S rRNA gene</i>), <i>P. falciparum</i> specific (<i>18S rRNA gene</i>), <i>P. vivax</i> specific (<i>18S rRNA gene</i>)	Holding	Pre-Incubation	50°C	2 minutes
	Holding	Activation of Taq polymerase	95°C	10 minutes
	Cycling (45x)	Denature	95°C	15 seconds
		Anneal/Extend	58°C	1 minute

Table S1.2. Primers and probes used for malaria molecular diagnosis.

Assay	Primers/Probes	PCR Efficiency	Assay detection limit
Qmal (<i>18S rRNA gene</i>)	Fw-TTA GAT TGC TTC CTT CAG TRC CTT ATG	90.6%	1 copy/uL
	Rev-GT TGA GTC AAA TTA AGC CGC AA		
	Probe: FAM – TCA ATT CTT TTA ACT TTC TCG CTT GCG CGA – BHQ1		
<i>P. falciparum</i> -specific (<i>18S rRNA gene</i>)	Fw-TAT TGC TTT TGA GAG GTT TTG TTA CTT TG	90.5%	3 copies/uL
	Rev-TATCCATGCTGTAGTATTCAAACACAA		
	Probe: FAM – ACG GGT AGT CAT GAT TGA GTT – MGB – NFQ		

Table S1.3. Quantitative results for *P. vivax* and *P. falciparum* infection

ID	Target	Ct	Quantity	Target	Ct	Quantity
P1_D0	VIVAX	24,3	115,386.0	FALCIPARUM	>45 cycles	Undetermined
P1_D42	VIVAX	>45 cycles	Undetermined	FALCIPARUM	>45 cycles	Undetermined
P4_D0	VIVAX	27.4	3,798.6	FALCIPARUM	>45 cycles	Undetermined
P4_D42	VIVAX	>45 cycles	Undetermined	FALCIPARUM	>45 cycles	Undetermined
P5_D0	VIVAX	28.0	3,014.4	FALCIPARUM	>45 cycles	Undetermined
P5_D42	VIVAX	>45 cycles	Undetermined	FALCIPARUM	>45 cycles	Undetermined
P6_D0	VIVAX	27.5	3,798.6	FALCIPARUM	>45 cycles	Undetermined

P6_D42	VIVAX	>45 cycles	Undetermined	FALCIPARUM	>45 cycles	Undetermined
P7_D0	VIVAX	30.67	532.5	FALCIPARUM	>45 cycles	Undetermined
P7_D42	VIVAX	>45 cycles	Undetermined	FALCIPARUM	>45 cycles	Undetermined
P9_D0	VIVAX	27.2	4,491.4	FALCIPARUM	>45 cycles	Undetermined
P9_D42	VIVAX	>45 cycles	Undetermined	FALCIPARUM	>45 cycles	Undetermined
P13_D0	VIVAX	27.8	3,206.6	FALCIPARUM	>45 cycles	Undetermined
P13_D42	VIVAX	>45 cycles	Undetermined	FALCIPARUM	>45 cycles	Undetermined

References

Almeida ACG, Kuehn A, Castro AJM, Vitor-Silva S, Figueiredo EFG, Brasil LW, et al. High proportions of asymptomatic and submicroscopic *Plasmodium vivax* infections in a peri-urban area of low transmission in the Brazilian Amazon. *Parasit Vectors*. 2018;11:194. doi: 10.1186/s13071-018-2787-7.u

Wampfler R, Mwingira F, Javati S, Robinson L, Betuela I, Siba P, et al. Strategies for detection of *Plasmodium* species gametocytes. *PLoS One*. 2013;8:e76316. doi: 10.1371/journal.pone.0076316.

Rosanas-Urgell A, Mueller D, Betuela I, Barnadas C, Iga J, Zimmerman PA, et al. Comparison of diagnostic methods for the detection and quantification of the four sympatric *Plasmodium* species in field samples from Papua New Guinea. *Malar J*. 2010;9:361. doi: 10.1186/1475-2875-9-361.

Table S2. Hematological and clinical data from patients at D0 and D42.

ID	Age	Gender	Parasitemia (Pv/μL)	BM aspirate purity (%)	Hemoglobin level (mg/dL)		Reticulocytes count (%)		Leukocytes (cells/mm3)		Platelets (cells/mm3)		HIV	Helminths	Protozoan
					D0	D42	D0	D42	D0	D42	D0	D42			
P1	48	M	12792,2	81	13,98	15,86	0,7	1,3	8300	99000	74000	293000	negative	negative	<i>G. lamblia</i>
P4	23	M	1204	85	13,2	13,83	0,9	0,7	5600	4520	59000	223000	negative	negative	negative
P5	46	M	6688,5	69	16,63	16,29	0,8	1	3900	6780	66000	88000	negative	negative	negative
P6	36	M	6545	83	15,45	15,4	1,2	NA	7770	7000	216000	323000	negative	<i>A. lumbricoides</i>	<i>E. nana</i>
P7	57	F	299	82	13,14	12,4	1,77	1,08	2300	5700	167000	241000	negative	negative	negative
P9	51	M	4425	92	11,8	13,98	1,06	1,8	5900	4800	112000	202000	negative	negative	negative
P13	52	M	603,75	45	11,53	14,2	2,8	2	1150	6430	64000	243000	negative	negative	negative

Table S3. Top 20 GSEA GO terms enriched at 42 days and at 0 days relative to the counterpart preranked by normalized enrichment score (NES) (padj<0.05).

D0					D42					
pathway	pval	padj	ES	NES	pathway	pval	padj	ES	NES	
GO_CELLULAR_RESPONSE_TO_INTERFERON_GAMMA	0,001	0,015	-0,767	-2,601	GO_CHROMATIN_SILENCING		0,008	0,047	0,633	2,81
GO_RESPONSE_TO_INTERFERON_GAMMA	0,001	0,015	-0,75	-2,574	GO_NUCLEAR_NUCLEOSOME		0,005	0,033	0,754	2,787
GO_CYTOKINE_ACTIVITY	0,001	0,015	-0,758	-2,561	GO_DNA_REPLICATION_DEPENDENT_NUCLEOSOME_ORGANIZATION		0,004	0,03	0,749	2,641
GO_LEUKOCYTE_CHEMOTAXIS	0,001	0,015	-0,77	-2,551	GO_CHROMATIN_SILENCING_AT_RDNA		0,004	0,031	0,72	2,593
GO_INFLAMMATORY_RESPONSE	0,001	0,015	-0,698	-2,551	GO_GAS_TRANSPORT		0,003	0,026	0,835	2,567
GO_INTERFERON_GAMMA_MEDIATED_SIGNALING_PATHWAY	0,001	0,015	-0,775	-2,54	GO_DNA_REPLICATION_INDEPENDENT_NUCLEOSOME_ORGANIZATION		0,006	0,04	0,616	2,557
GO_MYELOID_LEUKOCYTE_MIGRATION	0,001	0,015	-0,756	-2,466	GO_HEMOGLOBIN_COMPLEX		0,003	0,025	0,889	2,506
GO_RESPONSE_TO_TYPE_I_INTERFERON	0,001	0,015	-0,764	-2,464	GO_OXYGEN_TRANSPORT		0,003	0,025	0,88	2,482
GO_CELL_CHEMOTAXIS	0,001	0,015	-0,718	-2,458	GO_CENTROMERE_COMPLEX_ASSEMBLY		0,007	0,04	0,612	2,469
GO_POSITIVE_REGULATION_OF_CYTOKINE_SECRETION	0,001	0,015	-0,739	-2,436	GO_HISTONE_EXCHANGE		0,006	0,04	0,597	2,45
GO_DEFENSE_RESPONSE_TO_BACTERIUM	0,001	0,015	0,7	-2,426	GO_LYSINE_ACETYLATED_HISTONE_BINDING		0,003	0,026	0,796	2,401
GO_RESPONSE_TO_MOLECULE_OF_BACTERIAL_ORIGIN	0,001	0,015	-0,67	-2,426	GO_POSITIVE_REGULATION_OF_GENE_EXPRESSION_EPIGENETIC		0,008	0,047	0,523	2,342
GO GRANULOCYTE_MIGRATION	0,001	0,015	-0,766	-2,418	GO_ATP_DEPENDENT_CHROMATIN_REMODELING		0,008	0,047	0,529	2,335
GO INNATE_IMMUNE_RESPONSE	0,001	0,015	-0,652	-2,411	GO_TELOMERE_CAPPING		0,004	0,03	0,658	2,281
GO_RESPONSE_TO_BACTERIUM	0,001	0,015	-0,655	-2,407	GO_NON_RECOMBINATIONAL_REPAIR		0,008	0,047	0,51	2,264
GO_POSITIVE_REGULATION_OF_INFLAMMATORY_RESPONSE	0,001	0,015	0,732	-2,401	GO_CONDENSED_NUCLEAR_CHROMOSOME		0,008	0,047	0,505	2,244
GO_MYELOID_LEUKOCYTE_ACTIVATION	0,001	0,015	-0,716	-2,399	GO_CHROMOSOME_CONDENSATION		0,004	0,03	0,636	2,235
GO PEPTIDE ANTIGEN BINDING	0,001	0,015	-0,854	-2,385	GO_NUCLEAR_HETEROCHROMATIN		0,005	0,033	0,594	2,195
GO_REGULATION_OF_CYTOKINE_SECRETION	0,001	0,015	-0,69	-2,368	GO_PEPTIDYL_LYSINE_METHYLATION		0,008	0,046	0,488	2,156
GO_IMMUNE_RESPONSE	0,001	0,015	-0,635	-2,366	GO_HISTONE_H3_K4_METHYLATION		0,004	0,03	0,597	2,145

3.4 Article 4 (Unpublished): Transcriptional analysis of *Plasmodium vivax* during acute infections in the human bone marrow

Objective 1: Identification and validation of genes differentially expressed in the spleen & bone marrow through global transcriptional and computational analysis.

Title: Morphological and Transcriptional Changes in Human Bone Marrow During Natural *Plasmodium vivax* Malaria Infections.

Authors: **Alberto Ayllon-Hermida**, Marcelo A. M. Brito, Bàrbara Baro, Marcus V. G. Lacerda, Lauro Sumoy, Hernando A. del Portillo, Carmen Fernandez-Becerra.

Journal: -

Year: -

Volume: -

Issue: -

Pages: -

Impact Factor: -

Quartile and Research area: -

DOI: -

Transcriptional analysis of *Plasmodium vivax* during acute infections in the human bone marrow

Alberto Ayllon-Hermida^{1,2,3}, Marcelo A. M. Brito^{4,5}, Bàrbara Baro^{1,4}, Marcus V. G. Lacerda^{4,5,7}, Lauro Sumoy², Hernando A. del Portillo^{1,2,6*}, Carmen Fernandez-Becerra^{1,2,7*}

¹ISGlobal, Barcelona Institute for Global Health, Hospital Clínic-Universitat de Barcelona, Barcelona, Spain; ²IGTP Institut d'Investigació Germans Trias i Pujol, Badalona, Barcelona, Spain; ³School of Medicine and Health Sciences, University of Barcelona, Barcelona, Spain; ⁴Fundação de Medicina Tropical Dr Heitor Vieira Dourado, Manaus, Amazonas, Brazil; ⁵Universidade do Estado do Amazonas, Manaus, Amazonas, Brazil; ⁶ICREA, Institució Catalana de Recerca i Estudis Avançats, Barcelona, Spain; ⁷CIBERINFEC, ISCIII-CIBER de Enfermedades Infecciosas, Instituto de Salud Carlos III, Madrid, Spain

*present address: Single Cell Discoveries B.V., Utrecht, the Netherlands

*corresponding authors: hernandoa.delportillo@isglobal.org & carmen.fernandez@isglobal.org

Abstract

The bone marrow (BM) have been proved to be a key point for *Plasmodium vivax* cryptic infection. Previous studies have demonstrated the presence of the parasite inside the BM, including gametocytes. Here, we investigated the transcriptomic profile of *P. vivax* parasites isolated from BM aspirates collected from adult patients diagnosed with *P. vivax* malaria. *In silico* analysis identified a diverse set of highly expressed genes in BM parasites, including metabolic enzymes, like the GAPDH or enolase, structural proteins and antigenic proteins like the PvETRAMP. Gametocyte-specific genes were highly expressed, corroborating the presence of sexual stages in this erythroid tissue. Comparative analysis with previously available peripheral blood transcriptomes highlighted 116 genes preferentially expressed in the BM, many belonging to the *vir* superfamily and mainly associated with membrane localization. Attempts to express selected BM-dependent genes heterologously in *P. falciparum* 3D7 parasites were unsuccessful. However, we overcome this by expressing immunogenic domains of PHIST proteins in HEK293 cells, enabling future studies about its immune stimulatory potential. Overall, this study provides comprehensive insights into the BM transcriptome of *P. vivax*, shedding light on its biological adaptations and potential therapeutic targets.

Introduction

Malaria caused by *Plasmodium vivax* (*vivax* malaria) is a significant global health issue, being the most widely distributed human malaria parasite, mostly spanning regions from South-East Asia and the Americas. An estimated 2.5 billion people live at risk of transmission, and in 2022 alone, there were almost 7.7 million clinical cases. (World Health Organization, 2023). However, current diagnostic methods only detect a small percentage of infections (Fernandez-Becerra et al., 2022) as epidemiological studies suggest that up to 90% of chronic infections are asymptomatic (M. T. White et al., 2018) and 50-80% are below the sensitivity of current diagnostic methods (Okell et al., 2009, 2012). These infections vary across different endemic regions (Angrisano & Robinson,

2022). A better understanding of asymptomatic infections is crucial for malaria elimination (Fernandez-Becerra et al., 2022),.

Historically, the dormant liver stage, termed hypnozoite, was thought to be the sole cause of these asymptomatic infections (Krotoski, 1985; Krotoski et al., 1982; N. J. White, 2011). Recently, however, the reticulocyte-rich spleen has been identified as a major cryptic niche for *P. vivax*, harbouring over 95% of the total parasite biomass in natural asymptomatic chronic infections (Kho, et al., 2021a; Kho, et al., 2021b). This splenic tropism is not well understood but is linked to severe anaemia (Kho et al., 2024). *P. vivax* also impacts the bone marrow (BM), a niche for parasites recognized since 1894 (Marchiafava & Bignami, 1892). Sternal puncture evaluations and experimental infections in splenectomised monkeys have confirmed the presence of the parasite in the BM (Aitken, 1943; Obaldia et al., 2018), as well as BM dyserythropoiesis and ineffective erythropoiesis during human natural acute infections (Brito et al., 2022). The mechanisms behind these effects involve both direct parasite actions and host immune responses (Brito et al., 2022). Moreover, *in vitro* studies have demonstrated that *P. vivax*-infected cells can suppress erythroid development and promote cell cycle arrest (Panichakul et al., 2012, 2015).

Here, using BM aspirates from infected individuals from the Amazonas region (Brito et al., 2022), we identified *P. vivax* genes preferentially transcribed in this tissue as compared to previously available transcriptome data from parasites in peripheral blood (PB) (Zhu et al., 2016). Moreover, we used CRISPR/Cas9, to generate *P. falciparum* transgenic lines expressing selected *P. vivax* genes expressed in the BM for functional characterization (Ayllon-Hermida et al., 2024; Marin-Mogollon et al., 2018; Miyazaki et al., 2020). This research thus provides novel information of the intricate and complex interactions of *P. vivax* in the human bone marrow.

Materials & Methods

Human plasma samples

The protocol was reviewed and approved by the Ethics Review Board of the Fundação de Medicina Tropical Heitor Vieira Dourado (PB_1.065.022/2015). Adult patients diagnosed with vivax malaria via microscopy were enrolled after providing signed informed consent

Sample Collection, CD71 Purification of Aspirates and Parasite count

This process has been described before as samples belonging to the same cohort were used in a previous study (Brito et al., 2022). Following sample collection, BM punctures from the iliac crest were performed under aseptic conditions and local anaesthesia using appropriate needles by an expert physician and immediately afterwards treated according to the Brazilian Ministry of Health's guidelines for uncomplicated *P. vivax* malaria. This included chloroquine (600 mg on day 1 and 450 mg on days 2 and 3) followed by primaquine (30 mg daily for 7 days). 42 days later, a new BM aspirate was obtained from these same individuals. Haematological parameters were measured using a Sysmex KX-28N haematology analyser. CD71+ cells were enriched as described in previous studies (Baro et al., 2017; Brito et al., 2022). After removing the plasma, blood cells were washed twice with ice-cold incomplete Roswell Park Memorial Institute (iRPMI) 1640 medium, resuspended at 30% haematocrit, and filtered through a 50- μ m cell strainer. The cell suspensions were then brought to 50% haematocrit and incubated with CD71 microbeads for 15 minutes at 4°C (Miltenyi Biotech). Magnetic isolation was performed using LS columns (Miltenyi Biotech, USA). The cell suspensions

were loaded into a pre-hydrated column with iRPMI and allowed to flow through. From the recovered CD71+ pellet, 2 μ L was used for a smear, 2 μ L for staining with anti-CD71 and anti-glycophorin A antibodies (Miltenyi Biotech) to confirm purification, and the remainder was resuspended in Trizol reagent and stored at -80°C until RNA extraction. Thin smears containing CD71+ cells were stained with rapid panoptic stain to quantify erythroid cells and leukocyte contaminants under light microscopy.

Malaria parasitaemia was estimated using Giemsa-stained thin blood smears. For this, 10,000 enucleated red blood cells were counted, and the parasitaemia was calculated as the percentage of infected red blood cells. Both whole BM and PB samples were used for these counts. *P. vivax* mono-infection and the absence of parasites during convalescence were confirmed through quantitative polymerase chain reaction (qPCR).

RNA extraction and isolation

This process was performed as described previously (Brito et al., 2022). To note, CD71+ cells were resuspended in 200 μ L of Trizol reagent and stored at -80°C until RNA extraction. After thawing, cell suspensions were vigorously homogenized with 200 μ L of chloroform and incubated at room temperature for 15 minutes. The mixture was then centrifuged at 12,000g for 15 minutes at 4°C . The supernatant was mixed with isopropanol and incubated overnight for RNA precipitation. The RNA was then washed with 75% ethanol, and the resulting pellet was resuspended in diethyl pyrocarbonate-treated water and stored at -80°C until RNA sequencing. Aliquots were used to assess RNA integrity and concentration using the High Sensitivity RNA ScreenTape system (Agilent Technologies). RNA quality control was performed by the translational genomics core facility at Institut de Recerca Germans Trias i Pujol (IGTP).

Messenger RNA Sequencing Library Construction, Sequencing, and Bioinformatic Analysis

CD71+ fractions were used for transcriptomic studies. RNA from four patients (patients 1, 3, 9 and 15) had sufficient quality (RNA integrity number >7) on both day 0 and day 42 to generate RNA sequencing libraries using TruSeq stranded mRNA (Illumina). Next-generation sequencing library preparation and Illumina sequencing were conducted by the Genomics Unit of the Center for Genomic Regulation at Institut de Recerca Germans Trias i Pujol (IGTP). After sequencing, and in order to allow the following comparison with PB parasite transcriptome comparison (Zhu et al., 2016), the sequencing raw reads were aligned using Tophat2 version 2.1.0 with 4 nucleotides mismatches allowed. The parameters were specified as -mate-inner-dist 0, -mate-std-dev 80, -i 10, -I 10000, -library fr-firststrand, -min-segment-intron 10, -max-segment-intron 10000, -N 4, -read-edit-dist 4, following the parameters used in the comparative transcriptome **Supplementary Figure 1**. Two different mapping strategies have been used to identify the transcripts sequenced: a) mapping reads to a genome composed of genes of human + genes of *P. vivax* or b) mapping the unmapped reads from human to *P. vivax*. Both Sal1 strain and P01 genomes were used.

Data normalization, identification of top-50 expressed genes and comparison with genes expressed during asexual blood stages

Count data was normalized using DESeq2 considering only Day0 samples, as Day42 samples had zero counts for the vast majority of genes. DESeq2 is a widely used R package for high-throughput sequencing, enhanced in the specifics of counting data, such as non-normality, dependence of the variance on the mean, small number of samples and low read counts. DESeq performs its own normalization. A heat map of the top 50 most abundant transcripts (ranked by average normalised read counts) was performed and the list of genes retrieved after alignments against the *P. vivax* Sal1 and

P. vivax P01 genomes (**Supplementary Figure 1**). The top 50 expressed genes were analysed using PlasmoDB Gene Ontology Enrichment for Biological process, Cellular Component and Molecular Function (<https://plasmodb.org/plasmo/app/search/transcript/GeneByLocusTag>). Data was graphed using Cytoscape software v3.10.2.

The parasite transcriptome has also been compared against the gametocyte specific transcriptome (Westenberger et al., 2010) and comparison results have been graphed using GraphPad Prism version 10.0.0 for Windows, GraphPad Software, Boston, Massachusetts USA, www.graphpad.com.

Then, we compared the given dataset with Bozdech dataset (New insights into the *Plasmodium vivax* transcriptome using RNASeq) (Zhu et al., 2016). Firstly, we converted data to log₂(fpkm) using Cufflinks version 2.2.1, as Bozdech dataset were expressed in this format (**Supplementary Figure 1**). Then, a list of genes preferentially expressed in the BM is retrieved and heat map for comparing the samples sequenced is performed using TBtools-II (Chen et al., 2023). Briefly, *log2* was used to express the abundance of each individual gene and, as well as the clusterization of the genes using Euclidian distance method and clustering via average expression.

Analysis of RNAseq data

After the list of accession numbers were generated, GeneIDs were submitted to PlasmoDB for analysis (Alvarez-Jarreta et al., 2024). First, the list of preferentially expressed genes and the top 50 BM genes were searched for annotated subcellular localization. Then, the top 50 BM genes were analysed by GO enrichment analysis using PlasmoDB built-in application.

For the preferentially expressed genes of *P. vivax* in the BM and based on the annotated name on PlasmoDB, genes were clustered manually in different subcategories: *vir* superfamily, tRNAs, enzymes, resistance-related proteins, PvETRAMPs, cysteine-rich proteins, PHIST, merozoite surface protein, LISP1, gametocytes and WD-domain. Those annotated as hypothetical genes, conserved proteins and putative genes were counted as Unknown. Finally, retrieved preferentially expressed genes by RNAseq analysis and posterior comparison with PB parasites were compared with genes sequenced in a single-cell RNAseq analysis previously published by Sà and colleagues (Sà et al., 2020) and genes whose transcription was determined to be spleen-dependent (Fernandez-Becerra et al., 2020). Venn diagrams were generated using InteractiVenn suite (Heberle et al., 2015).

Also, we used ShinyGo 0.80 online suite (<http://bioinformatics.sdstate.edu/go/>) (Ge et al., 2020) for investigating GO enriched pathways or cellular components in the RNAseq data and result visualization.

Selection of genes to be expressed heterogously in *P. falciparum* parasites

From the top 50 expressed genes in the BM as well as the list of genes exclusively found in the BM sample after comparing with the PB transcriptome (Zhu et al., 2016), genes identified were annotated and searched for selected genes for functional analysis. potentially Decision criteria involved: (i) to pertain to the *vir* multigene family, (ii) to be a predicted exported protein, (iii) to have been previously identified (Fernandez-Becerra et al., 2020; Sà et al., 2020) or (iv) to have immunogenic potential. The list of selected genes is presented in **Supplementary Figure 2A**.

Primer design and gene amplification

Primers to amplify the selected genes and to be cloned into pHH1_CRT-3HA_Lisp1 plasmid (Ayllon-Hermida et al., 2024), were designed manually. Briefly, genes were amplified from a cDNA template obtained from total RNA of the Sal-I strain (kind gift of Dr. John Barnwell) using primers described in **Supplementary Table 1** and Platinum™ Taq (Invitrogen 11304011). Genes were cloned into pHH1_CRT-3HA_Lisp1 plasmid using In-Fusion® HD Cloning Plus CE (Takara 638916) or Gibson Assembly® Cloning Kit (NEB E5510S).

Parasite culture and transfection

Parasite were cultured with B+ human erythrocytes (3% haematocrit) in RPMI media (Sigma 51800-035) supplemented with 0.5% Albumax, 0.23% NaHCO₃, 0.59% HEPES, 0.05% gentamicin and 0.05 mg/ml of hypoxanthine using standard methods (Trager & Jensen, 1976).

P. falciparum 3D7 WT parasites were transfected as described previously (Llorà-Batlle et al., 2020). Briefly, 60 µg of pDC2_Cas9_hDHFryFCU1_LISP1 and 12 µg of pHH1_CRT-PvBMgene-3HA_LISP1 (corresponding to a specific BM gene) linearized using BsaI site (located in the ampicillin resistance cassette at the backbone of the plasmid) were used for transfection (**Supplementary Figure 2B**). Seven ml of 8% ring stage-synchronised culture were electroporated (310 V, 950 µF and 2 mm cuvette) with the above-mentioned plasmids. 24 h after electroporation, 10 nM WR99210 was added to the culture and maintained for 4 days. Parasites were maintained in culture for up to 40 days after drug removal and discarded if viable parasites were not observed in culture.

Results

Patients characteristics, demographical data, infection data can be found elsewhere (Brito et al., 2022).

Quantification of RNAseq reads confirm presence of *P. vivax* in the BM

RNA material from all four patients had enough quality for generating RNA libraries from both day 0 and day 42 (**Supplementary Table 2**). After RNAseq, the number of raw reads extracted per sample showed not significant differences among the samples, ranging from 3.5×10^7 to 4.9×10^7 reads (**Figure 1A**). When mapping the samples to the human genome, to samples from all four patients result in over 84% of read identity belonging to human transcripts. In contrast, when mapping to a database composed by human and *P. vivax* genome, the mapping percentage against one or the other organism exceeded 94%. If we only consider the reads not mapped against the human database and we map them against *P. vivax* genome, in to over 70% of the raw reads are mapped against vivax malaria parasite genome (**Figure 1B**). Interestingly, at t42, over 94% of the raw reads map directly to human genome, with no significant variation when mapping against the combined human and *P. vivax* database. Again, if we take the not mapped raw reads against human genome and map them against *P. vivax* genome, at t42, almost none of the reads map against the parasite genome, indicating complete clearance of *P. vivax* parasites in the BM aspirates after the antimalarial treatment in 3 patients. Interestingly, in patient we observe a detection of 2.7×10^3 reads matching to *P. vivax* Sal I genome. This might indicate the presence of some parasites in the tissue after the treatment that the patient has received (**Figure 1C**).

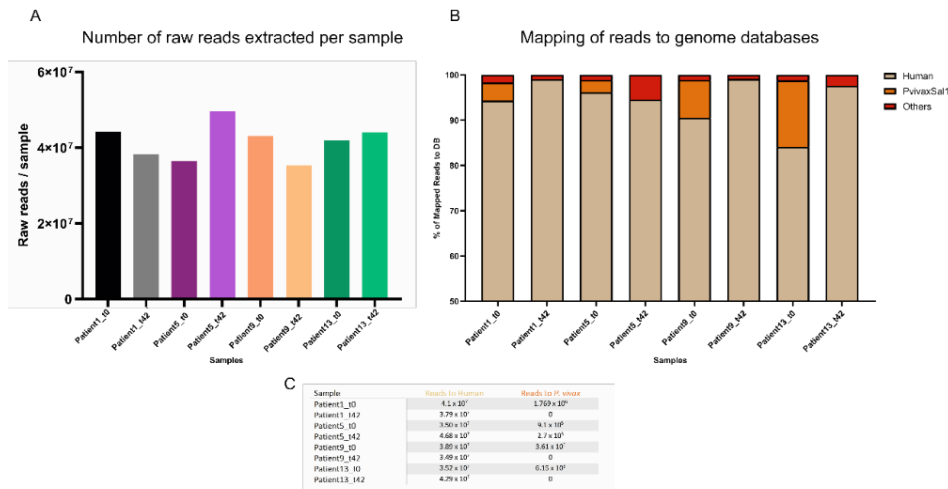


Figure 1. Comparison among samples of RNAseq. A) Raw number of reads sequenced by RNA from BM aspirates. No statistical significant differences were observed among samples. **B)** Mapping of raw reads to human genome or *P. vivax* Sal-1 genome across BM samples. **C)** Read count mapped to each genome DB

Top50 BM genes is formed by enzymes and other antigenic proteins

After sequencing and mapping the raw reads to the *P. vivax* genome, around 9.1×10^5 up to 6.35×10^6 reads mapped against the malaria parasite genome (Figure 1C). In total, 5,361 genes have been detected when analysing the raw data generated after RNAseq. After mapping the reads obtained from the RNAseq, and considering the quantification of the reads obtained from each patient, a list of the top 50 more abundantly expressed genes was obtained (Figure 2A). When analysing the list of genes, notably the presence of diverse enzymes involved in parasite metabolism like the PVX_117322 coding for the GAPDH, PVX_095015 coding for the enolase enzyme or PVX_080650 transcribing the inositol-3-phosphate synthase, were identified. Besides metabolic enzymes, structural proteins, such as the glideosome-associated protein PVX_099320, or antigenic proteins like the PvETRAMP, PVX_090230 (Chuquiyaui et al., 2015), were also observed. GO network analysis showed the interaction among enriched metabolic processes involving carbohydrate, monosaccharide, phospholipids and nucleosides compounds by *P. vivax* (Figure 2B). When looking into the subcellular localization of the proteins coded by the detected genes, the plastid and the apicoplast, with 22% of the genes in this category, are abundantly transcribed. Also, the plasma membrane as well as the parasite's pellicle appeared to be enriched. Of note, 38% of the genes abundantly expressed in the BM have no cellular component annotated (Figure 2C). Finally, using the ShinyGo algorithm against the top 50 most abundantly expressed genes of *P. vivax* in the BM, terms relating to a predicted function in the bone, including terms like bone growth, as well as cell surface and signalling genes, all predicted to play a role in the bone appeared upregulated (Figure 2D).

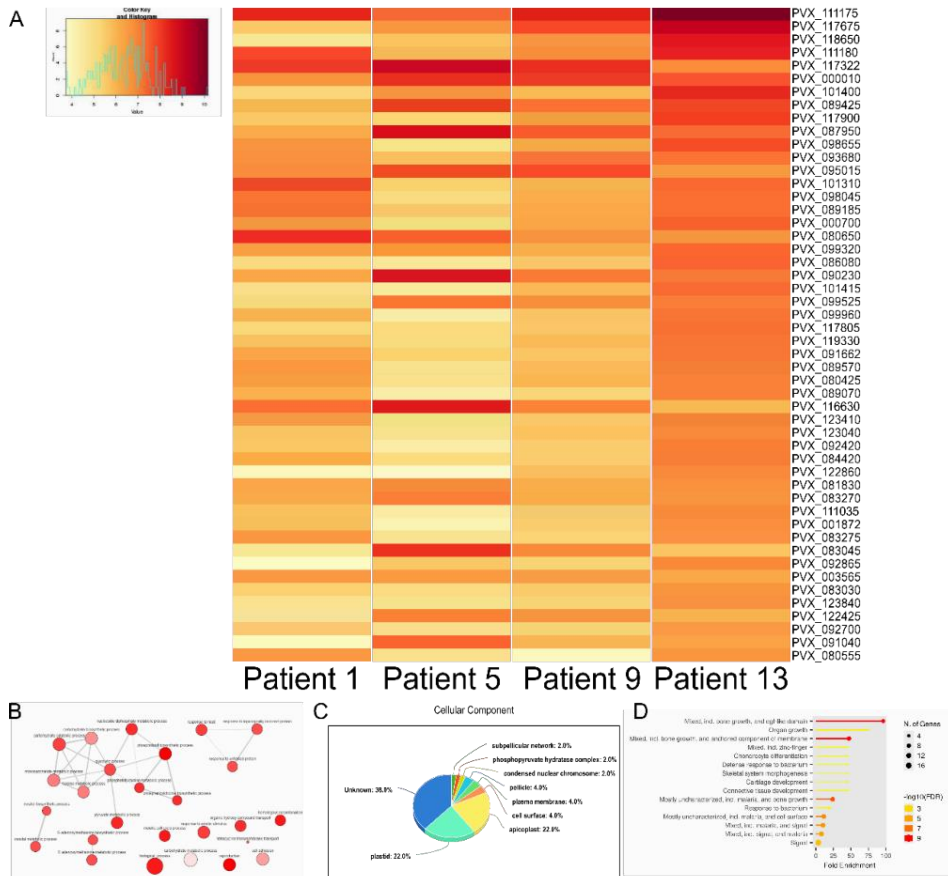


Figure 2. Analysis of top 50 expressed genes in the BM **A)** Heatmap with the abundance of the top 50 actively transcribed genes in the BM by *P. vivax* per patient **B)** Network with the enriched GO terms regarding Biological process in which the BM genes are involved. **C)** Pie-chart with the cellular component annotated for the top 50 expressed genes. **D)** ShinyGO GO and KEGG pathways enrichment analysis of the top 50 BM genes transcribed by the parasite.

RNaseq data confirm presence of *P. vivax* gametocytes in the BM during malaria infection

As expected, several gametocyte-related genes were identified, albeit variably, among the top 50 expressed genes by the parasite in the BM (**Figure 3A**). Patient 13 showed the highest overall expression of gametocyte-related genes while Patient 5 displayed smaller representation of gametocytes specific genes being actively transcribed. PVX_111175, the ookinete surface protein Pvs25 appeared to be the most expressed gametocyte gene among all samples (**Figure 3A**). Also, other important and well characterized genes related to the gametocytogenesis process, like the *pvs28*, *plasmepsins VIII*, and other crystalloid protein coding genes appeared in our list. Again, using the ShinyGo suite, we are able to identify enrichment in terms related to the bone as well as cellular compartments linking the detected genes to the parasite membrane (**Figure 3B**)

Wild variety of *vir*-genes expressed in the BM.

After comparison with the peripheral blood transcriptome of *P. vivax* parasites (Zhu et al., 2016), a list of genes preferentially (if not exclusively) expressed in the BM was generated. A total of 116 genes were found to be absent in the transcriptome from Zhu et al. and actively transcribed among the four patients analysed. The proportion of transcription of the genes among the patients is heterogeneous among individual patients, with some genes being active in only one patient and not in the others. We were able to determine a total of 6 clusters of genes based on the average expression among them (**Figure 4A**). Clusters 1 and 2 contain highly expressed genes in all 4 patients BM aspirates sequenced. Clusters 3 and 4 contain genes with medium or heterogenous expression pattern among the patients. Clusters 5 and 6 contain genes with low expression among the BM aspirates (**Figure 4A**). Among clusters 5 and 6, the majority of genes correspond to the tRNAs group of genes, with low to absent expression in some patients (**Figure 4A and 4B**).

We were able to observe how the *vir* superfamily is the most enriched category of genes expressed in the BM with 55 genes (out of 116) belonging to this superfamily (**Figure 4B**). Noticeably, there are some genes that are not annotated in the PlasmoDB. Also, subcellular localization of these genes is poorly annotated in the available databases with half of genes without any predicted or annotated subcellular localization in PlasmoDB (**Figure 4C**). However, 45% of the genes preferentially expressed in the BM are predicted to have membrane localization, mainly from the *vir* superfamily (**Figure 4C**).

Finally, some of the preferentially expressed genes have been already been described in other works, like the PVX_096410 coding for the cysteine repeat modular protein 2, which has been described as spleen-dependent gene (Fernandez-Becerra et al., 2020), or the PVX_121865, which appears in the Single-Cell RNAseq transcriptome published by Sà et colleagues (Sà et al., 2020), coding for a PHIST superfamily protein (**Figure 4D**). The complete list of genes that are shared with the compared works is present in **Figure 4D**.

Transgenic *P. falciparum* 3D7 parasites expressing BM-dependent genes from *P. vivax*

Plasmids carrying *P. vivax* dependent genes have been efficiently generated using pHH1_CRT-3HA_LISP1 backbone plasmid (Ayllon-Hermida et al., 2024). For transgenic parasite line generation, pDC2_Cas9_hDHFryFCU1_LISP1 (Ayllon-Hermida et al., 2024; Llorà-Batlle et al., 2020) was used as Cas9 and sgRNA carrier. Unexpectedly, without explanation and despite numerous try-outs of different pHH1 plasmids carrying an individual BM-dependent gene, we were unable to generate a stable transgenic parasite line expressing cloned genes for functional analysis (**Supplementary Figure 2A**).

Discussion

The bone marrow as a cryptic niche for infection of *Plasmodium vivax* parasites has been pointed as a major factor contributing to the parasite resilience to control, elimination and future eradication (Fernandez-Becerra et al., 2022; Silva-Filho et al., 2020). Our study provides a comprehensive analysis of RNA sequencing (RNAseq) data from bone marrow (BM) aspirates of patients infected with *P. vivax*, revealing insights into the transcriptional landscape of the parasite within this niche.

The RNAseq data yielded comparable numbers of raw reads across all samples, indicating the robustness of the procedure of sample obtention and RNA processing. The observed disappearance of *P. vivax* reads at t42 samples in 3 patients underscores the

efficacy of the treatment administered to patients (**Figure 1**). However, *P. vivax* reads were observed in one of the patients after treatment, thus indicating the presence of parasites that either were resistant to treatment or were hidden in niches where drug concentration was unable to completely remove them from this tissue. It has been observed that *P. vivax* can be transmitted through bone marrow transplantations even years after drug treatment in travellers after returning to non-endemic regions (O'Donnell et al., 1998). It is tempting to speculate that these parasites are in part responsible for asymptomatic cryptic infections contributing to transmission. In the absence of any other supporting data, this remains to be demonstrated.

The presence of gametocytes in the bone marrow have been demonstrated in experimental infections using malaria rodent models (Niz et al., 2018) as well as in post-mortem analysis of human BM samples (Joyce et al., 2014). In the context of *P. vivax*, the first unequivocal report showing the presence of parasites in this tissue (Baro et al., 2017) demonstrated the presence of gametocytes (Baro et al., 2017) and a later report confirmed this finding in other patients (Brito et al., 2022). Of interest, the presence of gametocyte-specific genes among the top 50 expressed genes indicates that *P. vivax* gametocytes reside and are actively transcribing in the BM during infection (**Figure 2 and 3**). However, a big heterogeneity of expression patterns highlights individual variability in gametocyte burden and possibly different stages of infection or immune response among patients (**Figure 3**).

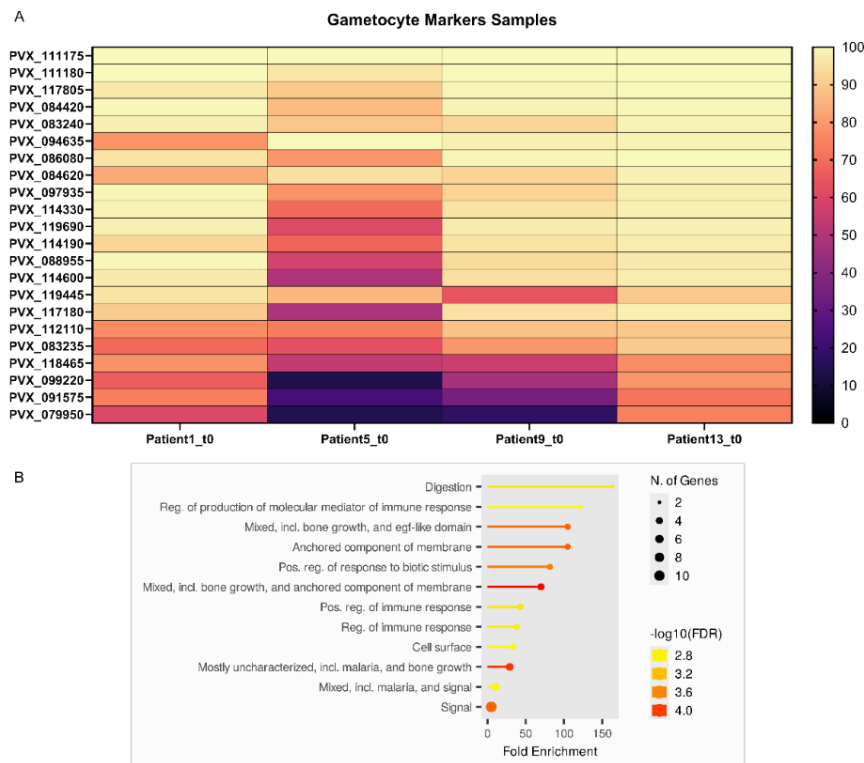


Figure 3. Gametocyte genes detected in the BM aspirates of four *P. vivax* patients. **A)** Heat map of gametocyte genes detected in BM samples at to. Scale bar represents the percentile ranking of each gene in the RNAseq data of each BM aspirate. **B)** ShinyGO GO and KEGG pathways enrichment analysis of the gametocytes genes detected.

Translational control is a key process during the transmission of gametocytes from humans to mosquitos (Dessens et al., 2021; Mair et al., 2006). In fact, several hundreds of genes are actively transcribed yet not translated in gametocytes. These include, among others, *p25*, *p28*, (PSOP family proteins), regulatory proteases (plasmepsins VII and VIII), as well as many of the known crystalloid proteins (e.g., PH-like proteins, MOLO1, NTH, and CPW-WPC proteins) (Dessens et al., 2021). Remarkably, orthologues of these genes were identified in our list of gametocyte markers (**Supplementary Table 3**), given for what we believe is the first time, full support of this mechanism in natural infections by *P. vivax*. In fact, the four most actively transcribe parasite genes in the bone marrow corresponds to the ookinete *pvs25* and *pvs28* genes as well as LCCLdomain-containing protein whose expression is associated with the plasma membrane in mature gametocytes.

Contrary to its often-benign reputation, *Plasmodium vivax* can cause severe disease (Anstey et al., 2012; Naing et al., 2014). In *P. falciparum* malaria, the disease process is linked to the parasite's ability to stick to endothelial cells and uninfected red blood cells in a phenomenon known as cytoadherence and rosetting (Lee et al., 2019; Newbold et al., 1999; Smith et al., 2013; Su et al., 1995). However, much less is known about cytoadherence in *P. vivax* malaria. Although *P. vivax* lacks of classical cytoadherence proteins like PfEMP1 or RIFIN proteins (Carlton et al., 2008), a different multigene family has been implicated in its adhesion and antigenic variation. The *P. vivax* variant genes (*vir*) family is the largest multigene family in *P. vivax*. Initially, 346 *vir* genes were identified in the *P. vivax* genome, mostly located in subtelomeric regions and grouped into 12 subfamilies (Carlton et al., 2008; Del Portillo et al., 2001; Fernandez-Becerra et al., 2005). Later, more than a 1000 *vir* genes were identified in *P. vivax* genomes (Auburn et al., 2016)

Our study also revealed a significant number of genes (116) that were preferentially expressed in the BM compared to peripheral blood (Zhu et al., 2016), with a substantial portion belonging to the *vir* superfamily (**Figure 4**). This superfamily, known for its role in immune evasion, antigenic variation (Bernabeu et al., 2012; Fernandez-Becerra et al., 2009; Lopez et al., 2013), and cytoadherence (Bernabeu et al., 2012; Carvalho et al., 2010; Fernandez-Becerra et al., 2020) underscores the complexity of *P. vivax* interactions within the BM. Clustering analysis revealed distinct patterns of gene expression, with some genes ubiquitously expressed across all patients and others showing more variable expression. Notably, 55 of the preferentially expressed genes were from the *vir* superfamily, with many predicted to have membrane localization, emphasizing their potential role in host-parasite interactions within the BM. These findings suggest that the BM environment uniquely influences the expression of *vir* genes, potentially contributing to the persistence and cytoadherence of *P. vivax*. Several genes identified in our study have been previously reported, reinforcing their relevance. For instance, the cysteine repeat modular protein 2 (PVX_096410) and PHIST superfamily proteins (PVX_121865) were also found in spleen-dependent (Fernandez-Becerra et al., 2020) and single-cell RNAseq studies (Sà et al., 2020), respectively. This overlap with previous research supports the robustness of our findings and highlights the critical role these genes play in the parasite's biology. The presence of these genes across different studies underscores their importance in the life cycle and pathogenicity of *P. vivax*.

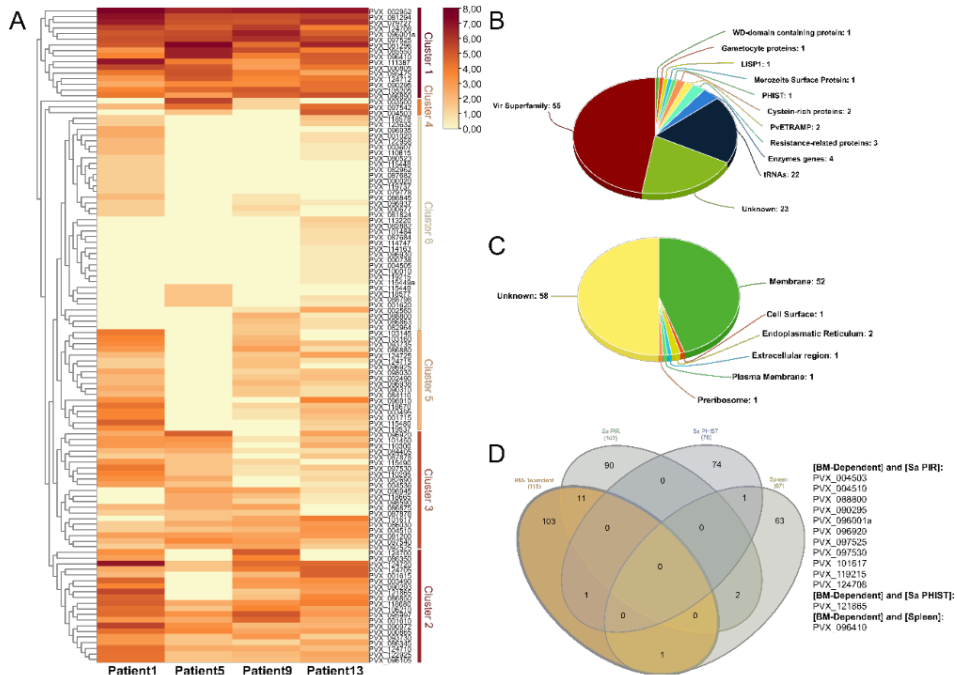


Figure 4. Analysis of transcriptome from BM parasite compared to previously published PB parasites from Zhu et al 2016 (Zhu et al., 2016). **A**) Clustered heatmap of not detected genes in Zhu et al. 2016 **B**) Pie chart of superfamily representation of the preferentially expressed BM genes **C**) Predicted subcellular localization of preferentially expressed genes in the BM **D**) Venn diagram comparing our own RNAseq data of preferentially expressed genes with Sa et al 2020 (Sa et al., 2020) and with spleen-dependent genes (Fernandez-Becerra et al., 2020). Venn diagram generated with InterctiVenn (Heberle et al., 2015).

We strongly aimed towards the functional characterization of those genes preferentially expressed through transgenic *P. falciparum* line generation, which in the past have enable our group to characterize some *P. vivax* genes (Ayllon-Hermida et al., 2024; Bernabeu et al., 2012). Unfortunately, we have not been able to generate a stable transgenic parasite line expressing any of the 5 genes we have selected during this study. The difficulty of generating stable transgenic *P. falciparum* parasite lines is well-known in the field and even stable parasites might be obtained, there are reports that those parasites are non-functional (Marin-Mogollon et al., 2018). More recently, the use of *P. knowlesi* for expressing *P. vivax* genes seems a solid alternative likely due to their closer phylogenetic relationship (Mohring et al., 2019; Moon et al., 2013). Implementation of such heterologous system is warranted for furthering functional studies of *P. vivax* genes preferentially expressed in the human bone marrow.

We are conscious of some limitations of this work: (i) the difficulty of the obtention of the BM, with the possible contamination with PB parasites might confound the parasite transcript detection (ii) not comparing the transcriptome of BM and PB from the same patient might not reveal the complete difference in both transcriptomes (iii) the incapability of generating stable transgenic lines of *P. falciparum* require future experimentation, maybe using a more similar parasite like *P. knowlesi*, which has been recently adapted to *in vitro* culture.

In conclusion, our study highlights the BM as a critical reservoir for *P. vivax*, harbouring a complex and active transcriptional profile that includes metabolic, structural, gametocyte, and *vir* genes. The data presented here provide valuable insights into the parasite's survival strategies and interactions within the BM, offering potential targets for therapeutic interventions and a deeper understanding of *P. vivax* biology. However, further research is needed to elucidate the functional roles of these preferentially expressed genes and their contributions to the parasite's lifecycle and pathogenicity.

Acknowledgments & Funding

We kindly acknowledge all participants that have given permission to be included in this project. We thank Alfred Cortes for the kind gift of the *pHH1_DiCre_lisp1* plasmid vector and Marc Nicolau for technical help. We thank the Center for Genomic Regulation's Genomics Unit for next-generation sequencing services.

CFB and HAP acknowledge support from the Spanish Ministry of Science and Innovation (MICINN) (PID2022- 142908OB-I00) and by AGAUR-SGR (2021 SGR 01554). We also acknowledge support from the grant CEX2023-0001290-S funded by MCIN/AEI/10.13039/501100011033, and support from the Generalitat de Catalunya through the CERCA Program". This research is part of the ISGlobal's Program on the Molecular Mechanisms of Malaria which is partially supported by the Fundació Ramón Areces. CFB is also part of the CIBER-Consortio Centro de Investigación Biomédica en Red (CB 2021), Instituto de Salud Carlos III, Ministerio de Ciencia e Innovación, and Unión Europea-NextGenerationEU

Author Contributions

AAH: Formal Analysis; Investigation; Methodology; Writing- original draft; Writing-review & editing. **MAMB, BB,** and **MVGL,** Resources. **LS,** Methodology, Formal analysis. **HAP** and **CFB,** Conceptualization, Formal analysis, Writing- original draft; Writing- review & editing.

Disclosure and competing interest statement

The authors declare that the research was conducted in the absence of any commercial or financial relationships that could be construed as a potential conflict of interest.

Data Availability

RNAseq data is available upon request to CFB or HAP.

References

- Aitken, G. J. (1943). Sternal puncture in the diagnosis of malaria. *The Lancet*, 242(6268), 466–468. [https://doi.org/10.1016/S0140-6736\(00\)87486-3](https://doi.org/10.1016/S0140-6736(00)87486-3)
- Alvarez-Jarreta, J., Amos, B., Aurrecochea, C., Bah, S., Barba, M., Barreto, A., Basenko, E. Y., Belnap, R., Blevins, A., Böhme, U., Brestelli, J., Brown, S., Callan, D., Campbell, L. I., Christophides, G. K., Crouch, K., Davison, H. R., DeBarry, J. D., Demko, R., ... Zheng, J. (2024). VEuPathDB: the eukaryotic pathogen, vector and host bioinformatics resource center in 2023. *Nucleic Acids Research*, 52(D1), D808–D816. <https://doi.org/10.1093/NAR/GKAD1003>
- Angrisano, F., & Robinson, L. J. (2022). Plasmodium vivax – How hidden reservoirs hinder global malaria elimination. *Parasitology International*, 87, 102526. <https://doi.org/10.1016/J.PARINT.2021.102526>

- Anstey, N. M., Douglas, N. M., Poespoprodjo, J. R., & Price, R. N. (2012). Plasmodium vivax: Clinical Spectrum, Risk Factors and Pathogenesis. In *Advances in Parasitology* (Vol. 80). Elsevier. <https://doi.org/10.1016/B978-0-12-397900-1.00003-7>
- Auburn, S., Böhme, U., Steinbiss, S., Trimarsanto, H., Hostetler, J., Sanders, M., Gao, Q., Nosten, F., Newbold, C. I., Berriman, M., Price, R. N., & Otto, T. D. (2016). A new Plasmodium vivax reference sequence with improved assembly of the subtelomeres reveals an abundance of pir genes. *Wellcome Open Research*, 1. <https://doi.org/10.12688/WELLCOMEOPENRES.9876.1/DOI>
- Ayllon-Hermida, A., Nicolau-Fernandez, M., Larrinaga, A. M., Aparici-Herraiz, I., Tintó-Font, E., Lorà-Batlle, O., Orban, A., Yasnot, M. F., Graupera, M., Esteller, M., Popovici, J., Cortés, A., del Portillo, H. A., & Fernandez-Becerra, C. (2024). Plasmodium vivax spleen-dependent protein 1 and its role in extracellular vesicles-mediated intrasplenic infections. *Frontiers in Cellular and Infection Microbiology*, 14. <https://doi.org/10.3389/fcimb.2024.1408451>
- Baro, B., Deroost, K., Raiol, T., Brito, M., Almeida, A. C. G., de Menezes-Neto, A., Figueiredo, E. F. G., Alencar, A., Leitão, R., Val, F., Monteiro, W., Oliveira, A., Armengol, M. del P., Fernández-Becerra, C., Lacerda, M. V., & del Portillo, H. A. (2017). Plasmodium vivax gametocytes in the bone marrow of an acute malaria patient and changes in the erythroid miRNA profile. *PLoS Neglected Tropical Diseases*, 11(4), 6–13. <https://doi.org/10.1371/journal.pntd.0005365>
- Bernabeu, M., Lopez, F. J., Ferrer, M., Martin-Jaular, L., Razaname, A., Corradin, G., Maier, A. G., del Portillo, H. A., & Fernandez-Becerra, C. (2012). Functional analysis of Plasmodium vivax VIR proteins reveals different subcellular localizations and cytoadherence to the ICAM-1 endothelial receptor. *Cellular Microbiology*, 14(3), 386–400. <https://doi.org/10.1111/J.1462-5822.2011.01726.X>
- Brito, M. A. M., Baro, B., Raiol, T. C., Ayllon-Hermida, A., Safe, I. P., Deroost, K., Figueiredo, E. F. G., Costa, A. G., Armengol, M. D. P., Sumoy, L., Almeida, A. C. G., Hounkpe, B. W., De Paula, E. V., Fernandez-Becerra, C., Monteiro, W. M., Del Portillo, H. A., & Lacerda, M. V. G. (2022). Morphological and Transcriptional Changes in Human Bone Marrow during Natural Plasmodium vivax Malaria Infections. *Journal of Infectious Diseases*, 225(7), 1274–1283. <https://doi.org/10.1093/infdis/jiaa177>
- Carlton, J. M., Adams, J. H., Silva, J. C., Bidwell, S. L., Lorenzi, H., Caler, E., Crabtree, J., Angiuoli, S. V., Merino, E. F., Amedeo, P., Cheng, Q., Coulson, R. M. R., Crabb, B. S., Del Portillo, H. A., Essien, K., Feldblyum, T. V., Fernandez-Becerra, C., Gilson, P. R., Gueye, A. H., ... Fraser-Liggett, C. M. (2008). Comparative genomics of the neglected human malaria parasite Plasmodium vivax. *Nature*, 455(7214), 757–763. <https://doi.org/10.1038/NATURE07327>
- Carvalho, B. O., Lopes, S. C. P., Nogueira, P. A., Orlandi, P. P., Bargieri, D. Y., Blanco, Y. C., Mamoni, R., Leite, J. A., Rodrigues, M. M., Soares, I. S., Oliveira, T. R., Wunderlich, G., Lacerda, M. V. G., Del Portillo, H. A., Araújo, M. O. G., Russell, B., Suwanarusk, R., Snounou, G., Rénia, L., & Costa, F. T. M. (2010). On the cytoadhesion of Plasmodium vivax-infected erythrocytes. *The Journal of Infectious Diseases*, 202(4), 638–647. <https://doi.org/10.1086/654815>
- Chen, C., Wu, Y., Li, J., Wang, X., Zeng, Z., Xu, J., Liu, Y., Feng, J., Chen, H., He, Y., & Xia, R. (2023). TBtools-II: A “one for all, all for one” bioinformatics platform for

- biological big-data mining. *Molecular Plant*, 16(11), 1733–1742. <https://doi.org/10.1016/J.MOLP.2023.09.010>
- Chuquiyaauri, R., Molina, D. M., Moss, E. L., Wang, R., Gardner, M. J., Brouwer, K. C., Torres, S., Gilman, R. H., Llanos-Cuentas, A., Neafsey, D. E., Felgner, P., Liang, X., & Vinetz, J. M. (2015). Genome-scale protein microarray comparison of human antibody responses in plasmodium vivax relapse and reinfection. *American Journal of Tropical Medicine and Hygiene*, 93(4), 801–809. https://doi.org/10.4269/AJTMH.15-0232/-/DC6/SD6_TAB2.XLSX
- Del Portillo, H. A., Fernandez-Becerra, C., Bowman, S., Oliver, K., Preuss, M., Sanchez, C. P., Schneider, N. K., Villalobos, J. M., Rajandream, M. A., Harris, D., Da Silva, L. H. P., Barrell, B., & Lanzer, M. (2001). A superfamily of variant genes encoded in the subtelomeric region of Plasmodium vivax. *Nature*, 410(6830), 839–842. <https://doi.org/10.1038/35071118>
- Dessens, J. T., Tremp, A. Z., & Saeed, S. (2021). Crystalloids: Fascinating Parasite Organelles Essential for Malaria Transmission. *Trends in Parasitology*, 37(7), 581–584. <https://doi.org/10.1016/J.PT.2021.04.002>
- Fernandez-Becerra, C., Aparici-Herraiz, I., & del Portillo, H. A. (2022). Cryptic erythrocytic infections in Plasmodium vivax, another challenge to its elimination. *Parasitology International*, 87. <https://doi.org/10.1016/j.parint.2021.102527>
- Fernandez-Becerra, C., Bernabeu, M., Castellanos, A., Correa, B. R., Obadía, T., Ramirez, M., Rui, E., Hentzschel, F., López-Montañés, M., Ayllon-Hermida, A., Martín-Jaular, L., Elizalde-Torrent, A., Siba, P., Vêncio, R. Z., Arevalo-Herrera, M., Herrera, S., Alonso, P. L., Mueller, I., & del Portillo, H. A. (2020). Plasmodium vivax spleen-dependent genes encode antigens associated with cytoadhesion and clinical protection. *Proceedings of the National Academy of Sciences of the United States of America*, 117(23), 13056–13065. <https://doi.org/10.1073/pnas.1920596117>
- Fernandez-Becerra, C., Pein, O., De Oliveira, T. R., Yamamoto, M. M., Cassola, A. C., Rocha, C., Soares, I. S., De Bragança Pereira, C. A., & Del Portillo, H. A. (2005). Variant proteins of Plasmodium vivax are not clonally expressed in natural infections. *Molecular Microbiology*, 58(3), 648–658. <https://doi.org/10.1111/j.1365-2958.2005.04850.x>
- Fernandez-Becerra, C., Yamamoto, M. M., Vêncio, R. Z. N., Lacerda, M., Rosanas-Urgell, A., & del Portillo, H. A. (2009). Plasmodium vivax and the importance of the subtelomeric multigene vir superfamily. *Trends in Parasitology*, 25(1), 44–51. <https://doi.org/10.1016/j.pt.2008.09.012>
- Ge, S. X., Jung, D., Jung, D., & Yao, R. (2020). ShinyGO: a graphical gene-set enrichment tool for animals and plants. *Bioinformatics*, 36(8), 2628–2629. <https://doi.org/10.1093/BIOINFORMATICS/BTZ931>
- Heberle, H., Meirelles, V. G., da Silva, F. R., Telles, G. P., & Minghim, R. (2015). InteractiVenn: a web-based tool for the analysis of sets through Venn diagrams. *BMC Bioinformatics*, 16(1). <https://doi.org/10.1186/S12859-015-0611-3>
- Joice, R., Nilsson, S. K., Montgomery, J., Dankwa, S., Egan, E., Morahan, B., Seydel, K. B., Bertuccini, L., Alano, P., Williamson, K. C., Duraisingh, M. T., Taylor, T. E., Milner, D. A., & Marti, M. (2014). Plasmodium falciparum transmission stages accumulate in the human bone marrow. *Science Translational Medicine*, 6(244). <https://doi.org/10.1126/SCITRANSLMED.3008882>

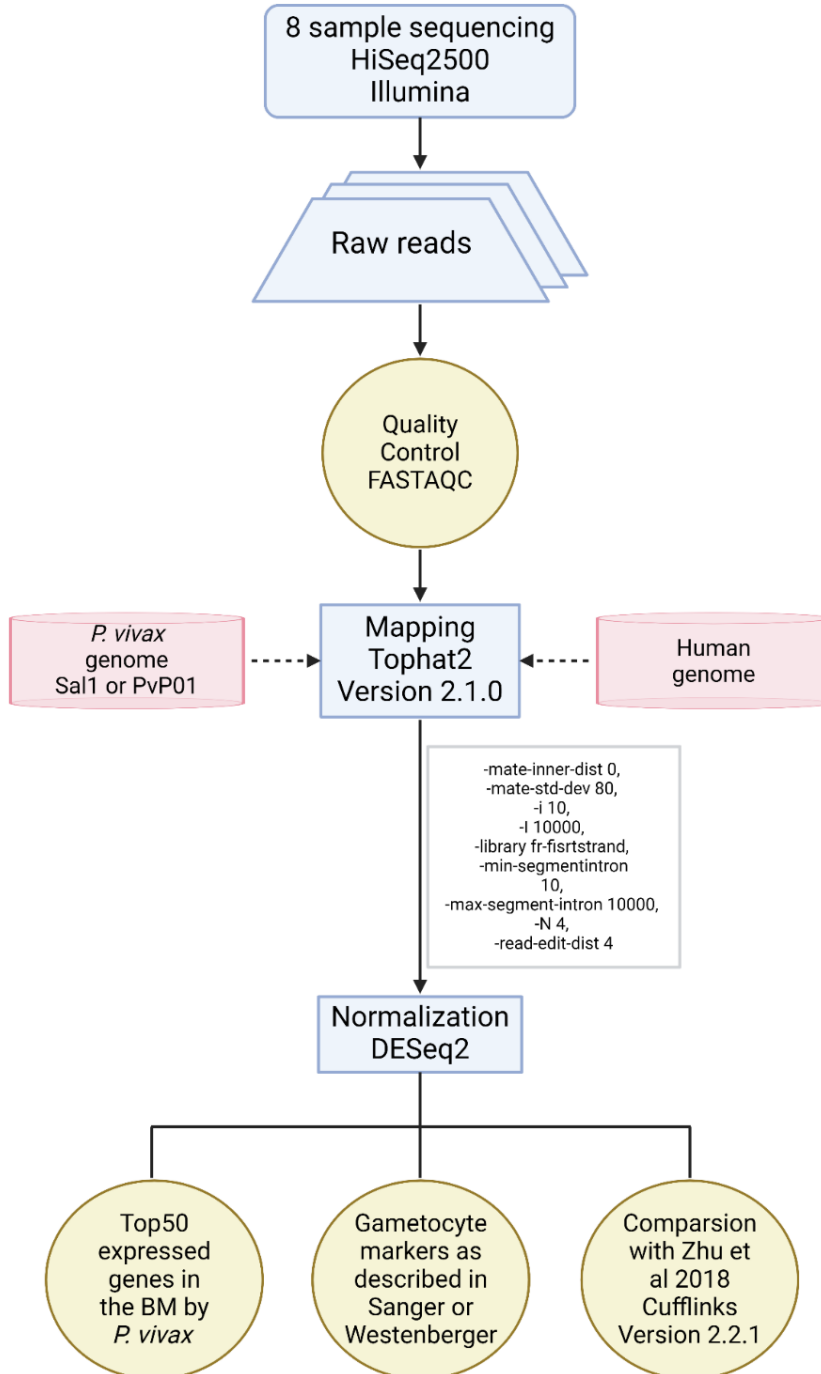
- Kho, S., Qotrunnada, L., Leonardo, L., Andries, B., Wardani, P. A. I., Fricot, A., Henry, B., Hardy, D., Margyaningsih, N. I., Apriyanti, D., Puspitasari, A. M., Prayoga, P., Trianty, L., Kenangalem, E., Chretien, F., Brousse, V., Safeukui, I., del Portillo, H. A., Fernandez-Becerra, C., ... Anstey, N. M. (2021). Evaluation of splenic accumulation and colocalization of immature reticulocytes and Plasmodium vivax in asymptomatic malaria: A prospective human splenectomy study. *PLOS Medicine*, 18(5), e1003632. <https://doi.org/10.1371/JOURNAL.PMED.1003632>
- Kho, S., Qotrunnada, L., Leonardo, L., Andries, B., Wardani, P. A. I., Fricot, A., Henry, B., Hardy, D., Margyaningsih, N. I., Apriyanti, D., Puspitasari, A. M., Prayoga, P., Trianty, L., Kenangalem, E., Chretien, F., Safeukui, I., del Portillo, H. A., Fernandez-Becerra, C., Meibalan, E., ... Anstey, N. M. (2021). Hidden Biomass of Intact Malaria Parasites in the Human Spleen. *New England Journal of Medicine*, 384(21), 2067–2069. https://doi.org/10.1056/NEJMC2023884/SUPPL_FILE/NEJMC2023884_DISCLOSURES.PDF
- Kho, S., Siregar, N. C., Qotrunnada, L., Fricot, A., Sissoko, A., Shanti, P. A. I., Candrawati, F., Kambuaya, N. N., Rini, H., Andries, B., Hardy, D., Margyaningsih, N. I., Fadllan, F., Rahmayenti, D. A., Puspitasari, A. M., Aisah, A. R., Leonardo, L., Yayang, B. T. G., Margayani, D. S., ... Buffet, P. A. (2024). Retention of uninfected red blood cells causing congestive splenomegaly is the major mechanism of anemia in malaria. *American Journal of Hematology*, 99(2), 223–235. <https://doi.org/10.1002/AJH.27152>
- Krotoski, W. A. (1985). Discovery of the hypnozoite and a new theory of malarial relapse. *Transactions of the Royal Society of Tropical Medicine and Hygiene*, 79(1), 1. [https://doi.org/10.1016/0035-9203\(85\)90221-4](https://doi.org/10.1016/0035-9203(85)90221-4)
- Krotoski, W. A., Garnham, P. C. C., Bray, R. S., Killick-Kendrick, R., Draper, C. C., Targett, G. A., & Guy, M. W. (1982). Observations on Early and Late Post-Sporozoite Tissue Stages in Primate Malaria: I. Discovery of a New Latent Form of Plasmodium cynomolgi (the Hypnozoite), and Failure to Detect Hepatic Forms Within the First 24 Hours After Infection. *The American Journal of Tropical Medicine and Hygiene*, 31(1), 24–35. <https://doi.org/10.4269/AJTMH.1982.31.24>
- Lee, W. C., Russell, B., & Rénia, L. (2019). Sticking for a Cause: The Falciparum Malaria Parasites Cytoadherence Paradigm. *Frontiers in Immunology*, 10(JUN). <https://doi.org/10.3389/FIMMU.2019.01444>
- Llorà-Batlle, O., Michel-Todó, L., Witmer, K., Toda, H., Fernández-Becerra, C., Baum, J., & Cortés, A. (2020). Conditional expression of PfAP2-G for controlled massive sexual conversion in Plasmodium falciparum. *Science Advances*, 6(24). https://doi.org/10.1126/SCIADV.AAZ5057/SUPPL_FILE/AAZ5057_SM.PDF
- Lopez, F. J., Bernabeu, M., Fernandez-Becerra, C., & del Portillo, H. A. (2013). A new computational approach redefines the subtelomeric vir superfamily of Plasmodium vivax. *BMC Genomics*, 14(1), 1. <https://doi.org/10.1186/1471-2164-14-8>
- Mair, G. R., Braks, J. A. M., Garver, L. S., Wiegant, J. C. A. G., Hall, N., Dirks, R. W., Khan, S. M., Dimopoulos, G., Janse, C. J., & Waters, A. P. (2006). Regulation of sexual development of Plasmodium by translational repression. *Science (New York, N.Y.)*, 313(5787), 667–669. <https://doi.org/10.1126/SCIENCE.1125129>

- Marchiafava, E., & Bignami, A. (1892). *Sulle febbri malariche estivo-autunnali* (I. Artero, Ed.; 1st ed.). Reale Accademia Medica di Roma. <https://wellcomecollection.org/works/zn2r62kh>
- Marin-Mogollon, C., Van Pul, F. J. A., Miyazaki, S., Imai, T., Ramesar, J., Salman, A. M., Winkel, B. M. F., Othman, A. S., Kroeze, H., Chevalley-Maurel, S., Reyes-Sandoval, A., Roestenberg, M., Franke-Fayard, B., Janse, C. J., & Khan, S. M. (2018). Chimeric Plasmodium falciparum parasites expressing Plasmodium vivax circumsporozoite protein fail to produce salivary gland sporozoites. *Malaria Journal*, 17(1). <https://doi.org/10.1186/S12936-018-2431-1>
- Miyazaki, S., Yang, A. S. P., Geurten, F. J. A., Marin-Mogollon, C., Miyazaki, Y., Imai, T., Kolli, S. K., Ramesar, J., Chevalley-Maurel, S., Salman, A. M., van Gemert, G. J. A., van Waardenburg, Y. M., Franke-Fayard, B., Hill, A. V. S., Sauerwein, R. W., Janse, C. J., & Khan, S. M. (2020). Generation of Novel Plasmodium falciparum NF135 and NF54 Lines Expressing Fluorescent Reporter Proteins Under the Control of Strong and Constitutive Promoters. *Frontiers in Cellular and Infection Microbiology*, 10. <https://doi.org/10.3389/fcimb.2020.00270>
- Mohring, F., Hart, M. N., Rawlinson, T. A., Henrici, R., Charleston, J. A., Diez Benavente, E., Patel, A., Hall, J., Almond, N., Campino, S., Clark, T. G., Sutherland, C. J., Baker, D. A., Draper, S. J., & Moon, R. W. (2019). Rapid and iterative genome editing in the malaria parasite Plasmodium knowlesi provides new tools for P. vivax research. *ELife*, 8. <https://doi.org/10.7554/ELIFE.45829>
- Moon, R. W., Hall, J., Rangkuti, F., Ho, Y. S., Almond, N., Mitchell, G. H., Pain, A., Holder, A. A., & Blackman, M. J. (2013). Adaptation of the genetically tractable malaria pathogen Plasmodium knowlesi to continuous culture in human erythrocytes. *Proceedings of the National Academy of Sciences of the United States of America*, 110(2), 531–536. https://doi.org/10.1073/PNAS.1216457110/SUPPL_FILE/PNAS.201216457SI.PDF
- Naing, C., Whittaker, M. A., Nyunt Wai, V., & Mak, J. W. (2014). Is Plasmodium vivax malaria a severe malaria?: a systematic review and meta-analysis. *PLoS Neglected Tropical Diseases*, 8(8). <https://doi.org/10.1371/JOURNAL.PNTD.0003071>
- Newbold, C., Craig, A., Kyes, S., Rowe, A., Fernandez-Reyes, D., & Fagan, T. (1999). Cytoadherence, pathogenesis and the infected red cell surface in Plasmodium falciparum. *International Journal for Parasitology*, 29(6), 927–937. [https://doi.org/10.1016/S0020-7519\(99\)00049-1](https://doi.org/10.1016/S0020-7519(99)00049-1)
- Niz, M. De, Meibalan, E., Mejia, P., Ma, S., Brancucci, N. M. B., Agop-nersesian, C., Mandt, R., Ngotho, P., Hughes, K. R., Waters, A. P., Huttenhower, C., Mitchell, J. R., Martinelli, R., Frischknecht, F., Seydel, K. B., Taylor, T., Milner, D., Heussler, V. T., & Marti, M. (2018). Plasmodium gametocytes display homing and vascular transmigration in the host bone marrow. 1–15.
- Obaldia, N., Meibalan, E., Sa, J. M., Ma, S., Clark, M. A., Mejia, P., Moraes Barros, R. R., Otero, W., Ferreira, M. U., Mitchell, J. R., Milner, D. A., Huttenhower, C., Wirth, D. F., Duraisingh, M. T., Wellem, T. E., & Marti, M. (2018). Bone marrow is a major parasite reservoir in plasmodium vivax infection. *MBio*, 9(3), 1–16. <https://doi.org/10.1128/mBio.00625-18>

- O'Donnell, J., Goldman, J. M., Wagner, K., Ehinger, G., Martin, N., Leahy, M., Kariuki, N., Dokal, I., & Roberts, I. (1998). Donor-derived *Plasmodium vivax* infection following volunteer unrelated bone marrow transplantation. *Bone Marrow Transplantation*, 21(3), 313–314. <https://doi.org/10.1038/sj.bmt.1701073>
- Okell, L. C., Bousema, T., Griffin, J. T., Ouédraogo, A. L., Ghani, A. C., & Drakeley, C. J. (2012). Factors determining the occurrence of submicroscopic malaria infections and their relevance for control. *Nature Communications*, 3. <https://doi.org/10.1038/ncomms2241>
- Okell, L. C., Ghani, A. C., Lyons, E., & Drakeley, C. J. (2009). Submicroscopic Infection in *Plasmodium falciparum*-Endemic Populations: A Systematic Review and Meta-Analysis. *The Journal of Infectious Diseases*, 200(10), 1509–1517. <https://doi.org/10.1086/644781>
- Panichakul, T., Payuhakrit, W., Panburana, P., Wongborisuth, C., Hongeng, S., & Udomsangpetch, R. (2012). Suppression of erythroid development in vitro by *Plasmodium vivax*. *Malaria Journal*, 11. <https://doi.org/10.1186/1475-2875-11-173>
- Panichakul, T., Ponnikorn, S., Roytrakul, S., Paemane, A., Kittisenachai, S., Hongeng, S., & Udomsangpetch, R. (2015). *Plasmodium vivax* inhibits erythroid cell growth through altered phosphorylation of the cytoskeletal protein ezrin. *Malaria Journal*, 14(1). <https://doi.org/10.1186/S12936-015-0648-9>
- Sà, J. M., Cannon, M. V., Caleon, R. L., Wellems, T. E., & Serre, D. (2020). Single-cell transcription analysis of *Plasmodium vivax* blood-stage parasites identifies stage- and species-specific profiles of expression. *PLOS Biology*, 18(5), e3000711. <https://doi.org/10.1371/JOURNAL.PBIO.3000711>
- Silva-Filho, J. L., Lacerda, M. V. G., Recker, M., Wassmer, S. C., Marti, M., & Costa, F. T. M. (2020). *Plasmodium vivax* in Hematopoietic Niches: Hidden and Dangerous. *Trends in Parasitology*, 36(5), 447–458. <https://doi.org/10.1016/j.pt.2020.03.002>
- Smith, J. D., Rowe, J. A., Higgins, M. K., & Lavstsen, T. (2013). Malaria's deadly grip: cytoadhesion of *Plasmodium falciparum*-infected erythrocytes. *Cellular Microbiology*, 15(12), 1976–1983. <https://doi.org/10.1111/CMI.12183>
- Su, X. zhuan, Heatwole, V. M., Wertheimer, S. P., Guinet, F., Herrfeldt, J. A., Peterson, D. S., Ravetch, J. A., & Wellems, T. E. (1995). The large diverse gene family var encodes proteins involved in cytoadherence and antigenic variation of *Plasmodium falciparum*-infected erythrocytes. *Cell*, 82(1), 89–100. [https://doi.org/10.1016/0092-8674\(95\)90055-1](https://doi.org/10.1016/0092-8674(95)90055-1)
- Trager, W., & Jensen, J. B. (1976). Human malaria parasites in continuous culture. *Science*, 193(4254), 673–675. <https://doi.org/10.1126/science.781840>
- Westenberger, S. J., McClean, C. M., Chattopadhyay, R., Dharia, N. V., Carlton, J. M., Barnwell, J. W., Collins, W. E., Hoffman, S. L., Zhou, Y., Vinetz, J. M., & Winzeler, E. A. (2010). A Systems-Based Analysis of *Plasmodium vivax* Lifecycle Transcription from Human to Mosquito. *PLoS Neglected Tropical Diseases*, 4(4). <https://doi.org/10.1371/JOURNAL.PNTD.0000653>
- White, M. T., Walker, P., Karl, S., Hetzel, M. W., Freeman, T., Waltmann, A., Laman, M., Robinson, L. J., Ghani, A., & Mueller, I. (2018). Mathematical modelling of the impact of expanding levels of malaria control interventions on *Plasmodium vivax*. *Nature Communications*, 9(3300). <https://doi.org/10.1038/s41467-018-05860-8>

- White, N. J. (2011). Determinants of relapse periodicity in *Plasmodium vivax* malaria. *Malaria Journal*, 10(1), 1–36. <https://doi.org/10.1186/1475-2875-10-297/TABLES/3>
- World Health Organization. (2023). *World malaria report 2022*. <https://www.wipo.int/amc/en/mediation/>
- Zhu, L., Mok, S., Imwong, M., Jaidee, A., Russell, B., Nosten, F., Day, N. P., White, N. J., Preiser, P. R., & Bozdech, Z. (2016). New insights into the *Plasmodium vivax* transcriptome using RNA-Seq. *Scientific Reports*, 6. <https://doi.org/10.1038/srep20498>

Supplementary Figures

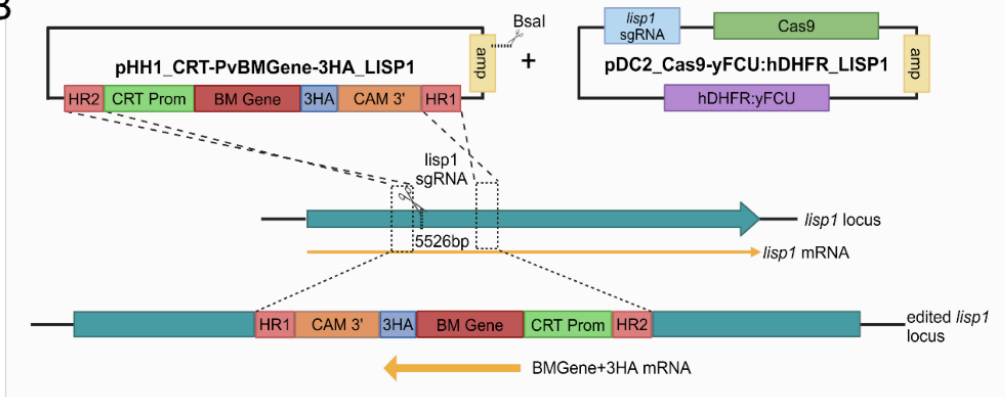


Supplementary Figure 1. Schematic representation of the workflow followed for the analysis of the RNAseq sequencing data.

A

GeneID	PlasmoDB Annotation	Organ	CDS Length	Amplified?	Cloned pHH1?	Sequenced?	Maxiprep?	Transfected?	Transgenic Line?
PVX_000010	Plasmodium exported protein, unknown function (3)	BM	1041						
PVX_093680	Phist protein (Pf-fam-b)	BM	2357					x2	
PVX_097525	variable surface protein Vir 12, putative	BM	1785					x2	
PVX_121865	RAD protein (Pv-fam-e)	BM	804					x2	
PVX_111175	ookinete surface protein Pvs25	BM	660					x3	

B



Supplementary Figure 2. CRISPR/Cas9 generation of transgenic *P. falciparum* parasites. **A)** List of preferentially expressed genes in the BM targeted for cloning, detailing in which step of the CRISPR/Cas9 editing workflow have failed. **B)** Schematic representation of the CRISPR/Cas9 editing strategy. Left plasmid represents the pHH1 plasmid carrying the distinct PvBM genes and the right plasmid represents the plasmid carrying the Cas9 endonuclease. Both aim to the *lisp1* gene of *P. falciparum*.

Supplementary Tables & Figures

Supplementary Table 1

GeneID	PlasmoDB Annotation	Primer Forward	Primer Reverse	Amplicon Length
PVX_000010	Plasmodium exported protein, unknown function	ACTCGACCCGGGATG GTACCATGATATCTCT TACGAAACTCTC	TGGGACGTCGTATGG GTACCAATTCCTCTTG ATTCTTAGA	1041
PVX_093680	Phist protein (Pf-fam-b)	ACTCGACCCGGGATG GTACCATGAGTCCCTG CAACATCCC	TGGGACGTCGTATGG GTACCGAGTTTGCTGT GTTCTTCATC	2357
PVX_097525	variable surface protein Vir 12, putative	ACTCGACCCGGGATG GTACCATGGCAGCTTC AACAGGAAAC	ACGTCGTATGGGTAG GTACCATAATATGAGT CTTGATCAGGGTGG	1785
PVX_121865	RAD protein (Pv-fam-e)	ACTCGACCCGGGATG GTACCATGAATAATCT CTCGATGTCAAGA	ACGTCGTATGGGTAG GTACCTGACTTTGATT TTAGGGTTCT	804
PVX_111175	ookinete surface protein Pvs25	ACTCGACCCGGGATG GTACCATGAACTCCTA CTACAGCCTCTTCG	TGGGACGTCGTATGG GTACCTATGACGTAC GAAAGGACAAGCAGG	660

Supplementary Table 1. Primers used for gene amplification of the targeted genes.

Supplementary Table 2

Individual identifier	Time (days) / <i>P. vivax</i> infection status	Anemia status	Hb level (g/dl)	RNA integrity number (RIN)	Number of raw reads extracted per sample (CRG):
1	0 / infected	Borderline	13.9	9.1	44234231
	42 / cured	Healthy	15.9	8.8	38289963
5	0 / infected	Healthy	16.6	7.4	36437431
	42 / cured	Healthy	16.3	8.7	49585366
9	0 / infected	Anaemic	11.8	8.8	43054913
	42 / cured	Healthy	14	9.1	35262973
13	0 / infected	Anaemic	11.5	7.3	41854986
	42 / cured	Healthy	14.2	7.4	44000844

Supplementary Table 2. Sample information. 4 different patients were enrolled in the study, with samples collected at t0 (when they were admitted at healthcare facility) and t42 (after treatment).

Supplementary Table 3

Gene	Product (Sanger GeneDB <i>P. vivax</i> P01 annotation 170)	<i>P. falciparum</i> orthologues GeneID	<i>P. falciparum</i> orthologues name
PVX_111175	ookinete surface protein P25	PF3D7_1030900	ookinete surface protein P28
PVX_111180	ookinete surface protein P28	PF3D7_1031000	ookinete surface protein P25
PVX_117805	pyridine nucleotide transhydrogenase, putative	PF3D7_1453500	NAD(P) transhydrogenase, putative
PVX_084420	41K blood stage antigen precursor 41-3, putative	PF3D7_1207700	41-3 protein
PVX_083240	6-cysteine protein	PF3D7_1346800	6-cysteine protein P47
PVX_094635	tubulin beta chain, putative	PF3D7_1008700	tubulin beta chain
PVX_086080	LCCL domain-containing protein, putative	PF3D7_1407000	LCCL domain-containing protein
PVX_084620	polyubiquitin 5, putative	PF3D7_1211800	polyubiquitin
PVX_097935	subtilisin-□like protease 1	PF3D7_0507500	subtilisin-like protease 1
PVX_114330	CPW-□WPC family protein Plasmodium falciparum	PF3D7_0624300	CPW-WPC family protein
PVX_119690	plasmepsin VI, putative	PF3D7_0311700	plasmepsin VI
PVX_114190	inner membrane complex protein 1j, putative	PF3D7_0621400	Pf77 protein
PVX_088955	rhomboid protease ROM3, putative	PF3D7_0828000	rhomboid protease ROM3
PVX_114600	CPW-WPC family protein Plasmodium falciparum	PF3D7_0630000	CPW-WPC family protein
PVX_119445	FAD-dependent glycerol-3-phosphate dehydrogenase, putative	PF3D7_0306400	FAD-dependent glycerol-3-phosphate dehydrogenase, putative
PVX_117180	plasmepsin VIII, putative	PF3D7_1465700	plasmepsin VIII, putative
PVX_112110	Plasmodium exported protein (PHIST)	PF3D7_0219700	Plasmodium exported protein (PHISTc), unknown function
PVX_083235	6-cysteine protein	PF3D7_1346700	6-cysteine protein P48/45
PVX_118465	allantoicase, putative	PF3D7_0729100	apicomplexan kinetochore protein 8, putative
PVX_099220	glycolipid transfer protein, putative	PF3D7_0915800	glycolipid transfer protein, putative
PVX_091575	actin-related protein 2/3 complex subunit 1, putative	PF3D7_1118800	actin-related protein 2/3 complex subunit 1, putative
PVX_079950	NIMA related kinase 2, putative	PF3D7_0525900	NIMA related kinase 2

Supplementary Table 3. Gametocyte markers detected in the transcriptome of the parasites from the BM and their correspondent orthologue in *P. falciparum*.

4. DISCUSSION



"Don't Do to Bed with Malaria Mosquito". Office for Emergency Management. Office of War Information. Domestic Operations Branch. Bureau of Special Services. Series: World War II Posters, compiled 1942 - 1945

Vivax malaria, a classically neglected disease

Classically, *P. vivax* malaria has been considered to be a “benign” or mild infection, and even to date, this misconception still prevails. One of the main reasons for this idea is the extremely low peripheral blood parasitaemia and self-limiting infection found in circulation, especially when comparing it to *P. falciparum* infection, where blood parasitaemia is clearly higher (73,360). In semi-immune individuals, parasitaemia is reduced to levels that are undetectable by standard methods (sub-patent), and acute illness is uncommon. In acute *P. vivax* malaria, sub-patency is not merely due to low parasitaemia but also results from parasite biomass that remains concealed beyond the vascular system (360). Even in severe and complicated cases of acute *P. vivax* malaria, parasitaemia is typically minimal (361). This species is not inherently mild, but rather elusive and subtly dangerous.

Despite any clinical data demanding our attention to this disease, is the re-appearance of *P. vivax* in geographic areas where efficient and effective measures to control *P. falciparum* malaria are being displayed what should also drive our attention towards this neglected parasite (3). Furthermore, there have been reports of outbreaks of *P. vivax* occurring occasionally in zones with favourable conditions to have seasonally abundance of anopheline mosquitoes, like Greece, the Republic of Korea or even the United States (362–366).

On the other hand, it has been always believed that *P. vivax* is absent in West, Central and Tropical Africa, where the Duffy-negative blood group, which have been fixed in around 95-100% of the population (34,367). The absence of the Duffy antigen/chemokine receptor (DARC) characteristic of this blood group, prevent the interaction between the antigen and the parasite Duffy-binding Protein (PvDBP), which is crucial for the infection of *P. vivax* (368). However, several recent reports indicate that *P. vivax* is circulating in Sub-Saharan countries with high prevalence of Duffy-negative population (32,369–372), which recently have been attributed to transient expression of Duffy antigen in

Duffy-negative individuals, explaining the susceptibility to *P. vivax*, which is a major implication and challenge for *P. vivax* malaria eradication (373).

Considering all these facts, it is critical to gain better understanding of the mechanisms for the parasite sub-patency, which maintain the ability of transmission (3), in an everyday more globalised world.

P. vivax cryptic infections

For decades, the hypnozoite (from the Greek words *hypnos* – sleep – and *zoon* – animal) stage in the liver has been considered to be the only cryptic stage of *Plasmodium vivax* and moreover the solely contributor for clinical relapses (50,158). Krotoski and Garnham attributed the phenomenon of extended prepatent periods and periodic reappearance of detectable *P. vivax* parasites in circulation by microscopy to an activation of quiescent hepatic hypnozoites (50).

Malaria relapses occur at varying intervals after initial inoculation of the parasite and subsequent infection and pose one of the main challenges in the study and prediction of malaria epidemiology (49). Relapses are solely originated from dormant hypnozoites in the case of *P. vivax* and *P. ovale* in humans. This trait makes *P. vivax* particularly predominant of persistent malaria diseases in regions of Asia, Central and South America and the oriental region of Africa (374). It is believed that *P. vivax* strains from different geographical areas have distinct relapse timing, being longer in temperate regions, where relapse time might occur around 6-12 months post infection (375). However, the epidemiology of these different relapse patterns and the factors triggering them are not well understood yet. This lack of knowledge is a significant gap and entangles malaria control and elimination strategies, given the potential for transmission across diverse environmental conditions. Though, the paradigm of the exclusivity of the hypnozoite as unique contributor for clinical relapses and maintenance of infectivity and transmission of malaria parasites have been questioned for a couple of decades already.

Several studies have suggested the existence of non-hypnozoite stages that persist longer than the acute phase of malaria. In endemic regions, it is common to find *Plasmodium* species, including those not known to relapse, in the blood of individuals who remain asymptomatic for extended periods (55,187,376).

Cryptic niches: The spleen

The spleen is a complex organ perfectly adapted to filter and destroy senescent RBCs, infectious microorganisms and *Plasmodium*-parasitized RBCs during malaria disease (187,376). Del Portillo and Fernandez-Becerra have been working for long time in the role of the spleen during cryptic infection of *P. vivax*. What started as a hypothesis, later was proved to be right. It was believed that *P. vivax* primarily causes infection of hematopoietic tissues rich in reticulocytes, such as the bone marrow and the spleen (73,377). Science advances sometimes occur just by pure serendipity, and back in 2012, del Portillo and Fernandez-Becerra had one of these lucky moments when they bumped into a 19-year-old individual that suffered from a traffic accident which caused him to undergo splenectomy surgery to later find out that he was infected with *Plasmodium vivax* (9). The spleen of the boy was analysed and showed incredibly amounts of intact *P. vivax*-infected reticulocytes. This initial observation led to hypothesize that the spleen might be a cryptic niche where the parasite accumulate during vivax malaria (9).

Later, Steven Kho and the group of Nicholas Anstey had made a major contribution to the field thanks to their research in the examination of spleen in Papua New Guinea, confirming that the initial hypothesis was indeed correct (8,13,184). This caused a shift in the paradigm of how *P. vivax* infection is seen as now it is clear that what we see in circulation is just the tip of the iceberg (3,184). However, a major key gap in the mechanistic of how this gathering of the parasite inside the spleen was occurring.

To solve this, we utilized experimental infection of *Aotus* monkeys (378) similarly to what was done previously by Barnwell and collaborators (379). As shown in the first paper of this thesis, using custom microarray representing all

coding genes of the Salvador I reference strain and then deploying two distinct algorithms to assess expression of those genes, enabled us to generate a list of genes whose expression was dependent of an intact spleen in experimental infection of *P. vivax*. Interestingly, it was found that VIR14 (PVX_108770) was clearly upregulated upon infection of spleen-intact monkeys and moreover, using transgenic *P. falciparum* parasites expressing this VIR protein, it was proven that this protein was mediating the cytoadherence to human spleen fibroblasts (hSFs) (378). From the detected spleen-dependent genes, many of the detected transcripts belonged to the *vir* multigenic family, *pvfam* or predicted exported proteins, which have been proven before to be playing a role in immune evasion, antigenic variation and cytoadherence (100,105,107,189). All these findings, together with the previously available data and reports (8,9,184), clearly shows the key role of the spleen as an important contributor for maintaining asexual multiplication of the parasite inside the organ.

Interestingly, from this same work, and based on evidences on possible clinical protection conferred by higher titers of antibody against a hypothetical *P. vivax* spleen-dependent protein (PVX_114580), we deepen into the characterization of this protein in the second paper presented in this thesis (226). PVX_114580 is completely conserved across *P. vivax* isolates from regions including Mauritania, North Korea, India, and Brazil, and shows up to 90% conservation among other *Plasmodium* species. These findings underscore the potential of this hypothetical *P. vivax* spleen-dependent gene (PVX_114580) protein as a promising target for vaccines aimed at the asexual blood stages of *P. vivax*.

Through the characterization of the PVX_114580, which we proposed to be named *P. vivax* spleen dependent protein 1 (PvSDP1), we were able to observe how EVs from natural infections facilitate parasite binding to hSFs. To be able to functional characterize this protein we use CRISPR/Cas9 genome editing technology to achieve so. This technology implementation has advanced significantly our knowledge of malaria parasites biology (208,380), even in studying *P. vivax* genes have been studied, like the CSP protein of *P. vivax* for the sporozoite formation and infectiveness (203,225). The PvSDP1 stands out

as an excellent potential vaccine, both because of what we have shown in the first paper of this thesis (378) regarding its association with protection against clinical manifestation of vivax malaria, its conservation among *P. vivax* strains and other *Plasmodium* species and its surface localization in natural isolates from Cambodian patient (226). Also, its role in cytoadhesion of the transgenic parasites to hSFs enhances the importance of spleen-dependent genes in this phenomenon, as reported in this thesis and previously (105,378).

Multigenic families with cytoadhesive or binding properties have been described in *P. falciparum*, like the well-studied PfEMP1 (66,88,89), but also in other infectious entities, like bacterial *Babesia bovis* (381), *Mycoplasma hyoshinis* (382) or *Neisseria* spp (383,384) to *Trypanosoma brucei* DNA binding capacity (385). Cytoadhesion was classically questioned to be occurring in *P. vivax* infection as all parasite stages were found in circulation, to opposition to mainly ring-staged parasite found in *P. falciparum* malaria. However, this dogma has been constantly questioned since first evidences of vivax parasite cytoadhering to lung endothelial cells, brain endothelial cells and placental cryosections (189). This cytoadhesion, in the case of *P. vivax*, enable and mediated the parasite accumulation found in the spleen (8,9), mainly by *vir* and other genes, whose expression its dependent of the spleen (105,226,378).

Cryptic niches: The BM

Regarding the bone marrow, and although *P. vivax* presence in the organ was first noted in 1894 (25), research on parasites in this tissue has been limited and sometimes contradictory. Initial observations reported specific morphological changes and nuclear abnormalities in the erythroblasts during vivax infections (386). However, a detailed ultrastructural examination of bone marrow samples from children with severe anaemia did not detect parasites in this tissue (181). But more recently, our group made the first unequivocal confirmation of the presence of *P. vivax* parasite in the BM of an infected individual (10). This trait was also confirmed in experimental infection of monkeys, confirming that the BM is a major parasite reservoir (12).

From the work of Baro in our group, it was proven that *P. vivax* can be found in the bone marrow during an active infection and, similar to *P. falciparum*, act as a niche for gametocyte production and maturation and as reservoir for vivax malaria (10). Gametocytes in *P. vivax* malaria appear in peripheral blood before the onset of any clinical manifestation, and also, the presence of asymptomatic patients, may serve as reservoir capable of maintaining transmission (4). But more interestingly, it was found that the presence of *P. vivax* in the bone marrow of the patient analysed in that project was associated with transcriptional changes of miRNAs involved in erythropoiesis (10).

This observation has been confirmed and further investigated in the third paper presented in this thesis (387). In our study, 3 of the 7 patients showed a 2-3-fold enrichment of parasites in the BM compared to PB. We were also able to notice a tendency for an increase in rings, schizonts and gametocytes in the tissue when compared to BM. However, due to the frequently low levels of parasitaemia of vivax malaria patients, it was difficult to make an accurate counting and would be necessary to generate antibodies or identify specific molecular markers to each parasite stage to accurately quantify *P. vivax* gametocytes stages. Also, no nucleated cells were observed to be infected by *P. vivax*, which has been previously documented (388). In our paper, not just we were able to confirm the enrichment of parasites in the BM, but also we were able to further investigate the affectation in erythropoiesis suffered by vivax malaria patients. Through a RNAseq, we detected down-regulation of major erythroid maturation related genes like the *gata1*, *nfe*, *tali* and *arid3a*. We concluded that during active *P. vivax* infections, parasites are consistently present in the bone marrow and cause dyserythropoiesis and ineffective erythropoiesis, regardless of whether the patient is anaemic. These abnormalities are associated with transcriptional changes in immune-related and erythropoietic-related genes, apparently driven by the downregulation of GATA-1. A major question arose from this paper and is why *P. vivax* targets CD71+ reticulocytes, which are primarily found in the BM, while simultaneously inducing erythropoietic defect during infections

Using this same RNAseq data, but now focusing in the parasite transcriptome present in the BM, we revealed crucial insights into the transcriptional landscape of the parasite within this niche (unpublished data, article 4). The analysis of 5,361 *Plasmodium vivax* genes in the BM confirms the active metabolic and replicative state of the parasite within this hematopoietic tissue, supporting the presence of both asexual life cycle and gametocytogenesis in the BM (10,387). This aligns with earlier studies that identified *Plasmodium* gametocytes in the BM in both rodent models and humans (10,389). Specifically, our findings reveal that *P. vivax* gametocytes are actively produced in the BM during infection, as indicated by the expression of gametocyte-specific genes (unpublished data, article 4). However, the variability in gene expression patterns among patients suggests differences in infection stages or immune responses. The detection of gametocyte specific genes, not only prove the presence of the parasite but detecting transcripts like the *pvs25* or the *pvs80*, which are ookinete proteins, confirm the strong translational control that the malaria parasite has, delaying the translation of transcribed genes to the moment when they are necessary (390).

Furthermore, our study identified 116 genes preferentially expressed in the BM compared to peripheral blood (16), many of which belong to the *vir* superfamily. These genes, as stated before, are known for their roles in immune evasion and antigenic variation, as well as cytoadhesion (105,378), underscoring the complexity of *P. vivax* interactions within the BM. The presence of these *vir* genes, particularly those predicted to have membrane localization, highlights their potential role in host-parasite interactions and suggests that the BM environment may uniquely influence their expression. Additionally, several genes identified in our study, such as the cysteine repeat modular protein 2 (PVX_096410) and PHIST (PVX_121865) superfamily proteins, were previously reported, in the first paper of this thesis (378) and in Sà and colleagues work (378,391), reinforcing their importance in the life cycle and pathogenicity of *P. vivax*.

Considering both cryptic niches, the bone marrow and the spleen, *P. vivax* life cycle as well as their pathways for physiopathology must be revisited. It is now evident that *P. vivax* has developed a cryptic erythrocytic infections within the BM and the spleen, with splenic infection gathering nearly 90% of the total parasite biomass during natural chronic infections, mainly harbouring asexual blood stages (184), and the bone marrow serving primarily as a niche for gametocytogenesis (10)(unpublished data, article 4).

Furthermore, and thanks to the transcriptomics analysis from both the spleen and the BM we have performed in this thesis, the *vir* multigenic family stands out as a key player for this interaction. This multigenic family, found in the sub telomeric region of the parasite chromosomes (5,103), have been demonstrated to play a crucial role in cytoadhesion and immune evasion (105). Of interest, and in contrast to *P. falciparum var* genes, more than one *vir* gene is expressed at any time (6,107), increasing the capability of the parasite to evade immune response, maintaining parasitaemia.

However, and knowing that *vir* genes might have other subcellular localizations other than in the membrane of the iRBCs (100,105), its crucial in the near future to investigate *in depth* the *vir* genes detected in both transcriptomics analysis performed in this thesis (378,387), as other functions rather than cytoadhesion and immune evasion might be done by proteins of the VIR family. To do so, CRISPR/Cas9 genome editing turns into a key tool for investigating this. It has been demonstrated the usefulness of this molecular technique to generate transgenic lines of *Plasmodium* parasites expressing *P. vivax* genes (225,226), but unfortunately, it is not trivial.

Lacking a robust *in vitro* continuous culture for *P. vivax* parasite, transfection of culturable *P. falciparum* parasites emerged as the way to proceed. In this thesis we faced the struggle to generate efficient transgenic parasite, as we have not been able to create *P. falciparum* expressing BM-dependent genes from vivax malaria parasite, something that have been also reported in the literature (203). Some questions arose from this failure, like up to what extent *P. falciparum* is able to recognize *P. vivax* genes, transcribe them and efficiently

translate the mRNAs. Not only that proteins might not be properly exported, trafficked and displayed at the correct subcellular localization, but also the fact that the generated protein might be toxic or harmful for the parasite due to unknown reasons, possibly explaining the constant failure to produce stable transgenic lines expressing *P. vivax* genes we have faced with the BM-dependent genes (unpublished data, article 4).

In the near future, alternative approaches are going to be explored, basically using a recipient specie of parasite more phylogenetically close to *P. vivax*, *P. knowlesi*. The use of the recently culture-adapted simian parasite (392) to generate parasites expressing *P. vivax* genes using CRISPR/Cas9 have been achieved already (222,393), opening new perspectives and tools for the functional characterization of the BM-dependent genes.

The role of EVs for *P. vivax* infection

Prokaryotes and eukaryotes have several strategies for cell-to-cell communication. Bacteria are in coordination among them by quorum sensing through the measurement of the environment and adapting their behaviour to their population density, as well as to others species growth (394,395). Eukaryotic cells can communicate among them using soluble factors like cytokines or hormones, and, of our particular interest, extracellular vesicles. All these messengers can have an effect over the producer cell itself (autocrine), surrounding cells (paracrine) or reach distant cells through circulation (endocrine).

EVs have been shown to be excellent intercellular communicators in physiological condition as in disease pathogenesis, susceptibility, intercellular signalling and immune responses (228,319,320). For example, in the context of cancer, it has been shown that EVs are involved in the metastatic niche organization and promotion (263,396). When looking into parasitic diseases, EVs have been described to be produced by either parasite cells itself or parasitized cells in many infections from protozoa parasites (*Plasmodium* spp., *Toxoplasma gondii*), kinetoplastids (*Trypanosoma* spp. and *Leishmania* spp.,

etc.) and helminths (*Fasciola* spp., flatworms and roundworms) (319). Malaria EVs derived from these infections have been proved to be excellent intercellular communicators, not just among parasites (14,329), but also with the human host (323,357), always being an excellent source for potential biomarker discovery source (292,336,397). In this thesis we also investigated the role of EVs in the formation of this cryptic niches, through analysing its role for facilitating parasite cytoadhesion to splenic cells (226).

Using single-cell RNA sequencing analysis we were able to characterize the response of hSFs to PvEVs. The increase of expression levels of adhesins like *cd36*, *icam1*, *thbs1*, *cd44* or genes like *fgf8* revealed that EVs from natural infection not just interact with hSFs, but facilitates the binding of *P. vivax*-infected reticulocytes to these cells, favouring the formation of intrasplenic niches, avoiding splenic clearance of parasitized reticulocytes.

This observation was made previously in our group (15), but here we were able to have the complete picture of this phenomenon (226). The over-expression of important molecules (188,398–403) in the context of malaria produced by the stimulation caused by PvEVs highlights the crucial role that those particles might be having in the organ to produce and, in some ways, prepare the cryptic splenic niche. Here we only assessed the effect of these cells over a specific type of splenic cells, but in the near future will be crucial to further investigate of those EVs in other cell type from the organ, from endothelial and vascular cells to immune cells homed in the white pulp of the spleen. So far, we have been able to test the effect of PvEVs over an immortalized hematopoietic cell line (Bel-A). Preliminary results shown downregulation of genes involved in erythropoiesis and haemoglobin synthesis, however further validations need to be performed (data not shown, unpublished).

Then, considering the importance of EVs during malaria infection, the effect in gametocytogenesis that has been reported before (14,329) and the over representation of gametocytes we found and described in this thesis, is easy to hypothesise that this phenomenon might be regulated and promoted via EVs. Future studies characterising EVs from the BM will help the scientific

community to clarify the mechanisms underlying the complex and regulated process of gametocytogenesis.

In the field of EV research there is a continuous discussion about the different existing subsets or subpopulation of EVs, mainly caused by the heterogeneity in both cells producing the vesicle as well as cargo, size and composition. By using direct immunocapture of specific subpopulation of reticulocyte-derived EVs we were able to increase the binding of our transgenic line to hSFs (226). This technique has enabled in the past our group to increase parasite protein detection in EVs (292), and considering the increasement on the effect we observed here, it is easy to think that previous mechanistic studies might be limited due to the above commented heterogeneity of EVs, especially those derived from plasma of infected individuals, where virtually all cells from the host might be shedding EVs into the fluid, thus, masking the effect of a specific subpopulation of EVs.

Improvement and implementation of new isolation techniques for specific subpopulation of EVs interesting for a particular reason is a must, and this thesis we have used this rationale to enrich in reticulocyte-derived EVs. Besides isolation methods, a universal marker for EVs characterization is yet to arrive, and at the same time, tremendously challenging to achieve, since each vesicle reflect the content and diversity of the producer cell. Synthenin-1 have been reported to possibly be a universal marker for EVs despite its origin (404), yet, in our group, we have experienced troubles to identify this protein in western blot analysis.

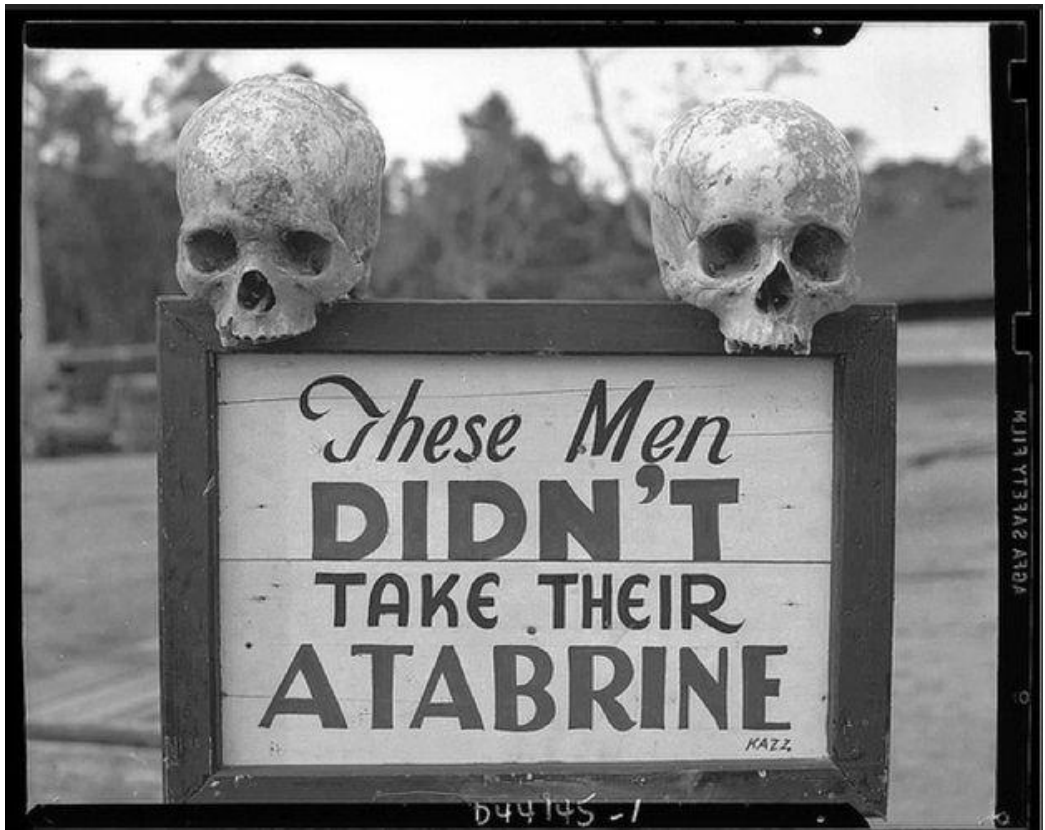
Limitations & Summary

During this thesis, some limitations have been noticed, and some of them have been commented so far. First, not being able to generate stable transgenic line expressing BM-dependent genes have been compromising the characterization of more *P. vivax* genes, thus, slowing the advance in gaining better understanding about the function of those genes in the BM. Also, the comparison we have performed in the transcriptome of the parasites from the

BM has to be carefully considered, as unfortunately we were not able to compare peripheral blood parasites with bone marrow parasites from the same patient, as blood samples from the same patients was impossible to be collected, which forced us to compare our results with previously available PB parasites transcriptome. Finally, and considering the limitation of the lack of an *in vitro* culture for *P. vivax*, always forces us to work with transgenic parasites, which might be affecting the observed function of the characterized genes.

Altogether, in this thesis we explored the complex relationship between *P. vivax* and its host, elucidating some mechanisms underlying the infection process. The importance of *vir* multigenic families have been widely commented in this thesis, in both hematopoietic organs, the spleen and the BM. The expression of this multigenic family, being affected by the parasite organ of origin highlights its role in the formation of the cryptic niches. PVX_108770 VIR14 and PVX_114580 PvSDP1 proteins have been shown to mediate the cytoadherence to hSFs, contributing to the formation of the splenic cryptic niche. Then, it is clear now that EVs are facilitating the formation of the splenic niche via stimulating the expression of adhesins by the splenic fibroblasts. The great overrepresentation of *vir* genes in the BM insinuates the function of those genes for the BM cryptic niche, however we have not been able to achieve functional characterization of any BM-dependent gene. To finish, both organs, the spleen and the BM needs to be further investigated, but for sure, taken into consideration when deploying future control and elimination strategies to face *Plasmodium vivax* malaria.

5. CONCLUSIONS



Malaria drug warning. Skulls on a warning sign at a US Army hospital during World War II (1939-1945). Photographed at the 363rd Station Hospital, Port Moresby, Papua New Guinea.

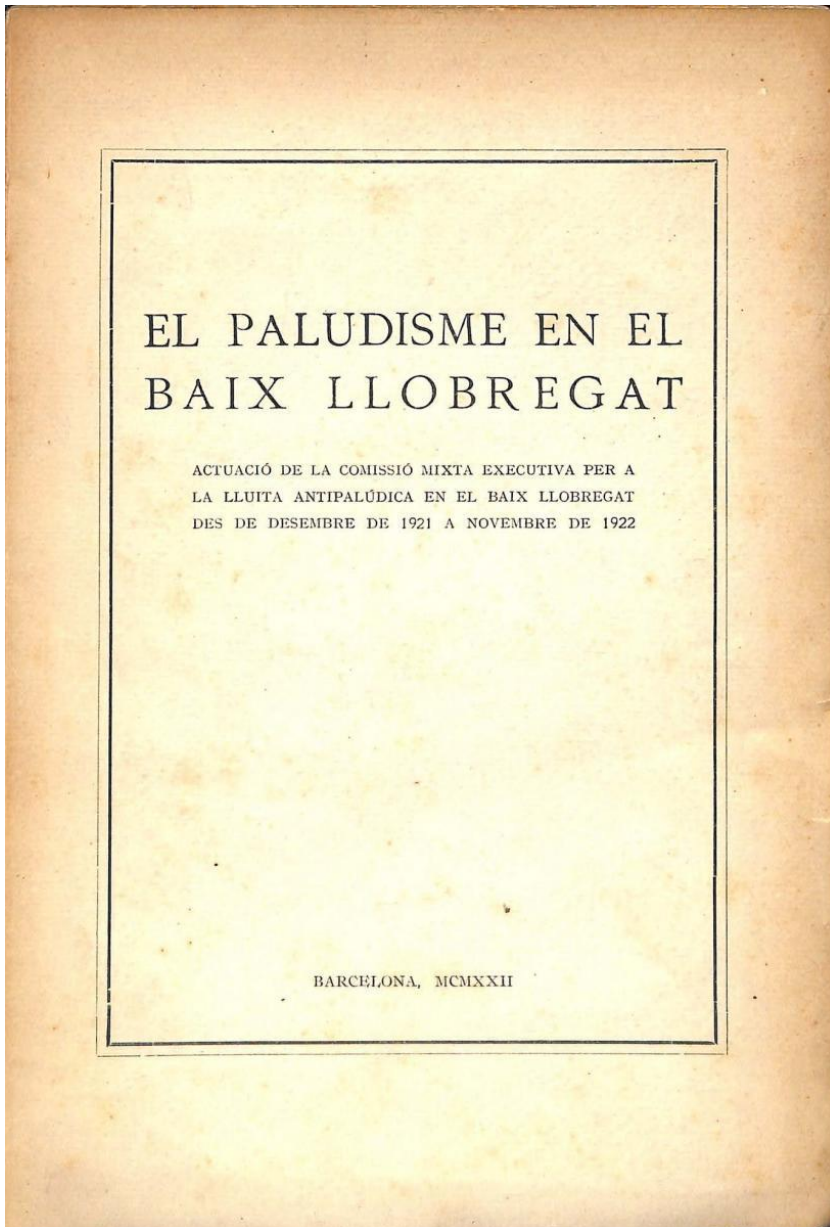
The main conclusions deduced from this thesis are as follows:

1. The spleen plays a major role in modulating the expression of certain parasite genes, controlling its transcription. In total, 67 coding genes, largely located at subtelomeric regions, are dependent on the spleen for expression and such antigens are targets of naturally acquired immune responses.
2. PVX_108770 (VIR14), presented the highest positivity of all antigens tested against sera from children from Papua New Guinea. Furthermore, this protein mediate adhesion to spleen fibroblasts.
3. When adjusting for difference in exposure, children with antibodies against the PVX_114580 (PvSDP1) showed significant association with protection against clinical *P. vivax* episodes during follow-up. Furthermore, this protein is highly conserved among *P. vivax* strains and other *Plasmodium* species.
4. Using CRISPR/Cas9 to edit *P. falciparum* to express vivax malaria gene PVX_114580 allowed us to functional characterise the protein, showing its membrane localization, both in the transgenic line as well as in *P. vivax* field isolates.
5. PvSDP1 protein is a ligand in interactions with human spleen fibroblasts. Moreover, such interactions are increased after human spleen fibroblasts stimulation with circulating extracellular vesicles from *P. vivax* infected patients.
6. Extracellular vesicles from *P. vivax* natural infections interact with human spleen fibroblasts, increasing the expression of cell adhesins, thus facilitating binding of *Plasmodium vivax*-infected reticulocytes and formation of intrasplenic niches.
7. *P. vivax* parasites are found in the bone marrow and induce dyserythropoiesis and ineffective erythropoiesis, independently of patients' anemic status. Such defects are related to transcriptional

changes affecting immune-related as well as erythropoietic-related genes like *gata1*, *nfe*, *tal1*, or *arid3a*, down-regulating its expression.

8. Transcriptomic analysis of bone marrow parasites revealed expression of gametocyte specific markers among top 50 expressed genes in the tissue, indicating residence and active transcriptional status of *Plasmodium vivax* gametocytes.
9. A total of 116 parasite genes were preferentially expressed in the bone marrow compared to previously available transcriptome from peripheral blood parasites, with a substantial portion belonging to the *vir* superfamily.

6. BIBLIOGRAPHY



Cover of the book *El Paludisme en el Baix Llobregat: actuació de la Comissió Mixta Executiva per a la lluita antipalúdica en el Baix Llobregat des de desembre de 1921 a novembre de 1922*. Barcelona. Imp.de la casa de la caritat, 1922.

6.1 References

1. World Health Organization. World malaria report 2022. 2023. Available from: <https://www.who.int/teams/global-malaria-programme/reports/world-malaria-report-2022>
2. Anstey NM, Russell B, Yeo TW, Price RN. The pathophysiology of vivax malaria. *Trends Parasitol.* 2009;25(5):220-227. doi:10.1016/j.pt.2009.02.003
3. Fernandez-Becerra C, Aparici-Herraiz I, del Portillo HA. Cryptic erythrocytic infections in *Plasmodium vivax*, another challenge to its elimination. *Parasitol Int.* 2022;87:102527. doi:10.1016/j.parint.2021.102527
4. Mueller I, Galinski MR, Baird JK, Carlton JM, Kochar DK, Alonso PL, et al. Key gaps in the knowledge of *Plasmodium vivax*, a neglected human malaria parasite. *Lancet Infect Dis.* 2009;9(9):555-566. doi:10.1016/S1473-3099(09)70177-X
5. Del Portillo HA, Fernandez-Becerra C, Bowman S, Oliver K, Preuss M, Sanchez CP, et al. A superfamily of variant genes encoded in the subtelomeric region of *Plasmodium vivax*. *Nature.* 2001;410(6830):839-842. doi:10.1038/35071118
6. Fernandez-Becerra C, Pein O, De Oliveira TR, Yamamoto MM, Cassola AC, Rocha C, et al. Variant proteins of *Plasmodium vivax* are not clonally expressed in natural infections. *Mol Microbiol.* 2005;58(3):648-658. doi:10.1111/j.1365-2958.2005.04850.x
7. Son UH, Dinzouna-Boutamba SD, Lee S, Yun HS, Kim JY, Joo SY, et al. Diversity of vir genes in *Plasmodium vivax* from endemic regions in the Republic of Korea: an initial evaluation. *Korean J Parasitol.* 2017;55(2):149-158. doi:10.3347/kjp.2017.55.2.149
8. Kho S, Qotrunnada L, Leonardo L, Andries B, Wardani PAI, Fricot A, et al. Hidden biomass of intact malaria parasites in the human spleen. *N Engl J Med.* 2021;384(21):2067-2069. doi:10.1056/NEJMc2023884
9. Siqueira M, Maria B, Magalha L, Melo GC, Ferrer M, Castillo P, et al. Spleen rupture in a case of untreated *Plasmodium vivax* infection. *PLoS Negl Trop Dis.* 2012;6(12):e1934. doi:10.1371/journal.pntd.0001934.
10. Baro B, Deroost K, Raiol T, Brito M, Almeida ACG, de Menezes-Neto A, et al. *Plasmodium vivax* gametocytes in the bone marrow of an acute malaria patient and changes in the erythroid miRNA profile. *PLoS Negl Trop Dis.* 2017;11(4):e0005365. doi:10.1371/journal.pntd.0005365.
11. Joice R, Nilsson SK, Montgomery J, Dankwa S, Egan E, Morahan B, et al. *Plasmodium falciparum* transmission stages accumulate in the human bone marrow. *Sci Transl Med.* 2014;6(244):244re5. doi:10.1126/scitranslmed.3008882
12. Obaldia N, Meibalan E, Sa JM, Ma S, Clark MA, Mejia P, et al. Bone marrow is a major parasite reservoir in *Plasmodium vivax* infection. *mBio.* 2018;9(3):e00625-18. doi:10.1128/mBio.00625-18
13. Kho S, Siregar NC, Qotrunnada L, Fricot A, Sissoko A, Shanti PAI, et al. Retention of uninfected red blood cells causing congestive splenomegaly is the major mechanism of anemia in malaria. *Am J Hematol.* 2024;99(2):223-235. doi:10.1002/ajh.27152

14. Regev-Rudzki N, Wilson DW, Carvalho TG, Sisquella X, Coleman BM, Rug M, et al. Cell-cell communication between malaria-infected red blood cells via exosome-like vesicles. *Cell*. 2013;153(5):1120-1133. doi:10.1016/j.cell.2013.04.029.
15. Toda H, Diaz-Varela M, Segui-Barber J, Roobsoong W, Baro B, Garcia-Silva S, et al. Plasma-derived extracellular vesicles from Plasmodium vivax patients signal spleen fibroblasts via NF-κB facilitating parasite cytoadherence. *Nat Commun*. 2020;11(1):2761. doi:10.1038/s41467-020-16337-y.
16. Zhu L, Mok S, Imwong M, Jaidee A, Russell B, Nosten F, et al. New insights into the Plasmodium vivax transcriptome using RNA-Seq. *Sci Rep*. 2016;6:20498. doi:10.1038/srep20498.
17. Garnham PCC. Malaria parasites and other haemosporidia. Science. Oxford: Blackwell Science Ltd; 1966. Available from: <https://api.semanticscholar.org/CorpusID:162385487>
18. Arrow KJ, Panosian CB, Gellband H. Saving lives, buying time. Institute of Medicine. 2004 Sep 9. Available from: <https://nap.nationalacademies.org/catalog/11017/saving-lives-buying-time-economics-of-malaria-drugs-in-an>
19. Cox FE. History of the discovery of the malaria parasites and their vectors. *Parasit Vectors*. 2010;3. Available from: <http://www.parasitesandvectors.com/content/3/1/5>
20. Hawass Z, Gad YZ, Ismail S, Khairat R, Fathalla D, Hasan N, et al. Ancestry and pathology in king Tutankhamun's family. *JAMA*. 2010;303(7):638-647. doi:10.1001/jama.2010.121
21. Sherman I. A brief history of malaria and discovery of the parasite's life cycle. Malaria: Parasite Biology. Washington, DC: ASM; 1998.
22. Communicable Disease Center. CDC. 2019. Our History - Our Story | CDC. Available from: <https://www.cdc.gov/museum/history/our-story.html>
23. Laveran A. Nature parasitaire des accidents de l'impaludisme: description d'un nouveau parasite trouvé dans le sang des malades atteints de fièvre palustre. J.-B. Baillière et fils, editor. Paris. 1881. Available from: <https://gallica.bnf.fr/ark:/12148/bpt6k9761344p>
24. Golgi C. Sul ciclo evolutivo dei parassiti malarici nella febbre terzana: diagnosi differenziale tra i parassiti endoglobulari malarici della terzana e quelli della quartana. Torino: Archivio per le scienze mediche. 1889. Available from: <https://wellcomecollection.org/works/rtfmcbsa>
25. Marchiafava E, Bignami A. Sulle febbri malariche estivo-autunnali. Artero I, editor. Roma: Reale Accademia Medica di Roma; 1892. Available from: <https://wellcomecollection.org/works/zn2r62kh>
26. Ross R. The rôle of the mosquito in the evolution of the malarial parasite. *The Lancet*. 1898 Aug 20;152(3912):488-90. doi.org/10.1016/S0140-6736(01)81400-8
27. Datawrapper. 2024. Available from: <https://app.datawrapper.de/>
28. WHO. Global Malaria Programme. 2024. Available from: <https://www.who.int/teams/global-malaria-programme>
29. World Health Organization. A framework for malaria elimination Global Malaria Programme. Geneva; 2017. Available from: <https://www.who.int/publications/i/item/9789241511988>

30. Price RN, Commons RJ, Battle KE, Thriemer K, Mendis K. Plasmodium vivax in the era of the shrinking P. falciparum map. *Trends Parasitol.* 2020;36(6):560-570. doi:10.1016/j.pt.2020.03.009.
31. Twohig KA, Pfeffer DA, Baird JK, Price RN, Zimmerman PA, Hay SI, et al. Growing evidence of Plasmodium vivax across malaria-endemic Africa. *PLoS Negl Trop Dis.* 2019 Jan 31;13(1):e0007140. doi: 10.1371/journal.pntd.0007140. Erratum in: *PLoS Negl Trop Dis.* 2019;13(6):e0007525. doi: 10.1371/journal.pntd.0007525.
32. Quaye IK, Aleksenko L, Ouevray C, Yewhalaw D, Duah N, Gyan B, et al. The Pan African Vivax and Ovale Network (PAVON): Refocusing on Plasmodium vivax, ovale and asymptomatic malaria in sub-Saharan Africa. *Parasitol Int.* 2021;84:102415. doi:10.1016/j.parint.2021.102415.
33. Cheng Q, Cunningham J, Gatton ML. Systematic review of sub-microscopic P. vivax infections: prevalence and determining factors. *PLoS Negl Trop Dis.* 2015;9(1):e3413. doi: 10.1371/journal.pntd.0003413.
34. Howes RE, Battle KE, Mendis KN, Smith DL, Cibulskis RE, Baird JK, et al. Global epidemiology of Plasmodium vivax. *Am J Trop Med Hyg.* 2016;95(6 Suppl):15-34. doi:10.4269/ajtmh.16-0141
35. Wampfler R, Mwingira F, Javati S, Robinson L, Betuela I, Siba P, et al. Strategies for detection of Plasmodium species gametocytes. *PLoS One.* 2013;8(9):e76316. doi:10.1371/journal.pone.0076316
36. Alves FP, Gil LHS, Marrelli MT, Ribolla PEM, Camargo EP, Da Silva LHP. Asymptomatic carriers of Plasmodium spp. as infection source for malaria vector mosquitoes in the Brazilian Amazon. *J Med Entomol.* 2005;42(5):777-779. doi:10.1093/jmedent/42.5.777
37. Barbosa S, Gozze AB, Lima NF, Batista CL, Bastos M da S, Nicolete VC, et al. Epidemiology of disappearing Plasmodium vivax malaria: a case study in rural Amazonia. *PLoS Negl Trop Dis.* 2014;8(8):e3109. doi:10.1371/journal.pntd.0003109.
38. Leander BS, Keeling PJ. Morphostasis in alveolate evolution. *Trends Ecol Evol.* 2003;18(8):395-402. doi:10.1016/S0169-5347(03)00152-6
39. Fikadu M, Ashenafi E. Malaria: An overview. *Infect Drug Resist.* 2023;16:3339-3347. doi:10.2147/IDR.S405668
40. Nureye D, Assefa S. Old and recent advances in life cycle, pathogenesis, diagnosis, prevention, and treatment of malaria including perspectives in Ethiopia. *The Scientific World Journal.* 2020;2020(1):1295381. doi:10.1155/2020/1295381
41. Phillips MA, Burrows JN, Manyando C, Van Huijsduijnen RH, Van Voorhis WC, Wells TNC. Malaria. *Nat Rev Dis Primers.* 2017;3:17050. doi:10.1038/nrdp.2017.50.
42. Baron S. Medical Microbiology. 4th ed. Galveston (TX): University of Texas Medical Branch at Galveston; 1996. Available from: <https://www.ncbi.nlm.nih.gov/books/NBK7627/>.
43. Sato S. Plasmodium—a brief introduction to the parasites causing human malaria and their basic biology. *J Physiol Anthropol.* 2021;40(1):1. doi:10.1186/s40101-020-00251-9.

44. Shute PG, Maryon M. A study of gametocytes in a West African strain of *Plasmodium falciparum*. *Trans R Soc Trop Med Hyg*. 1951;44(4):421-438. doi:10.1016/s0035-9203(51)80020-8.
45. Hang JW, Tukijan F, Lee EQH, Abdeen SR, Aniwah Y, Malleret B. Zoonotic malaria: Non-laverania plasmodium biology and invasion mechanisms. *Pathogens*. 2021;10(7):889. doi:10.3390/pathogens10070889.
46. Poostchi M, Silamut K, Maude RJ, Jaeger S, Thoma G. Image analysis and machine learning for detecting malaria. *Transl Res*. 2018;194:36-55. doi:10.1016/j.trsl.2017.12.004.
47. Collins WE, Jeffery GM. *Plasmodium malariae*: parasite and disease. *Clin Microbiol Rev*. 2007;20(4):579-592. doi:10.1128/CMR.00027-07
48. Lee KS, Cox-Singh J, Singh B. Morphological features and differential counts of *Plasmodium knowlesi* parasites in naturally acquired human infections. *Malar J*. 2009;8:73. doi:10.1186/1475-2875-8-73.
49. White MT, Shirreff G, Karl S, Ghani AC, Mueller I. Variation in relapse frequency and the transmission potential of *Plasmodium vivax* malaria. *Proc Biol Sci*. 2016;283(1827):20160048. doi:10.1098/rspb.2016.0048.
50. Krotoski WA, Collins WE, Bray RS, Garnham PC, Cogswell FB, Gwadz RW, et al. Demonstration of hypnozoites in sporozoite-transmitted *Plasmodium vivax* infection. *Am J Trop Med Hyg*. 1982;31(6):1291-1293. doi:10.4269/ajtmh.1982.31.1291.
51. Commons RJ, Simpson JA, Watson J, White NJ, Price RN. Estimating the proportion of *Plasmodium vivax* recurrences caused by relapse: a systematic review and meta-analysis. *Am J Trop Med Hyg*. 2020;103(3):1094-1099. doi:10.4269/ajtmh.20-0186.
52. Veletzky L, Groger M, Lagler H, Walochnik J, Auer H, Fuehrer HP, et al. Molecular evidence for relapse of an imported *Plasmodium ovale wallikeri* infection. *Malar J*. 2018;17(1):78. doi:10.1186/s12936-018-2226-4
53. Groger M, Fischer HS, Veletzky L, Lalremruata A, Ramharther M. A systematic review of the clinical presentation, treatment and relapse characteristics of human *Plasmodium ovale* malaria. *Malar J*. 2017;16(1):112. doi:10.1186/s12936-017-1759-2
54. Richter J, Franken G, Mehlhorn H, Labisch A, Häussinger D. What is the evidence for the existence of *Plasmodium ovale* hypnozoites?. *Parasitol Res*. 2010;107(6):1285-1290. doi:10.1007/s00436-010-2071-z
55. Vinetz JM, Li J, McCutchan TF, Kaslow DC. *Plasmodium malariae* infection in an asymptomatic 74-year-old Greek woman with splenomegaly. *N Engl J Med*. 1998;338(6):367-371. doi:10.1056/NEJM199802053380605
56. Newbold C, Craig A, Kyes S, Rowe A, Fernandez-Reyes D, Fagan T. Cytoadherence, pathogenesis and the infected red cell surface in *Plasmodium falciparum*. *Int J Parasitol*. 1999;29(6):927-937. doi:10.1016/s0020-7519(99)00049-1.
57. Udomsangpetch R, Wahlin B, Carlson J, Berzins K, Torii M, Aikawa M, et al. *Plasmodium falciparum*-infected erythrocytes form spontaneous erythrocyte rosettes. *J Exp Med*. 1989;169(5):1835-1840. doi:10.1084/jem.169.5.1835
58. Pain A, Ferguson DJP, Kai O, Urban BC, Lowe B, Marsh K, et al. Platelet-mediated clumping of *Plasmodium falciparum*-infected erythrocytes is a

- common adhesive phenotype and is associated with severe malaria. *Proc Natl Acad Sci U S A*. 2001;98(4):1805-1810. doi:10.1073/pnas.98.4.1805
59. Rowe JA, Claessens A, Corrigan RA, Arman M. Adhesion of Plasmodium falciparum-infected erythrocytes to human cells: molecular mechanisms and therapeutic implications. *Expert Rev Mol Med*. 2009;11:e16. doi:10.1017/S1462399409001082
60. Nunes MC, Scherf A. Plasmodium falciparum during pregnancy: a puzzling parasite tissue adhesion tropism. *Parasitology*. 2007;134(Pt 13):1863-1869. doi:10.1017/S0031182007000133
61. Hartman TK, Rogerson SJ, Fischer PR. The impact of maternal malaria on newborns. *Ann Trop Paediatr*. 2010;30(4):271-282. doi:10.1179/146532810X12858955921032
62. Miller LH, Baruch DI, Marsh K, Doumbo OK. The pathogenic basis of malaria. *Nature*. 2002;415(6872):673-679. doi:10.1038/415673a
63. Lee WC, Russell B, Rénia L. Sticking for a cause: The Falciparum malaria parasites cytoadherence paradigm. *Front Immunol*. 2019;10:1444. doi:10.3389/fimmu.2019.01444
64. Smith JD, Rowe JA, Higgins MK, Lavstsen T. Malaria's deadly grip: cytoadhesion of Plasmodium falciparum-infected erythrocytes. *Cell Microbiol*. 2013;15(12):1976-1983. doi:10.1111/cmi.12183
65. Wassmer SC, Cianciolo GJ, Combes V, Grau GE. Inhibition of endothelial activation: a new way to treat cerebral malaria? *PLoS Med*. 2005;2(9):e245. doi:10.1371/journal.pmed.0020245
66. Jensen AR, Adams Y, Hviid L. Cerebral Plasmodium falciparum malaria: The role of PfEMP1 in its pathogenesis and immunity, and PfEMP1-based vaccines to prevent it. *Immunol Rev*. 2020;293(1):230-252. doi:10.1111/imr.12807
67. Jakobsen PH, Bate CAW, Taverne J, Playfair JHL. Malaria: toxins, cytokines and disease. *Parasite Immunol*. 1995;17(5):223-231. doi:10.1111/j.1365-3024.1995.tb01019.x
68. Schofield L, Hackett F. Signal transduction in host cells by a glycosylphosphatidylinositol toxin of malaria parasites. *J Exp Med*. 1993;177(1):145-153. doi:10.1084/jem.177.1.145
69. Dunst J, Kamena F, Matuschewski K. Cytokines and chemokines in cerebral malaria pathogenesis. *Front Cell Infect Microbiol*. 2017;7:324. Published 2017 Jul 20. doi:10.3389/fcimb.2017.00324
70. Chen Q, Schlichtherle M, Wahlgren M. Molecular aspects of severe malaria. *Clin Microbiol Rev*. 2000;13(3):439-450. doi:10.1128/CMR.13.3.439
71. Kochar DK, Saxena V, Singh N, Kochar SK, Kumar SV, Das A. Plasmodium vivax malaria. *Emerg Infect Dis*. 2005 Jan;11(1):132-4. doi: 10.3201/eid1101.040519.
72. Price RN, Tjitra E, Guerra CA, Yeung S, White NJ, Anstey NM. Vivax malaria: neglected and not benign. *Am J Trop Med Hyg*. 2007;77(6 Suppl):79-87. doi: 10.4269/ajtmh.2007.77.79
73. Baird JK. Evidence and implications of mortality associated with acute plasmodium vivax malaria. *Clin Microbiol Rev*. 2013;26(1):36-57. doi:10.1128/CMR.00074-12
74. Whorton CM, Yount E, Jones R, Craige B, Alving AS, Pullman TN, et al. The Chesson strain of Plasmodium vivax malaria; clinical aspects. *J Infect Dis*. 1947;80(3):237-249. doi:10.1093/infdis/80.3.237.

75. Anstey NM, Douglas NM, Poespoprodjo JR, Price RN. Plasmodium vivax: clinical spectrum, risk factors and pathogenesis. *Adv Parasitol.* 2012;80:151-201. doi:10.1016/B978-0-12-397900-1.00003-7
76. Covell G. Spontaneous rupture of the spleen. *Trop Dis Bull.* 1955;52(8):705-723.
77. Williams TN, Maitland K, Phelps L, Bennett S, Peto TEA, Viji J, et al. Plasmodium vivax: a cause of malnutrition in young children. *QJM.* 1997;90(12):751-757. doi:10.1093/qjmed/90.12.751
78. Genton B, D'Acremont V, Rare L, Baea K, Reeder JC, Alpers MP, et al. Plasmodium vivax and mixed infections are associated with severe malaria in children: a prospective cohort study from Papua New Guinea. *PLoS Med.* 2008;5(6):e127. doi:10.1371/journal.pmed.0050127
79. Beg MA, Khan R, Baig SM, Gulzar Z, Hussain R, Smego RA. Cerebral involvement in benign tertian malaria. *Am J Trop Med Hyg.* 2002;67(3):230-232. doi:10.4269/ajtmh.2002.67.230
80. McGready R, Davison BB, Stepniwska K, Cho T, Shee H, Brockman A, et al. The effects of Plasmodium falciparum and P. vivax infections on placental histopathology in an area of low malaria transmission. *Am J Trop Med Hyg.* 2004;70(4):398-407.
81. Bardají A, Martínez-Espinosa FE, Arévalo-Herrera M, Padilla N, Kochar S, Ome-Kaius M, et al. Burden and impact of Plasmodium vivax in pregnancy: A multi-centre prospective observational study. *PLoS Negl Trop Dis.* 2017;11(6):e0005606. doi:10.1371/journal.pntd.0005606
82. Brabin BJ, Romagosa C, Abdelgalil S, Menéndez C, Verhoeff FH, McGready R, et al. The sick placenta - The role of malaria. *Placenta.* 2004;25(5):359-378. doi:10.1016/j.placenta.2003.10.019
83. Nosten F, McGready R, Simpson JA, Thwai KL, Balkan S, Cho T, et al. Effects of Plasmodium vivax malaria in pregnancy. *Lancet.* 1999;354(9178):546-549. doi:10.1016/S0140-6736(98)09247-2
84. Duffy PE, Gorres JP, Healy SA, Fried M. Malaria vaccines: a new era of prevention and control. *Nat Rev Microbiol.* doi:10.1038/s41579-024-01065-7
85. Bachmann A, Metwally NG, Allweier J, Cronshagen J, del Pilar Martinez Tauler M, Murk A, et al. CD36-A host receptor necessary for malaria parasites to establish and maintain infection. *Microorganisms.* 2022;10(12):2356. doi:10.3390/microorganisms10122356
86. Cserti-Gazdewich CM, Dhabangi A, Musoke C, Ssewanyana I, Ddungu H, Nakiboneka-Ssenabulya D, et al. Cytoadherence in paediatric malaria: ABO blood group, CD36, and ICAM1 expression and severe Plasmodium falciparum infection. *Br J Haematol.* 2012;159(2):223-236. doi:10.1111/bjh.12014
87. Hermand P, Cicéron L, Pionneau C, Vaquero C, Combadière C, Deterre P. Plasmodium falciparum proteins involved in cytoadherence of infected erythrocytes to chemokine CX3CL1. *Sci Rep.* 2016;6:33786. doi:10.1038/srep33786
88. Nacer A, Claes A, Roberts A, Scheidig-Benatar C, Sakamoto H, Ghorbal M, et al. Discovery of a novel and conserved Plasmodium falciparum exported protein that is important for adhesion of PfEMP1 at the surface of infected erythrocytes. *Cell Microbiol.* 2015;17(8):1205-16. doi: 10.1111/cmi.12430
89. Su X zhuan, Heatwole VM, Wertheimer SP, Guinet F, Herrfeldt JA, Peterson DS, et al. The large diverse gene family var encodes proteins involved in

- cytoadherence and antigenic variation of *Plasmodium falciparum*-infected erythrocytes. *Cell*. 1995;82(1):89-100. doi:10.1016/0092-8674(95)90055-1
90. Smith JD, Chitnis CE, Craig AG, Roberts DJ, Hudson-Taylor DE, Peterson DS, et al. Switches in expression of *Plasmodium falciparum* var genes correlate with changes in antigenic and cytoadherent phenotypes of infected erythrocytes. *Cell*. 1995;82(1):101-110. doi:10.1016/0092-8674(95)90056-x
91. Baruch DI, Pasloske BL, Singh HB, Bi X, Ma XC, Feldman M, et al. Cloning the *P. falciparum* gene encoding PfEMP1, a malarial variant antigen and adherence receptor on the surface of parasitized human erythrocytes. *Cell*. 1995;82(1):77-87. doi:10.1016/0092-8674(95)90054-3
92. Gardner MJ, Hall N, Fung E, White O, Berriman M, Hyman RW, et al. Genome sequence of the human malaria parasite *Plasmodium falciparum*. *Nature*. 2002;419(6906):498-511. doi:10.1038/nature01097
93. Scherf A, Lopez-Rubio JJ, Riviere L. Antigenic variation in *Plasmodium falciparum*. *Annu Rev Microbiol*. 2008;62:445-470. doi:10.1146/annurev.micro.61.080706.093134
94. Scherf A, Hernandez-Rivas R, Buffet P, Bottius E, Benatar C, Pouvelle B, et al. Antigenic variation in malaria: in situ switching, relaxed and mutually exclusive transcription of var genes during intra-erythrocytic development in *Plasmodium falciparum*. *EMBO J*. 1998;17(18):5418-5426. doi:10.1093/emboj/17.18.5418
95. Wahlgren M, Goel S, Akhouri RR. Variant surface antigens of *Plasmodium falciparum* and their roles in severe malaria. *Nat Rev Microbiol*. 2017;15(8):479-491. doi:10.1038/nrmicro.2017.47
96. Niang M, Bei AK, Madnani KG, Pelly S, Dankwa S, Kanjee U, et al. STEVOR is a *Plasmodium falciparum* erythrocyte binding protein that mediates merozoite invasion and rosetting. *Cell Host Microbe*. 2014;16(1):81-93. doi:10.1016/j.chom.2014.06.004
97. Goel S, Palmkvist M, Moll K, Joannin N, Lara P, R Akhouri R, et al. RIFINs are adhesins implicated in severe *Plasmodium falciparum* malaria. *Nat Med*. 2015;21(4):314-317. doi:10.1038/nm.3812
98. Camargo AA, Fischer K, Lanzer M, Del Portillo HA. Construction and characterization of a *Plasmodium vivax* genomic library in yeast artificial chromosomes. *Genomics*. 1997;42(3):467-473. doi:10.1006/geno.1997.4758.
99. Oliveira TR, Fernandez-Becerra C, Jimenez MCS, Del Portillo HA, Soares IS. Evaluation of the acquired immune responses to *Plasmodium vivax* VIR variant antigens in individuals living in malaria-endemic areas of Brazil. *Malar J*. 2006;5:83. doi:10.1186/1475-2875-5-83
100. Lopez FJ, Bernabeu M, Fernandez-Becerra C, del Portillo HA. A new computational approach redefines the subtelomeric vir superfamily of *Plasmodium vivax*. *BMC Genomics*. 2013;14:8. doi:10.1186/1471-2164-14-8
101. Auburn S, Böhme U, Steinbiss S, Trimarsanto H, Hostetler J, Sanders M, et al. A new *Plasmodium vivax* reference sequence with improved assembly of the subtelomeres reveals an abundance of pir genes. *Wellcome Open Res*. 2016;1:4. doi:10.12688/wellcomeopenres.9876.1
102. Merino EF, Fernandez-Becerra C, Durham AM, Ferreira JE, Tumilasci VF, d'Arc-Neves J, et al. Multi-character population study of the vir subtelomeric multigene superfamily of *Plasmodium vivax*, a major human malaria parasite.

- Mol Biochem Parasitol.* 2006;149(1):10-16. doi:10.1016/j.molbiopara.2006.04.002
103. Carlton JM, Adams JH, Silva JC, Bidwell SL, Lorenzi H, Caler E, et al. Comparative genomics of the neglected human malaria parasite *Plasmodium vivax*. *Nature*. 2008;455(7214):757-763. doi:10.1038/nature07327
104. Jalah R, Sarin R, Sud N, Alam MT, Parikh N, Das TK, et al. Identification, expression, localization and serological characterization of a tryptophan-rich antigen from the human malaria parasite *Plasmodium vivax*. *Mol Biochem Parasitol.* 2005;142(2):158-169. doi:10.1016/j.molbiopara.2005.01.020
105. Bernabeu M, Lopez FJ, Ferrer M, Martin-Jaular L, Razaname A, Corradin G, et al. Functional analysis of *Plasmodium vivax* VIR proteins reveals different subcellular localizations and cytoadherence to the ICAM-1 endothelial receptor. *Cell Microbiol.* 2012;14(3):386-400. doi:10.1111/j.1462-5822.2011.01726.x
106. Schappo AP, Bittencourt NC, Bertolla LP, Forcellini S, da Silva ABIE, Dos Santos HG, et al. Antigenicity and adhesiveness of a *Plasmodium vivax* VIR-E protein from Brazilian isolates. *Mem Inst Oswaldo Cruz.* 2022;116:e210227. doi:10.1590/0074-02760210227
107. Fernandez-Becerra C, Yamamoto MM, Vêncio RZN, Lacerda M, Rosanas-Urgell A, del Portillo HA. *Plasmodium vivax* and the importance of the subtelomeric multigene *vir* superfamily. *Trends Parasitol.* 2009;25(1):44-51. doi:10.1016/j.pt.2008.09.012.
108. World Health Organization. Guidelines for the treatment of malaria. 2015. 313 p. Available from: <https://www.who.int/publications/i/item/guidelines-for-malaria>
109. Greenwood BM, Armstrong JRM. Comparison of two simple methods for determining malaria parasite density. *Trans R Soc Trop Med Hyg.* 1991;85(2):186-188. doi:10.1016/0035-9203(91)90015-q
110. Wilcox A. Manual for the microscopical diagnosis of malaria in man. *Bull Natl Inst Health.* 1951;180:1-49.
111. World Health Organization. Parasitological confirmation of malaria diagnosis. Geneva; 2009. Available from: <https://www.who.int/publications/i/item/789241599412>
112. World Health Organization. Malaria rapid diagnostic test performance results of WHO product testing of malaria RDTs: Round 4. 2012. Available from: https://iris.who.int/bitstream/handle/10665/77748/9789241504720_eng.pdf?sequence=1
113. Abba K, Kirkham AJ, Olliaro PL, Deeks JJ, Donegan S, Garner P, et al. Rapid diagnostic tests for diagnosing uncomplicated nonfalciparum or *Plasmodium vivax* malaria in endemic countries. *Cochrane Database Syst Rev.* 2014;2014(12):CD011431. doi:10.1002/14651858.CD011431
114. Kakkilaya BS. Rapid Diagnosis of Malaria. *Laboratory Medicine.* 2003;34(8):602-608, Pages 602-608. doi:10.1309/J4ANKCCJ147JB2FR
115. Snounou G, Viriyakosol S, Xin Ping Zhu, Jarra W, Pinheiro L, do Rosario VE, et al. High sensitivity of detection of human malaria parasites by the use of nested polymerase chain reaction. *Mol Biochem Parasitol.* 1993;61(2):315-320. doi:10.1016/0166-6851(93)90077-b
116. Hänscheid T, Grobusch MP. How useful is PCR in the diagnosis of malaria? *Trends Parasitol.* 2002;18(9):395-398. doi:10.1016/s1471-4922(02)02348-6

117. Visser MT, Zonneveld R, Peto TJ, van Vugt M, Dondorp AM, van der Pluijm RW. Are national treatment guidelines for falciparum malaria in line with WHO recommendations and is antimalarial resistance taken into consideration? – A review of guidelines in non-endemic countries. *Trop Med Int Health*. 2022;27(2):129-136. doi: 10.1111/tmi.13715
118. Cappellini M, Fiorelli G. Glucose-6-phosphate dehydrogenase deficiency. *Lancet*. 2008;371(9606):64-74. doi:10.1016/S0140-6736(08)60073-2
119. Baird JK, Valecha N, Duparc S, White NJ, Price RN. Diagnosis and treatment of plasmodium vivax malaria. *Am J Trop Med Hyg*. 2016;95(6 Suppl):35-51. doi:10.4269/ajtmh.16-0171
120. Lobo NF, Achee NL, Greico J, Collins FH. Modern vector control. *Cold Spring Harb Perspect Med*. 2018;8(1):a025643. doi:10.1101/cshperspect.a025643
121. Dato MS, Dicko A, Tinto H, Ouédraogo JB, Hamaluba M, Olotu A, et al. Safety and efficacy of malaria vaccine candidate R21/Matrix-M in African children: a multicentre, double-blind, randomised, phase 3 trial. *Lancet*. 2024;403(10426):533-544. doi:10.1016/S0140-6736(23)02511-4
122. Nnaji CA, Amaechi UA, Wiysonge CS. R21/Matrix-M vaccine: optimising supply, maximising impact. [published correction appears in *Lancet*. 2024;403(10441):2292. doi: 10.1016/S0140-6736(24)01042-0]. *Lancet*. 2024;403(10426):525. doi:10.1016/S0140-6736(23)02716-2
123. White M, Chitnis CE. Potential role of vaccines in elimination of Plasmodium vivax. *Parasitol Int*. 2022;90:102592. doi:10.1016/j.parint.2022.102592
124. Mueller I, Shakri AR, Chitnis CE. Development of vaccines for Plasmodium vivax malaria. *Vaccine*. 2015;33(52):7489-7495. doi:10.1016/j.vaccine.2015.09.060
125. Yadava A, Sattabongkot J, Washington MA, Ware LA, Majam V, Zheng H, et al. A novel chimeric Plasmodium vivax circumsporozoite protein induces biologically functional antibodies that recognize both VK210 and VK247 sporozoites. *Infect Immun*. 2007;75(3):1177-1185. doi:10.1128/IAI.01667-06
126. Bennett JW, Yadava A, Tosh D, Sattabongkot J, Komisar J, Ware LA, et al. Phase 1/2a trial of Plasmodium vivax malaria vaccine candidate VMPO01/ASO1B in malaria-naive adults: safety, immunogenicity, and efficacy. *PLoS Negl Trop Dis*. 2016;10(2):e0004423. doi:10.1371/journal.pntd.0004423
127. Vanloubbeeck Y, Pichyangkul S, Bayat B, Yongvanitchit K, Bennett JW, Sattabongkot J, et al. Comparison of the immune responses induced by soluble and particulate Plasmodium vivax circumsporozoite vaccine candidates formulated in ASO1 in rhesus macaques. *Vaccine*. 2013;31(52):6216-6224. doi:10.1016/j.vaccine.2013.10.041
128. Salman AM, Montoya-Díaz E, West H, Lall A, Atcheson E, Lopez-Camacho C, et al. Rational development of a protective P. vivax vaccine evaluated with transgenic rodent parasite challenge models. *Sci Rep*. 2017;7:46482. doi:10.1038/srep46482
129. Blagborough AM, Yoshida S, Sattabongkot J, Tsuboi T, Sinden RE. Intranasal and intramuscular immunization with baculovirus dual expression system-based Pvs25 vaccine substantially blocks Plasmodium vivax transmission. *Vaccine*. 2010;28(37):6014-6020. doi:10.1016/j.vaccine.2010.06.100
130. Miyata T, Harakuni T, Sugawa H, Sattabongkot J, Kato A, Tachibana M, et al. Adenovirus-vectored Plasmodium vivax ookinete surface protein, Pvs25, as a

- potential transmission-blocking vaccine. *Vaccine*. 2011;29(15):2720-2726. doi:10.1016/j.vaccine.2011.01.083
131. Blagborough AM, Musiyuchuk K, Bi H, Jones RM, Chichester JA, Streatfield S, et al. Transmission blocking potency and immunogenicity of a plant-produced Pvs25-based subunit vaccine against *Plasmodium vivax*. *Vaccine*. 2016;34(28):3252-3259. doi:10.1016/j.vaccine.2016.05.007
 132. Malkin EM, Durbin AP, Diemert DJ, Sattabongkot J, Wu Y, Miura K, et al. Phase 1 vaccine trial of Pvs25H: a transmission blocking vaccine for *Plasmodium vivax* malaria. *Vaccine*. 2005;23(24):3131-3138. doi:10.1016/j.vaccine.2004.12.019
 133. Wu Y, Ellis RD, Shaffer D, Fontes E, Malkin EM, Mahanty S, et al. Phase 1 trial of malaria transmission blocking vaccine candidates Pfs25 and Pvs25 formulated with montanide ISA 51. *PLoS One*. 2008;3(7):e2636. doi:10.1371/journal.pone.0002636
 134. Lopez-Perez M, Jain A, Davies DH, Vásquez-Jiménez JM, Herrera SM, Oñate J, et al. Profiling the antibody response of humans protected by immunization with *Plasmodium vivax* radiation-attenuated sporozoites. *Sci Rep*. 2024;14(1):2790. doi:10.1038/s41598-024-53175-0
 135. Arévalo-Herrera M, Vásquez-Jiménez JM, Lopez-Perez M, Vallejo AF, Amado-Garavito AB, Céspedes N, et al. Protective Efficacy of *Plasmodium vivax* Radiation-Attenuated Sporozoites in Colombian Volunteers: A Randomized Controlled Trial. *PLoS Negl Trop Dis*. 2016;10(10):e0005070. doi:10.1371/journal.pntd.0005070
 136. Michon P, Fraser T, Adams JH. Naturally acquired and vaccine-elicited antibodies block erythrocyte cytoadherence of the *Plasmodium vivax* Duffy binding protein. *Infect Immun*. 2000;68(6):3164-3171. doi:10.1128/IAI.68.6.3164-3171.2000
 137. Yazdani SS, Shakri AR, Mukherjee P, Baniwal SK, Chitnis CE. Evaluation of immune responses elicited in mice against a recombinant malaria vaccine based on *Plasmodium vivax* Duffy binding protein. *Vaccine*. 2004;22(27-28):3727-3737. doi:10.1016/j.vaccine.2004.03.030
 138. Rawlinson TA, Barber NM, Mohring F, Cho JS, Kosaisavee V, Gérard SF, et al. Structural basis for inhibition of *Plasmodium vivax* invasion by a broadly neutralizing vaccine-induced human antibody. *Nat Microbiol*. 2019;4(9):1497-1507. doi:10.1038/s41564-019-0462-1
 139. Moreno A, Caro-Aguilar I, Yazdani SS, Shakri AR, Lapp S, Strobert E, et al. Preclinical assessment of the receptor-binding domain of *Plasmodium vivax* Duffy-binding protein as a vaccine candidate in rhesus macaques. *Vaccine*. 2008;26(34):4338-4344. doi:10.1016/j.vaccine.2008.06.010
 140. de Cassan SC, Rushdi Shakri A, Llewellyn D, Elias SC, Cho JS, Goodman AL, et al. Preclinical Assessment of Viral Vected and Protein Vaccines Targeting the Duffy-Binding Protein Region II of *Plasmodium Vivax*. *Front Immunol*. 2015;6:348. doi:10.3389/fimmu.2015.00348
 141. Bhardwaj R, Shakri AR, Hans D, Gupta P, Fernandez-Becerra C, del Portillo HA, et al. Production of recombinant PvDBP-II, receptor binding domain of *Plasmodium vivax* Duffy binding protein, and evaluation of immunogenicity to identify an adjuvant formulation for vaccine development. *Protein Expr Purif*. 2017;136:52-57. doi:10.1016/j.pep.2015.06.011

142. Singh K, Mukherjee P, Shakri AR, Singh A, Pandey G, Bakshi M, et al. Malaria vaccine candidate based on Duffy-binding protein elicits strain transcending functional antibodies in a Phase I trial. *NPJ Vaccines*. 2018;3:48. doi:10.1038/s41541-018-0083-3
143. Payne RO, Silk SE, Elias SC, Milne KH, Rawlinson TA, Llewellyn D, et al. Human vaccination against Plasmodium vivax Duffy-binding protein induces strain-transcending antibodies. *JCI Insight*. 2017;2(12):e93683. doi:10.1172/jci.insight.93683
144. Martinez FJ, White M, Guillotte-Blisnick M, Huon C, Boucharlat A, Agou F, et al. PvDBPII elicits multiple antibody-mediated mechanisms that reduce growth in a Plasmodium vivax challenge trial. *NPJ Vaccines*. 2024;9(1):10. doi:10.1038/s41541-023-00796-7
145. Hou MM, Barrett JR, Themistocleous Y, Rawlinson TA, Diouf A, Martinez FJ, et al. Vaccination with Plasmodium vivax Duffy-binding protein inhibits parasite growth during controlled human malaria infection. *Sci Transl Med*. 2023;15(704):eadf1782. doi:10.1126/scitranslmed.adf1782
146. Martinez FJ, Guillotte-Blisnick M, Huon C, England P, Popovici J, Laude H, et al. Immunogenicity of a Plasmodium vivax vaccine based on the duffy binding protein formulated using adjuvants compatible for use in humans. *Sci Rep*. 2023;13(1):13904. doi:10.1038/s41598-023-40043-6
147. Bennett JW, Yadava A, Tosh D, Sattabongkot J, Komisar J, Ware LA, et al. Phase 1/2a trial of Plasmodium vivax malaria vaccine candidate vmp001/as01b in malaria-naive adults: safety, immunogenicity, and efficacy. *PLoS Negl Trop Dis*. 2016;10(2):e0004423. doi:10.1371/journal.pntd.0004423
148. Herrera S, Fernández OL, Vera O, Cárdenas W, Ramírez O, Palacios R, et al. Phase I Safety and Immunogenicity Trial of Plasmodium vivax CS Derived Long Synthetic Peptides Adjuvanted with Montanide ISA 720 or Montanide ISA 51. *Am J Trop Med Hyg*. 2011 Feb;84(2 Suppl):12-20. doi: 10.4269/ajtmh.2011.09-0516
149. Arévalo-Herrera M, Gaitán X, Larmat-Delgado M, Caicedo MA, Herrera SM, Henao-Giraldo J, et al. Randomized clinical trial to assess the protective efficacy of a Plasmodium vivax CS synthetic vaccine. *Nat Commun*. 2022;13(1):1603. doi:10.1038/s41467-022-29226-3
150. Arévalo-Herrera M, Vásquez-Jiménez JM, Lopez-Perez M, Vallejo AF, Amado-Garavito AB, Céspedes N, et al. Protective Efficacy of Plasmodium vivax Radiation-Attenuated Sporozoites in Colombian Volunteers: A Randomized Controlled Trial. *PLoS Negl Trop Dis*. 2016;10(10):e0005070. doi:10.1371/journal.pntd.0005070
151. Payne RO, Silk SE, Elias SC, Milne KH, Rawlinson TA, Llewellyn D, et al. Human vaccination against Plasmodium vivax Duffy-binding protein induces strain-transcending antibodies. *JCI Insight*. 2017;2(12):e93683. doi:10.1172/jci.insight.93683
152. Wu Y, Ellis RD, Shaffer D, Fontes E, Malkin EM, Mahanty S, et al. Phase 1 trial of malaria transmission blocking vaccine candidates Pfs25 and Pvs25 formulated with montanide ISA 51. *PLoS One*. 2008;3(7):e2636. doi:10.1371/journal.pone.0002636

153. Veiga GTS da, Moriggi MR, Vettorazzi JF, Müller-Santos M, Albrecht L. Plasmodium vivax vaccine: What is the best way to go? *Front Immunol.* 2023;13:910236. doi:10.3389/fimmu.2022.910236
154. Morrison DA. Evolution of the Apicomplexa: where are we now? *Trends Parasitol.* 2009;25(8):375-382. doi:10.1016/j.pt.2009.05.010
155. Singh B, Sung LK, Matusop A, Radhakrishnan A, Shamsul SSG, Cox-Singh J, et al. A large focus of naturally acquired Plasmodium knowlesi infections in human beings. *Lancet.* 2004;363(9414):1017-1024. doi:10.1016/S0140-6736(04)15836-4
156. Coppi A, Natarajan R, Pradel G, Bennett BL, James ER, Roggero MA, et al. The malaria circumsporozoite protein has two functional domains, each with distinct roles as sporozoites journey from mosquito to mammalian host. *J Exp Med.* 2011;208(2):341-356. doi:10.1084/jem.20101488
157. Sturm A, Amino R, Van De Sand C, Regen T, Retzlaff S, Rennenberg A, et al. Manipulation of host hepatocytes by the malaria parasite for delivery into liver sinusoids. *Science.* 2006;313(5791):1287-1290. doi:10.1126/science.1129720
158. Krotoski WA. Discovery of the hypnozoite and a new theory of malarial relapse. *Trans R Soc Trop Med Hyg.* 1985;79(1):1-11. doi: 10.1016/0035-9203(85)90221-4
159. Pigeault R, Ruiz De Paz A, Baur M, Isaia J, Glaizot O, Christe P. Impact of host stress on the replication rate of Plasmodium: take it easy to avoid malaria recurrences. *Front Ecol Evol.* 2023;11:1191664. doi: doi.org/10.3389/fevo.2023.1191664
160. Cornet S, Bichet C, Larcombe S, Faivre B, Sorci G. Impact of host nutritional status on infection dynamics and parasite virulence in a bird-malaria system. *J Anim Ecol.* 2014;83(1):256-265. doi:10.1111/1365-2656.12113
161. Kitchen SF. The infection of reticulocytes by Plasmodium Vivax. *Am J Trop Med Hyg.* 1938;1(4):347-59. doi: 10.4269/AJTMH.1938.S1-18.347
162. Cowman AF, Healer J, Marapana D, Marsh K. Malaria: biology and disease. *Cell.* 2016;167(3):610-624. doi:10.1016/j.cell.2016.07.055
163. Galinski MR, Medina CC, Ingravallo P, Barnwell JW. A reticulocyte-binding protein complex of plasmodium vivax merozoites. *Cell.* 1992;69(7):1213-1226. doi:10.1016/0092-8674(92)90642-p
164. Chitnis CE, Miller LH. Identification of the erythrocyte binding domains of Plasmodium vivax and Plasmodium knowlesi proteins involved in erythrocyte invasion. *J Exp Med.* 1994;180(2):497-506. doi:10.1084/jem.180.2.497
165. Gruszczyk J, Kanjee U, Chan LJ, Menant S, Malleret B, Lim NTY, et al. Transferrin receptor 1 is a reticulocyte-specific receptor for Plasmodium vivax. *Science.* 2018;359(6371):48-55. doi:10.1126/science.aan1078
166. Malleret B, Rénia L, Russell B. The unhealthy attraction of Plasmodium vivax to reticulocytes expressing transferrin receptor 1 (CD71). *Int J Parasitol.* 2017;47(7):379-383. doi:10.1016/j.ijpara.2017.03.001
167. Malleret B, El Sahili A, Tay MZ, Carissimo G, Ong ASM, Novera W, et al. Plasmodium vivax binds host CD98hc (SLC3A2) to enter immature red blood cells. *Nat Microbiol.* 2021;6(8):991-999. doi:10.1038/s41564-021-00939-3
168. Meibalan E, Marti M. Biology of malaria transmission. *Cold Spring Harb Perspect Med.* 2017;7(3):a025452. doi:10.1101/cshperspect.a025452

169. Boyd MF, Kitchen SF. On the infectiousness of patients infected with *Plasmodium Vivax* and *Plasmodium Falciparum*. *Am J Trop Med Hyg*. 1937;17(2):253–62. doi: 10.4269/ajtmh.1937.s1-17.253
170. Krotoski WA, Garnham PCC, Bray RS, Killick-Kendrick R, Draper CC, Targett GA, et al. Observations on early and late post-sporozoite tissue stages in primate malaria: Discovery of a new latent form of *Plasmodium cynomolgi* (the Hypnozoite), and failure to detect hepatic forms within the first 24 hours after infection. *Am J Trop Med Hyg*. 1982;31(1):24–35. doi: 10.4269/ajtmh.1982.31.24
171. Anwar MN, Smith L, Devine A, Mehra S, Walker CR, Ivory E, et al. Mathematical models of *Plasmodium vivax* transmission: A scoping review. *PLoS Comput Biol*. 2024;20(3):e1011931. doi:10.1371/journal.pcbi.1011931
172. Adekunle AI, Pinkevych M, McGready R, Luxemburger C, White LJ, Nosten F, et al. Modeling the dynamics of *Plasmodium vivax* infection and hypnozoite reactivation in vivo. *PLoS Negl Trop Dis*. 2015;9(3):e0003595. doi: 10.1371/journal.pntd.0003595
173. Lee RS, Waters AP, Brewer JM. A cryptic cycle in haematopoietic niches promotes initiation of malaria transmission and evasion of chemotherapy. *Nat Commun*. 2018;9(1):1689. doi:10.1038/s41467-018-04108-9
174. Cooper B. The origins of bone marrow as the seedbed of our blood: from antiquity to the time of Osler. *Proc (Bayl Univ Med Cent)*. 2011;24(2):115–118. doi:10.1080/08998280.2011.11928697
175. Yeo JH, Lam YW, Fraser ST. Cellular dynamics of mammalian red blood cell production in the erythroblastic island niche. *Biophys Rev*. 2019;11(6):873–894. doi:10.1007/s12551-019-00579-2
176. Kuttikrishnan S, Prabhu KS, Khan AQ, Uddin S. Signaling networks guiding erythropoiesis. *Curr Opin Hematol*. 2024;31(3):89–95. doi:10.1097/MOH.0000000000000808
177. Smalley ME, Abdalla S, Brown J. The distribution of *Plasmodium falciparum* in the peripheral blood and bone marrow of Gambian children. *Trans R Soc Trop Med Hyg*. 1981;75(1):103–105. doi:10.1016/0035-9203(81)90019-5
178. Thomson JG, Robertson A. The structure and development of plasmodium falciparum gametocytes in the internal organs and peripheral circulation. *Trans R Soc Trop Med Hyg*. 1935;29(1):31–40. doi: 10.1016/S0035-9203(35)90015-3
179. Aguilar R, Magallon-Tejada A, Achtman AH, Moraleda C, Joice R, Cisteró P, et al. Molecular evidence for the localization of *Plasmodium falciparum* immature gametocytes in bone marrow. *Blood*. 2014;123(7):959–966. doi:10.1182/blood-2013-08-520767
180. Neveu G, Richard C, Dupuy F, Behera P, Volpe F, Subramani PA, et al. Red Cells, iron, and erythropoiesis: *Plasmodium falciparum* sexual parasites develop in human erythroblasts and affect erythropoiesis. *Blood*. 2020;136(12):1381–1393. doi: 10.1182/blood.2019004746
181. Wickramasinghe SN, Looareesuwan S, Nagachinta B, White NJ. Dyserythropoiesis and ineffective erythropoiesis in *Plasmodium vivax* malaria. *Br J Haematol*. 1989;72(1):91–99. doi:10.1111/j.1365-2141.1989.tb07658.x
182. O'Donnell J, Goldman JM, Wagner K, Ehinger G, Martin N, Leahy M, et al. Donor-derived *Plasmodium vivax* infection following volunteer unrelated bone

- marrow transplantation. *Bone Marrow Transplant.* 1998;21(3):313-314. doi:10.1038/sj.bmt.1701073
183. Raina V, Sharma A, Gujral S, Kumar R. Plasmodium vivax causing pancytopenia after allogeneic blood stem cell transplantation in CML. *Bone Marrow Transplant.* 1998;22(2):205-206. doi:10.1038/sj.bmt.1701299
184. Kho S, Qotrunnada L, Leonardo L, Andries B, Wardani PAI, Fricot A, et al. Evaluation of splenic accumulation and colocalization of immature reticulocytes and Plasmodium vivax in asymptomatic malaria: A prospective human splenectomy study. *PLoS Med.* 2021;18(5):e1003632. doi:10.1371/journal.pmed.1003632
185. Wilkins BS. The spleen. *Br J Haematol.* 2002;117(2):265-274. doi:10.1046/j.1365-2141.2002.03425.x
186. Freedman MH, Saunders EF. Hematopoiesis in the human spleen. *Am J Hematol.* 1981;11(3):271-275. doi:10.1002/ajh.2830110307
187. Engwerda CR, Beattie L, Amante FH. The importance of the spleen in malaria. *Trends Parasitol.* 2005;21(2):75-80. doi:10.1016/j.pt.2004.11.008
188. Martin-Jaular L, Ferrer M, Calvo M, Rosanas-Urgell A, Kalko S, Graewe S, et al. Strain-specific spleen remodelling in Plasmodium yoelii infections in Balb/c mice facilitates adherence and spleen macrophage-clearance escape. *Cell Microbiol.* 2011 Jan;13(1):109-22. doi: 10.1111/j.1462-5822.2010.01523
189. Carvalho BO, Lopes SCP, Nogueira PA, Orlandi PP, Bargieri DY, Blanco YC, et al. On the cytoadhesion of Plasmodium vivax-infected erythrocytes. *J Infect Dis.* 2010;202(4):638-647. doi:10.1086/654815
190. Aparici Herraiz I, Caires HR, Castillo-Fernández Ó, Sima N, Méndez-Mora L, Risueño RM, et al. Advancing key gaps in the knowledge of Plasmodium vivax cryptic infections using humanized mouse models and organs-on-chips. *Front Cell Infect Microbiol.* 2022;12:920204. doi: 10.3389/fcimb.2022.920204
191. Oberstaller J, Otto TD, Rayner JC, Adams JH. Essential genes of the parasitic apicomplexa. *Trends Parasitol.* 2021;37(4):304-316. doi:10.1016/j.pt.2020.11.007
192. Goonewardene R, Daily J, Kaslow D, Sullivan TJ, Duffy P, Carter R, et al. Transfection of the malaria parasite and expression of firefly luciferase. *Proc Natl Acad Sci U S A.* 1993;90(11):5234-6. doi: 10.1073/pnas.90.11.5234
193. Crabb BS, Cooke BM, Reeder JC, Waller RF, Caruana SR, Davern KM, et al. Targeted gene disruption shows that knobs enable malaria-infected red cells to cytoadhere under physiological shear stress. *Cell.* 1997;89(2):287-296. doi:10.1016/s0092-8674(00)80207-x
194. Crabb BS, Cowman AF. Characterization of promoters and stable transfection by homologous and nonhomologous recombination in Plasmodium falciparum. *Proc Natl Acad Sci U S A.* 1996;93(14):7289-7294. doi:10.1073/pnas.93.14.7289
195. Wu Y, Kirkman LA, Wellems TE. Transformation of Plasmodium falciparum malaria parasites by homologous integration of plasmids that confer resistance to pyrimethamine. *Proc Natl Acad Sci U S A.* 1996;93(3):1130-1134. doi:10.1073/pnas.93.3.1130
196. Van Dijk MR, Waters AP, Janse CJ. Stable transfection of malaria parasite blood stages. *Science.* 1995;268(5215):1358-1362. doi:10.1126/science.7761856

197. Santos JM, Josling G, Ross P, Joshi P, Orchard L, Campbell T, et al. Red blood cell invasion by the malaria parasite is coordinated by the PfAP2-I Transcription Factor. *Cell Host Microbe*. 2017;21(6):731-741.e10. doi:10.1016/j.chom.2017.05.006
198. Wezena CA, Alisch R, Golzmann A, Liedgens L, Staudacher V, Pradel G, et al. The cytosolic glyoxalases of *Plasmodium falciparum* are dispensable during asexual blood-stage development. *Microb Cell*. 2017;5(1):32-41. doi:10.15698/mic2018.01.608
199. Chi J, Cova M, De Las Rivas M, Medina A, Junqueira Borges R, Leivar P, et al. *Plasmodium falciparum* apicomplexan-specific glucosamine-6-phosphate N-Acetyltransferase is key for amino sugar metabolism and asexual blood stage development. *mBio*. 2020;11(5):e02045-20. doi:10.1128/mBio.02045-20
200. Lamonte G, Lim MYX, Wree M, Reimer C, Nachon M, Corey V, et al. Mutations in the *Plasmodium falciparum* Cyclic Amine Resistance Locus (PfCARL) confer multidrug resistance. *mBio*. 2016;7(4):e00696-16. doi:10.1128/mBio.00696-16
201. Lim MYX, LaMonte G, Lee MCS, Reimer C, Tan BH, Corey V, et al. UDP-galactose and acetyl-CoA transporters as *Plasmodium* multidrug resistance genes. *Nat Microbiol*. 2016;1:16166. doi:10.1038/nmicrobiol.2016.166
202. Llorà-Batlle O, Michel-Todó L, Witmer K, Toda H, Fernández-Becerra C, Baum J, et al. Conditional expression of PfAP2-G for controlled massive sexual conversion in *Plasmodium falciparum*. *Sci Adv*. 2020;6(24):eaaz5057. doi:10.1126/sciadv.aaz5057
203. Marin-Mogollon C, Van Pul FJA, Miyazaki S, Imai T, Ramesar J, Salman AM, et al. Chimeric *Plasmodium falciparum* parasites expressing *Plasmodium vivax* circumsporozoite protein fail to produce salivary gland sporozoites. *Malar J*. 2018;17(1):288. doi:10.1186/s12936-018-2431-1
204. Lee MCS, Lindner SE, Lopez-Rubio JJ, Llinás M. Cutting back malaria: CRISPR/Cas9 genome editing of *Plasmodium*. *Brief Funct Genomics*. 2019;18(5):281-289. doi:10.1093/bfpg/elz012.
205. Berzsenyi I, Pantazi V, Borsos BN, Pankotai T. Systematic overview on the most widespread techniques for inducing and visualizing the DNA double-strand breaks. *Mutat Res Rev Mutat Res*. 2021;788:108397. doi:10.1016/j.mrrev.2021.108397
206. Kirkman LA, Lawrence EA, Deitsch KW. Malaria parasites utilize both homologous recombination and alternative end joining pathways to maintain genome integrity. *Nucleic Acids Res*. 2014;42(1):370-379. doi:10.1093/nar/gkt881
207. Singer M, Marshall J, Heiss K, Mair GR, Grimm D, Mueller AK, et al. Zinc finger nuclease-based double-strand breaks attenuate malaria parasites and reveal rare microhomology-mediated end joining. *Genome Biol*. 2015;16:249. doi:10.1186/s13059-015-0811-1
208. Ghorbal M, Gorman M, MacPherson CR, Martins RM, Scherf A, Lopez-Rubio JJ. Genome editing in the human malaria parasite *Plasmodium falciparum* using the CRISPR-Cas9 system. *Nat Biotechnol*. 2014;32(8):819-821. doi:10.1038/nbt.2925
209. Marin-Mogollon C, Salman AM, Koolen KMJ, Bolscher JM, Van Pul FJA, Miyazaki S, et al. A *P. falciparum* NF54 reporter line expressing mCherry-

- luciferase in gametocytes, sporozoites, and liver-stages. *Front Cell Infect Microbiol.* 2019;9:96. doi: 10.3389/fcimb.2019.00096
210. Knuepfer E, Napiorkowska M, Van Ooij C, Holder AA. Generating conditional gene knockouts in Plasmodium - A toolkit to produce stable DiCre recombinase-expressing parasite lines using CRISPR/Cas9. *Sci Rep.* 2017;7(1):3881. doi:10.1038/s41598-017-03984-3
 211. Pfahler JM, Galinski MR, Barnwell JW, Lanzer M. Transient transfection of Plasmodium vivax blood stage parasites. *Mol Biochem Parasitol.* 2006;149(1):99-101. doi:10.1016/j.molbiopara.2006.03.018
 212. Barros RRM, Straimer J, Sa JM, Salzman RE, Melendez-Muniz VA, Mu J, et al. Editing the Plasmodium vivax genome, using zinc-finger nucleases. *J Infect Dis.* 2015;211(1):125-129. doi:10.1093/infdis/jiu423
 213. Van Der Wel AM, Tomás AM, Kocken CHM, Malhotra P, Janse CJ, Waters AP, et al. Transfection of the primate malaria parasite Plasmodium knowlesi using entirely heterologous constructs. *J Exp Med.* 1997;185(8):1499-1503. doi:10.1084/jem.185.8.1499
 214. Kocken CHM, Van Der Wel A, Thomas AW. Plasmodium cynomolgi: transfection of blood-stage parasites using heterologous DNA constructs. *Exp Parasitol.* 1999;93(1):58-60. doi:10.1006/expr.1999.4430
 215. Voorberg-van der Wel A, Zeeman AM, van Amsterdam SM, van den Berg A, Klooster EJ, Iwanaga S, et al. Transgenic fluorescent Plasmodium cynomolgi liver stages enable live imaging and purification of Malaria hypnozoite-forms. *PLoS One.* 2013;8(1):e54888. doi:10.1371/journal.pone.0054888
 216. Voorberg-van der Wel AM, Zeeman AM, Nieuwenhuis IG, van der Werff NM, Klooster EJ, Klop O, et al. A dual fluorescent Plasmodium cynomolgi reporter line reveals in vitro malaria hypnozoite reactivation. *Commun Biol.* 2020;3:7. doi:10.1038/s42003-019-0737-3
 217. Sá JM, Yamamoto MM, Fernandez-Becerra C, de Azevedo MF, Papakrivos J, Naudé B, et al. Expression and function of pvcrt-o, a Plasmodium vivax ortholog of pfert, in Plasmodium falciparum and Dictyostelium discoideum. *Mol Biochem Parasitol.* 2006;150(2):219-228. doi:10.1016/j.molbiopara.2006.08.006
 218. Rehn T, Lubiana P, Nguyen THT, Pansegrau E, Schmitt M, Roth LK, et al. Ectopic expression of Plasmodium vivax vir genes in P. falciparum affects cytoadhesion via increased expression of specific var genes. *Microorganisms.* 2022;10(6):1183. doi:10.3390/microorganisms10061183
 219. Somsak V, Uthapibull C, Prommana P, Srichairatanakool S, Yuthavong Y, Kamchonwongpaisan S. Transgenic Plasmodium parasites stably expressing Plasmodium vivax dihydrofolate reductase-thymidylate synthase as in vitro and in vivo models for antifolate screening. *Malar J.* 2011;10:291. doi: 10.1186/1475-2875-10-291
 220. Mohring F, van Schalkwyk DA, Henrici RC, Blasco B, Leroy D, Sutherland CJ, et al. Cation atpase (ATP4) orthologue replacement in the malaria parasite Plasmodium knowlesi reveals species-specific responses to ATP4-targeting drugs. *mBio.* 2022;13(5):e0117822. doi:10.1128/mbio.01178-22
 221. Moraes Barros RR, Thawnashom K, Gibson TJ, Armistead JS, Caleon RL, Kaneko M, et al. Activity of Plasmodium vivax promoter elements in Plasmodium knowlesi, and a centromere-containing plasmid that expresses

- NanoLuc throughout the parasite life cycle. *Malar J.* 2021;20(1):247. doi:10.1186/s12936-021-03773-4
222. Mohring F, Hart MN, Rawlinson TA, Henrici R, Charleston JA, Diez Benavente E, et al. Rapid and iterative genome editing in the malaria parasite *Plasmodium knowlesi* provides new tools for *P. vivax* research. *Elife.* 2019;8:e45829. doi:10.7554/eLife.45829
223. Salman AM, Mogollon CM, Lin JW, Van Pul FJA, Janse CJ, Khan SM. Generation of transgenic rodent malaria parasites expressing human malaria parasite proteins. *Methods Mol Biol.* 2015;1325:257-286. doi:10.1007/978-1-4939-2815-6_21
224. Moita D, Maia TG, Duarte M, Andrade CM, Albuquerque IS, Dwivedi A, et al. A genetically modified *Plasmodium berghei* parasite as a surrogate for whole-sporozoite vaccination against *P. vivax* malaria. *NPJ Vaccines.* 2022;7(1):163. Published 2022 Dec 16. doi:10.1038/s41541-022-00585-8
225. Miyazaki Y, Marin-Mogollon C, Imai T, Mendes AM, van der Laak R, Sturm A, et al. Generation of a genetically modified chimeric *Plasmodium falciparum* parasite expressing *Plasmodium vivax* circumsporozoite protein for malaria vaccine development. *Front Cell Infect Microbiol.* 2020;10:591046. doi:10.3389/fcimb.2020.591046
226. Ayllon-Hermida A, Nicolau-Fernandez M, Larrinaga AM, Aparici-Herraiz I, Tintó-Font E, Llorà-Batlle O, et al. *Plasmodium vivax* spleen-dependent protein 1 and its role in extracellular vesicles-mediated intrasplenic infections. *Front Cell Infect Microbiol.* 2024;14:1408451. doi:10.3389/fcimb.2024.1408451
227. Yáñez-Mó M, Siljander PR. Editorial- Insights of extracellular vesicles in cell biology. *Eur J Cell Biol.* 2023;102(3):151327. doi:10.1016/j.ejcb.2023.151327
228. Yáñez-Mó M, Siljander PRM, Andreu Z, Zavec AB, Borràs FE, Buzas EI, et al. Biological properties of extracellular vesicles and their physiological functions. *J Extracell Vesicles.* 2015;4:27066. doi:10.3402/jev.v4.27066
229. Théry C, Zitvogel L, Amigorena S. Exosomes: composition, biogenesis and function. *Nat Rev Immunol.* 2002;2(8):569-579. doi:10.1038/nri855
230. Raposo G, Stoorvogel W. Extracellular vesicles: exosomes, microvesicles, and friends. *J Cell Biol.* 2013;200(4):373-383. doi:10.1083/jcb.201211138
231. Colombo M, Raposo G, Théry C. Biogenesis, secretion, and intercellular interactions of exosomes and other extracellular vesicles. *Annu Rev Cell Dev Biol.* 2014;30:255-289. doi:10.1146/annurev-cellbio-101512-122326
232. Johnstone RM, Adam M, Hammond JR, Orr L, Turbide C. Vesicle formation during reticulocyte maturation. Association of plasma membrane activities with released vesicles (exosomes). *J Biol Chem.* 1987;262(19):9412-9420.
233. Harding C, Heuser J, Stahl P. Receptor-mediated endocytosis of transferrin and recycling of the transferrin receptor in rat reticulocytes. *J Cell Biol.* 1983;97(2):329-339. doi:10.1083/jcb.97.2.329
234. Raposo G, Nijman HW, Stoorvogel W, Leijendekker R, Harding C V., Melief CJM, et al. B lymphocytes secrete antigen-presenting vesicles. *J Exp Med.* 1996;183(3):1161-1172. doi:10.1084/jem.183.3.1161
235. Kalluri R, LeBleu VS. The biology, function, and biomedical applications of exosomes. *Science.* 2020;367(6478):eaau6977. doi:10.1126/science.aau6977
236. Hessvik NP, Llorente A. Current knowledge on exosome biogenesis and release. *Cell Mol Life Sci.* 2018;75(2):193-208. doi:10.1007/s00018-017-2595-9

237. Van Niel G, D'Angelo G, Raposo G. Shedding light on the cell biology of extracellular vesicles. *Nat Rev Mol Cell Biol.* 2018;19(4):213-228. doi:10.1038/nrm.2017.125
238. Jeppesen DK, Zhang Q, Franklin JL, Coffey RJ. Extracellular vesicles and nanoparticles: emerging complexities. *Trends Cell Biol.* 2023;33(8):667-681. doi:10.1016/j.tcb.2023.01.002
239. Mathieu M, Martin-Jaular L, Lavieu G, Théry C. Specificities of secretion and uptake of exosomes and other extracellular vesicles for cell-to-cell communication. *Nat Cell Biol.* 2019;21(1):9-17. doi:10.1038/s41556-018-0250-9
240. Hurley JH. ESCRT complexes and the biogenesis of multivesicular bodies. *Curr Opin Cell Biol.* 2008;20(1):4-11. doi:10.1016/j.ceb.2007.12.002
241. Stuffers S, Sem Wegner C, Stenmark H, Brech A. Multivesicular endosome biogenesis in the absence of ESCRTs. *Traffic.* 2009;10(7):925-937. doi:10.1111/j.1600-0854.2009.00920.x
242. van Niel G, Charrin S, Simoes S, Romao M, Rochin L, Saftig P, et al. The tetraspanin CD63 regulates ESCRT-independent and -dependent endosomal sorting during melanogenesis. *Dev Cell.* 2011;21(4):708-721. doi:10.1016/j.devcel.2011.08.019
243. Theos AC, Truschel ST, Tenza D, Hurbain I, Harper DC, Berson JF, et al. A lumenal domain-dependent pathway for sorting to intraluminal vesicles of multivesicular endosomes involved in organelle morphogenesis. *Dev Cell.* 2006;10(3):343-354. doi:10.1016/j.devcel.2006.01.012
244. Trajkovic K, Hsu C, Chiantia S, Rajendran L, Wenzel D, Wieland F, et al. Ceramide triggers budding of exosome vesicles into multivesicular endosomes. *Science.* 2008;319(5867):1244-1247. doi:10.1126/science.1153124
245. Cocucci E, Meldolesi J. Ectosomes and exosomes: shedding the confusion between extracellular vesicles. *Trends Cell Biol.* 2015;25(6):364-372. doi:10.1016/j.tcb.2015.01.004.
246. de la Torre-Escudero E, Bennett APS, Clarke A, Brennan GP, Robinson MW. Extracellular vesicle biogenesis in helminths: more than one route to the surface? *Trends Parasitol.* 2016;32(12):921-929. doi:10.1016/j.pt.2016.09.001
247. Kowal J, Arras G, Colombo M, Jouve M, Morath JP, Primdal-Bengtson B, et al. Proteomic comparison defines novel markers to characterize heterogeneous populations of extracellular vesicle subtypes. *Proc Natl Acad Sci U S A.* 2016;113(8):E968-E977. doi:10.1073/pnas.1521230113
248. Zhang H, Freitas D, Kim HS, Fabijanic K, Li Z, Chen H, et al. Identification of distinct nanoparticles and subsets of extracellular vesicles by asymmetric flow field-flow fractionation. *Nat Cell Biol.* 2018;20(3):332-343. doi:10.1038/s41556-018-0040-4
249. White R, Sotillo J, Ancarola ME, Borup A, Boysen AT, Brindley PJ, et al. Special considerations for studies of extracellular vesicles from parasitic helminths: A community-led roadmap to increase rigour and reproducibility. *J Extracell Vesicles.* 2023;12(1):e12298. doi:10.1002/jev2.12298
250. Abou Karam P, Rosenhek-Goldian I, Ziv T, Ben Ami Pilo H, Azuri I, Rivkin A, et al. Malaria parasites release vesicle subpopulations with signatures of different destinations. *EMBO Rep.* 2022;23(7):e54755. doi:10.15252/embr.202254755

251. Leung KF, Dacks JB, Field MC. Evolution of the Multivesicular Body ESCRT Machinery; Retention Across the Eukaryotic Lineage. *Traffic*. 2008;9(10):1698-1716. doi:10.1111/j.1600-0854.2008.00797.x
252. Rojas A, Regev-Rudzki N. Biogenesis of extracellular vesicles from the pathogen perspective: Transkingdom strategies for delivering messages. *Curr Opin Cell Biol*. 2024;88:102366. doi:10.1016/j.ceb.2024.102366
253. Martin C, Ligat G, Malnou CE. The Yin and the Yang of extracellular vesicles during viral infections. *Biomed J*. doi:10.1016/j.bj.2023.100659.
254. Hoen EN, Cremer T, Gallo RC, Margolis LB. Extracellular vesicles and viruses: Are they close relatives? *Proc Natl Acad Sci U S A*. 2016;113(33):9155-61. doi:10.1073/pnas.1605146113
255. Théry C, Boussac M, Véron P, Ricciardi-Castagnoli P, Raposo G, Garin J, et al. Proteomic analysis of dendritic cell-derived exosomes: a secreted subcellular compartment distinct from apoptotic vesicles. *J Immunol*. 2001;166(12):7309-7318. doi:10.4049/jimmunol.166.12.7309
256. De Gassart A, Géminard C, Février B, Raposo G, Vidal M. Lipid raft-associated protein sorting in exosomes. *Blood*. 2003;102(13):4336-4344. doi:10.1182/blood-2003-03-0871
257. Thakur BK, Zhang H, Becker A, Matei I, Huang Y, Costa-Silva B, et al. Double-stranded DNA in exosomes: a novel biomarker in cancer detection. *Cell Res*. 2014;24(6):766-769. doi:10.1038/cr.2014.44
258. Valadi H, Ekström K, Bossios A, Sjöstrand M, Lee JJ, Lötvall JO. Exosome-mediated transfer of mRNAs and microRNAs is a novel mechanism of genetic exchange between cells. *Nat Cell Biol*. 2007;9(6):654-659. doi:10.1038/ncb1596
259. Jeppesen DK, Fenix AM, Franklin JL, Higginbotham JN, Zhang Q, Zimmerman LJ, et al. Reassessment of exosome composition. *Cell*. 2019;177(2):428-445.e18. doi:10.1016/j.cell.2019.02.029
260. Villarroya-Beltri C, Gutiérrez-Vázquez C, Sánchez-Cabo F, Pérez-Hernández D, Vázquez J, Martín-Cofreces N, et al. Sumoylated hnRNP A2B1 controls the sorting of miRNAs into exosomes through binding to specific motifs. *Nat Commun*. 2013;4:2980. doi:10.1038/ncomms3980
261. Munro TP, Magee RJ, Kidd GJ, Carson JH, Barbarese E, Smith LM, et al. Mutational analysis of a heterogeneous nuclear ribonucleoprotein A2 response element for RNA trafficking. *J Biol Chem*. 1999;274(48):34389-34395. doi:10.1074/jbc.274.48.34389
262. Villarroya-Beltri C, Baixauli F, Gutiérrez-Vázquez C, Sánchez-Madrid F, Mittelbrunn M. Sorting it out: regulation of exosome loading. *Semin Cancer Biol*. 2014;28:3-13. doi:10.1016/j.semcancer.2014.04.009
263. Minciacci VR, Freeman MR, Di Vizio D. Extracellular vesicles in cancer: exosomes, microvesicles and the emerging role of large oncosomes. *Semin Cell Dev Biol*. 2015;40:41-51. doi:10.1016/j.semcdb.2015.02.010
264. Clancy JW, Schmidtman M, D'Souza-Schorey C. The ins and outs of microvesicles. *FASEB Bioadv*. 2021;3(6):399-406. doi:10.1096/fba.2020-00127
265. Del Conde I, Shrimpton CN, Thiagarajan P, López JA. Tissue-factor-bearing microvesicles arise from lipid rafts and fuse with activated platelets to initiate coagulation. *Blood*. 2005;106(5):1604-1611. doi:10.1182/blood-2004-03-1095

266. Li B, Antonyak MA, Zhang J, Cerione RA. RhoA triggers a specific signaling pathway that generates transforming microvesicles in cancer cells. *Oncogene*. 2012;31(45):4740-4749. doi:10.1038/onc.2011.636
267. Shen B, Fang Y, Wu N, Gould SJ. Biogenesis of the posterior pole is mediated by the exosome/microvesicle protein-sorting pathway. *J Biol Chem*. 2011;286(51):44162-44176. doi:10.1074/jbc.M111.274803
268. Welsh JA, Goberdhan DCI, O'Driscoll L, Buzas EI, Blenkiron C, Bussolati B, et al. Minimal information for studies of extracellular vesicles (MISEV2023): From basic to advanced approaches. *J Extracell Vesicles*. 2024;13(2):e12404. doi:10.1002/jev2.12404
269. Théry C, Amigorena S, Raposo G, Clayton A. Isolation and Characterization of Exosomes from Cell Culture Supernatants and Biological Fluids. *Curr Protoc Cell Biol*. 2006;Chapter 3:. doi:10.1002/0471143030.cb0322s30
270. Momen-Heravi F, Balaj L, Alian S, Trachtenberg AJ, Hochberg FH, Skog J, et al. Impact of biofluid viscosity on size and sedimentation efficiency of the isolated microvesicles. *Front Physiol*. 2012;3:162. doi:10.3389/fphys.2012.00162
271. Cvjetkovic A, Lötval J, Lässer C. The influence of rotor type and centrifugation time on the yield and purity of extracellular vesicles. *J Extracell Vesicles*. 2014;3:10.3402/jev.v3.23111. doi:10.3402/jev.v3.23111
272. Baranyai T, Herczeg K, Onódi Z, Voszka I, Módos K, Marton N, et al. Isolation of exosomes from blood plasma: qualitative and quantitative comparison of ultracentrifugation and size exclusion chromatography methods. *PLoS One*. 2015;10(12):e0145686. doi:10.1371/journal.pone.0145686
273. Linares R, Tan S, Gounou C, Arraud N, Brisson AR. High-speed centrifugation induces aggregation of extracellular vesicles. *J Extracell Vesicles*. 2015;4:29509. Published 2015 Dec 23. doi:10.3402/jev.v4.29509
274. Fischer H, Polikarpov I, Craievich AF. Average protein density is a molecular-weight-dependent function. *Protein Sci*. 2004;13(10):2825-8. doi:10.1110/ps.04688204
275. Webber J, Clayton A. How pure are your vesicles? *J Extracell Vesicles*. 2013;2:10.3402/jev.v2i0.19861. doi:10.3402/jev.v2i0.19861
276. Monguió-Tortajada M, Gálvez-Montón C, Bayes-Genis A, Roura S, Borràs FE. Extracellular vesicle isolation methods: rising impact of size-exclusion chromatography. *Cell Mol Life Sci*. 2019;76(12):2369-2382. doi:10.1007/s00018-019-03071-y
277. Böing AN, van der Pol E, Grootemaat AE, Coumans FAW, Sturk A, Nieuwland R. Single-step isolation of extracellular vesicles by size-exclusion chromatography. *J Extracell Vesicles*. 2014;3:10.3402/jev.v3.23430. doi:10.3402/jev.v3.23430
278. Pan BT, Johnstone RM. Fate of the transferrin receptor during maturation of sheep reticulocytes in vitro: Selective externalization of the receptor. *Cell*. 1983;33(3):967-978. doi:10.1016/0092-8674(83)90040-5
279. Grubisic Z, Rempp P, Benoit H. A universal calibration for gel permeation chromatography. *J Polym Sci B*. 1967;5(9):753-9. doi:10.1002/pol.1967.110050903
280. Monguió-Tortajada M, Morón-Font M, Gámez-Valero A, Carreras-Planella L, Borràs FE, Franquesa M. Extracellular-vesicle isolation from different

- biological fluids by size-exclusion chromatography. *Curr Protoc Stem Cell Biol.* 2019;49(1):e82. doi:10.1002/cpsc.82
281. Gámez-Valero A, Monguió-Tortajada M, Carreras-Planella L, Franquesa M, Beyer K, Borràs FE. Size-Exclusion Chromatography-based isolation minimally alters Extracellular Vesicles' characteristics compared to precipitating agents. *Sci Rep.* 2016;6:33641. doi:10.1038/srep33641
282. Monguió-Tortajada M, Roura S, Gálvez-Montón C, Pujal JM, Aran G, Sanjurjo L, et al. Nanosized UCMSC-derived extracellular vesicles but not conditioned medium exclusively inhibit the inflammatory response of stimulated T cells: implications for nanomedicine. *Theranostics.* 2017;7(2):270-284. doi:10.7150/thno.16154
283. Gámez-Valero A, Lozano-Ramos SI, Bancu I, Lauzurica-Valdemoros R, Borràs FE. Urinary extracellular vesicles as source of biomarkers in kidney diseases. *Front Immunol.* 2015;6:6. doi:10.3389/fimmu.2015.00006
284. de Menezes-Neto A, Sáez MJ, Lozano-Ramos I, Seguí-Barber J, Martín-Jaular L, Ullate JME, et al. Size-exclusion chromatography as a stand-alone methodology identifies novel markers in mass spectrometry analyses of plasma-derived vesicles from healthy individuals. *J Extracell Vesicles.* 2015;4:27378. doi:10.3402/jev.v4.27378
285. Li P, Kaslan M, Lee SH, Yao J, Gao Z. Progress in Exosome Isolation Techniques. *Theranostics.* 2017;7(3):789-804. doi:10.7150/thno.18133
286. Koliha N, Wiencek Y, Heider U, Jüngst C, Kladt N, Krauthäuser S, et al. A novel multiplex bead-based platform highlights the diversity of extracellular vesicles. *J Extracell Vesicles.* 2016;5:29975. doi:10.3402/jev.v5.29975.
287. Fortunato D, Giannoukakos S, Giménez-Capitán A, Hackenberg M, Molina-Vila MA, Zarovni N. Selective isolation of extracellular vesicles from minimally processed human plasma as a translational strategy for liquid biopsies. *Biomark Res.* 2022;10(1):57. doi:10.1186/s40364-022-00404-1
288. Koksál AR, Thevenot P, Aydın Y, Nunez K, Sandow T, Widmer K, et al. Impaired autophagy response in hepatocellular carcinomas enriches glypican-3 in exosomes, not in the microvesicles. *J Hepatocell Carcinoma.* 2022;9:959-972. doi:10.2147/JHC.S376210
289. Wiklander OPB, Bostancioglu RB, Welsh JA, Zickler AM, Murke F, Corso G, et al. Systematic Methodological Evaluation of a Multiplex Bead-Based Flow Cytometry Assay for Detection of Extracellular Vesicle Surface Signatures. *Front Immunol.* 2018;9:1326. doi:10.3389/fimmu.2018.01326
290. Yoo CE, Kim G, Kim M, Park D, Kang HJ, Lee M, et al. A direct extraction method for microRNAs from exosomes captured by immunoaffinity beads. *Anal Biochem.* 2012;431(2):96-98. doi:10.1016/j.ab.2012.09.008
291. Yang F, Liao X, Tian Y, Li G. Exosome separation using microfluidic systems: size-based, immunoaffinity-based and dynamic methodologies. *Biotechnol J.* 2017;12(4):10.1002/biot.201600699. doi:10.1002/biot.201600699
292. Aparici-Herraiz I, Gualdrón-López M, Castro-Cavada CJ, Carmona-Fonseca J, Yasnot MF, Fernandez-Becerra C, et al. Antigen Discovery in Circulating Extracellular Vesicles From Plasmodium vivax Patients. *Front Cell Infect Microbiol.* 2022;11:811390. doi:10.3389/fcimb.2021.811390

293. Coccozza F, Grisard E, Martin-Jaular L, Mathieu M, Théry C. SnapShot: Extracellular Vesicles. *Cell*. 2020;182(1):262-262.e1. doi:10.1016/j.cell.2020.04.054
294. Brown R. A brief account of microscopical observations made in the months of June, July and August 1827, on the particles contained in the pollen of plants; and on the general existence of active molecules in organic and inorganic bodies. *The Philosophical Magazine* 1828;4(21):161-73. Available from: <https://www.tandfonline.com/doi/abs/10.1080/14786442808674769>
295. Einstein A. Zur Theorie der Brownschen Bewegung. *Ann Phys*. 1906;324(2):371-81. Available from: <https://onlinelibrary.wiley.com/doi/full/10.1002/andp.19063240208>
296. Dragovic RA, Gardiner C, Brooks AS, Tannetta DS, Ferguson DJP, Hole P, et al. Sizing and phenotyping of cellular vesicles using Nanoparticle Tracking Analysis. *Nanomedicine*. 2011;7(6):780-788. doi:10.1016/j.nano.2011.04.003
297. Szatanek R, Baj-Krzyworzeka M, Zimoch J, Lekka M, Siedlar M, Baran J. The methods of choice for extracellular vesicles (EVs) characterization. *Int J Mol Sci*. 2017;18(6):1153. doi:10.3390/ijms18061153
298. Ricklefs FL, Maire CL, Reimer R, Dührsen L, Kolbe K, Holz M, et al. Imaging flow cytometry facilitates multiparametric characterization of extracellular vesicles in malignant brain tumours. *J Extracell Vesicles*. 2019;8(1):1588555. doi:10.1080/20013078.2019.1588555
299. Midekessa G, Godakumara K, Dissanayake K, Hasan MM, Reshi QUA, Rinken T, et al. Characterization of extracellular vesicles labelled with a lipophilic dye using fluorescence nanoparticle tracking analysis. *Membranes (Basel)*. 2021;11(10):779. doi:10.3390/membranes11100779
300. Rupert DLM, Claudio V, Lässer C, Bally M. Methods for the physical characterization and quantification of extracellular vesicles in biological samples. *Biochim Biophys Acta Gen Subj*. 2017;1861(1 Pt A):3164-3179. doi:10.1016/j.bbagen.2016.07.028
301. Linares R, Tan S, Gounou C, Brisson AR. Imaging and quantification of extracellular vesicles by transmission electron microscopy. Methods in molecular biology. *Methods Mol Biol*. 2017;1545:43-54. doi:10.1007/978-1-4939-6728-5_4
302. Reimer L. Transmission Electron Microscopy. 1997;36. Available from: <https://link.springer.com/10.1007/978-3-662-14824-2>
303. Pisitkun T, Shen RF, Knepper MA. Identification and proteomic profiling of exosomes in human urine. *Proc Natl Acad Sci U S A*. 2004;101(36):13368-13373. doi:10.1073/pnas.0403453101
304. Peterson MF, Otoc N, Sethi JK, Gupta A, Antes TJ. Integrated systems for exosome investigation. *Methods*. 2015;87:31-45. doi:10.1016/j.ymeth.2015.04.015.
305. van der Vlist EJ, Nolte-'t Hoen ENM, Stoorvogel W, Arkesteijn GJA, Wauben MHM. Fluorescent labeling of nano-sized vesicles released by cells and subsequent quantitative and qualitative analysis by high-resolution flow cytometry. *Nat Protoc*. 2012;7(7):1311-1326. doi:10.1038/nprot.2012.065
306. Suárez H, Gámez-Valero A, Reyes R, López-Martín S, Rodríguez MJ, Carrascosa JL, et al. A bead-assisted flow cytometry method for the semi-quantitative

- analysis of Extracellular Vesicles. *Sci Rep.* 2017;7(1):11271. doi:10.1038/s41598-017-11249-2
307. Pocsfalvi G, Stanly C, Vilasi A, Fiume I, Capasso G, Turiák L, et al. Mass spectrometry of extracellular vesicles. *Mass Spectrom Rev.* 2016;35(1):3-21. doi:10.1002/mas.21457
308. Mayr M, Grainger D, Mayr U, Leroyer AS, Leseche G, Sidibe A, et al. Proteomics, metabolomics, and immunomics on microparticles derived from human atherosclerotic plaques. *Circ Cardiovasc Genet.* 2009;2(4):379-388. doi:10.1161/CIRCGENETICS.108.842849
309. Dean WL, Lee MJ, Cummins TD, Schultz DJ, Powell DW, Dean B. Proteomic and functional characterisation of platelet microparticle size classes. *Thromb Haemost.* 2009;102(4):711-718. doi:10.1160/TH09-04-243
310. Kreimer S, Belov AM, Ghiran I, Murthy SK, Frank DA, Ivanov AR. Mass-spectrometry-based molecular characterization of extracellular vesicles: lipidomics and proteomics. *J Proteome Res.* 2015;14(6):2367-2384. doi:10.1021/pr501279t
311. Shelke GV, Lässer C, Gho YS, Lötval J. Importance of exosome depletion protocols to eliminate functional and RNA-containing extracellular vesicles from fetal bovine serum. *J Extracell Vesicles.* 2014;3:10.3402/jev.v3.24783. doi:10.3402/jev.v3.24783
312. Pigati L, Yaddanapudi SCS, Iyengar R, Kim DJ, Hearn SA, Danforth D, et al. Selective Release of MicroRNA Species from Normal and Malignant Mammary Epithelial Cells. *PLoS One.* 2010;5(10):e13515. doi:10.1371/journal.pone.0013515
313. Valadi H, Ekström K, Bossios A, Sjöstrand M, Lee JJ, Lötval JO. Exosome-mediated transfer of mRNAs and microRNAs is a novel mechanism of genetic exchange between cells. *Nat Cell Biol.* 2007;9(6):654-659. doi:10.1038/ncb1596
314. Ahadi A, Brennan S, Kennedy PJ, Hutvagner G, Tran N. Long non-coding RNAs harboring miRNA seed regions are enriched in prostate cancer exosomes. *Sci Rep.* 2016;6:24922. doi:10.1038/srep24922
315. Van Balkom BWM, Eisele AS, Michiel Pegtel D, Bervoets S, Verhaar MC. Quantitative and qualitative analysis of small RNAs in human endothelial cells and exosomes provides insights into localized RNA processing, degradation and sorting. *J Extracell Vesicles.* 2015;4:26760. doi:10.3402/jev.v4.26760
316. Miranda KC, Bond DT, Levin JZ, Adiconis X, Sivachenko A, Russ C, et al. Massively parallel sequencing of human urinary exosome/microvesicle rna reveals a predominance of non-coding RNA. *PLoS One.* 2014;9(5):e96094. doi:10.1371/journal.pone.0096094
317. Guduric-Fuchs J, O'Connor A, Camp B, O'Neill CL, Medina RJ, Simpson DA. Selective extracellular vesicle-mediated export of an overlapping set of microRNAs from multiple cell types. *BMC Genomics.* 2012;13:357. doi:10.1186/1471-2164-13-357
318. Lässer C, Shelke GV, Yeri A, Kim DK, Crescitelli R, Raimondo S, et al. Two distinct extracellular RNA signatures released by a single cell type identified by microarray and next-generation sequencing. *RNA Biol.* 2017;14(1):58-72. doi:10.1080/15476286.2016.1249092

319. Marcilla A, Martin-Jaular L, Trelis M, de Menezes-Neto A, Osuna A, Bernal D, et al. Extracellular vesicles in parasitic diseases. *J Extracell Vesicles*. 2014;3:25040. doi:10.3402/jev.v3.25040
320. Buzas EI. The roles of extracellular vesicles in the immune system. *Nat Rev Immunol*. *Nat Rev Immunol*. 2023;23(4):236-250. doi:10.1038/s41577-022-00763-8
321. Combes V, Taylor TE, Juhan-Vague I, Mège JL, Mwenechanya J, Tembo M, et al. Circulating endothelial microparticles in Malawian children with severe falciparum malaria complicated with coma. *JAMA*. 2004;291(21):2542-2544. doi:10.1001/jama.291.21.2542-b
322. Sampaio NG, Emery SJ, Garnham AL, Tan QY, Sisquella X, Pimentel MA, et al. Extracellular vesicles from early stage Plasmodium falciparum-infected red blood cells contain PfEMP1 and induce transcriptional changes in human monocytes. *Cell Microbiol*. 2018;20(5):e12822. doi:10.1111/cmi.12822
323. Dey S, Mohapatra S, Khokhar M, Hassan S, Pandey RK. Extracellular Vesicles in Malaria: Shedding Light on Pathogenic Depths. *ACS Infect Dis*. 2024;10(3):827-844. doi: 10.1021/acscinfecdis.3c00649
324. Campos FM, Franklin BS, Teixeira-Carvalho A, Filho AL, De Paula SC, Fontes CJ, et al. Augmented plasma microparticles during acute Plasmodium vivax infection. *Malar J*. 2010;9:327. doi:10.1186/1475-2875-9-327
325. Nantakomol D, Dondorp AM, Krudsood S, Udomsangpetch R, Pattanapanyasat K, Combes V, et al. Circulating red cell-derived microparticles in human malaria. *J Infect Dis*. 2011;203(5):700-706. doi:10.1093/infdis/jiq104.
326. Juan T, Fürthauer M. Biogenesis and function of ESCRT-dependent extracellular vesicles. *Semin Cell Dev Biol*. 2018;74:66-77. doi:10.1016/j.semcdb.2017.08.022
327. Avalos-Padilla Y, Georgiev VN, Lantero E, Pujals S, Verhoef R, Borghetti-Cardoso LN, et al. The ESCRT-III machinery participates in the production of extracellular vesicles and protein export during Plasmodium falciparum infection. *PLoS Pathog*. 2021;17(4). doi: 10.1371/journal.ppat.1009455
328. Ofir-Birin Y, Abou karam P, Rudik A, Giladi T, Porat Z, Regev-Rudzki N. Monitoring extracellular vesicle cargo active uptake by imaging flow cytometry. *Front Immunol*. 2018;9:1011. doi:10.3389/fimmu.2018.01011
329. Mantel PY, Hoang AN, Goldowitz I, Potashnikova D, Hamza B, Vorobjev I, et al. Malaria-infected erythrocyte-derived microvesicles mediate cellular communication within the parasite population and with the host immune system. *Cell Host Microbe*. 2013;13(5):521-534. doi:10.1016/j.chom.2013.04.009
330. Dekel E, Yaffe D, Rosenhek-Goldian I, Ben-Nissan G, Ofir-Birin Y, Morandi MI, et al. 20S proteasomes secreted by the malaria parasite promote its growth. *Nat Commun*. 2021;12(1):1172. doi:10.1038/s41467-021-21344-8
331. Pilo HBA, Khilji SK, Lühle J, Biskup K, Gal BL, Goldian IR, et al. Sialylated N-glycans mediate monocyte uptake of extracellular vesicles secreted from Plasmodium falciparum-infected red blood cells. *J Extracell Biol*. 2022;1(2):e33. doi: 10.1002/jex2.33.
332. Opadokun T, Agyapong J, Rohrbach P. Protein Profiling of Malaria-Derived Extracellular Vesicles Reveals Distinct Subtypes. *Membranes (Basel)*. 2022;12(4):397. doi:10.3390/membranes12040397

333. Abdi A, Yu L, Goulding D, Rono MK, Bejon P, Choudhary J, et al. Proteomic analysis of extracellular vesicles from a *Plasmodium falciparum* Kenyan clinical isolate defines a core parasite secretome. *Wellcome Open Res.* 2017;2:50. doi:10.12688/wellcomeopenres.11910.2.
334. Vimontpatranon S, Roytrakul S, Phaonakrop N, Lekmanee K, Atipimonpat A, Srimark N, et al. Extracellular Vesicles Derived from Early and Late Stage *Plasmodium falciparum*-Infected Red Blood Cells Contain Invasion-Associated Proteins. *J Clin Med.* 2022;11(14):4250. doi:10.3390/jcm11144250
335. Sisquella X, Nebl T, Thompson JK, Whitehead L, Malpede BM, Salinas ND, et al. *Plasmodium falciparum* ligand binding to erythrocytes induce alterations in deformability essential for invasion. *Elife.* 2017;6:e21083. doi:10.7554/eLife.21083
336. Gualdrón-López M, Díaz-Varela M, Zanghi G, Aparici-Herraiz I, Steel RWJ, Schäfer C, et al. Mass spectrometry identification of biomarkers in extracellular vesicles from *Plasmodium vivax* liver hypnozoite infections. *Mol Cell Proteomics.* 2022;21(10):100406. doi:10.1016/j.mcpro.2022.100406
337. Gualdrón-López M, Flannery EL, Kangwanransan N, Chuenchob V, Fernandez-Orth D, Segui-Barber J, et al. Characterization of *Plasmodium vivax* Proteins in plasma-derived exosomes from Malaria-infected liver-chimeric humanized mice. *Front Microbiol.* 2018 Jun 25;9:1271. doi:10.3389/fmicb.2018.01271
338. Babatunde KA, Mbagwu S, Hernández-Castañeda MA, Adapa SR, Walch M, Filgueira L, et al. Malaria infected red blood cells release small regulatory RNAs through extracellular vesicles. *Sci Rep.* 2018;8(1):884. doi:10.1038/s41598-018-19149-9
339. Vetter L, Bajalan A, Ahamed MT, Scasso C, Shafeeq S, Andersson B, et al. Starvation induces changes in abundance and small RNA cargo of extracellular vesicles released from *Plasmodium falciparum* infected red blood cells. *Sci Rep.* 2023;13(1):18423. doi:10.1038/s41598-023-45590-6
340. Sisquella X, Ofir-Birin Y, Pimentel MA, Cheng L, Abou Karam P, Sampaio NG, et al. Malaria parasite DNA-harboring vesicles activate cytosolic immune sensors. *Nat Commun.* 2017;8(1):1985. doi:10.1038/s41467-017-02083-1
341. Rathjen T, Nicol C, McConkey G, Dalmay T. Analysis of short RNAs in the malaria parasite and its red blood cell host. *FEBS Lett.* 2006;580(22):5185-5188. doi:10.1016/j.febslet.2006.08.063
342. Xue X, Zhang Q, Huang Y, Feng L, Pan W. No miRNA were found in *Plasmodium* and the ones identified in erythrocytes could not be correlated with infection. *Malar J.* 2008;7:4. doi:10.1186/1475-2875-7-47
343. Rubio M, Bassat Q, Estivill X, Mayor A. Tying malaria and microRNAs: from the biology to future diagnostic perspectives. *Malar J.* 2016;15:167. doi:10.1186/s12936-016-1222-9
344. Li J jing, Huang M jun, Li Z, Li W, Wang F, Wang L, et al. Identification of potential whole blood MicroRNA biomarkers for the blood stage of adult imported falciparum malaria through integrated mRNA and miRNA expression profiling. *Biochem Biophys Res Commun.* 2018;506(3):471-477. doi:10.1016/j.bbrc.2018.10.072
345. Mantel PY, Hjelmqvist D, Walch M, Kharoubi-Hess S, Nilsson S, Ravel D, et al. Infected erythrocyte-derived extracellular vesicles alter vascular function via

- regulatory Ago2-miRNA complexes in malaria. *Nat Commun.* 2016;7:12727. doi: 10.1038/ncomms12727
346. Gurung S, Perocheau D, Touramanidou L, Baruteau J. The exosome journey: from biogenesis to uptake and intracellular signalling. *Cell Commun Signal.* 2021;19(1):47. doi: 10.1186/s12964-021-00730-1
347. Khowawisetsut L, Vimontpatranon S, Lekmanee K, Sawasdipokin H, Srimark N, Chotivanich K, et al. Differential effect of extracellular vesicles derived from Plasmodium falciparum-infected red blood cells on monocyte polarization. *Int J Mol Sci.* 2023;24(3):2631. doi: 10.3390/ijms24032631
348. Gualdrón-López M, Díaz-Varela M, Toda H, Aparici-Herraiz I, Pedró-Cos L, Lauzurica R, et al. Multiparameter flow cytometry analysis of the human spleen applied to studies of plasma-derived EVs from Plasmodium vivax patients. *Front Cell Infect Microbiol.* 2021;11:596104. doi: 10.3389/fcimb.2021.596104.
349. Yang Y, Liu Q, Lu J, Adah D, Yu S, Zhao S, et al. Exosomes from Plasmodium-infected hosts inhibit tumor angiogenesis in a murine Lewis lung cancer model. *Oncogenesis.* 2017;6(6):e351. doi:10.1038/oncsis.2017.52
350. Gilles HM, World Health Organization, World Health Organization. Global Malaria Programme. Management of severe malaria : a practical handbook. WHO. 2013;0–92.
351. Combes V, Coltel N, Alibert M, Van Eck M, Raymond C, Juhan-Vague I, et al. ABCA1 gene deletion protects against cerebral malaria: potential pathogenic role of microparticles in neuropathology. *Am J Pathol.* 2005;166(1):295-302. doi:10.1016/S0002-9440(10)62253-5
352. Sahu U, Mohapatra BN, Kar SK, Ranjit M. Promoter polymorphisms in the ATP binding cassette transporter gene influence production of cell-derived microparticles and are highly associated with susceptibility to severe malaria in humans. *Infect Immun.* 2013;81(4):1287-1294. doi:10.1128/IAI.01175-12
353. Thomas JJ, Harp KO, Bashi A, Hood JL, Botchway F, Wilson MD, et al. MiR-451a and let-7i-5p loaded extracellular vesicles attenuate heme-induced inflammation in hiPSC-derived endothelial cells. *Front Immunol.* 2022;13:1082414. doi:10.3389/fimmu.2022.1082414.
354. Coltel N, Combes V, Wassmer SC, Chimini G, Grau GE. Cell vesiculation and immunopathology: implications in cerebral malaria. *Microbes Infect.* 2006;8(8):2305-2316. doi:10.1016/j.micinf.2006.04.006
355. Kioko M, Mwangi S, Pance A, Ochola-Oyier LI, Kariuki S, Newton C, et al. The mRNA content of plasma extracellular vesicles provides a window into molecular processes in the brain during cerebral malaria. *Sci Adv.* 2024;10(33):eadl2256. doi:10.1126/sciadv.adl2256
356. Mfonkeu JB, Gouado I, Fotso Kuate H, Zambou O, Combes V, Raymond Grau GE, et al. Biochemical markers of nutritional status and childhood malaria severity in Cameroon. *Br J Nutr.* 2010;104(6):886-892. doi:10.1017/S0007114510001510
357. Mbagwu SI, Lannes N, Walch M, Filgueira L, Mantel PY. Human microglia respond to malaria-induced extracellular vesicles. *Pathogens.* 2019;9(1):21. doi:10.3390/pathogens9010021
358. Huang K, Huang L, Zhang X, Zhang M, Wang Q, Lin H, et al. Mast cells-derived exosomes worsen the development of experimental cerebral malaria. *Acta Trop.* 2021;224:106145. doi:10.1016/j.actatropica.2021.106145

359. Moro L, Bardají A, Macete E, Barrios D, Morales-Prieto DM, España C, et al. Placental microparticles and microRNAs in pregnant women with *Plasmodium falciparum* or HIV infection. *PLoS One*. 2016;11(1):e0146361. doi:10.1371/journal.pone.0146361
360. Baird JK. Basic research of *Plasmodium vivax* biology enabling its management as a clinical and public health problem. *Front Cell Infect Microbiol*. 2021;11:696598. doi:10.3389/fcimb.2021.696598
361. Silva-Filho JL, Lacerda MVG, Recker M, Wassmer SC, Marti M, Costa FTM. *Plasmodium vivax* in hematopoietic niches: hidden and dangerous. *Trends Parasitol*. 2020;36(5):447-458. doi:10.1016/j.pt.2020.03.002
362. Blackburn D, Drennon M, Broussard K, Morrison AM, Stanek D, Sarney E, et al. Outbreak of Locally Acquired Mosquito-Transmitted (Autochthonous) Malaria - Florida and Texas, May-July 2023. *MMWR Morb Mortal Wkly Rep*. 2023;72(36):973-978. doi:10.15585/mmwr.mm7236a1
363. Spanakos G, Snounou G, Pervanidou D, Alifrangis M, Rosanas-Urgell A, Baka A, et al. Genetic Spatiotemporal Anatomy of *Plasmodium vivax* Malaria Episodes in Greece, 2009-2013. *Emerg Infect Dis*. 2018;24(3):541-548. doi:10.3201/eid2403.170605
364. Bahk YY, Lee HW, Na BK, Kim J, Jin K, Hong YS, et al. Epidemiological Characteristics of Re-emerging *Vivax* Malaria in the Republic of Korea (1993-2017). *Korean J Parasitol*. 2018;56(6):531-543. doi:10.3347/kjp.2018.56.6.531
365. Muneer A, Adapa SR, Silbert S, Scanlan K, Vore H, Cannons A, et al. Autochthonous *Plasmodium vivax* Infections, Florida, USA, 2023. *Emerg Infect Dis*. 2024;30(6):1214-1217. doi:10.3201/eid3006.240336
366. Andriopoulos P, Economopoulou A, Spanakos G, Assimakopoulos G. A local outbreak of autochthonous *Plasmodium vivax* malaria in Laconia, Greece--a re-emerging infection in the southern borders of Europe? *Int J Infect Dis*. 2013;17(2):e125-e128. doi:10.1016/j.ijid.2012.09.009
367. Howes RE, Patil AP, Piel FB, Nyangiri OA, Kabaria CW, Gething PW, et al. The global distribution of the Duffy blood group. *Nat Commun*. 2011;2:266. doi:10.1038/ncomms1265
368. Miller LH, Mason SJ, Clyde DF, McGinniss MH. The resistance factor to *Plasmodium vivax* in blacks. The Duffy-blood-group genotype, FyFy. *N Engl J Med*. 1976;295(6):302-304. doi:10.1056/NEJM197608052950602
369. Twohig KA, Pfeffer DA, Baird JK, Price RN, Zimmerman PA, Hay SI, et al. Growing evidence of *Plasmodium vivax* across malaria-endemic Africa. *PLoS Negl Trop Dis*. 2019;13(1):e0007140. doi:10.1371/journal.pntd.0007140
370. Culleton R, Ndounga M, Zeyrek FY, Coban C, Casimiro PN, Takeo S, et al. Evidence for the transmission of *Plasmodium vivax* in the Republic of the Congo, West Central Africa. *J Infect Dis*. 2009;200(9):1465-1469. doi:10.1086/644510
371. Dhorda M, Nyehangane D, Rénia L, Piola P, Guerin PJ, Snounou G. Transmission of *Plasmodium vivax* in south-western Uganda: report of three cases in pregnant women. *PLoS One*. 2011;6(5):e19801. doi:10.1371/journal.pone.0019801
372. Bernabeu M, Gomez-Perez GP, Sissoko S, Niambélé MB, Haibala AA, Sanz A, et al. *Plasmodium vivax* malaria in Mali: a study from three different regions. *Malar J*. 2012;11:405. doi:10.1186/1475-2875-11-405

373. Dechavanne C, Dechavanne S, Bosch J, Metral S, Redinger KR, Watson QD, et al. Duffy antigen is expressed during erythropoiesis in Duffy-negative individuals. *Cell Host Microbe*. 2023;31(12):2093-2106.e7. doi:10.1016/j.chom.2023.10.019
374. Gething PW, Elyazar IRF, Moyes CL, Smith DL, Battle KE, Guerra CA, et al. A long neglected world malaria map: Plasmodium vivax endemicity in 2010. *PLoS Negl Trop Dis*. 2012;6(9):e1814. doi: 10.1371/journal.pntd.0001814
375. White NJ. Determinants of relapse periodicity in Plasmodium vivax malaria. *Malar J*. 2011;10:297. doi:10.1186/1475-2875-10-297
376. del Portillo HA, Ferrer M, Brugat T, Martin-Jaular L, Langhorne J, Lacerda MVG. The role of the spleen in malaria. *Cell Microbiol*. 2012;14(3):343-355. doi:10.1111/j.1462-5822.2011.01741.x
377. Del Portillo HA, Lanzer M, Rodriguez-Malaga S, Zavala F, Fernandez-Becerra C. Variant genes and the spleen in Plasmodium vivax malaria. *Int J Parasitol*. 2004;34(13-14):1547-1554. doi:10.1016/j.ijpara.2004.10.012
378. Fernandez-Becerra C, Bernabeu M, Castellanos A, Correa BR, Obadia T, Ramirez M, et al. *Proc Natl Acad Sci U S A*. 2020;117(23):13056-13065. doi:10.1073/pnas.1920596117
379. Barnwell JW, Howard RJ, Coon HG, Miller LH. Splenic requirement for antigenic variation and expression of the variant antigen on the erythrocyte membrane in cloned Plasmodium knowlesi malaria. *Infect Immun*. 1983;40(3):985-994. doi:10.1128/iai.40.3.985-994.1983
380. Adjalley S, Lee MCS. CRISPR/Cas9 editing of the Plasmodium falciparum genome. *Methods Mol Biol*. 2022;2470:221-239. doi:10.1007/978-1-0716-2189-9_17
381. Allred DR. Variable and variant protein multigene families in Babesia bovis persistence. *Pathogens*. 2019;8(2):76. doi:10.3390/pathogens8020076
382. Li J, Wang J, Shao J, Li Y, Yu Y, Shao G, et al. The variable lipoprotein family participates in the interaction of Mycoplasma hyorhinis with host extracellular matrix and plasminogen. *Vet Microbiol*. 2022;265:109310. doi:10.1016/j.vetmic.2021.109310
383. Merz AJ, So M. Interactions of pathogenic neisseriae with epithelial cell membranes. *Annu Rev Cell Dev Biol*. 2000;16:423-457. doi:10.1146/annurev.cellbio.16.1.423
384. Plant L, Jonsson AB. Contacting the host: insights and implications of pathogenic Neisseria cell interactions. *Scand J Infect Dis*. 2003;35(9):608-613. doi:10.1080/00365540310016349
385. Li B, Zhao Y. Regulation of antigenic variation by Trypanosoma brucei telomere proteins depends on their unique DNA binding activities. *Pathogens*. 2021;10(8):967. doi:10.3390/pathogens10080967
386. Aitken GJ. Sternal puncture in the diagnosis of malaria. *The Lancet*. 1943 Oct 16;242(6268):466-8.
387. Brito MAM, Baro B, Raiol TC, Ayllon-Hermida A, Safe IP, Deroost K, et al. Morphological and transcriptional changes in human bone marrow during natural Plasmodium vivax malaria infections. *J Infect Dis*. 2022;225(7):1274-1283. doi:10.1093/infdis/jiaa177
388. Ru YX, Mao BY, Zhang FK, Pang TX, Zhao SX, Liu JH, et al. Invasion of erythroblasts by Plasmodium vivax: a new mechanism contributing to malarial

- anemia. *Ultrastruct Pathol.* 2009;33(5):236-242. doi:10.3109/01913120903251643
389. De Niz M, Meibalan E, Mejia P, Ma S, Brancucci NMB, Agop-Nersesian C, et al. Plasmodium gametocytes display homing and vascular transmigration in the host bone marrow. *Sci Adv.* 2018;4(5):eaat3775. doi:10.1126/sciadv.aat3775
390. Mair GR, Braks JAM, Garver LS, Wiegant JCAG, Hall N, Dirks RW, et al. Regulation of sexual development of Plasmodium by translational repression. *Science.* 2006;313(5787):667-669. doi:10.1126/science.1125129
391. Sà JM, Cannon M V., Caleon RL, Wellems TE, Serre D. Single-cell transcription analysis of Plasmodium vivax blood-stage parasites identifies stage- and species-specific profiles of expression. *PLoS Biol.* 2020;18(5):e3000711. doi:10.1371/journal.pbio.3000711
392. Moon RW, Hall J, Rangkuti F, Ho YS, Almond N, Mitchell GH, et al. Adaptation of the genetically tractable malaria pathogen Plasmodium knowlesi to continuous culture in human erythrocytes. *Proc Natl Acad Sci U S A.* 2013;110(2):531-536. doi:10.1073/pnas.1216457110
393. Mohring F, Hart M, Patel A, Baker D, Moon R. CRISPR-Cas9 genome editing of Plasmodium knowlesi. *Bio Protoc.* 2020;10(4):e3522. doi:10.21769/BioProtoc.3522.
394. Waters CM, Bassler BL. Quorum sensing: Cell-to-cell communication in bacteria. *Annu Rev Cell Dev Biol.* 2005;21:319-346. doi:10.1146/annurev.cellbio.21.012704.131001
395. Jimenez JC, Federle MJ. Quorum sensing in group A Streptococcus. *Front Cell Infect Microbiol.* 2014 Sep 12;4:127. doi: 10.3389/fcimb.2014.00127
396. Tsering T, Laskaris A, Abdouh M, Bustamante P, Parent S, Jin E, et al. Uveal melanoma-derived extracellular vesicles display transforming potential and carry protein cargo involved in metastatic niche preparation. *Cancers (Basel).* 2020;12(10):2923. doi:10.3390/cancers12102923
397. Barnadas-Carceller B, del Portillo HA, Fernandez-Becerra C. Extracellular vesicles as biomarkers in parasitic disease diagnosis. *Curr Top Membr.* 2024;94:187-223. doi:10.1016/bs.ctm.2024.07.003.
398. Cabrera A, Neculai D, Kain KC. CD36 and malaria: friends or foes? A decade of data provides some answers. *Trends Parasitol.* 2014;30(9):436-444. doi:10.1016/j.pt.2014.07.006
399. Nguyen TS, Park JH, Nguyen TK, Nguyen T Van, Lee SK, Na SH, et al. Plasmodium vivax merozoite-specific thrombospondin-related anonymous protein (PvMTRAP) interacts with human CD36, suggesting a novel ligand-receptor interaction for reticulocyte invasion. *Parasit Vectors.* 2023;16(1):426. Published 2023 Nov 19. doi:10.1186/s13071-023-06031-5
400. Gill J, Singh H, Sharma A. Profiles of global mutations in the human intercellular adhesion molecule-1 (ICAM-1) shed light on population-specific malaria susceptibility. *BMC Genomics.* 2023;24(1):773. doi:10.1186/s12864-023-09846-9
401. Egan ES. Beyond hemoglobin: Screening for Malaria Host Factors. *Trends Genet.* 2018;34(2):133-141. doi:10.1016/j.tig.2017.11.004
402. Kanchan K, Pati SS, Mohanty S, Mishra SK, Sharma SK, Awasthi S, et al. Polymorphisms in host genes encoding NOSII, C-reactive protein, and adhesion molecules thrombospondin and E-selectin are risk factors for Plasmodium

- falciparum malaria in India. *Eur J Clin Microbiol Infect Dis*. 2015;34(10):2029-2039. doi:10.1007/s10096-015-2448-0
403. Martin-Jaular L, Nakayasu ES, Ferrer M, Almeida IC, del Portillo HA. Exosomes from *Plasmodium yoelii*-infected reticulocytes protect mice from lethal infections. *PLoS One*. 2011;6(10):e26588. doi:10.1371/journal.pone.0026588
404. Kugeratski FG, Hodge K, Lilla S, McAndrews KM, Zhou X, Hwang RF, et al. Quantitative proteomics identifies the core proteome of exosomes with syntenin-1 as the highest abundant protein and a putative universal biomarker. *Nat Cell Biol*. 2021;23(6):631-641. doi:10.1038/s41556-021-00693-y

7. ANNEX I

As part of my PhD, I've also participated in the following publications:

1. **Title:** Extracellular vesicles in malaria: proteomics insights, *in vitro* and *in vivo* studies indicate the need for transitioning to natural human infections

Authors: Nuria Sima*, Alberto Ayllon-Hermida*, Carmen Fernandez Becerra, Hernando A Del Portillo (*Equal Contribution)

Journal: mBio (*Under revision*)

Year: 2024

Impact Factor: -

DOI: -

Abstract:

Globally, an estimated 2.1 billion malaria cases and 11.7 million malaria deaths were averted in the period 2000–2022. Noticeably, in spite of effective control measurements, in 2022 there were an estimated 249 million malaria cases in 85 malaria endemic countries and an increase of 5 million cases compared with 2021. Further understanding the biology, epidemiology, and pathogenesis of human malaria is therefore essential for achieving malaria elimination. Extracellular vesicles (EVs) are membrane-enclosed nanoparticles pivotal in intercellular communication and secreted by all cell types. Here, we will review what is currently known about EVs in malaria, from biogenesis and cargo to molecular insights of pathophysiology. Of relevance, a meta-analysis of proteomics cargo, and comparisons between *in vitro* and *in vivo* animal studies revealed striking differences with those few studies reported from patients. Thus, indicating the need to transitioning to human infections to elucidate their physiological role. We conclude with a focus on translational aspects in diagnosis and vaccine development and highlight key gaps in the knowledge of EVs in malaria research.

2. **Title:** Proteomic profile of plasma-derived extracellular vesicles from Colombian pregnant women with *Plasmodium*-soil transmitted helminths coinfection

Authors: Jahnney A. Martinez Moreno, Alberto Ayllon-Hermida, Berta Barnadas-Carceller, Carmen Fernandez-Becerra, Hernando A. del Portillo, Jaime Carmona-Fonseca, Eliana María Arango Flórez

Journal: Frontiers in Malaria (Accepted)

Year:2024

Impact Factor: -

DOI: 10.3389/fmala.2024.1484359

Abstract:

Introduction: Extracellular vesicles (EVs) are lipid bilayer membrane-enclosed nanoparticles, secreted by all cell types. Information regarding EVs and their molecular cargo in gestational parasitic infections, particularly those caused by *Plasmodium* and soil-transmitted helminths (STH), remains largely unexplored. This study aimed to perform isolation and molecular characterization of plasma-derived EVs from Colombian pregnant women and compare quantity, size, concentration and protein cargo of those EVs according to the infectious status, to investigate if parasite-derived proteins could be detected as biological cargo of circulating EVs of pregnant women infected with *Plasmodium*, STH and co-infections. Thus, after isolation of circulating EVs, we compared their quantity, size, concentration and protein cargo according to the infectious status.

Material and methods: A descriptive study with 5 groups was performed: 1) Pregnant women with *Plasmodium* infection (n=10). 2) Pregnant women with STH infection (n=14). 3) Pregnant women with coinfection *Plasmodium* and STH (n=14). 4) Pregnant women without infection with *Plasmodium* nor STH (n=10). 5) Non-pregnant women without infection with *Plasmodium* nor STH (n=6). Plasma-derived EVs were isolated by size exclusion chromatography (SEC) and fractions containing EVs identified by a bead-based flow cytometric assay for tetraspanin CD9; the size and concentration of EVs were quantified by nanoparticle tracking analysis, and proteins associated with EVs were identified by liquid chromatography-mass spectrometry (LC-MS) in a pool of samples per study group.

Results: There were no statistical differences in expression of the CD9 EVs marker among study groups. The size range of EVs was more variable in the three infected groups (100-700 nm) compared to the size range of the uninfected groups (50-300 nm). A total of 823 quantifiable proteins with measurable abundance values were identified within the

five study groups by LC-MS. Of the total quantifiable proteins, 758 were identified as human, six proteins pertained to *P. vivax*, fifteen to *Trichiuris trichiura*, and one to hookworms. Data are available via ProteomeXchange with identifier PXD051270.

Discussion: This is the first study that identifies proteins from *Plasmodium* and STH in EVs isolated from pregnant women. The identification of such proteins from neglected tropical parasites accounting for a major burden of disease worldwide, open the possibilities of studying their physiological role during infections as well as exploring them for antigen discovery, vaccine development and biomarker discovery.

3. **Title:** Circulating Extracellular Vesicles Proteomics Reveals Diverse Clinical Presentations of COVID-19 but fails identifying viral peptides.

Authors: Melisa Gualdrón-López*, Alberto Ayllon-Hermida*, Nuria Cortes-Serra, Patricia Resa-Infante, Joan Josep Bech-Serra, Iris Aparici Herraiz, Marc Nicolau-Fernández, Itziar Erkizia, Lucia Gutierrez-Chamorro, Silvia Marfil, Edwards Pradenas, Carlos Avila Nieto, Bernat Cucurull, Sergio Roberto Montaner Tarbes, Magdalena Muelas, Ruth Sotil, Ester Ballana, Victor Urrea, Lorenzo Fraile, Maria Montoya, Júlia Vergara-Alert, Joaquim Segalés, Jorge Carrillo, Nuria Izquierdo-Useros, Julià Blanco, Carmen Fernandez-Becerra, Carolina De La Torre Gómez, Maria-Jesus Pinazo, Javier Martinez-Picado and Hernando A Del Portillo (*Equal Contribution)

Journal: Frontiers in Cellular and Infection Microbiology Virus and Host (Accepted)

Year:2024

Volume: 14

Impact Factor: 5.7

DOI: 10.3389/fcimb.2024.1442743

Abstract:

Extracellular vesicles (EVs) released by virus-infected cells have the potential to encapsulate viral peptides, a characteristic that could facilitate vaccine development. Furthermore, plasma-derived EVs may elucidate pathological changes occurring in distal tissues during viral infections. We hypothesized that molecular characterization of EVs isolated from COVID-19 patients would reveal peptides suitable for vaccine development. Blood samples were collected from three cohorts: severe COVID-19 patients (G1), mild/asymptomatic cases (G2), and SARS-CoV-2-negative healthcare workers (G3). Samples were obtained

at two time points: during the initial phase of the pandemic in early 2020 (m0) and eight months later (m8). Clinical data analysis revealed elevated inflammatory markers in G1. Notably, non-vaccinated individuals in G1 exhibited increased levels of neutralizing antibodies at m8, suggesting prolonged exposure to viral antigens. Proteomic profiling of EVs was performed using three distinct methods: immunocapture (targeting CD9), ganglioside-capture (utilizing Siglec-1) and size-exclusion chromatography (SEC). Contrary to our hypothesis, this analysis failed to identify viral peptides. These findings were subsequently validated through Western blot analysis targeting the RBD of the SARS-CoV-2 Spike protein's and comparative studies using samples from experimentally infected Syrian hamsters. Furthermore, analysis of the EV cargo revealed a diverse molecular profile, including components involved in the regulation of viral replication, systemic inflammation, antigen presentation, and stress responses. These findings underscore the potential significance of EVs in the pathogenesis and progression of COVID-19.

Also, as part of this PhD, and in collaboration with the group of Prof. Dr. Bernd Giebel, at the Universitätsmedizin Essen, a collaborative project for antigen discovery of *P. vivax* for vaccine development using extracellular vesicles was done.

4. **Title:** Antigen discovery and their expression in extracellular vesicles for vaccine development against *Plasmodium vivax*.

Authors: Alberto Ayllon-Hermida, Yanis Mouloud, Ali Al-Jipouri, Carmen Fernandez Becerra, Bernd Giebel, Hernando A Del Portillo

Journal: *Manuscript in preparation*

Year:2024

Abstract:

Plasmodium vivax, the most resilient malaria parasite, poses significant challenges to be eliminated due to its dormant liver stage, cryptic splenic and bone-marrow infections and early gametocyte production. A key approach to combat *P. vivax* would be the development of effective vaccines. Current efforts are focusing in targeting the Duffy-binding protein (PvDBPII), critical for parasite invasion of reticulocytes. However, traditional vaccine development has progressed slowly, with very few candidates reaching to clinical trials. Extracellular vesicles (EVs) offer a novel platform for vaccine development due to their ability to present antigens and modulate immune responses. This study explores the potential of engineered EVs to express immunogenic regions of the *P. vivax* proteins, specifically the pHISTc (PVX_093680) and the PvSDP1 (PVX_114580), using HEK-293 cells. The antigenicity and B-cell epitope productions identified immunogenic regions for loading into EVs, which were confirmed using advanced modelling techniques. Lentiviral transduction enabled the expression of these antigens in HEK-293 cells, leading to the production of EVs carrying the desired immunogenic domains. The resulting EVs showed potential for further investigation and development as potential vaccine candidates against *P. vivax*, which if achieved, would represent a promising step towards malaria control through an innovative vaccine design.